

University of Southampton

Faculty of Engineering and Physical Sciences

School of Chemistry

**Stereoselective synthesis of lupin alkaloids: total synthesis of (+)- β -isosparteine
and (-)-epilupinine**

by

Firas Mohammed Younus Al-Saffar

Thesis for the degree of Doctor of Philosophy

November_2019

University of Southampton

Abstract

Faculty of Engineering and Physical Sciences

School of Chemistry

Thesis for the degree of Doctor of Philosophy

Stereoselective synthesis of lupin alkaloids: total synthesis of (+)- β -isosparteine and (-)-epilupinine

By

Firas Mohammed Younus Al-Saffar

The first stereoselective total synthesis of the tetracyclic lupin alkaloid (+)- β -isosparteine (+)-**1.4** has been achieved in 15% yield over 4 steps using a two-directional, *syn*-selective, double imino-aldol reaction between diphenyl glutarate **2.1** and *tert*-butanesulfinimine **1.205**. The chiral auxiliary, *tert*-butyl sulfinamide **2.9**, was used to control the stereoselectivity of imino-aldol reaction. This methodology was applied to access diastereomerically pure product, introducing 4 stereogenic centres in a single step. In addition, the minor diastereoisomers from double imino-aldol reaction have been identified and used to synthesise (-)-sparteine (-)-**1.3** and (-)-10,17-dioxo- α -isosparteine ((-)-**1.43**). The stereochemistry of intermediates (+)-10,17-dioxo- β -isosparteine ((+)-**1.33**), and (-)-10,17-dioxo- α -isosparteine were confirmed by single crystal X-ray structure determination. A short total synthesis of the bicyclic lupin alkaloid (-)-epilupinine (-)-**1.1** has also been achieved in 31% yield over 2 steps from halo imine **1.205**. Formation of mono cyclised imino-aldol adduct **2.13** was obtained from reaction of the dianion of diphenyl glutarate **2.1** with one equivalent of halo *tert*-butanesulfinimine **1.205**. The stereochemistry of cyclised **2.13** and uncyclised **2.16** mono *syn* imino-aldols were confirmed by single crystal X-ray structure determination. As a part of synthetic studies towards (+)-allomatridine (+)-**1.5**, total synthesis of the bicyclic lupin alkaloid (-)-epilupinine ((-)-**1.1**) was completed in 55% overall yield over 6 steps using single imino-aldol reaction between phenyl ester **1.173** and unsaturated *tert*-butanesulfinimine **1.208**. The stereochemistry of unsaturated quinolizidinone **2.30** and tricyclic imide **2.40** were confirmed by single crystal X-ray structure determination.

Table of Contents

Table of Contents	i
List of Tables.....	v
List of Figures	vii
DECLARATION OF AUTHORSHIP	xi
Acknowledgements	xiii
Definitions and Abbreviations.....	xiv
Chapter 1: Introduction to lupin alkaloid sparteine and its isomers, and allomatridine and epilupinine.....	1
1.1 Introduction	1
1.1.1 Lupin alkaloids	1
1.1.2 Sparteine alkaloid and its identification	1
1.2 Application of sparteine as a chiral ligand in enantioselective reactions	4
1.2.1 Chiral diamine organolithium complexes.....	4
1.2.2 (–)-Sparteine and its isomers in metal catalysed enantioselective reactions	6
1.2.3 Enantioselective electrocatalytic oxidative coupling using (–)-sparteine ..	7
1.3 Previous synthetic studies on the lupin alkaloids.....	7
1.3.1 Ing's semi-synthesis of (–)-sparteine from anagyrene.....	7
1.3.2 Winterfeld and Rauch's semi-synthesis of (–)- α -isosparteine from (–)- sparteine	8
1.3.3 Clemo's syntheses of (\pm)-sparteine.....	8
1.3.4 Sorm and Keil's synthesis of (\pm)-sparteine and (\pm)- β -isosparteine	9
1.3.5 Leonard's synthesis of (\pm)-sparteine and (\pm)- β -isosparteine	11
1.3.6 Clemo, Raper, and Short's synthesis of (\pm)-dioxosparteine isomers	12
1.3.7 Anet, Hughes, and Ritchie's synthesis of (\pm)-sparteine.....	12
1.3.8 Moore and Marion semi-synthesis (–)- β -isosparteine and (+)-sparteine	13
1.3.9 Tsuda and Satoh's synthesis of three isomers of (\pm)-sparteine	13
1.3.10 Van Tamelen and Foltz biogenetic synthesis of (\pm)-sparteine	14
1.3.11 Bolmann's synthesis of (\pm)-sparteine.....	15

1.3.12	Kakisawa's total synthesis (\pm)- α -isosparteine	16
1.3.13	Otomasu's formal synthesis of (\pm)-sparteine	16
1.3.14	Koomen's synthesis of (\pm)-sparteine and (\pm)- β -isosparteine	17
1.3.15	Aube's synthesis of (+)-sparteine	18
1.3.16	O'Brien's synthesis of (-)-sparteine	19
1.3.17	Butler and Fleming's synthesis of (\pm)-sparteine	21
1.3.18	Blakemore's synthesis of (\pm)-sparteine, (\pm)- α -isosparteine and (\pm)- β - isosparteine.....	22
1.3.19	O'Brien's synthesis of (-)-sparteine	24
1.3.20	Breuing's synthesis of bisquinolizidine alkaloids	25
1.4	Matrine alkaloids.....	28
1.4.1	Previous total synthesis of (\pm)-matrine isomers	28
1.4.2	Bohlmann's Biogenetic synthesis of (\pm)-allomatridine and other tetracyclic lupin alkaloid	28
1.4.3	Mandell's total synthesis of (\pm)-matrine and (\pm)-allomatrine	30
1.4.4	Okuda's semi-synthesis of optically active of (\pm)-allomatrine	31
1.4.5	Matsunaga's synthesis of (\pm)-allomatridine	32
1.4.6	Chen's total synthesis of (\pm)-matrine.....	32
1.4.7	Brown's total synthesis of (+)-allomatrine	34
1.5	Epilupinine	35
1.5.1	Pohmakotr's synthesis of (\pm)-epilupinine and (\pm)-lupinine	35
1.5.2	Martin's synthesis of (\pm)-epilupinine	36
1.5.3	Hu, Wang's synthesis of (\pm)-epilupinine.....	37
1.5.4	Szymoniak's synthesis of (\pm)-epilupinine	38
1.5.5	Brown's total synthesis of (-)-epilupinine	38
1.5.6	Kise's synthesis of (\pm)-epilupinine <i>via</i> electroreductive coupling	40
1.5.7	Davies's synthesis of (+)-epilupinine <i>via</i> a double reductive cyclisation protocol.....	40
Chapter 2:	Results and Discussion	43
2.1	Synthesis of the tetracyclic alkaloid (+)- β -isospartiene	43
2.1.1	Retrosynthetic analysis of (+)- β -isospartiene.....	43
2.1.2	Double imino-aldol reaction of glutarate esters.....	44
2.1.3	Double imino-aldol reaction of diphenyl glutarate with unsaturated imine..	46

2.1.4	A concise double imino-aldol approach to the synthesis of (+)- β -isospartiene.....	47
2.1.5	Optimisation of the double imino-aldol reaction.....	51
2.1.6	Determination of the structures and stereochemistry of the major and minor products from the double imino-aldol reaction	52
2.1.7	Determination of the remaining structures from imino-aldol reaction.....	56
2.1.8	Determination of the absolute stereochemical assignments of sparteine isomers	58
2.1.9	Elaboration of <i>syn</i> mono imino-aldol product towards the synthesis of (–)-sparteine	60
2.1.10	Conclusions.....	62
2.2	Synthesis of (–)-epilupinine from mono imino-aldol adducts of diphenyl glutarate.....	63
2.2.1	Retrosynthetic analysis of (–)-epilupinine	63
2.2.2	The optimisation of mono imino-aldol adduct formation.....	63
2.2.3	Determination the diastereoselectivity of mono imino-aldole products.....	65
2.2.4	The mechanism of mono imino-aldole reaction	66
2.2.5	Completion the synthesis of (–)-epilupinine from cyclised- <i>syn</i> imino-aldol.....	67
2.2.6	Confirmation of the absolute stereochemistry of (–)-epilupinine.....	68
2.2.7	Comparison of the product distribution observed for the mono and double imino-aldol reactions	68
2.2.8	Structure determination of the minor imino-aldol products	69
2.2.9	Conclusions.....	71
2.3	RCM approach to the total synthesis of (–)-epilupinine from phenyl ester and unsaturated imine.....	72
2.3.1	Retrosynthetic analysis of (–)-epilupinine	72
2.3.2	Towards the synthesis of (–)-epilupinine	72
2.3.3	Imino-aldole reaction of unsaturated imine	73
2.3.4	Total synthesis of (–)-epilupinine from imino-aldol 1.208.....	74
2.3.5	Conclusions.....	77
2.4	Towards the synthesis of (+)-allomatridine and (–)-sparteine.....	78
2.4.1	Retrosynthetic analysis of (+)-allomatridine.....	78
2.4.1.1	The synthesis of tricyclic imide intermediate towards (+)-allomatridine.....	79

2.4.1.2	Efforts towards the synthesis of (+)-allomatridine	81
2.4.1.3	Further attempts to cyclise tricyclic intermediates.....	Error! Bookmark not defined.
2.4.2	Retrosynthetic analysis of (-)-sparteine	84
2.4.2.1	Towards stereocontrolled synthesis of (-)-sparteine.....	85
2.4.3	Conclusions	87
Chapter 3:	Experimental Details	91
3.1	General Methods.....	91
3.2	Procedures and Characterisation Data.....	92
Appendix A.....		147
Appendix B.....		153
List of References	Error! Bookmark not defined.	

213

List of Tables

1. Table 2.1.	¹³ C NMR data for (+)-10,17-dioxo- β -isosparteine ((+)- 1.33).	50
2. Table 2.2.	¹³ C NMR data for (+)- β -isosparteine ((+)- 1.4).	50
3. Table 2.3.	Optimisation of the double imino-aldol reaction.	51
4. Table 2.4.	¹³ C NMR data for (+)-10,17-dioxo-sparteine ((+)- 1.44) and recorded physical data.	58
5. Table 2.5.	¹³ C NMR data for (-)-sparteine ((-)- 1.3) and recorded physical data..	59
6. Table 2.6.	¹³ C NMR data for (-)-10,17-dioxo- α -isosparteine ((-)- 1.43) and recorded physical data	59
7. Table 2.7:	Optimisation of mono imino-aldol reaction using different imines ...	64
8. Table 2.8:	Comparison of recorded and literature spectroscopic data for (-)-epilupinine.	68
9. Table 2.9:	Summary of the main identified components from reaction under optimised double (conditions A) and mono (conditions B) imino-aldol reactions.	69
10. Table 2.10:	Optimisation and the deprotection-cyclisation reaction of the <i>syn</i> -adduct 1.209	75

List of Figures

Figure 1.1	Exemplar structures of Lupin alkaloids..... Error! Bookmark not defined.
Figure 1.2	Model of the structure proposed for sparteine by Clemo and Raper2
Figure 1.3	Structures of (-)-sparteine ((-)- 1.3), (-)- β -isoparteine ((-)- 1.4) and (-)- α -isoparteine ((-)- 1.8)3
Figure 1.4	The conformational-configurational isomerism of (-)-sparteine ((-)- 1.3).....4
Figure 1.5	Achiral and chiral diamine ligands for asymmetric synthesis.5
Figure 1.6	PdCl ₂ complexes of (-)-sparteine and its isomers.....6
Figure 1.7	Structures of (+)-allomatridine ((+)- 1.5), (+)-matrine ((+)- 1.138) and (+)-allomatrine ((+)- 1.139).28
Figure 1.8	Structure of (-)-epilupinine ((-)- 1.1) and (+)-lupinine ((+)- 1.181) and 1.182 .35
Figure 2.1	Overview of strategy towards the synthesis of lupin alkaloids43
Figure 2.2	Retrosynthetic analysis of (+)- β -isoparteine from unsaturated imin 1.208 .44
Figure 2.3	Retrosynthetic analysis of (+)- β -isoparteine from halo imin 1.20544
Figure 2.4	X-ray crystal structure of <i>syn,syn</i> double imino-aldol adduct 2.247
Figure 2.5	X-ray crystal structure of (+)-10,17-dioxo- β -isoparteine ((+)- 1.33).49
Figure 2.6	Representation of the TLC plate showing R _f values for different imino-aldol products.53
Figure 2.7	The ¹ H NMR spectrum of the crude double imino-aldol reaction mixture54
Figure 2.8	X-ray crystal structures of mono <i>syn</i> imino-aldol 2.16 and its cyclised product 2.1354
Figure 2.9	¹ H NMR spectra for mono <i>syn</i> imino-aldol 2.16 and its cyclised <i>syn</i> product 2.1355
Figure 2.10	Representation of the TLC plate showing R _f values for bicyclised products .57
Figure 2.11	X-ray crystal structure of (-)-10,17-dioxo- α -isoparteine ((-)- 1.43).....58

Figure 2.12	Proposed synthesis of (–)-sparteine from <i>syn</i> imino-aldol adduct 2.16	60
Figure 2.13	Retrosynthetic analysis of (–)-epilupinine from halo imine 1.205	63
Figure 2.14	¹ H NMR (400 MHz) for cyclised <i>syn</i> and <i>anti</i> -adducts 2.13 and 2.17	66
Figure 2.15	¹ H NMR (400 MHz) for comparison of <i>syn</i> - and <i>anti</i> -mono imino-aldol adducts	70
Figure 2.16	Retrosynthetic analysis of (–)-epilupinine	72
Figure 2.17	Proposed Zimmerman-Traxler transition state model for the imino-aldol reaction leading to the major <i>syn</i> product	73
Figure 2.18	Proposed routes towards the synthesis of (–)-epilupinine	74
Figure 2.19	X-ray crystal structure of the unsaturated quinolizidinone 2.30	76
Figure 2.20	Routes towards (+)-allomatridine ((+)- 1.5) and (–)-sparteine ((–)- 1.3) from piperidine and quinolizidine intermediates	78
Figure 2.21	Retrosynthetic analysis of (+)-allomatridine ((+)- 1.5)	79
Figure 2.22	X-ray crystal structure of tricyclic imide 2.40	81
Figure 2.23	Retrosynthetic analysis of (–)-sparteine over <i>N</i> -acyliminium ion cyclisation ..	85
Figure 2.24	Bohlmann’s reported synthesis of (±)-sparteine.....	85

DECLARATION OF AUTHORSHIP

I Firas Mohammad Al-Saffar declare that this thesis and the work presented in it are my own and has been generated by me as the result of my own original research.

Stereoselective synthesis of lupin alkaloids: total synthesis of (+)- β -isosparteine and (-)-epilupinine

I confirm that:

1. This work was done wholly or mainly while in candidature for a research degree at this University;
2. Where any part of this thesis has previously been submitted for a degree or any other qualification at this University or any other institution, this has been clearly stated;
3. Where I have consulted the published work of others, this is always clearly attributed;
4. Where I have quoted from the work of others, the source is always given. With the exception of such quotations, this thesis is entirely my own work;
5. I have acknowledged all main sources of help;
6. Where the thesis is based on work done by myself jointly with others, I have made clear exactly what was done by others and what I have contributed myself;
7. Part of this work have been published as:
Al-Saffar, F. M.; Brown, R. C. D., *Org. Lett.* **2017**, *19*, 3502-3504.

Signed:

Date:

Acknowledgements

I would first and foremost like to greatest thank to Professor Richard Brown, for the support throughout this journey and helped me to be better scientist. You have encouraged me to pursue my dream of a PhD, and while it has been a difficult situation faced these past few years, however your patience and appreciation of my circumstances made me continue to get my target. I will always appreciate your efforts with me to obtain my PhD and kept me on the right track.

I am grateful my family for standing and supporting me throughout my life, and also thanks to all the other academics in building 30 as well – Dr. Lynda J. Brown, Prof. Harrowven, Prof. Linclau, Dr. Bloodworth, Dr. Ramon Rios and Prof. Whitby: for taught me a lot, and encouraged me to try things I may not have thought of otherwise.

I would like to extend special thanks to the members of the Brown group, both past and present, for keeping me sane these past few years. Many thanks to Katie Jolley; Rob Green; Ana Folgueiras; Gamal Moustafa; Alex Pop; Alex Leeder; Alex MI; Alex Teuten; Sergio; Angelos; Domenico; Gorge; David Wheatley; Xiang Lyu (Sean); Azzam Mohammed; Aqeel Alaa; Victor; Faisal Al-Malki; Wei Sun for all the talks, support and wisdom you gave me, and unforgettable time. Assistance with all things analytical from Neil, Julie, John, Mark and Peter was always cheerfully provided and gratefully received.

All X-ray crystallography data included in this thesis was collected and processed by Mark Light, thank you.

Finally, I would like to thank the School of Chemistry at the University of Southampton.

Definitions and Abbreviations

$[\alpha]_D$	Alpha D
°C	Degrees Celsius
9-BBN	9-Borabicyclo[3.3.1]-nonane
Ac	Acetyl
acac	Acetylacetone
ADDP	1,1'-(Azodicarbonyl)dipiperidine
AM	Anti-Markovnikov
Aq	Aqueous
atm	Atmosphere
ATMS	Allyltrimethylsilane
Bn	Benzyl
br	Broad
BtH	1 <i>H</i> -Benzotriazole
Bu	Butyl
ca.	Circa
Cbz	Benzyloxycarbonyl
cm	Centimetre
CM	Cross metathesis
Conc.	Concentrated
d	Doublet
d.r.	Diastereomeric ratio
DBU	1,8-Diazabicyclo[5.4.0]undec-7-ene
DCC	<i>N,N'</i> -dicyclohexylcarbodiimide
DEAD	Diethyl azodicarboxylate
DIAD	Diisopropyl azodicarboxylate

DIBAL-H	Diisobutylaluminium hydride
DMAP	4-(Dimethylamino)-pyridine
DMF	<i>N,N'</i> -dimethylformamide
DMSO	Dimethylsulfoxide
e.e.	Enantiomeric excess
EI	Electron ionisation
Equiv.	Molar equivalents
ESI	Electrospray Ionisation
Et	Ethyl
FT	Fourier Transform
g	Gram
GC	Gas Chromatography
h	Hour(s)
HMDS	Hexamethyldisilazane
HMPA	Hexamethylphosphoramide
HPLC	High-Performance Liquid Chromatography
HRMS	High-Resolution Mass Spectrometry
HSQC	Heteronuclear Single Quantum Coherence Spectroscopy
<i>i</i>	Iso
IR	Infrared
<i>J</i>	Coupling constant
K	Kelvin
L	Litre
LDA	Lithium diisopropylamide
LiHMDS	Lithium bis(trimethylsilyl)amide
LRMS	Low-Resolution Mass Spectrometry

m	Multiplet
<i>m</i>-CPBA	<i>meta</i> -Chloroperbenzoic acid
Me	Methyl
min	Minute(s)
mmol	Millimole(s)
Ms	Mesyl
MS	Mass Spectrometry
MW	Molecular weight
n	Nano
NBS	<i>N</i> -Bromosuccinimide
NMO	<i>N</i> -Methylmorpholine <i>N</i> -Oxide
NMR	Nuclear Magnetic Resonance
NOE	Nuclear Overhauser Effect
O/N	Overnight
<i>p</i>	<i>Para</i>
Ph	Phenyl
ppm	Parts per million
Pr	Propyl
Py	Pyridine
q	Quartet
RBF	Round Bottom Flask
RCM	Ring Closing Metathesis
R_f	Retention factor
rt	Room Temperature
s	Singlet
sat.	Saturated
t	Tertiary

T	Temperature
T₃P	Propylphosphonic anhydride
TBS	<i>tert</i> -Dibutyldimethylsilyl
TFA	Trifluoroacetic Acid
THF	Tetrahydrofuran
TLC	Thin Layer Chromatography
TMS	Trimethylsilyl
Ts	Tosyl
V_t	Variable Temperature
Δ	Heating at reflux

Chapter 1: Introduction to the lupin alkaloids sparteine, its stereoisomers, and allomatridine and epilupinine.

1.1 Introduction

1.1.1 Lupin alkaloids

The Lupin alkaloids are a large family of natural products consisting of more than 200 compounds,¹ the majority of Lupin have a quinolizidine core. They have been isolated from several papilionaceous plant species^{1,2} which can be grouped into four structural series named after the parent alkaloids (**Figure 1.1**). These are the bicyclic “epilupinine” alkaloids tricyclic “cytisine” alkaloids tetracyclic “sparteine” alkaloids and another group of tetracyclic alkaloids known as “matrine” alkaloids. The focus of this thesis is the synthesis of compounds belonging to the epilupinine, sparteine and matrine structural classes, and an introduction to these compounds will be provided in the following sections.

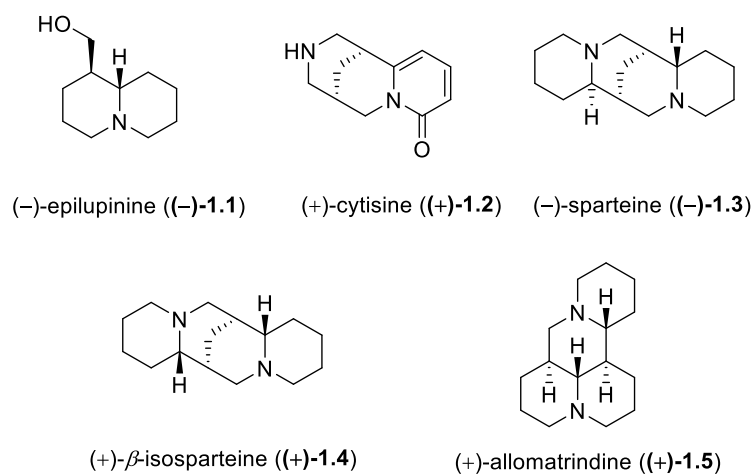
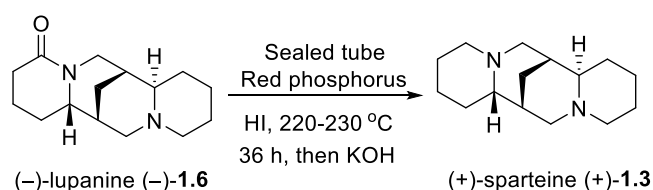


Figure 1.1: Exemplar structures of Lupin alkaloids

1.1.2 Sparteine alkaloid and its identification

(-)-Sparteine ((-)-1.3) is a tetracyclic lupin alkaloid isolated in 1851 by extraction from certain papilionaceous plants (e.g. *Cytisus scoparius*) by Stenhouse who also determined its molecular formula ($C_{15}H_{26}N_2$).³ In 1903, Moureu and Valeur correctly elucidated the presence of two tertiary nitrogen atoms and four rings,⁴ but later incorrectly concluded (-)-sparteine was an asymmetrical compound with bridgehead nitrogen atoms.⁵

In 1928 Clemo and Leitch reported on the reduction of (\pm)-lupanine ((\pm)-**1.6**), an alkaloid found as a racemate in *Lupinus albus*, *Lupinus termis*, *Podalyria buxifolia*, *Podalyria sericea*, and *Virgilia capensis*.⁶ Reduction of (\pm)-lupanine using a sealed tube containing red phosphorus and HI, led to a compound identified as “deoxylupanine”, which was later shown to be the same as (\pm)-sparteine ((\pm)-**1.3**) (found as a racemate in *Cytisus proliferus*). At that time, however, the structure of these alkaloids was not known and the relationship between “deoxylupanine” and sparteine was not recognised. After several years, in 1931, Clemo, Raper, and Tenniswood succeeded in resolving (\pm)-lupanine ((\pm)-**1.6**) and reducing (+)- and (-)-lupanine (**Scheme 1.1**).⁷ The enantiomeric alkaloids were converted to (-)-sparteine and (+)-sparteine respectively, confirming the equivalence of sparteine and “deoxylupanine”.



Scheme 1.1: Clemo, Raper, and Tenniswood’s reduction of lupanine to sparteine.

The structure of sparteine and lupanine were proposed by Clemo and Raper⁸ in 1933 adopting the formula suggested by Ing⁹ in 1932 for cytisine and also depending on a key factor of Ing’s work in 1933.^{10,11} The model of sparteine was suggested by Clemo and Raper, they expected the structure of sparteine as shown in photo (**Figure 1.2**).⁸

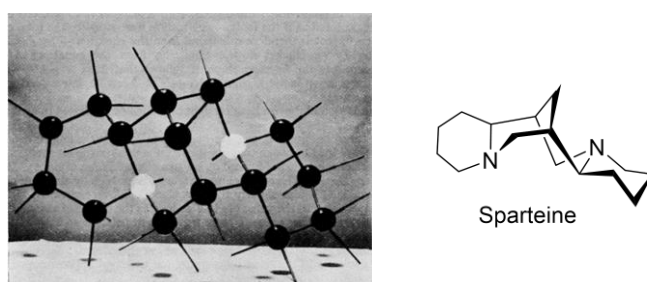
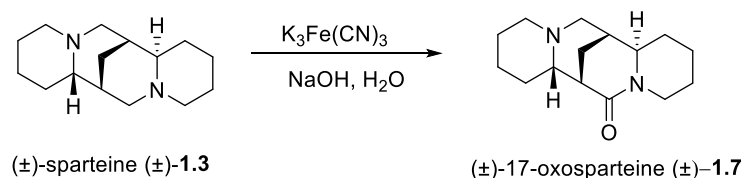


Figure 1.2: Model of the structure proposed for sparteine by Clemo and Raper

Furthermore, in 1936 Clemo *et al.* determined the correct structure of (\pm)-sparteine by its oxidation using potassium ferricyanide to (\pm)-17-oxosparteine ((\pm)-**1.7**) which was identical with the known compound (**Scheme 1.2**).¹²



Scheme 1.2: Oxidation of (±)-sparteine to (±)-17-oxosparteine by Clemo *et al.*

Three diastereoisomers of sparteine are known; sparteine, α -isosparteine and β -isosparteine (**Figure 1.3**). The absolute stereochemistry and configuration of sparteine were confirmed by Okuda *et al.* in 1965 through chemical interrelations between (–)-cytisine ((–)-**1.2**) and (–)-sparteine ((–)-**1.3**), in which the absolute configuration of the methylene bridge was confirmed to be the same as that of (–)-cytisine.¹³

(–)- α -Isosparteine ((–)-**1.8**) was first isolated from *Lupinus caudatus* by Marion *et al.* in 1951,¹⁴ but prior to its isolation, it was obtained *via* a semi-synthesis from (–)-sparteine ((–)-**1.3**) in 1934.¹⁵ (–)- β -Isosparteine ((–)-**1.4**) also called (spartalupine and pusilline) was isolated from *Lupinus sericeus* by Carmack *et al.* in 1955.¹⁶

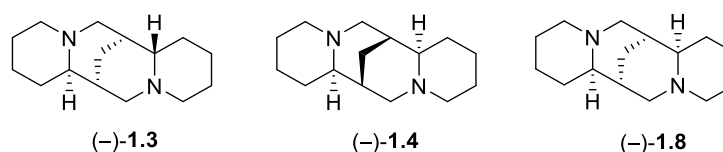


Figure 1.3: Structures of (–)-sparteine ((–)-**1.3**), (–)- β -isosparteine ((–)-**1.4**) and (–)- α -isosparteine ((–)-**1.8**)

In terms of pharmacological activity, (–)-sparteine ((–)-**1.3**) is limited in potency as a cardiac agent and has a moderate toxicity,¹⁷ causing unpredictable side effects. However, it has found use in clinical applications.¹⁸⁻²² At lower doses, increased blood pressure and diuretic effects are common, but dangerous heart rhythms and obstetrical complications are possible at moderately high doses. The use of sparteine as an *anti*-arrhythmic and oxytocic was banned in 1979, but later it was used in human studies related to metabolism by the CYP2D6 enzyme.²³

1.2 Applications of sparteine as a chiral ligand in enantioselective reactions

(–)-Sparteine ((–)-**1.3**) is used as a chiral ligand in asymmetric synthesis for a wide range of enantioselective transformations.²⁴ Since the initial publication of asymmetric deprotonation of alkyl carbamates with *sec*-butyl lithium / (–)-sparteine by Hoppe *et al.* in 1990,²⁵ there have been

numerous reviews published in the literature.^{24, 26-28} The first review was by Caddick and Jenkins in 1996 covering dynamic resolutions in asymmetric synthesis.²⁸ (–)-Sparteine has found applications as a chiral ligand in organolithium chemistry for enantioselective synthesis with lithium-carbanion pairs, where the metal exists in a tetrahedral coordination geometry with four donor ligands.²⁹ Studies of the suitability of (–)-sparteine as a chiral additive in carbanion reactions were reported by Nozaki *et al.* between 1968 and 1971.³⁰⁻³⁴ Examples included, asymmetric Grignard addition to benzaldehyde,³¹ and lithiation of isopropyl ferrocene and ethylbenzene.^{32,33} The favoured conformation of sparteine in metal coordination complexes between the two nitrogens was shown by theoretical calculations to adopt in the *chair-chair trans*-quinolizidine A/B system and *boat-chair trans*-quinolizidine C/D system.³⁵ Free (–)-sparteine exists mostly in *trans*-configuration **1.3b** (*chair/chair/boat/chair*) of the A/B/C/D system because the *cis*-configuration **1.3a** (*chair/chair/chair/chair*) has been computed to be higher in energy by 3.4 kcal/mol than the *trans*-configuration **1.3b** (**Figure 1.4**).³⁶ On the other hand, the *cis*-configuration was adopted when chelating to a metal centre. In fact, (–)-sparteine could behave as an efficient chiral bidentate ligand, since flipping of **1.3b** into **1.3a** favours formation of two coordinate bonds in the metal complexes (**Figure 1.4**).^{37,38}

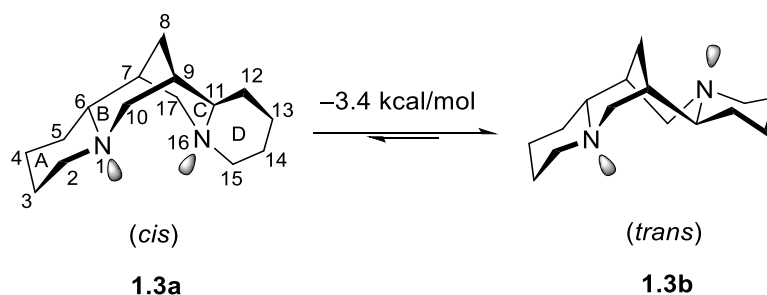


Figure 1.4: The conformational-configurational isomerism of (–)-sparteine ((–)-**1.3**)

1.2.1 Chiral diamine organolithium complexes

The first highly enantioselective asymmetric deprotonations to prepare organolithium reagents using (–)-sparteine were reported by Beak *et al.* in 1993.³⁹⁻⁴¹ The ligand tetramethylethylenediamine (**1.9**) (TMEDA) was used with an alkyllithium bases for α -deprotonation of *N*-heterocycles by Beak and Lee in 1989 (**Figure 1.5**). An asymmetric synthesis was later developed in 1994 using (–)-sparteine ((–)-**1.3**).⁴² Routes to the enantiomeric α -substituted *N*-heterocycles were realised by O'Brien and co-workers using a (+)-sparteine surrogate (+)-**1.10**, which provided similar levels of enantioselectivity to sparteine in many reactions.⁴³

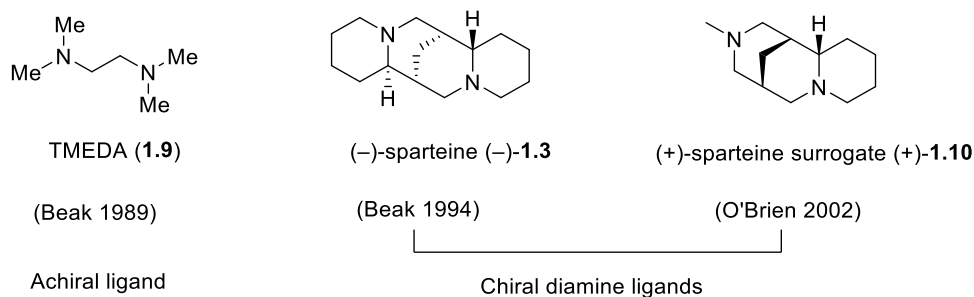
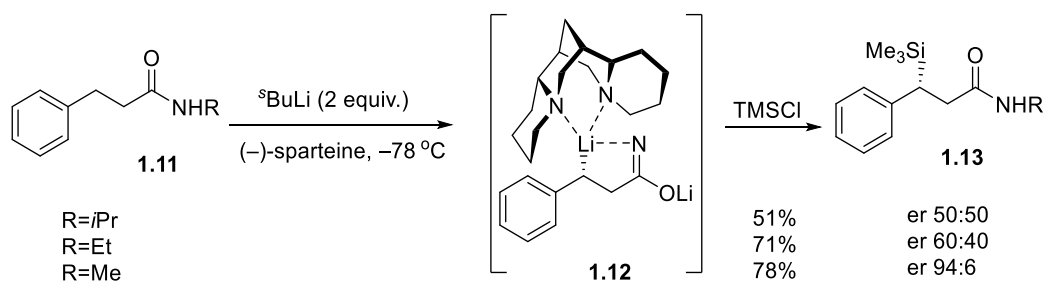


Figure 1.5: Achiral and chiral diamine ligands for asymmetric synthesis

The asymmetric lithiation-substitution of the *N*-methyl amide **1.11** using *sec*-BuLi/(-)-sparteine has been reported by Beak *et al.* (**Scheme 1.3**).⁴⁰ The amide nitrogen and (-)-sparteine form a chiral complex to the benzylic lithium which was shown to proceed through a process of dynamic thermodynamic resolution. The chiral organolithium **1.12** was obtained from double deprotonation of **1.11** in the presence of (-)-sparteine followed by trimethylsilyl chloride (TMSCl) trapping to afford amide **1.13** with high selectivity and good yield (R = Me). Poor or no selectivity was observed for bulkier amides (R = Et, *i*Pr), and this can be explained by the steric interactions of the substituents which prevented coordination of (-)-sparteine to the organolithium. There are many other reported examples of asymmetric lithiation using (-)-sparteine and these have been reviewed.⁴⁴⁻⁴⁷



Scheme 1.3: Dynamic thermodynamic resolution of benzylic carbanions.

1.2.2 (-)-Sparteine and its isomers in metal catalysed enantioselective reactions

(-)-Sparteine and its isomers ((-)- α -isoparteine, (-)- β -isoparteine) have been used with metal catalysts to form diastereoisomeric PdCl₂ complexes (**Figure 1.6**),⁴⁸ which provided new reactivity and selectivity in the oxidative kinetic resolution of phenyl ethanol secondary alcohols.

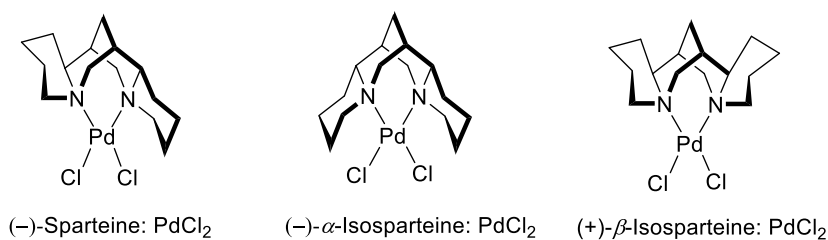
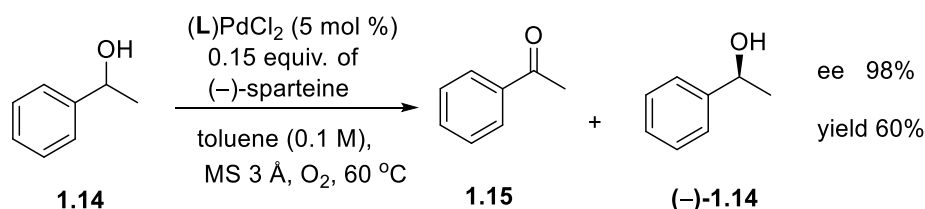


Figure 1.6: PdCl₂ complexes of (-)-sparteine and its isomers

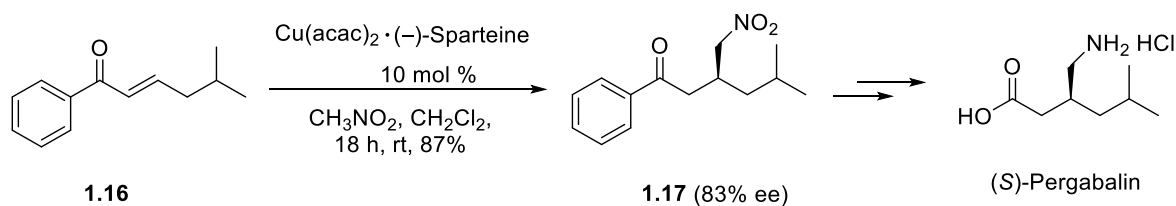
The stereoselectivity of the oxidative kinetic resolution of 1-phenylethanol (**1.14**) to the corresponding ketone **1.15** was carried out using (sparteine). PdCl₂ and indicated that C₁-symmetry of (-)-sparteine is particularly effective (**Scheme 1.4**). (-)-Sparteine was highly selective and more reactive than its C₂-symmetric diastereomers (-)- α -isosparteine and (-)- β -isosparteine.



L = (-)-Sparteine, (-)- α -Isosparteine and (+)- β -Isosparteine

Scheme 1.4: Oxidative kinetic resolution with three sparteine PdCl₂ diastereoisomers

In 2016, Chopade and co-worker used (-)-sparteine (-)-**1.3** and Cu(acac)₂ as a catalyst for the enantioselective Michael addition of nitromethane on chalcone **1.16** to give γ -nitro ketone **1.17** in 87% yield and 83% ee (**Scheme 1.5**).⁴⁹ This methodology was applied to the asymmetric synthesis of anticonvulsant drug (*S*)-pregabalin (88% ee) in four steps with 52% overall yield.

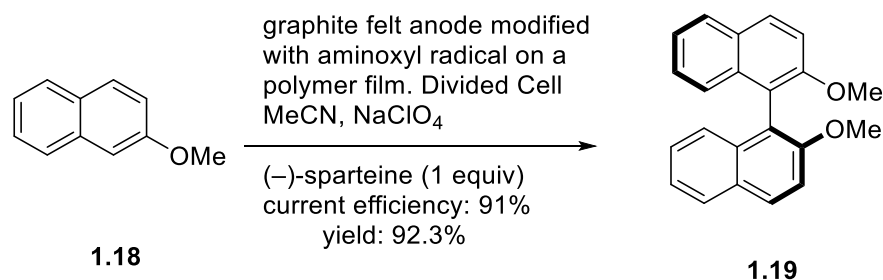


Scheme 1.5: The enantioselective Michael addition of nitromethane to chalcone using Cu(acac)₂·(-)-sparteine complex

1.2.3 Enantioselective electro catalytic oxidative coupling using (-)-sparteine

The enantioselective electrocatalytic oxidative coupling of naphthol (**1.18**) in the presence of (-)-sparteine on a TEMPO-modified electrode was reported by Kashiwagi *et al.* in 1994 (**Scheme 1.6**).⁵⁰ Electrolytic coupling of 2-methoxynaphthalene (**1.18**) to (*S*)-(-)-2,2'-dimethoxy-1,1'-binaphthyl

(**1.19**) was shown to proceed with high enantioselectivity (93.3% ee by polarimetry and 93.6% by HPLC). No explanation was given to indicate how enantioselectivity was achieved.



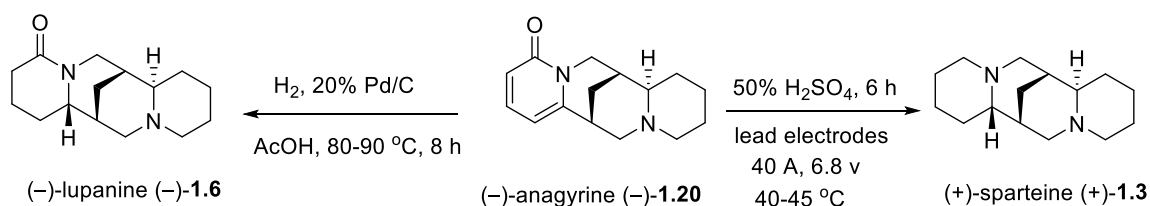
Scheme 1.6: The enantioselective oxidative coupling naphthol using sparteine

1.3 Previous synthetic studies on the sparteine alkaloids

Syntheses of sparteine have been attempted many times, originally to determine the absolute and relative configuration of the natural product and for the preparation of enantiomerically pure material. More recent synthetic work has focussed on the development of synthetic methodology. There have been over ten total syntheses of sparteine-type alkaloids; an overview of the synthetic work is documented below in chronological order.

1.3.1 Ing's semi-synthesis of (+)-sparteine from anagyrene.

In 1933, Ing reduced (-)-anagyrene ((-)-**1.20**) electrochemically to give "hexa-hydroanagyrene", which they found to be identical to (+)-sparteine (**Scheme 1.7**). In the same work hydrogenation of (-)-anagyrene afforded "tetra-hydroanagyrene", which was determined to be identical to (-)-lupanine ((-)-**1.6**).⁹

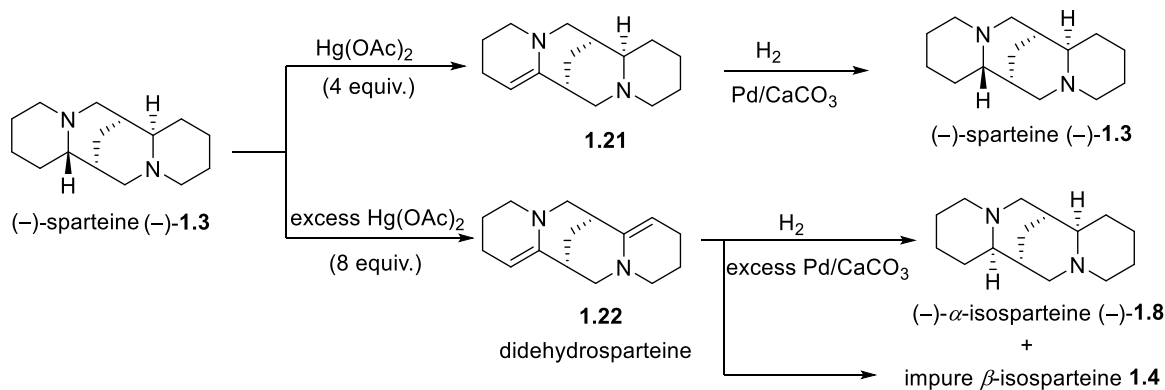


Scheme 1.7: Ing's semi-synthesis of (+)-sparteine ((-)-**1.3**) from (-)-anagyrene ((-)-**1.20**)

1.3.2 Winterfeld and Rauch's semi-synthesis of (-)- α -isoparteine from (-)-sparteine

A semi-synthesis of (-)- α -isoparteine ((-)-**1.8**) from (-)-sparteine was published by Winterfeld and Rauch in 1934 (**Scheme 1.8**).¹⁴ A dehydro-spartiene **1.21** was formed using mercuric acetate Hg(OAc)₂ under mild conditions. Hydrogenation of **1.21** over Pd/CaCO₃ generated (-)-sparteine.

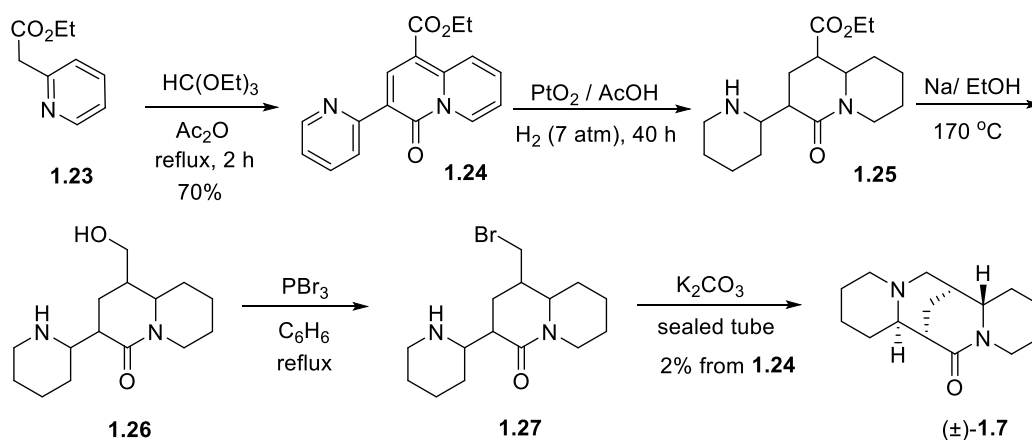
Using more equivalents of $\text{Hg}(\text{OAc})_2$, dihydrogenation of (-)-sparteine afforded dihydrosparteine **1.22**. Subsequent hydrogenation of α -dihydrosparteine **1.22** furnished (-)- α -isosparteine (-)-**1.8**, while β -isosparteine **1.4** was obtained as an impure product from β -dihydrosparteine **1.22** under the same conditions.



Scheme 1.8: Winterfeld and Rauch's semi-synthesis of (-)- α -isosparteine from (-)-sparteine

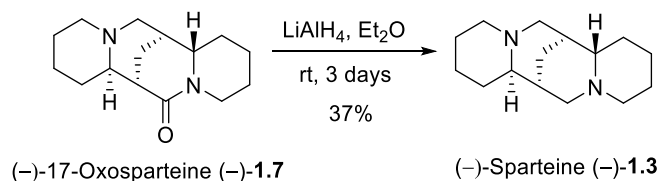
1.3.3 Clemo's syntheses of (\pm)-sparteine

In 1936, Clemo, Morgan, and Raper prepared (\pm)-17-oxosparteine ((\pm)-**1.7**) through a multi-step procedure from ethyl 2-pyridylacetate (**1.23**) and ethyl orthoformate (**Scheme 1.9**).¹¹ Adams' catalyst hydrogenation of pyridocoline **1.24** in AcOH provided piperidyl ethyl carboxylate **1.25**. Reduction of ethyl carboxylate **1.25** using Na in EtOH with heating afforded alcohol **1.26** which was then treated with PBr_3 to access bromide **1.27**. Cyclisation of **1.27** under basic conditions gave (\pm)-17-oxosparteine ((\pm)-**1.7**) in 14% overall yield from **1.23**. Reduction of (\pm)-17-oxosparteine to (\pm)-sparteine was not completed due to the lack availability of reducing agents at that time. Therefore, this should strictly be considered as formal synthesis of sparteine.



Scheme 1.9: Clemo, Morgan and Raper's synthesis of (\pm)-17-oxosparteine (\pm)-**1.7**

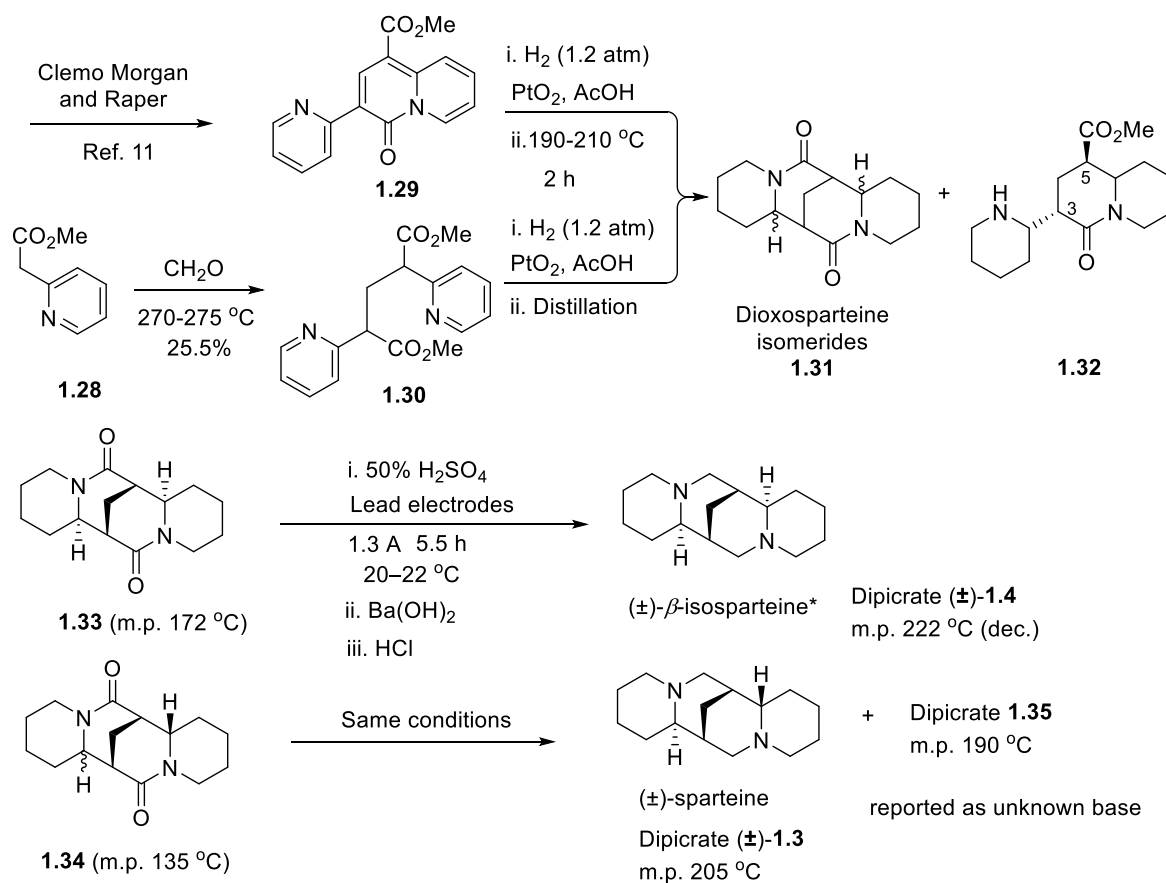
In 1949, following the discovery of LiAlH_4 , Clemo, Raper and Short showed that (–)-17-oxosparteine is reduced to (–)-sparteine (**Scheme 1.10**).⁵¹



Scheme 1.10: Clemo, Raper and Short's semi-synthesis of (–)-sparteine

1.3.4 Sorm and Keil's synthesis of (±)-sparteine and (±)-β-isosparteine

In 1948, Sorm and Keil successfully reported the first total syntheses of (±)-sparteine (±)-**1.3** and (±)-β-isosparteine (**1.4**) using electrolytic reduction (**Scheme 1.11**).^{52,53} The pyridocoline **1.24** was prepared in the previous work by Clemo *et al.* using Knoevenagel condensation of ethyl 2-pyridylacetate (**1.23**) with ethyl orthoformate (**Scheme 1.9**).¹¹ The same method was applied by Sorm *et al.* using methyl 2-pyridylacetate (**1.28**) as starting material. Condensation with ethyl orthoformate gave 4-oxo-3-(2'-pyridyl)-pyridocoline-1-methylcarboxylate (**1.29**). An alternative condensation of methyl 2-pyridylacetate (**1.28**) with formaldehyde, provided 2,4-di-(2'-pyridyl)-dimethylglutarate (**1.30**). Hydrogenation of pyridyl intermediates **1.29** or **1.30** using Adams's catalyst and subsequent heating of the products under vacuum generated crystalline compounds, after purification by column chromatography. Same conditions



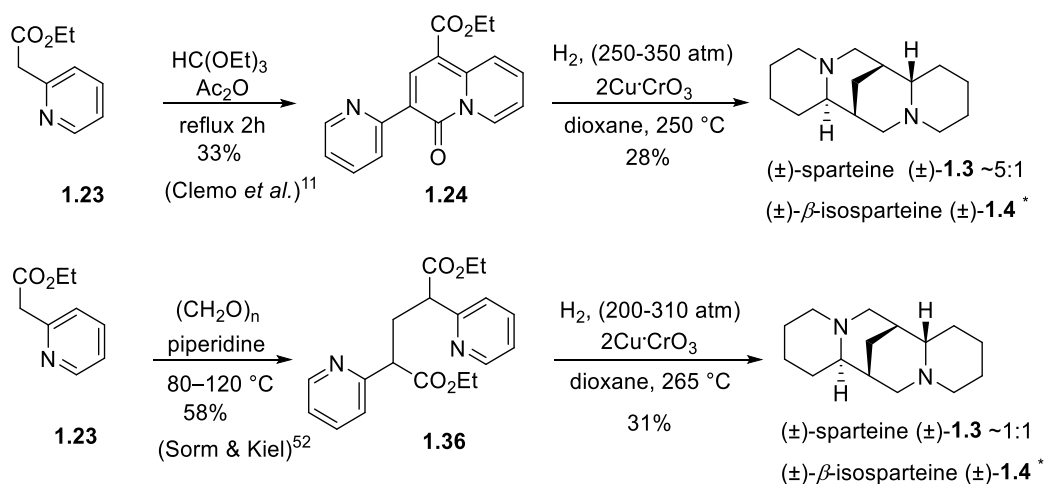
*Note that β-isosparteine was incorrectly reported as α-isosparteine in this work.

Scheme 1.11: Sorm & Keil's synthesis of (±)-sparteine & (±)-β-isosparteine (1948).

The first fraction of dioxosparteine isomers **1.31** were separated into (±)-dioxo-isosparteine (±)-**1.33** (m.p. 172 °C) and (±)-dioxosparteine (±)-**1.34** (m.p. 135 °C). Sorm and Keil reported (±)-α-Isosparteine (±)-**1.8** was the product after electrolytic reduction.⁵² However, (±)-dioxo-isosparteine (±)-**1.33** was shown later by Carmack *et al.* to be (±)-β-dioxo-isosparteine (±)-**1.4** (m.p. 172 °C) through repetition of this methodology. In the later work reduction of the dioxosparteine isomers was achieved using LiAlH₄ giving three sparteine diastereomers, which were identified by comparison with the literature.^{15,54,55} A second fraction was 4-oxo-3-(2'-piperidyl)-octahydropyridocoline-1-methylcarboxylate (**1.32**) m.p. 161 °C. Formation of uncyclised piperidyl **1.32** after catalytic hydrogenation is likely due to its *trans*-configuration between C3 and C5, therefore it is unable to cyclise. Electrolytic reduction of dioxosparteine isomerides using 50% sulphuric acid with activated lead electrodes gave three C₁₅H₂₆N₂ bases, isolated as their dipicrates (**1.3**, **1.4** and **1.35**). The dipicrates of m.p. 205 °C and 222 °C were identified as racemic (±)-sparteine ((±)-**1.3**) and (±)-β-isosparteine (±)-**1.4** respectively.

1.3.5 Leonard's synthesis of (\pm)-sparteine and (\pm)- β -isoparteine.

A closely related total synthesis of (\pm)-sparteine was published in 1948 by Leonard *et al.*⁵⁶ Leonard and co-workers developed synthesis of (\pm)-sparteine, from two different precursors.⁵⁷ (\pm)-Sparteine and (\pm)- β -isoparteine were synthesised as racemic mixtures in two linear steps (**Scheme 1.12**). The synthesis requires a one-step condensation and reductive cyclisation of either pyridyl intermediates, **1.24** or **1.36**, to furnish (\pm)-sparteine and (\pm)- β -isoparteine respectively. 1-Carboxy-4-keto-3-(2'-pyridyl)-pyridocoline (**1.24**) was prepared from condensation of ethyl pyridyl-2-acetate (**1.23**) with ethyl orthoformate in refluxing Ac_2O as reported above.

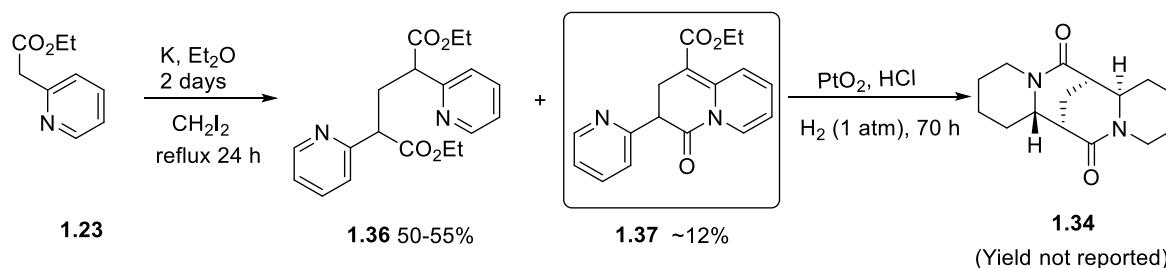


Scheme 1.12: Leonard's synthesis of (\pm)-sparteine and (\pm)- β -isoparteine.

Reductive cyclisation of **1.24** in dioxane at 250 °C and 250–350 atm of H_2 over copper chromite led to the formation of two bases: (\pm)-sparteine (\pm)-**1.3** and a compound identified as (\pm)- α -isoparteine (\pm)-**1.8**, present in a ratio of (\sim 5:1).⁵⁶ The identity of the samples was confirmed by comparison of the monoperochlorate and dipicrate salts which had been previously reported.⁵² However, in this work, (\pm)- α -isoparteine was reported by reference to Sorm and Kiel's isomer which was shown later to be (\pm)- β -isoparteine (not (\pm)- α -isoparteine). Using chemistry reported by Sorm *et al.* for the synthesis of dipyridyl dimethyl glutarate **1.30** (Scheme 1.11),⁵² dipyridyl ethyl glutarate **1.36** was synthesised. Reductive cyclisation of **1.36** in dioxane at 265 °C and 200–310 atm of H_2 over copper chromite catalyst led to the formation of an equimolar mixture of isomers: (\pm)-sparteine and (\pm)- β -isoparteine in a ratio of (\sim 1:1), which were separated chromatographically.⁵⁷ Resolution of racemic sparteine using either (+) or (–)- β -camphorsulfonic acid in EtOH, followed by recrystallisation from acetone, led to the isolation of either (+)-sparteine or (–)-sparteine.⁵⁸

1.3.6 Clemo, Raper, and Short's synthesis of (±)-dioxosparteine isomers

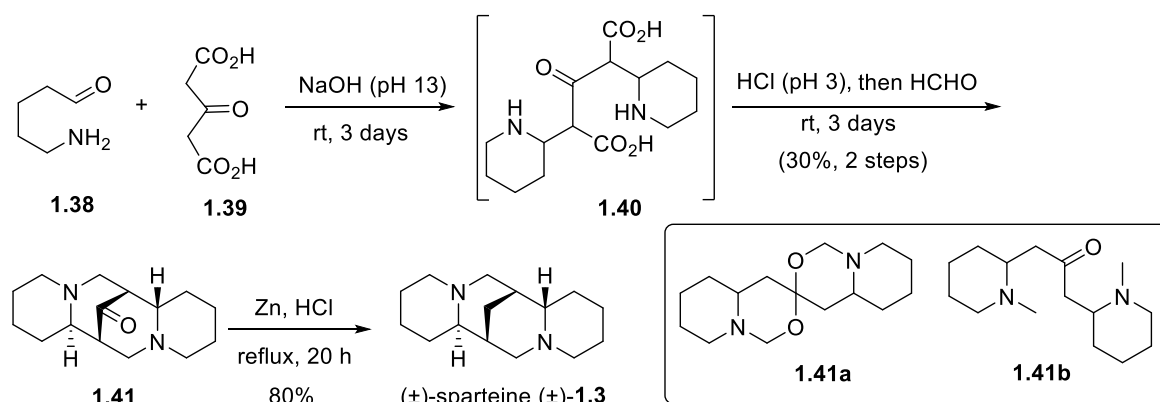
The synthesis of (±)-dioxosparteine isomer (**1.31**) was achieved by Clemo, Raper and Short⁵¹ in 1949 using a method subsequently adopted by Leonard⁵⁹ (**Scheme 1.13**).⁵¹ Condensation of ethyl 2-pyridylacetate (**1.23**) with methylene iodide in the presence of potassium metal gave two products: dihydropyridocoline **1.37** as a minor product in 12% and diethyl glutarate **1.36** as the major component in 50-55% yield.⁵¹ Dihydropyridocoline **1.37** was reduced with Adams's catalyst in HCl affording (±)-10,17-dioxosparteine ((±)-**1.34**) as previously described by Sorm and Keil.



Scheme 1.13: Clemo, Raper, and Short's synthesis of (±)-10,17-dioxosparteine isomer

1.3.7 Anet, Hughes, & Ritchie's synthesis of (±)-sparteine

A proposed biomimetic route to (±)-sparteine was reported by Anet, Hughes, and Ritchie in 1950 (**Scheme 1.14**).^{60,61} A dilute aqueous pH 13 solution of 5-aminopentanal (**1.38**) and acetone dicarboxylic acid (**1.39**) was allowed to stand for 3 days at rt to give dipiperidine glutaric acid derivative **1.40**. The solution of **1.40** was then acidified to pH 3 and was allowed to cyclise by adding formaldehyde to give (±)-8-oxo-sparteine ((±)-**1.41**).



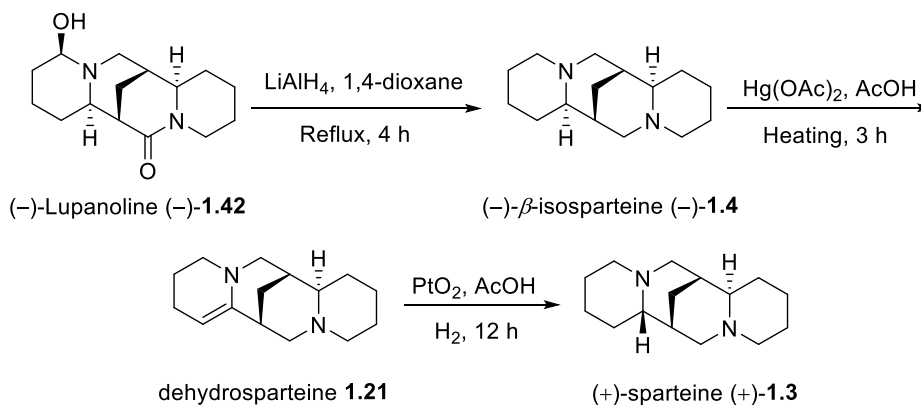
Scheme 1.14: Anet, Hughes, and Ritchie's synthesis of (±)-sparteine

Clemmensen reduction of (±)-8-oxo-sparteine ((±)-**1.41**) gave (±)-sparteine in high yield. Minor variations in pH were reported to give substantially lower yield, or none, of the ketone **1.41**. However, the synthetic (±)-sparteine obtained was identified only by a mixed melting point, and several years later the synthesis was questioned by Schöpf and co-workers.⁶² The Schöpf group

stated that the intermediate taken to be (\pm)-8-oxo-sparteine ((\pm)-**1.41**) was in fact acetal **1.41a**, with melting point 133 °C and a formula $C_{15}H_{26}N_2O_2$ consistent Anet's recorded data.⁶² The Clemmensen reduction of **1.41a** would lead to piperidyl propanone **1.41b** instead of (\pm)-sparteine. However, Schöpf *et al.* reported that (\pm)-**1.41** could be obtained from **1.41a** with acetic anhydride.⁶³

1.3.8 Moore and Marion semi-synthesis of (–)- β -isosparteine and (+)-sparteine

As a part of their work to investigate the relationship of sparteine alkaloids and proof of structures, Moore and co-workers investigated interconversion of alkaloid. (+)-Lupanoline ((+)-**1.42**) was described by Moore *et al.* in 1953,⁶⁴ which was previously isolated from the legume *Lupinus Sericeus*.⁶⁵ (+)-Lupanoline was identified as (+)-2-hydroxy-17-oxo- β -isosparteine ((+)-**1.42**) by analysis of the IR data and apparent inert character of the carbonyl. Elimination of (+)-2-hydroxy-17-oxo- β -isosparteine by treatment with mineral acid gave anhydrolupanoline, identifying the hydroxyl group to be at the α position to one of the nitrogen atoms of the ring. The semi-synthesis of (–)- β -isosparteine ((–)-**1.4**) was achieved by reduction of (+)-lupanoline using $LiAlH_4$ (Scheme 1.15). Dehydrogenation of (–)-**1.4** using mercuric acetate in acetic acid gave dehydrosparteine **1.21**. Initially, sparteine obtained by hydrogenation of **1.21** using Adam's catalyst and was identified as (–)-sparteine, but Marion later confirmed that the structure was (+)-sparteine ((+)-**1.3**).⁵⁴

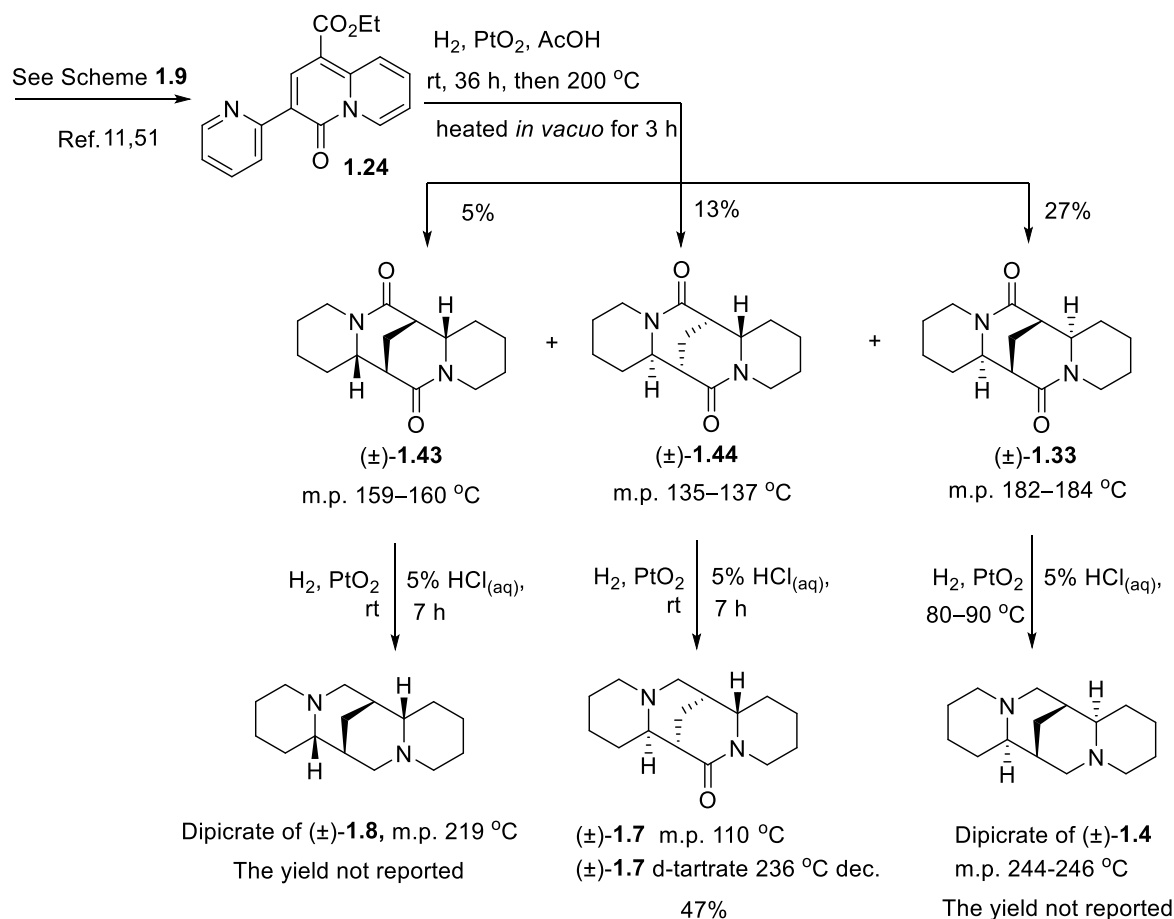


Scheme 1.15: Moore and Marion semi-synthesis of (–)- β -isosparteine and (+)-sparteine

1.3.9 Tsuda and Satoh's synthesis of three isomers of (\pm)-sparteine

In 1954, Tsuda and Satoh⁶⁶ repeated the synthesis of dioxo-sparteine according to the method of Clemo *et al.* and Galinovsky.^{11,51,67} Employing pyridocoline **1.24** as an intermediate to produce three isomers of (\pm)-10,17-dioxo-sparteine *via* catalytic reduction and then cyclisation (Scheme 1.16). The three (\pm)-10,17-dioxo-sparteine isomers were isolated by column chromatography through alumina and recrystallisation giving: (\pm)-10,17-dioxo- α -isosparteine ((\pm)-**1.43**), m.p. 159 – 160 °C, (\pm)-10,17-dioxosparteine ((\pm)-**1.44**), m.p. 135 – 137 °C and (\pm)-10,17-dioxo- β -isosparteine ((\pm)-

1.33), m.p. 182 – 184 °C). Reduction of (\pm)-**1.43** using platinum oxide as a catalyst in 5% HCl at rt yielded (\pm)- α -isosparteine ((\pm)-**1.8**) identified as the dipicrate salt, (m.p. 219 °C). Reduction of (\pm)-**1.44** using the same conditions provided (\pm)-17-oxosparteine ((\pm)-**1.7** m.p.109 – 111 °C). Treatment of (\pm)-**1.7** with a solution of D-tartaric acid gave oxosparteine tartrate (m.p. 236 °C (dec.)). (\pm)- β -Isosparteine ((\pm)-**1.4**) was obtained from (\pm)-dioxosparteine ((\pm)-**1.33**) using the same reagents with heating of the solution at 80 – 90 °C. The diastereoisomer (\pm)-**1.4** as its dipicrate salt gave a melting point of 244 – 246 °C was not consistent with the literatures data.⁵²

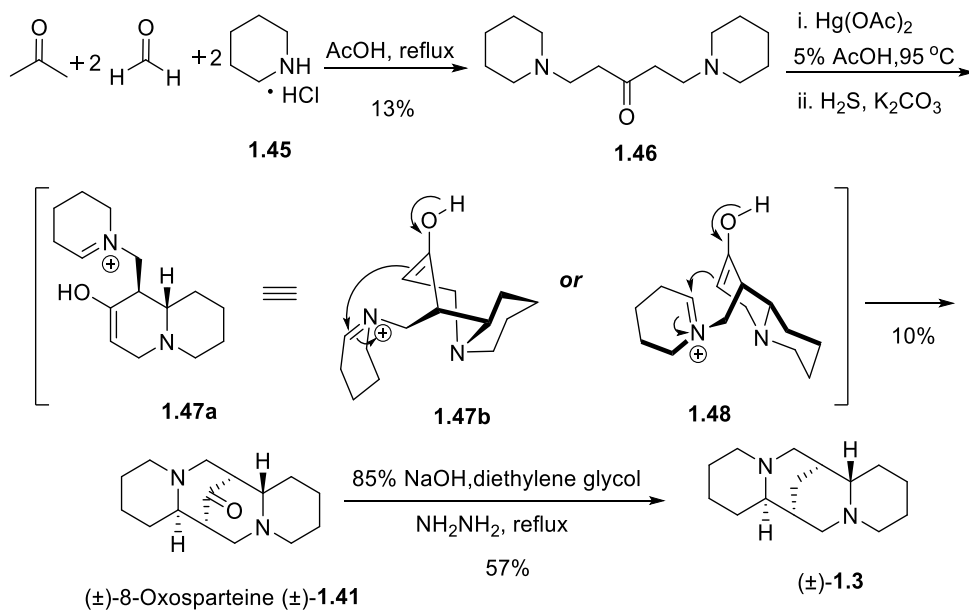


Scheme 1.16: Tsuda and Satoh's synthesis of three sparteine diastereoisomers

1.3.10 Van Tamelen and Foltz biogenetic synthesis of (\pm)-sparteine

A biogenic total synthesis of (\pm)-sparteine (\pm)-**1.3** was achieved by Van Tamelen *et al.* in 1960,⁶⁸ with full details reported in 1969,⁶⁹ using a Mannich type cyclisation as a key step (**Scheme 1.17**). Condensation of piperidine hydrochloride (**1.45**), formaldehyde and acetone in AcOH gave the bispiperidine **1.46** *via* a symmetrical bis-Mannich reaction in 13% yield. The activated diiminium ketone intermediate was established by treatment of the free base **1.46** with an excess of $\text{Hg}(\text{OAc})_2$ in 5% AcOH, giving the less stable intermediate **1.47b**. The more stable conformation **1.47a** yielded (\pm)-8-oxosparteine (\pm)-**1.41**. Alternatively, cyclisation from the epimer **1.48** provided racemic

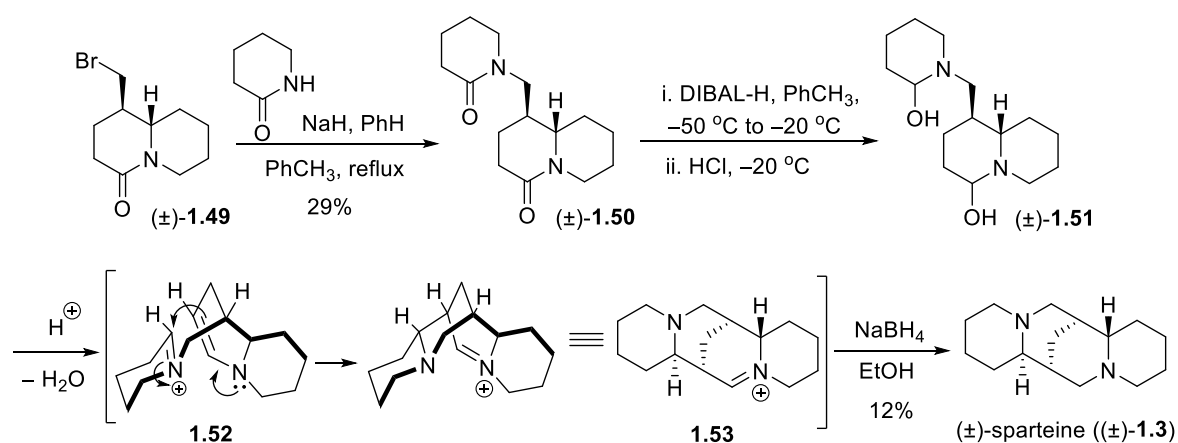
oxosparteine (\pm)-**1.41**. Reduction of ketone (\pm)-**1.41** using modified Wolf-Kishner reduction led to (\pm)-sparteine in 6% yield from **1.46**. The identity of the product was confirmed by comparison of the monoperchlorate and dipicrate salt reported previously by Leonard.⁵⁷



Scheme 1.17: Van Tamelen and Foltz's biogenetic synthesis of (\pm)-sparteine (**3**) synthesis

1.3.11 Bohlmann's synthesis of (\pm)-sparteine

A related approach was reported by Bohlmann *et al.* in 1973 using lactam reduction and Mannich-type cyclisation as the key step (**Scheme 1.18**).⁷⁰ Piperidinone was deprotonated using NaH in benzene and alkylated with bromide (\pm)-**1.49** to afford bisamide (\pm)-**1.50** in 29 % yield.



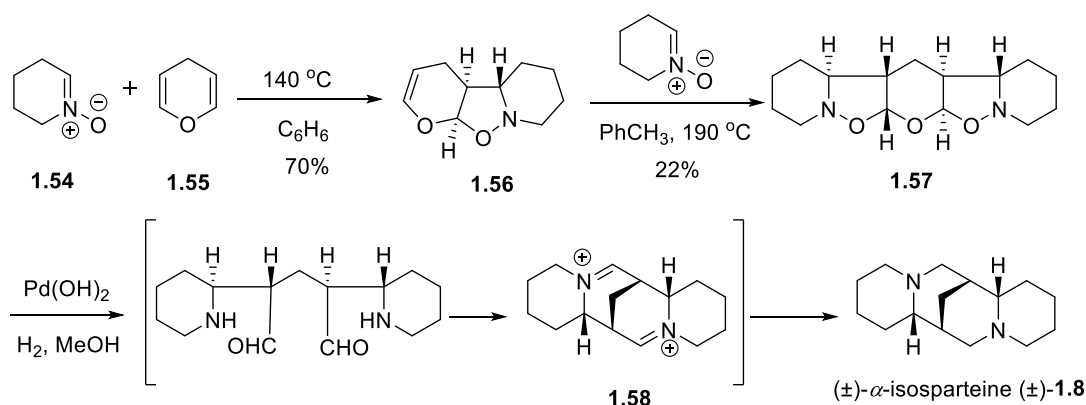
Scheme 1.18: Bohlmann's synthesis of (\pm)-sparteine

Reduction of (\pm)-**1.50** with DIBAL-H at -78°C afforded bis-hemiaminal (\pm)-**1.51**, which was dehydrated under acidic conditions. The intermediate **1.52** underwent intramolecular Mannich-type cyclisation to afford tetracyclic iminium **1.53**. The final reduction was achieved using NaBH_4 in

ethanol to access (\pm)-sparteine in low yield. No other stereoisomers were reported although the tetracycle was only isolated in very low yield from (\pm)-**1.50**.

1.3.12 Kakisawa's total synthesis of (\pm)- α -isopterine

In 1983, Kakisawa *et al.* established a diastereoselective synthesis of (\pm)- α -isopterine ((\pm)-**1.8**) using 1,3-dipolar cycloadditions as key steps (**Scheme 1.19**).^{71,72} Cycloaddition of nitron **1.54** and 4*H*-pyran (**1.55**) in refluxing benzene proceeded with the formation of adduct **1.56** in 70% yield with high regio- and stereoselectivity. A second cycloaddition reaction between **1.56** and nitron **1.54** secured **1.57** in 22% yield as 2:1 mixture of isomers. Catalytic hydrogenation of **1.57** over Pd(OH)₂ in MeOH provided tetracyclic diiminium cation **1.58**, which was subsequently reduced to give (\pm)- α -isopterine (\pm)-**1.8**. The identity of the sample was confirmed by comparison of physical and ¹H and ¹³C NMR data with an authentic sample of the natural product. The yield of the final step is not reported in the paper.

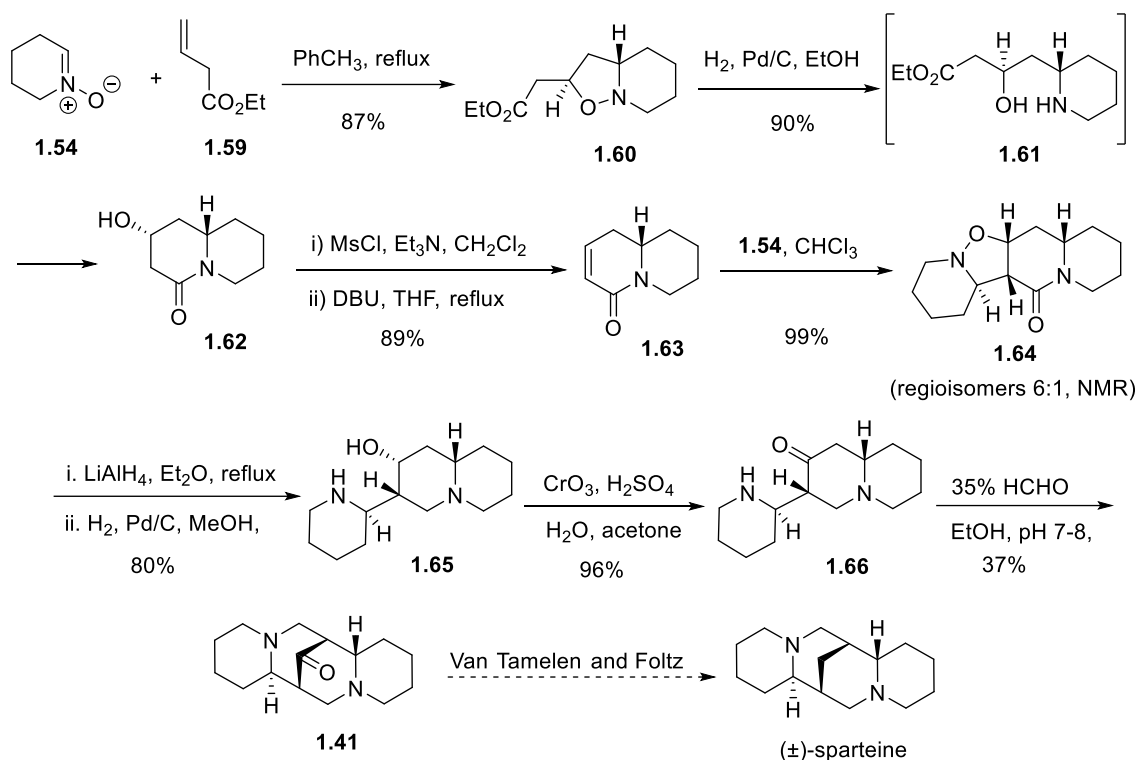


Scheme 1.19: Kakisawa's total synthesis of (\pm)- α -isopterine

1.3.13 Otomasu's formal synthesis of (\pm)-sparteine

Formal synthesis of (\pm)-sparteine was published by Otomasu *et al.* in 1987, also using a 1,3-dipolar cycloaddition as the key step in the synthesis (**Scheme 1.20**).^{73,74} Employing chemistry reported by Tufariello,⁷⁵ 1,3-dipolar cycloaddition reaction of 1-pyrrolidine nitron (**1.54**) and ethyl 3-butenoate (**1.59**) in refluxing toluene provided *exo*-adduct **1.60** as a single racemic diastereoisomer. Hydrogenation of **1.60** in EtOH over Pd/C caused a reductive N–O bond cleavage to produce intermediate **1.61**, which subsequently cyclised to bicyclic hydroxy amide **1.62** as a single isomer in 90% yield. Dehydration of hydroxy amide **1.62** by mesylation and elimination of the mesylate intermediate using DBU generated bicyclic enamide **1.63** in excellent yield. A second 1,3-dipolar cycloaddition reaction of nitron **1.54** and enamide **1.63** gave tetracycle **1.64**. An inseparable mixture of regioisomers was reported in ratio of approximately 6:1 due to the *exo*-addition of

nitron **1.54** from both sides of enone **1.63**. Reduction of the lactam **1.64** was completed with LiAlH_4 and the formation of (\pm)-2-hydroxyleontiformidine (**1.65**) by hydrogenolysis in MeOH over Pd/C. Oxidation of amino alcohol **1.65** using chromic acid generated amino ketone **1.66**. Mannich reaction of (\pm)-2-oxoleontiformidine (**1.66**) with formaldehyde generated (\pm)-8-oxosparteine (**1.41**) in 37% yield. Reduction of **1.41** to (\pm)-sparteine had previously been reported by Van Tamelen and Foltz (See Scheme 1.17).⁶⁸

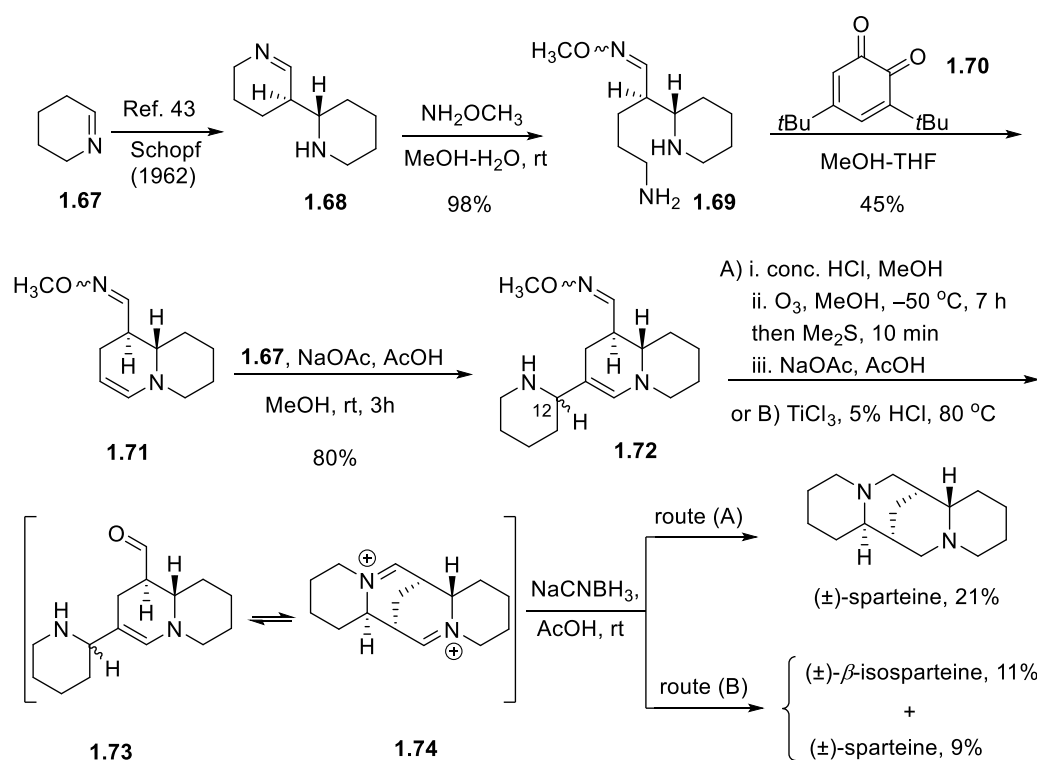


Scheme 1.20: Otomasu's synthesis of (\pm)-sparteine

1.3.14 Koomen's synthesis of (\pm)-sparteine and (\pm)- β -isosparteine

A biomimetic total synthesis of (\pm)-sparteine was reported in 1996 by Koomen *et al.* (Scheme 1.21).⁷⁶ Dipiperidine **1.68** was prepared using chemistry reported by Schöpf, starting from a dehydropiperidine **1.67** trimer.⁷⁷ (\pm)-*trans*-Tetrahydroanabasine (**1.68**) was ring-opened in the presence of methoxyamine in aq. MeOH to afford *O*-methoxyoxime **1.69** as a mixture of *cis/trans* isomers. Quinone derivative **1.70** was used to oxidise oxime **1.69** to the dehydroquinolizidine **1.71**. Condensation of enamine **1.71** with α -tripiperidine monomer (**1.67**), which was prepared *in situ* from trimer in buffered methanol, provided 3-piperidylquinolizidine **1.72** as a 1:1 mixture of epimers at C12.⁷⁸ The synthesis of sparteine followed two approaches (A) and (B). Firstly, oxidative

removal of the oxime **1.72** with ozone under acidic conditions progressed very slowly to obtain **1.73**, which subsequently gave the ring closed diiminium salt **1.74**. Reduction of the diiminium salt **1.74** with NaCNBH₃ gave (±)-sparteine in 21% yield. The second approach employed TiCl₃ in aq. HCl to achieve hydrolysis of oxime **1.72** followed by cyclisation, and finally reduction with NaCNBH₃ furnished a mixture of (±)-sparteine and (±)-β-isosparteine in 9% and 11% yields respectively. It is not clear why the second approach afforded β-isosparteine when none was isolated from the first route. The overall yield of (±)-sparteine over 7 steps (route A) was 7% from **1.68**, while route B gave (±)-sparteine and (±)-β-isosparteine over 5 steps in 3% and 4% yields respectively.

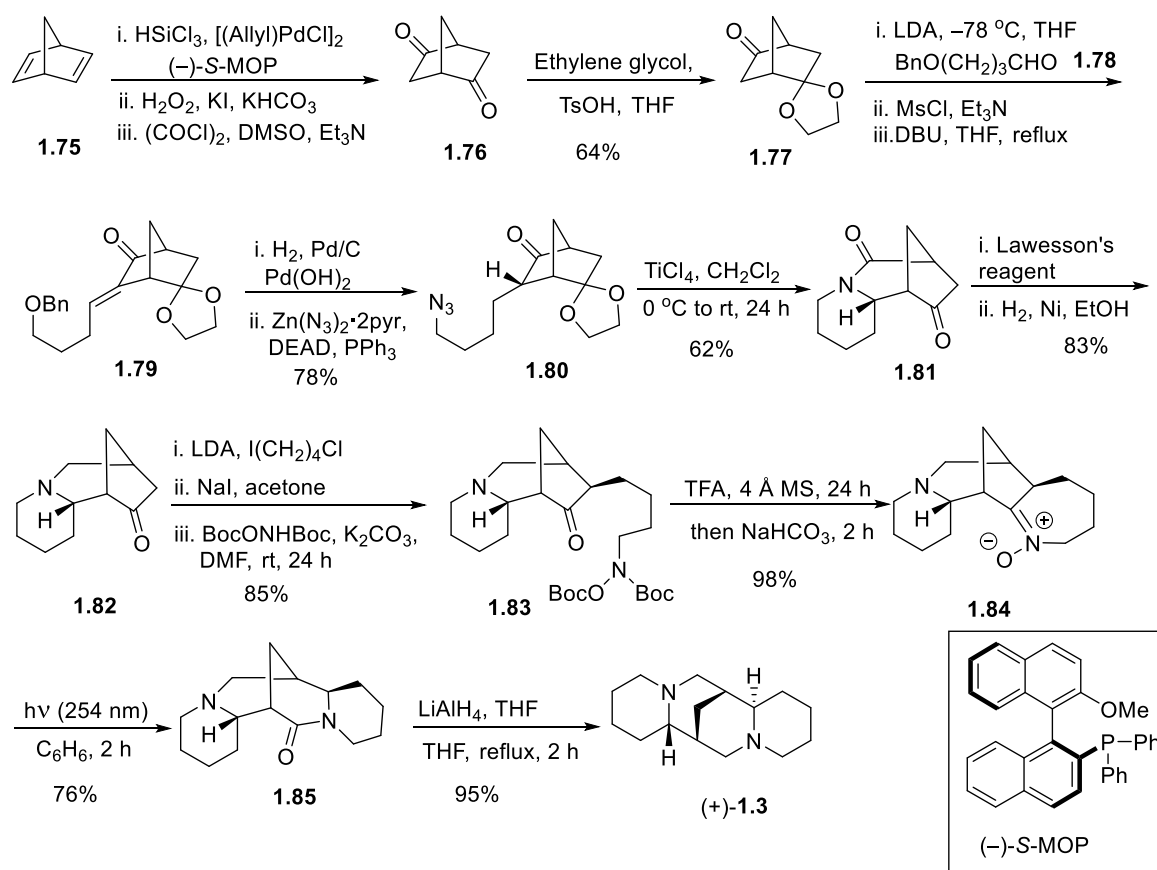


Scheme 1.21: Koomen's synthesis of (±)-sparteine and (±)-β-isosparteine

1.3.15 Aube's synthesis of (+)-sparteine

The first asymmetric total synthesis of optically pure (+)-sparteine ((+)-**1.3**) was reported by Aube *et al.* in 2002 (**Scheme 1.22**).⁷⁹ (+)-Sparteine was synthesised from 2,5-norbornadiene (**1.75**) which was converted to a diol with high enantio- and regio-selectivity using chemistry reported by Hayashi,⁸⁰ followed by Swern oxidation to form C2 symmetrical ketone **1.76**.⁸¹ Protection of diketone **1.76** as the mono acetal **1.77**, and then treatment with LDA at -78 °C followed by slow addition of aldehyde **1.78** yielded the aldol condensation product **1.79** after mesylation and

elimination. The benzyl protecting group was removed at the same time as hydrogenation of the *exo* face of the olefin, and the formation of the azide **1.80** was completed using a modified Mitsunobu azidation. An intramolecular Schmidt ring expansion of intermediate **1.80** with TiCl_4 furnished the functionalised lactam **1.81** as a single isomer.⁸² The thioamide of **1.81** was prepared using Lawesson's reagent, then hydrogenation over Raney-Ni accessed the desired quinolizidine **1.82**. Deprotonation of quinolizidine **1.82** using LDA at -78°C , chloroalkylation and subsequent BocONHBoc displacement afforded hydroxylamine derivative **1.83**. *N*-Boc deprotection using TFA and condensation gave tetracyclic nitron **1.84**. Photo-Beckmann rearrangement of **1.84** in benzene provided 10-oxosparteine (**1.85**).⁸³ The synthesis of (+)-sparteine ((+)-**1.3**) was completed by reduction of lactam **1.85** using LiAlH_4 in 95% yield. The overall synthetic route involved 15 steps and was achieved in 15.7% yield.

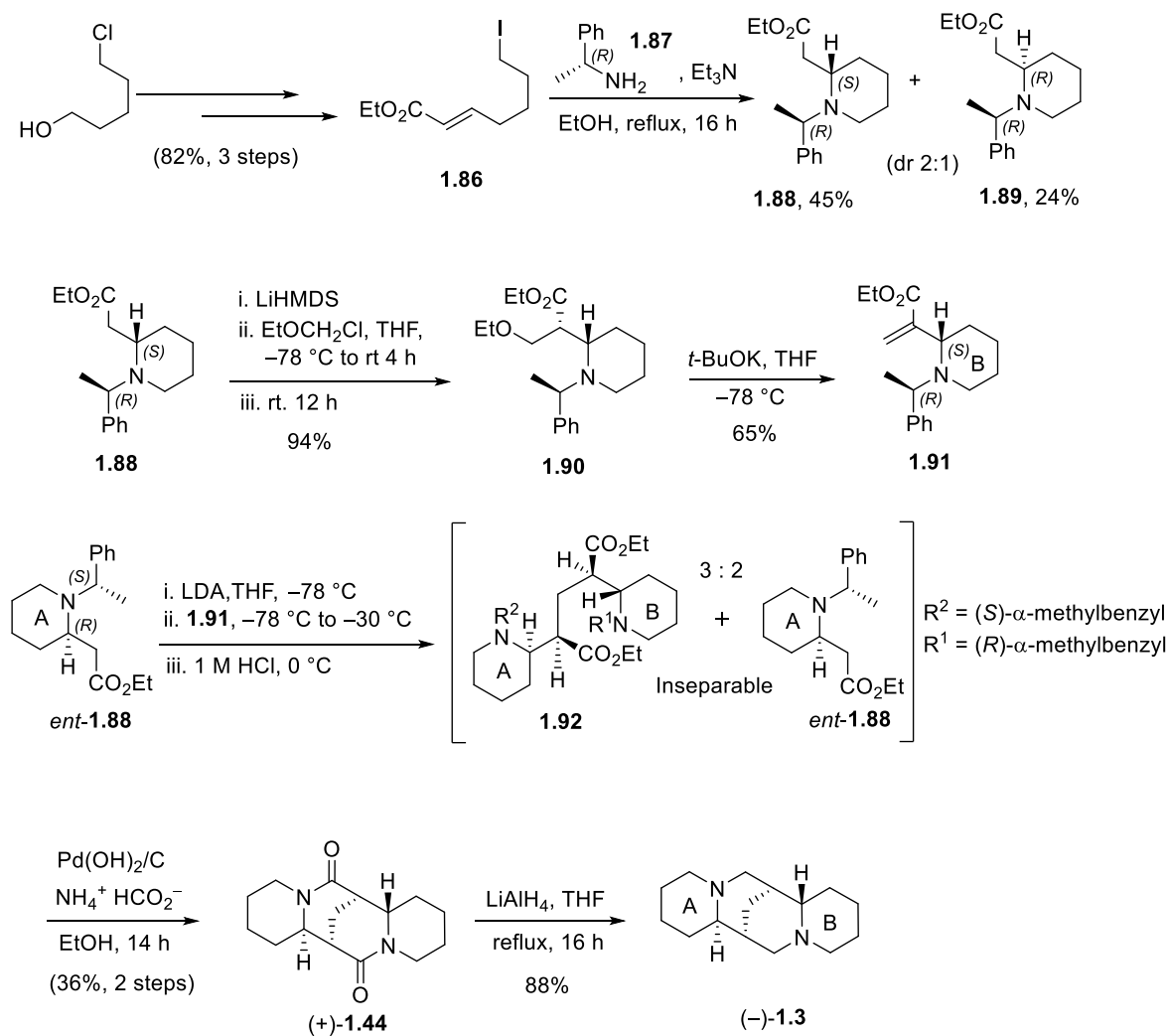


Scheme 1.22: Aube's synthesis of (+)-sparteine ((+)-**1.3**)

1.3.16 O'Brien's synthesis of (-)-sparteine

The first total synthesis of optically pure (-)-sparteine ((-)-**3**) was reported by O'Brien *et al.* in 2004 (**Scheme 1.23**).⁸⁴ Using chemistry reported by Hense,⁸⁵ ethyl-7-iodohept-2-enoate (**1.86**) was prepared in 82% yield over three steps from 5-chloropentanol. Alkylation of iodide **1.86** with (*R*)- α -methylbenzylamine **1.87** in refluxing EtOH and subsequent intramolecular Michael addition of the

amine furnished piperidine **1.88** and **1.89** as a mixture of diastereoisomer (2:1). Despite the poor selectivity in the conjugate addition, the mixture was readily separable and the major isomer **1.88** was accessed in gram quantities. Treatment of **1.88** with LiHMDS at $-78\text{ }^{\circ}\text{C}$ followed by enolate addition to EtOCH₂Cl accessed the functionalised piperidine **1.90** as a single isomer. Elimination of ethoxide from **1.90** was accomplished using a modified procedure reported by Sworin and Lin to secure the Michael acceptor **1.91**.⁸⁶

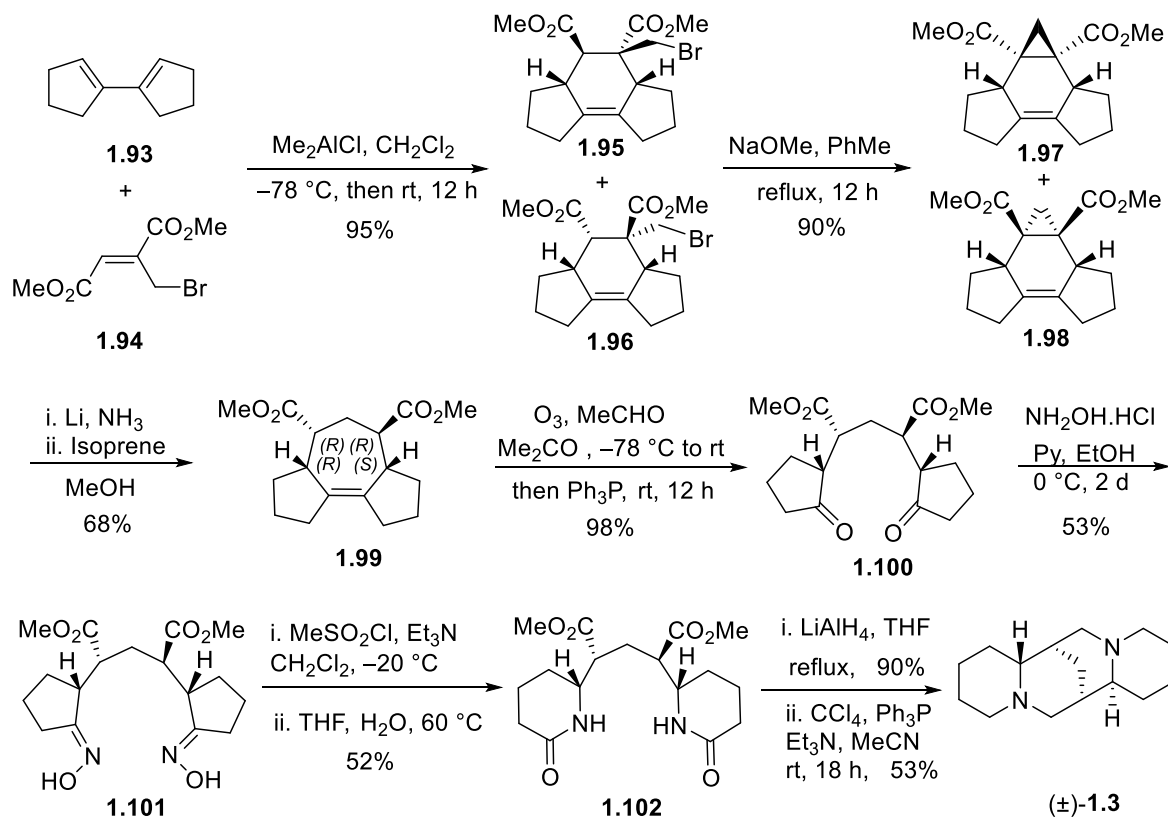


Scheme 1.23: O'Brien's synthesis of (–)-sparteine (–)-**1.3**

Deprotonation of *ent*-**1.88** at $-78\text{ }^{\circ}\text{C}$ using LDA and subsequent enolate addition to α, β -unsaturated amino ester **1.91** led to the formation of the bispiperidine **1.92**. Disappointingly, no pure sample could be isolated. As a result, an inseparable mixture of **1.92** and *ent*-**1.88** was submitted to transfer hydrogenation over Pd(OH)₂/C (Pearlman's catalyst) to furnish (+)-10,17-dioxosparteine (+)-**1.44** after removal of the α -methylbenzyl ether protecting group and cyclisation of the free amine. Final reduction of bislactam (+)-**1.44** with LiAlH₄ afforded (–)-sparteine (–)-**1.3**. Overall, the O'Brien group synthesis involved 6 steps from enoate **1.86** and was achieved in 9% yield.

1.3.17 Buttler and Fleming's synthesis of (±)-sparteine

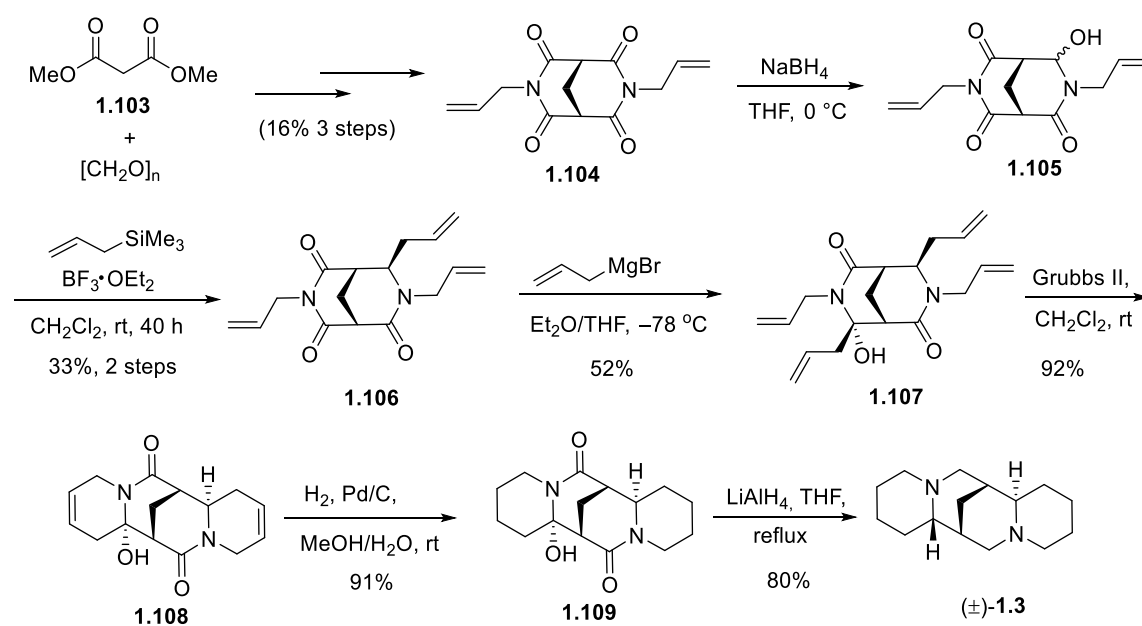
In 2005, Fleming and co-workers reported a synthesis of racemic (±)-sparteine ((±)-**1.3**) using a Diels-Alder reaction and a Beckman rearrangement as key steps (**Scheme 1.24**).^{87,88} Diels-Alder cycloaddition between diene **1.93** and Z-diester **1.94** gave a mixture of bromides **1.95** and **1.96** in a ratio of 3:1. Treatment of these intermediates with NaOMe in refluxing toluene afforded a mixture of cyclopropanes **1.97** and **1.98** in the same ratio. Reductive ring expansion of the mixture of cyclopropanes **1.97** and **1.98** with lithium in ammonia established a 68% yield of the *dissymmetric* *R,R,R,S*-diastereomer **1.99** and 21% of the corresponding *meso-R,S,R,S*-diastereomer. In theory, from protonation of the enolates, three possible diastereomers could be formed, and quenching with methanol was important for selective to formation of the *dissymmetric* diastereomer **1.99**. Biscyclopentanone **1.100** was obtained from the oxidative cleavage of alkene **1.99** with ozone in acetone at $-78\text{ }^{\circ}\text{C}$, which was optimized to prevent epimerization of intermediate ketone oxide by the addition of acetaldehyde. Bisoxime **1.101** obtained by treatment of **1.100** with hydroxylamine followed by Beckmann rearrangement to provide bislactam diester **1.102** in 52% yield over two steps. Reduction of bislactam diester **1.102** using LiAlH_4 afforded the corresponding bispiperidine diol which on cyclisation, *via* Appel reaction, furnished racemic sparteine. Overall, the synthesis was achieved in 8% yield and 9 steps from **1.93** & **1.94**.



Scheme 1.24: Butler & Fleming's synthesis of (±)-sparteine

1.3.18 Blakemore's synthesis of (\pm)-sparteine, (\pm)- α -isoparteine and (\pm)- β -isoparteine

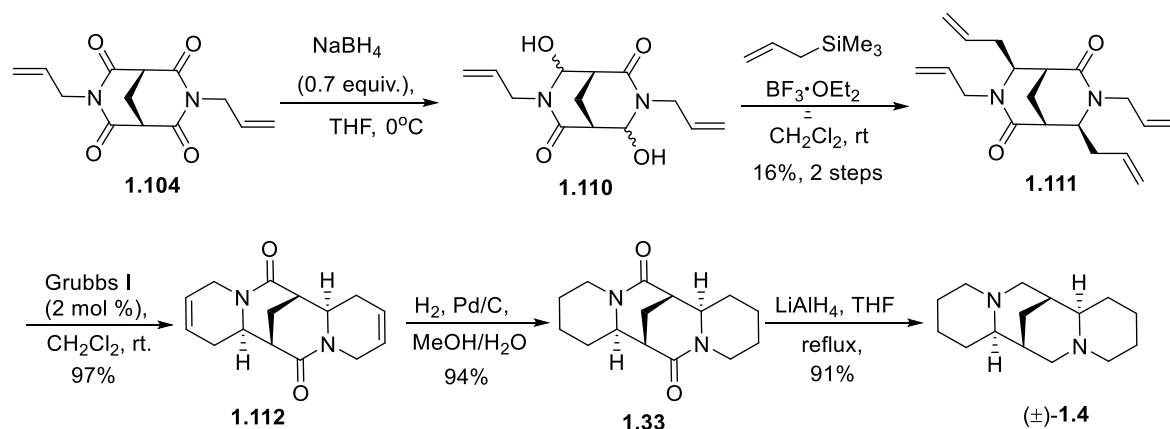
In 2008, Blakemore and co-workers developed a general strategy to access any of the three racemic sparteine diastereoisomers from a common tetraoxobispidine intermediate **1.104** (Scheme 1.25).^{55,89,90} Tetraoxobispidine **1.104** (obtained in 16% over three steps from dimethyl malonate **1.103** and paraformaldehyde),⁹⁰ was treated with NaBH₄ in THF to give hydroxylactam **1.105**. Using chemistry reported by Sakurai, the crude aminol **1.105** was alkylated with allyltrimethylsilane in the presence of BF₃•OEt₂, subsequent addition of the nucleophile afforded imidolactam **1.106** in 33% yield over two steps. The treatment of **1.106** with allylmagnesium bromide gave the functionalised pseudo-C2-symmetrical amide **1.107** as a single stereoisomer. Double RCM of **1.107** using Grubbs II afforded the tetracyclic diene **1.108** in 92% yield. Tetracyclic amide **1.109** was formed from hydrogenation of diene **1.108** over Pd/C, and reduction of bisamide **1.109** using LiAlH₄ completed the synthesis of (\pm)-sparteine in 6 steps and 12% yield from tetraoxobispidine **1.104**. The stereochemistry of **1.109** was confirmed by single crystal X-ray crystallography.



Scheme 1.25: Blakemore's synthesis of (\pm)-sparteine ((\pm)-**1.3**)

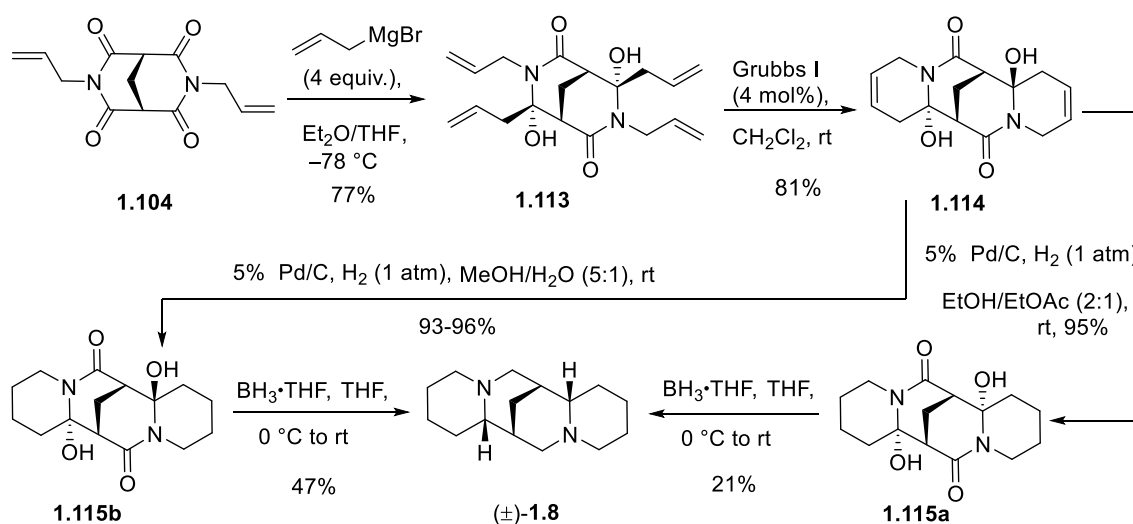
A similar approach was used for the stereocontrolled synthesis of (\pm)- β -isoparteine (Scheme 1.26),⁵⁵ again from tetraoxobispidine **1.104** as a key intermediate. Reduction of bispidine **1.104** using NaBH₄ gave the bishydroxylactam **1.110**. It is noteworthy that reduction of **1.104** using NaBH₄ showed a marked improvement in 16% overall yield in 2 steps instead of using LiBHET₃. Double Sakurai-type allylation of **1.110** using allyltrimethylsilane with BF₃•OEt₂ formed tetraene **1.111** in 16% yield over two steps. Double RCM of tetraene **1.111** using Grubbs I provided tetracyclic diene **1.112** in 97% yield, and hydrogenation of diene **1.112** over Pd/C afforded (\pm)-10,17-dioxo- β -

isosparteine, which was reduced to complete the synthesis of (\pm)- β -isosparteine. The total synthesis was achieved in 13% in 5 steps from **1.104**.



Scheme 1.26: Blakemore's synthesis of (\pm)- β -isosparteine (\pm)-**1.4**

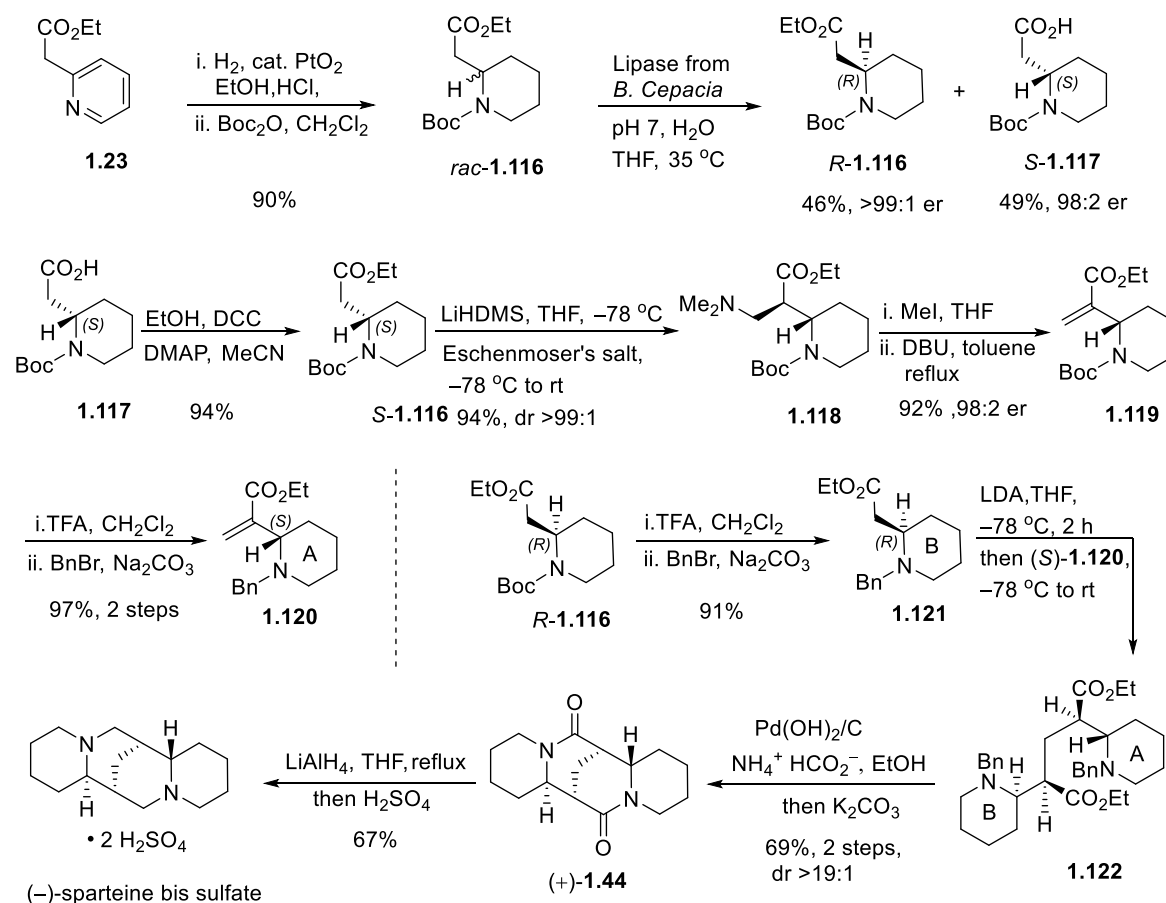
The reverse addition order of the allyl and hydride groups were used to obtain (\pm)- α -isosparteine ((\pm)-**1.8**) (**Scheme 1.27**), where double allylation of tetraoxobispidine **1.104** first formed bishydroxylactam **1.113**. Grubbs I was used to achieve double RCM of **1.113** to yield the tetracyclic diene **1.114** in 81%. Hydrogenation of **1.114** over of Pd/C in (EtOH/EtOAc, 2:1) furnished the symmetric bis-hemiaminal **1.115a** in 21% yield while the hydrogenation in a more polar solvent mixture (MeOH/H₂O, 5:1) gave the nonsymmetric bis-hemiaminal **1.115b** as a single isomer in 93-96% yield. Reduction of the symmetric and nonsymmetric bis-hemiaminals was achieved in a stereocontrolled manner using a large excess of BH₃ to give (\pm)- α -isosparteine.⁹⁰ Overall, the synthesis was achieved in 28% yield and 4 steps from tetraoxobispidine **1.104**.



Scheme 1.27: Blakemore's synthesis of (\pm)- α -isosparteine ((\pm)-**1.8**)

1.3.19 O'Brien's synthesis of (-)-sparteine bis-sulfate

A synthesis of (-)-sparteine was published early 2018 by O'Brien *et al.* in using *B. cepacia* lipase to obtain enantiopure ester piperidine **R-1.116** as starting point (**Scheme 1.28**).⁹¹ Racemic ester (**rac-1.116**) was prepared by hydrogenation of pyridine and *N*-Boc protection by following previous method.^{92,93} Using chemistry reported by Pousset *et al.* in 2004,⁹⁴ enzymatic resolution of **rac-1.116** using lipase gave enantiopure ester piperidine **R-1.116** in 46% yield and chiral β -amino acid **1.117** in 49% yield. β -Amino acid **1.117** is the first fragment to access (-)-sparteine, which was esterified to obtain **S-1.116**. Enolisation of **S-1.116** using LiHMDS and reaction with Eschenmoser's salt gave methyl amine **1.118** as a single diastereoisomer. Methylation and elimination using MeI and DBU formed α,β -unsaturated ester **1.119** with no racemisation. Deprotection *N*-Boc of **1.119** and then benzyl protection gave **1.120** in 97% over 2 steps.



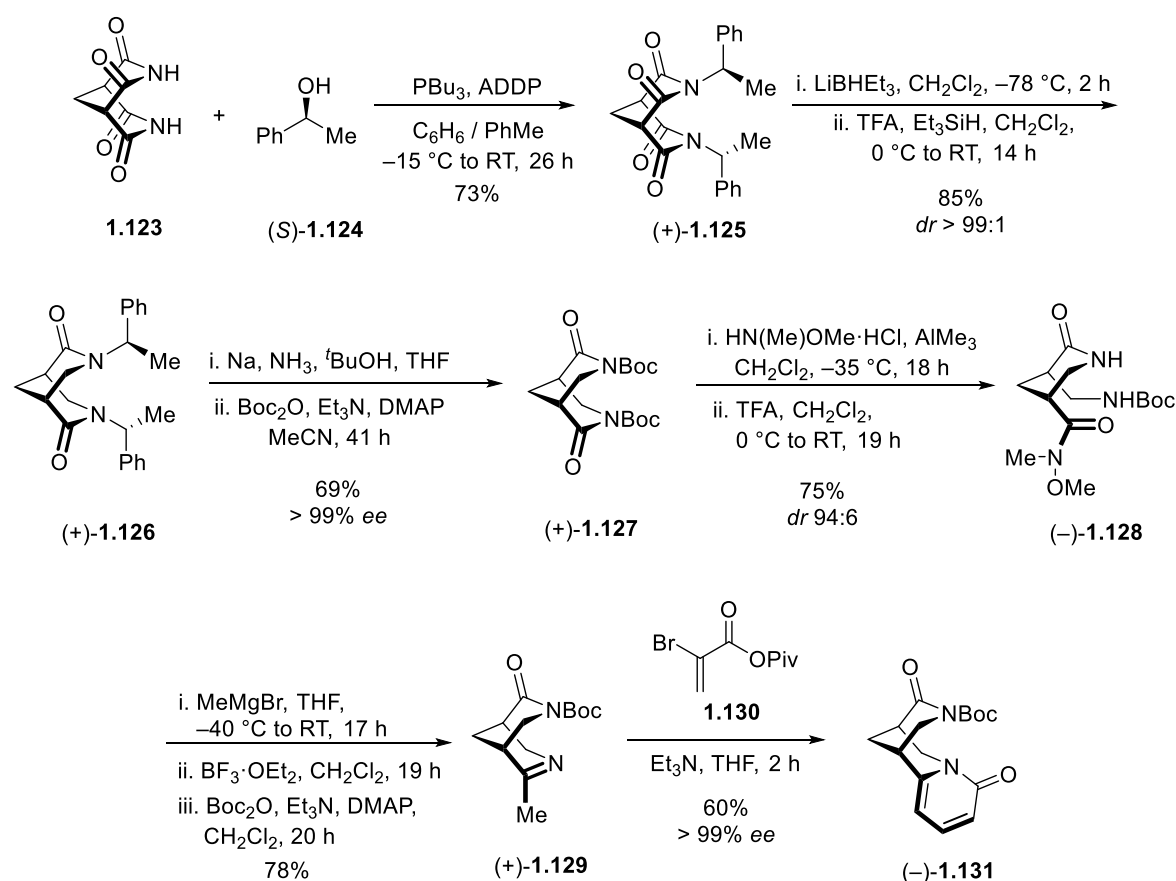
Scheme 1.28: O'Brien's synthesis of (-)-sparteine bis-sulfate

The second fragment is **R-1.116** which was also deprotected and re-protected using a benzyl group under the previously described conditions giving **1.121**. Deprotonation of ester **1.121** using LDA followed by addition of α,β -unsaturated ester **1.120** produced **1.122**. Transfer hydrogenation of **1.122** over $\text{Pd(OH)}_2/\text{C}$ cleaved the *N*-benzyl protecting groups, and subsequently, cyclisation using K_2CO_3 provided (+)-10,17-dioxo-sparteine as a single diastereoisomer in 69% yield over 2 steps.

Finally, the synthesis of (-)-sparteine bis sulfate was completed by reduction of bis-lactam **1.44** in the presence of LiAlH_4 and then salt formation with H_2SO_4 in 67%. Overall, the synthesis was achieved in 31% yield over 10 steps, on a scale of one gram.

1.3.20 Breuning and co-workers synthesis of bisquinolizidine alkaloids

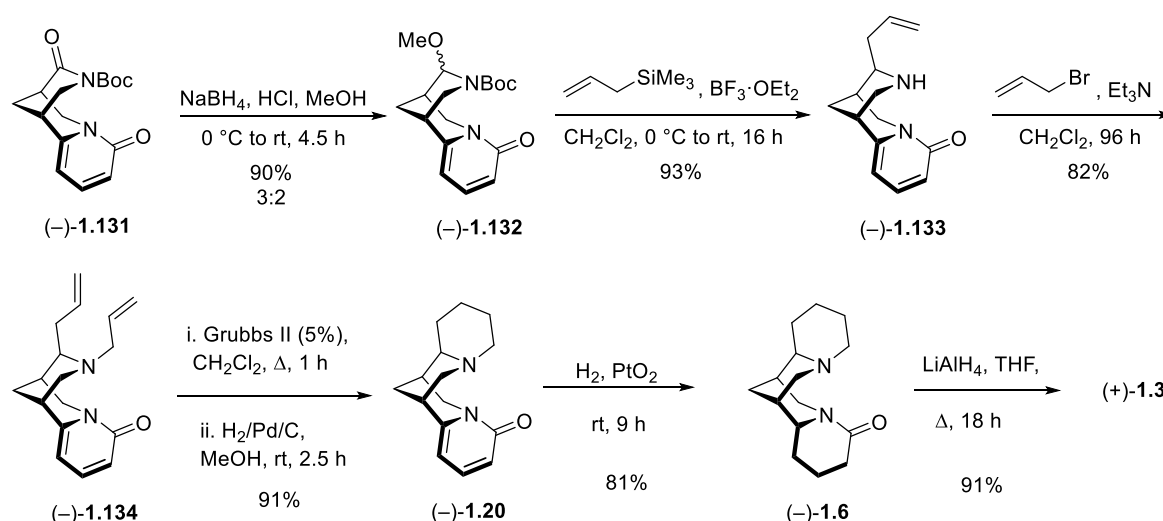
Breuning *et al.* published the asymmetric syntheses of 21 natural products in total in 2018 using bispidine **1.123** which was reported by Blakemore to build the tetracyclic cores of the sparteine isomers (**Scheme 1.25**).⁹⁵ Breuning succeeded in directly desymmetring achiral 2,4,6,8-tetraoxobisbidine **1.123** (**Scheme 1.29**). The bispidine **1.123** used by Blakemore as an excellent key starting point to an “inside out” route towards the core of the lupin alkaloids. Breuning attempted to desymmetrise this core.⁸⁹ With careful manipulation, this would allow the preparation of a key late-stage tricyclic intermediate that could be further functionalised to afford the desired alkaloids. The authors used Blakemore’s originally reported synthesis of **1.123**, which presumably suffered the same modest yields, but gave high throughput of material.⁹⁰



Scheme 1.29: Breuning’s desymmetrization of achiral bispidine **1.123**, and subsequent preparation of key intermediate **(-)-1.131**.

Deoxygenation one pair of enantiotopic carbonyls from achiral bispidine **1.123** began with a Mitsunobu-type reaction using (*S*)-phenyl ethanol ((*S*)-**1.124**) to give diimide (+)-**1.125**. Diastereoselective reduction of **1.125** using LiBHET₃ followed by treatment with TFA provided diamide (+)-**1.126** with excellent regio- and stereo-control. Removal of the chiral auxiliary using Birch conditions and subsequent Boc protection afforded the successfully desymmetrised dioxo-bispidine (+)-**1.127**. Selective modification of one of the amide groups was carried out by Lewis acid-catalysed ring opening with *N,O*-Dimethyl hydroxylamine. *N*-Boc removal of the resultant lactam furnished Weinreb amide (–)-**1.128**, with a slight loss in diastereoselectivity by epimerisation at the bridgehead positions. Grignard addition to the Weinreb amide (–)-**1.128** and subsequent reclosure of the amine *via* Boc deprotection and reprotection gave cyclic imine (+)-**1.129**. Michael addition to anhydride **1.130**, and elimination of HBr provided the key tricyclic bispidine (–)-**1.131**, the enantiomer of which was also prepared from **1.123** and (*R*)-**1.124**.

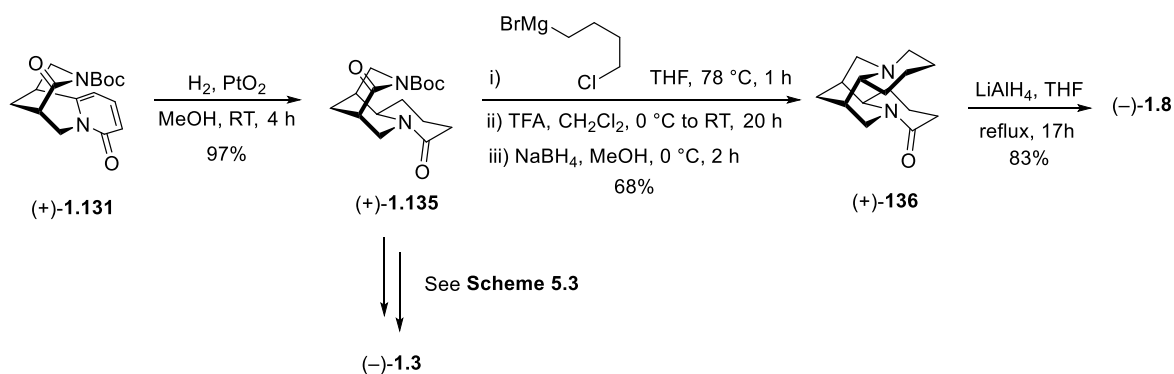
The synthesis of (+)-sparteine ((+)-**1.3**) was achieved using the key intermediate bispidine (–)-**1.131** (Scheme 1.30). Reduction of the imide functionality of (–)-**1.131** using NaBH₄ afforded *N,O*-acetal (–)-**1.132**, which was subjected to an *exo*-selective Sakurai allylation and simultaneous Boc deprotection to obtain alkene (–)-**1.133**. The free amine was allylated to provide diene (–)-**1.134**, which after RCM and hydrogenation afforded (–)-anagyryne ((–)-**1.20**) which was subsequently hydrogenated to (–)-lupanine ((–)-**1.6**), and finally reduced to ((+)-**1.3**). (–)-Sparteine ((–)-**1.3**) also obtained in this approach from (+)-**1.131**, with the exception that reduction of the pyridone moiety would occur at the start (Scheme 1.30).



Scheme 1.30: Breuning's total synthesis of (+)-**1.3** from tricyclic bispidine (–)-**1.131**

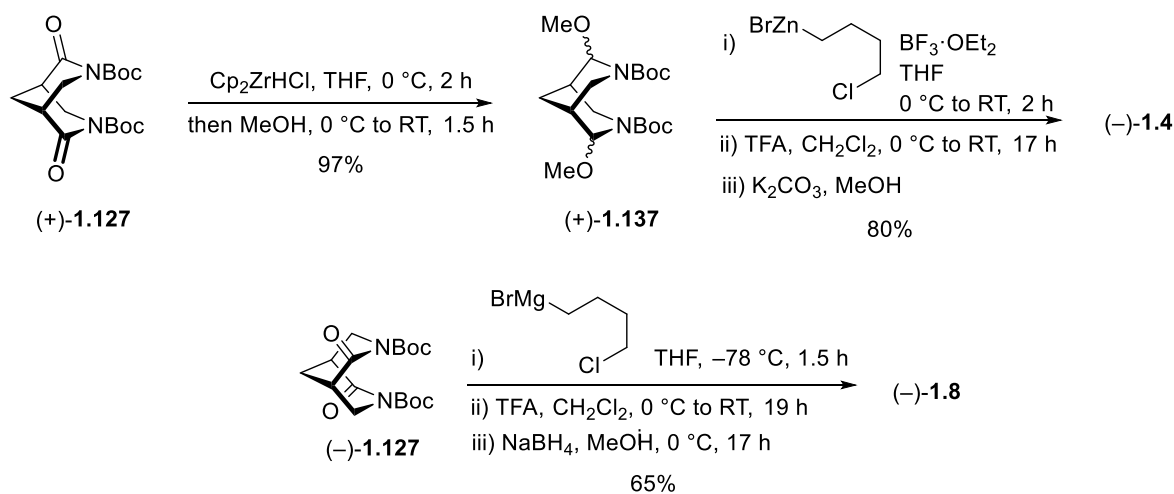
The synthesis of α -isoparteine ((–)-**1.8**) was accomplished by hydrogenation of imide (+)-**1.131** using H₂/PtO₂ to obtain piperidone (+)-**1.135** (Scheme 1.31). Treatment of (+)-**1.135** with 4-

chlorobutylmagnesium bromide, followed by *N*-deprotection and reductive amination afforded the *endo*-piperidone product (+)-isolupanine ((+)-**1.136**), which was converted into (–)- α -isosparteine ((–)-**1.8**) by LiAlH₄ reduction. The synthesis of (–)-**1.3** was obtained through *exo*-functionalisation by reduction of imide (+)-**1.135** to *N,O*-acetal, and then following the steps described earlier (Scheme 1.29).



Scheme 1.31: The total synthesis of (–)-**1.8** using of (+)-**1.131** by *endo*-annulation, and using *exo*-functionalisation to synthesise (–)-**1.3**

The ability to syntheses of (–)- β -isosparteine ((–)-**1.4**) and the (–)- α -isosparteine ((–)-**1.8**) from the *exo/endo* annulation strategies were applied using both antipodes of bispidine **1.127** (Scheme 1.32). Double reduction of the imides to bis-*N,O*-acetal (+)-**1.137** was effected by the use of Schwartz's reagent, which was found to be higher-yielding than other alternatives. Alkylation by Lewis acid assisted organozinc addition of the required alkyl chain, followed by cyclisation, subsequently delivered (–)-**1.4** by *exo* annulation. Double alkylation of (–)-**1.127** followed by *N*-deprotection and *endo* reduction as before completed a short route to (–)-**1.8**.



Scheme 1.32: Total syntheses of (–)-**1.4** and (–)-**1.8** following the *exo/endo* additions from enantiomeric bispidine precursors (+)- and (–)-**1.127**.

1.4 Matrine alkaloids

(+)-Matrine ((+)-**1.138**) was first isolated from the traditional medicinal herb *Sophora flavescens* by Nagai in 1889, and has been the subject of many studies due to its biological activities.⁹⁶ (+)-Allomatridine ((+)-**1.5**) is a tetracyclic lupin alkaloid of the matrine series, which can be obtained by the reduction of (+)-allomatrine ((+)-**1.139**) (**Figure 1.7**). (+)-Allomatrine has been reported as a chemical component from the *Sophora* species.⁹⁷⁻⁹⁹ It was found to have *anti*-nociceptive activity in mice through action at the opioid receptors,^{100,101} and also reported to possess antitumor activity *in vitro* and *in vivo*.¹⁰²

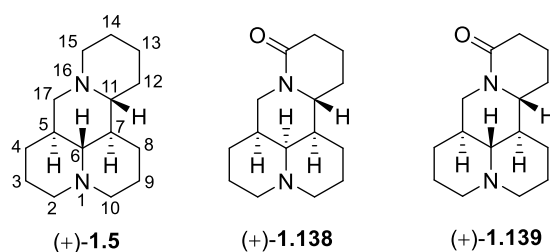


Figure 1.7: Structures of (+)-allomatridine ((+)-**1.5**), (+)-matrine ((+)-**1.138**) and (+)-allomatrine ((+)-**1.139**).

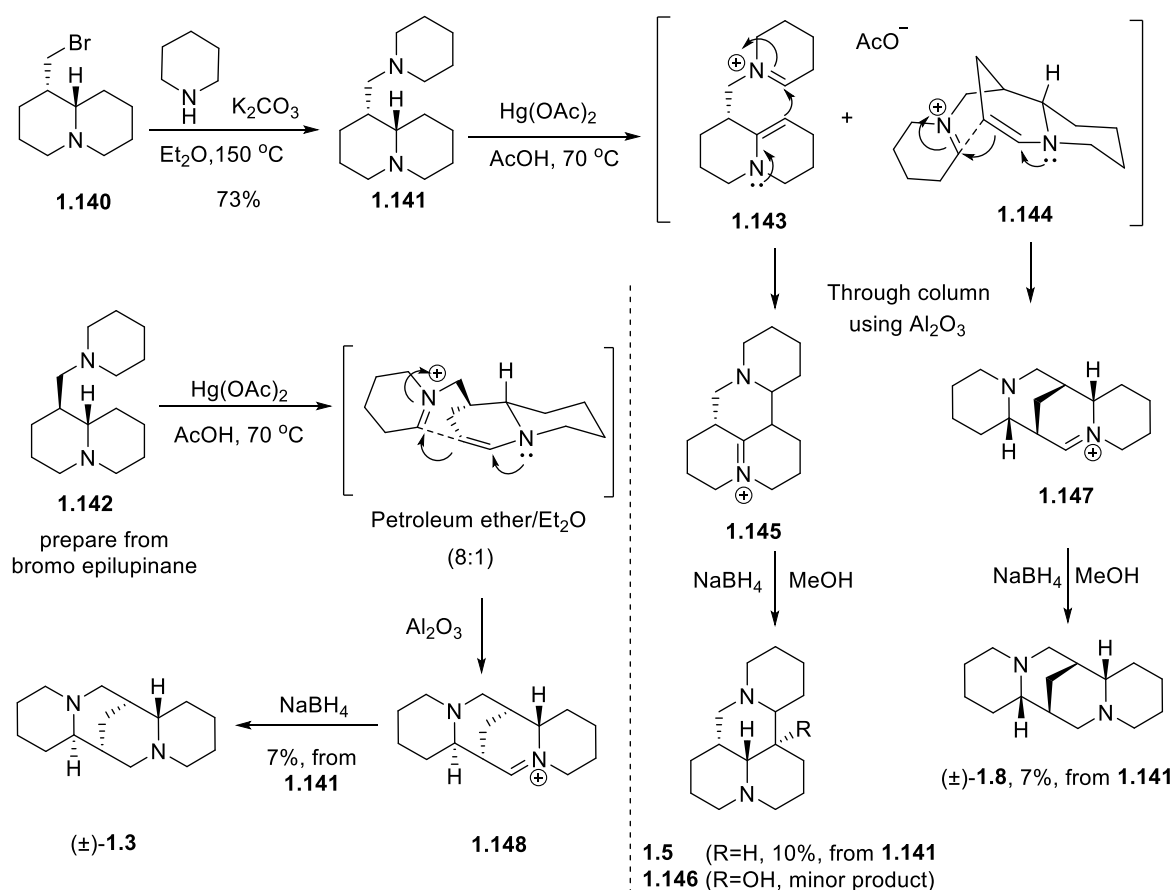
1.4.1 Previous total syntheses of matrine isomers

There have been several synthetic preparations of tetracyclic lupin alkaloids of the matrine structural series. The total synthesis approaches to this class of natural products and semi synthesis published have been documented below in chronological order of their publication in the literature.¹⁰³⁻¹⁰⁹ The target natural products were originally synthesised as mixtures of diastereoisomers and enantiomers with the first asymmetric total syntheses reported by Brown and co-workers.¹⁰⁹ The first preparation of (+)-allomatrine ((+)-**1.139**) was by epimerization of (+)-matrine ((+)-**1.138**) at C6.¹¹⁰ A semi synthesis detailed by Okuda¹⁰⁶ has been included in this brief overview as this publication details the first preparation of enantiomerically pure matrine and allomatrine *via* synthetic methods.

1.4.2 Bohlmann's "biogenetic" synthesis of (±)-allomatridine and other tetracyclic lupin alkaloids

The tetracyclic lupin alkaloids (±)-allomatridine ((±)-**1.5**), (±)- α -isosparteine ((±)-**1.8**) and (±)-sparteine ((±)-**1.3**) were prepared in 1963 by Bohlmann *et al.* using *N*-acyliminium ion cyclisation as a key step.¹⁰³ There are three routes to access the target compounds starting from bromo lupinine

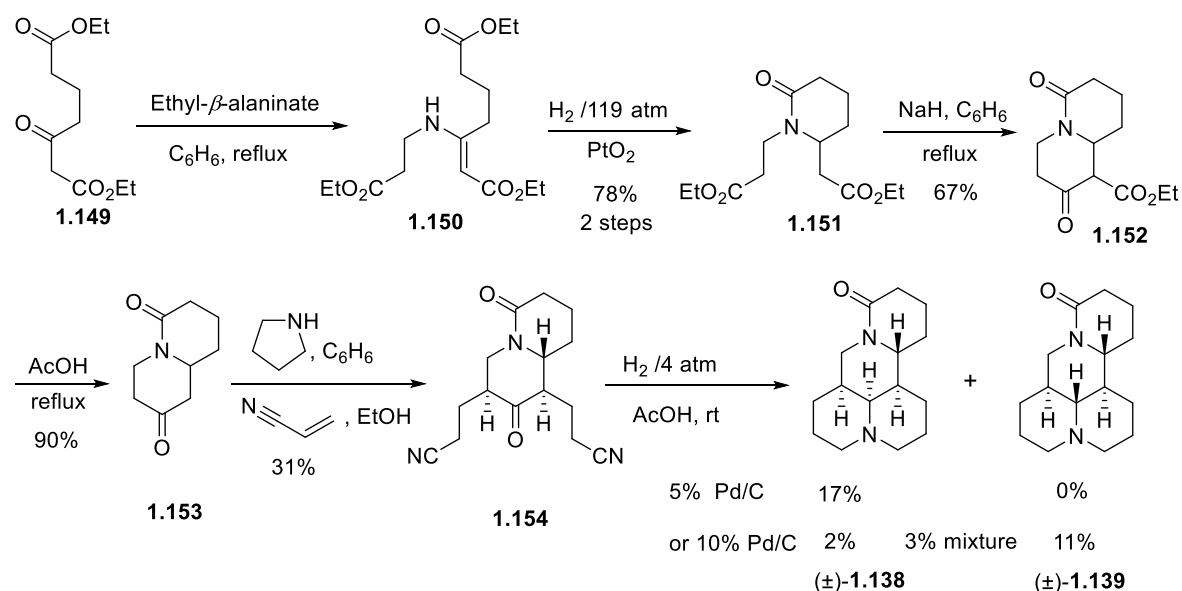
1.140 with piperidine in the presence of K_2CO_3 in Et_2O to produce piperidino-lupinine **1.141** (Scheme 1.33). The epimeric piperidino-epilupinine **1.142** was obtained analogously from bromo epilupinane. Dehydrogenation of piperidino-lupinine **1.141** in the presence of mercury acetate in acetic acid gave tricyclic diiminium cations **1.143** and **1.144**, which underwent a Mannich type cyclisation. The yield for this transformation was not reported. The iminium cation **1.145** was isolated through column chromatography on Al_2O_3 (eluent, petroleum ether: Et_2O , (1:1)). Subsequent reduction of **1.145** using sodium borohydride ($NaBH_4$) generated two tetracycles, (\pm)-allomatridine ((\pm)-**1.5**), and 5-hydroxy-allomatridine (**1.146**) as a minor component. While, using (eluent, Et_2O :MeOH, (10:1)), the iminium cation **1.147** was obtained by column chromatography on Al_2O_3 . Reduction of **1.147** using $NaBH_4$ gave (\pm)- α -isosparteine in 7% yield from **1.141**. (\pm)-Sparteine was obtained using the diastereoisomeric piperidino-epilupinine **1.142** as starting point followed by dehydrogenation and cyclisation using $Hg(OAc)_2$ and subsequent reduction of **1.148** using $NaBH_4$. The syntheses of (\pm)-allomatridine and (\pm)- α -isosparteine involved 3 steps each, which were achieved in 7% and 5% overall yields, respectively from **1.140**.



Scheme 1.33: Bohlmann's "biogenetic" syntheses of (\pm)-allomatridine and another tetracyclic lupin alkaloids

1.4.3 Mandell's total syntheses of (±)-matrine and (±)-allomatrine

Mandell *et al.* reported the first total synthesis of (±)-matrine ((±)-**1.138**) in 1963.¹⁰⁴ The same synthetic strategy was later reported in 1965 as a full paper including the synthesis of (±)-matrine and (±)-allomatrine ((±)-**1.139**) from a common intermediate **1.149** (Scheme 1.34).¹⁰⁵ Racemic mixtures of matrine and allomatrine were synthesised in 2.5% and 1.6% overall yield respectively in 6 linear steps from **1.149**. Condensation of ethyl β-alaninate with diethyl β-oxopimelate (**1.134**) in refluxing benzene afforded enamine **1.150**. Hydrogenation of the crude enamine **1.150** over Adam's catalyst led to formation of lactam **1.151** which was completed by heating on a steam bath. Dieckmann cyclisation using NaH led to the formation of quinolizidinedione **1.152**. Decarboxylation of ketoester **1.152** by refluxing in glacial AcOH produced 8-oxo-2-quinolizidone (**1.153**), which underwent double alkylation with acrylonitrile to give a mixture of the bis nitrile product **1.154**, along with the mono-addition product.

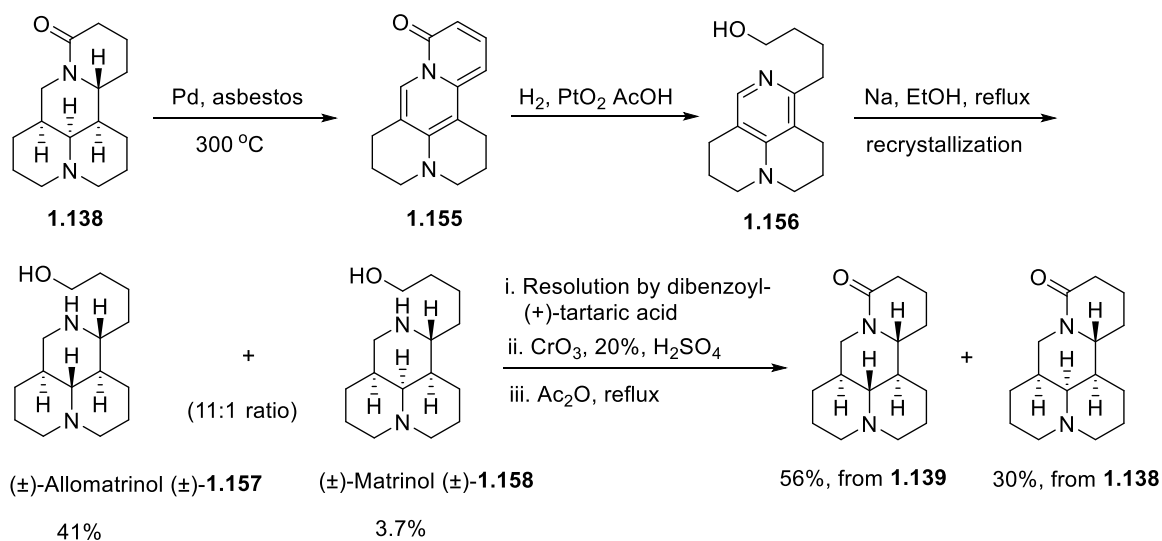


Scheme 1.34: Mandell's total synthesis of (±)-matrine and (±)-allomatrine

The major component was reductively cyclised to either (±)-matrine using 5% Pd on charcoal at rt under 4 atm of H₂ in 17% yield or the thermodynamically more stable (±)-allomatrine (±)-**1.139** using 10% Pd on charcoal at rt in 11% yield with 2% yield of (±)-matrine and 3% of a mixture. The identities of the products was confirmed by comparison of their infrared spectra and melting points with authentic samples obtained from natural sources.

1.4.4 Okuda's semi-synthesis of optically active (+)-allomatrine

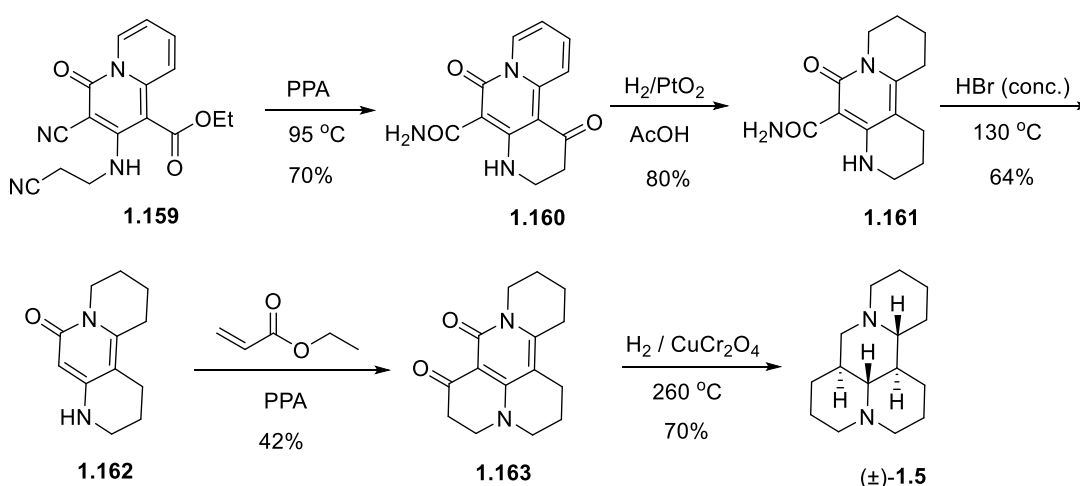
The semi-synthesis of optically active (+)-allomatrine ((+)-**1.139**) was accomplished by Okuda *et al.* in 1966 from (+)-matrine.¹⁰⁶ Their approach proceeded by oxidation of (+)-matrine ((+)-**1.138**) to didehydromatrine (**1.156**), using a procedure which was reported by Tsuda and co-workers in 1962.¹¹¹ Dehydrogenation of (+)-matrine over Pd/asbestos provided octadehydromatrine (**1.155**) (**Scheme 1.35**). Catalytic hydrogenation over PtO₂ in AcOH afforded didehydromatrine (**1.156**). Reduction of **1.156** with Na in refluxing EtOH generated a mixture of two racemic diastereoisomers; (±)-allomatrinol ((±)-**1.157**) and (±)-matrinol ((±)-**1.158**) present in a ratio of (11:1). The resolution of diastereoisomers (±)-allomatrinol and (±)-matrinol was performed by recrystallisation of the dibenzoyl-(+)-tartaric acid salts from acetone-ether. (+)-Allomatrinol ((+)-**1.157**) and (+)-matrinol ((+)-**1.158**) were transformed to corresponding amino acid derivatives by oxidation with CrO₃ in 20% H₂SO₄. The crude material was cyclised without purification in refluxing acetic anhydride to access (+)-allomatrine in 56% from (+)-allomatrinol, and (+)-matrine in 30% from (+)-matrinol ((+)-**1.158**).



Scheme 1.35: Okuda's semi-synthesis of (+)-allomatrine from (+)-matrine

1.4.5 Matsunaga's synthesis of (\pm)-allomatridine

(\pm)-Allomatridine (\pm)-**1.5** was synthesised by Matsunaga *et al.* in 1970.¹¹² Oxoquinolizine **1.159** was used as starting material, which was prepared as described in previous work in 1969 in 2 steps and 37% yield.¹¹³ Cyclization of oxoquinolizine **1.159** in the presence of polyphosphoric acid (PPA) provided keto-amide **1.160** in HBr (**Scheme 1.36**). Reduction of **1.160** using Adams' catalyst afforded a carboxamide **1.161**. Removal the carboxamide group from **1.161** to gave tricycle **1.162** under heating with conc. HBr. Formal cycloaddition of tricycle **1.162** with ethyl acrylate generated tetracycle **1.163**. Finally, reduction of tetracycle **1.163** using copper chromite catalyst (CuCr_2O_4) at high temperature gave (\pm)-allomatridine (\pm)-**1.5** in 70% yield. The identity of (\pm)-allomatridine was confirmed by mixed melting point, infrared comparison and elemental analysis. The synthesis was achieved in 5 steps and in 11% yield from oxoquinolizine **1.159**.

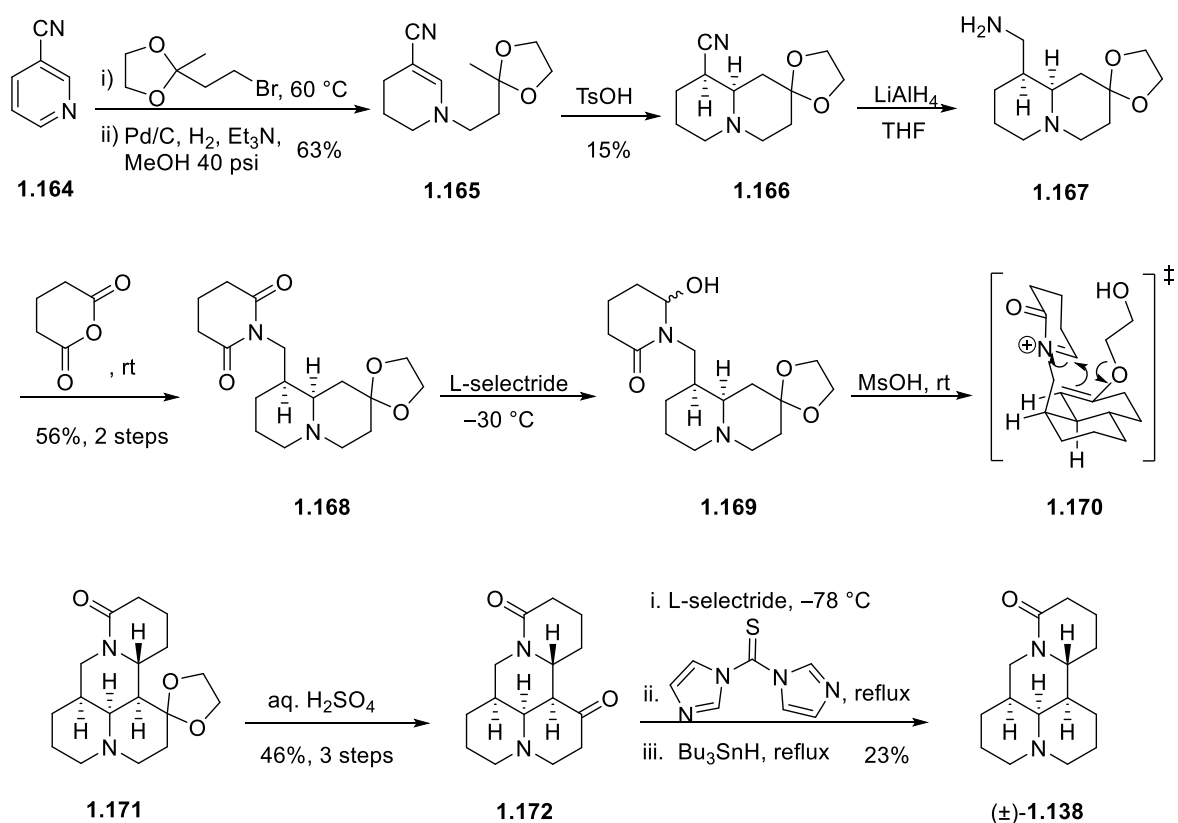


Scheme 1.36: Matsunaga's synthesis of (\pm)-allomatridine (\pm)-**1.5**

1.4.6 Chen's total synthesis of (\pm)-matrine

A synthesis of (\pm)-matrine ((\pm)-**1.138**) was published by Chen *et al.* in 1986 by employing an acetal mediated *N*-acyliminium ion cyclisation to assemble both the C and D rings of the natural product (**Scheme 1.37**).¹⁰⁷ Using the chemistry reported by Wenkert and Jeffcoat,¹¹⁴ alkylation of nicotinonitrile **1.164** with 4-bromo-2-butanone ethylene ketal followed by hydrogenation led to piperidine **1.165** in 63% yield. Treatment of piperidine **1.165** with TsOH furnished quinolizidine derivative **1.166** through addition of the enol to the iminium ion intermediate in 15% yield (these yields were reported by Wenkert and Jeffcoat).¹¹⁴ Reduction of the nitrile functionality of **1.166** using LiAlH_4 accessed primary amine **1.167**. Primary amine **1.167** was treated with glutaric anhydride to afford glutarimide intermediate **1.168** in 56% over 2 steps. The desired *N*-acyliminium cyclisation precursor **1.169** was obtained *via* the reduction of the imide moiety with L-selectride. The *N*-acyliminium cyclisation **1.170** was achieved using MsOH to generate the tetracyclic core **1.171**

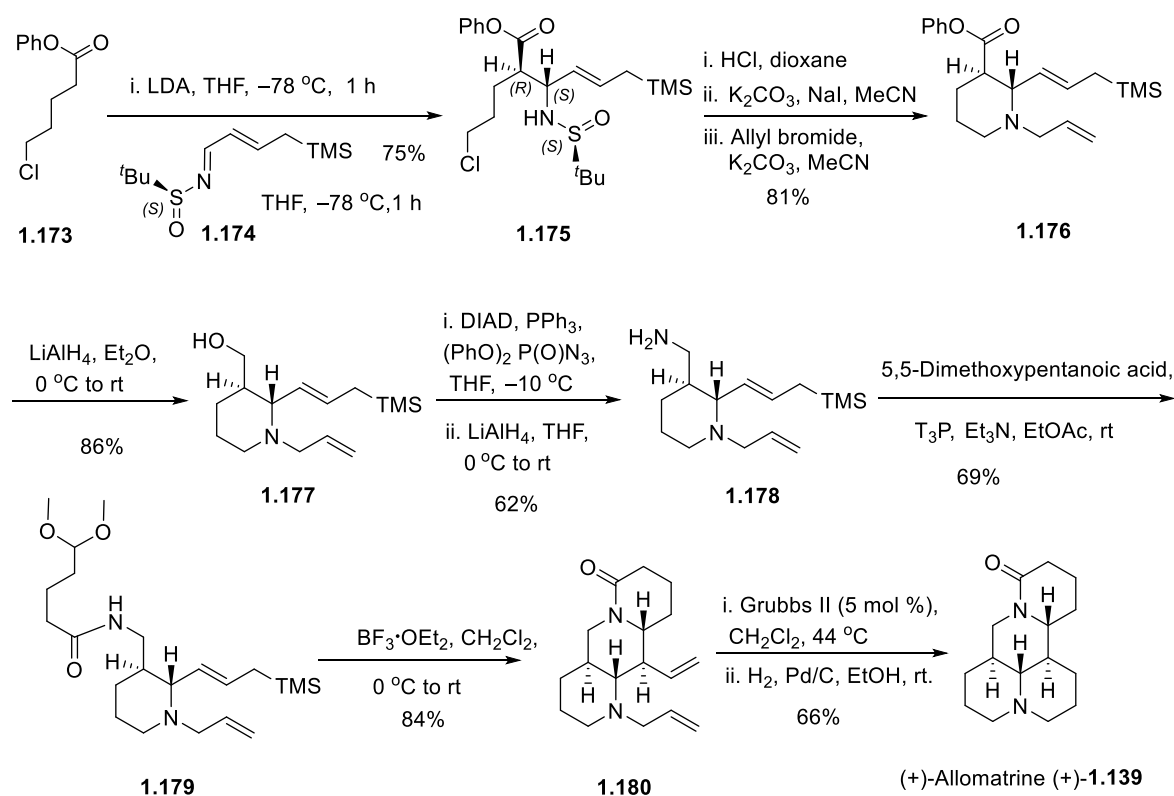
of the natural product which was deprotected with aq. H_2SO_4 to give 8-oxomatrine (**1.172**) in 46% yield over the three steps. The stereochemistry of 8-oxomatrine (**1.157**) was determined by single crystal X-ray analysis. The synthesis of (\pm)-matrine was completed by reduction of oxomatrine **1.172** followed by a Barton radical de-oxygenation in 23% yield. The synthesis was completed in 11 steps with 1% overall yield.



Scheme 1.37: Chen's total synthesis of (\pm)-matrine

1.4.7 Brown's total synthesis of (+)-allomatrine

The first stereocontrolled total synthesis of (+)-allomatrine ((+)-**1.139**) was accomplished in 2013 by Brown and co-workers (Scheme 1.38).¹⁰⁹ The synthesis was described utilising imino-aldol and *N*-acyliminium cyclisation reactions as key steps. The lithium enolate of phenyl 5-chlorovalerate (**1.173**) underwent addition to α,β -unsaturated imine **1.174** to provide *syn* β -amino acid **1.175** in 75% yield as a single diastereoisomer. Removal of the *N*-sulfinyl protecting group using 1 equiv. of HCl produced the primary amine, and subsequent treatment with K_2CO_3 and NaI furnished the piperidine intermediate. *N*-Alkylation of this piperidine intermediate *in situ* with allyl bromide to give the piperidine derivative **1.176**. Reduction of ester **1.176** using $LiAlH_4$ afforded alcohol **1.177**, which was subjected to modified Mitsunobu reaction to introduce the azide functionality. Subsequent reduction using $LiAlH_4$ generated the primary amine **1.178**, which was treated with 5,5-dimethoxypentanoic acid in the presence of propylphosphonic anhydride coupling agent (T_3P) to secure the acyliminium cyclisation precursor **1.179**.



Scheme 1.38: Brown's synthesis of (+)-allomatrine

Employing the Lewis acid $BF_3 \cdot OEt_2$ with the intermediate **1.179** initiated a sequence of reactions and with addition of the TMS activated alkene onto the *in situ* *N*-acyliminium ion to form the tricycle **1.180**. Treatment of diene **1.180** with Grubbs II catalyst followed by hydrogenation over Pd/C accessed (+)-allomatrine (**1.139**). The first total synthesis of (+)-allomatrine was completed in 13 steps and 14% overall yield.

1.5 Epilupinine

This section describes synthetic strategies of early and recent synthetic interest in the quinolizidine alkaloids. (+)-Epilupinine ((+)-**1.1**) was reported to show *in vitro* inhibitory activity against P-388 (LD₅₀=28 μg/mL) and L1210 (LD₅₀ = 20 μg/mL) cell lines.¹¹⁵ In recent years, quinolizidines have been employed as intermediates or pharmacophores in drug discovery. Many molecules bearing epilupinyl unit are antiviral, antiarrhythmic, antimalarial or platelet antiaggregation agents.¹¹⁶⁻¹²¹ Due to its biologically important properties, and the fact that it is an excellent structure for validation of new synthetic methodology and strategy, (–)-epilupinine ((–)-**1.1**) and lupinine ((+)-**1.181**) have attracted great interest as targets for total synthesis.

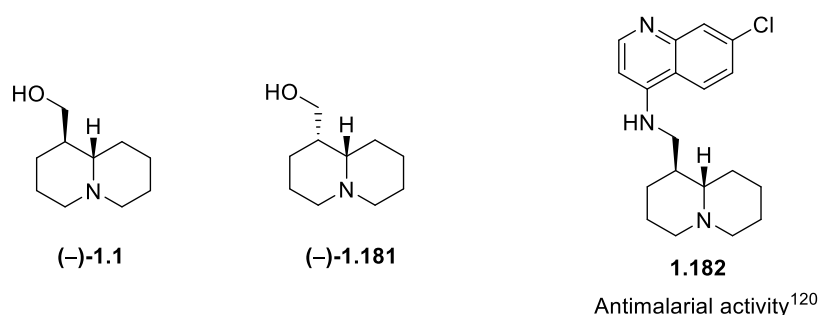
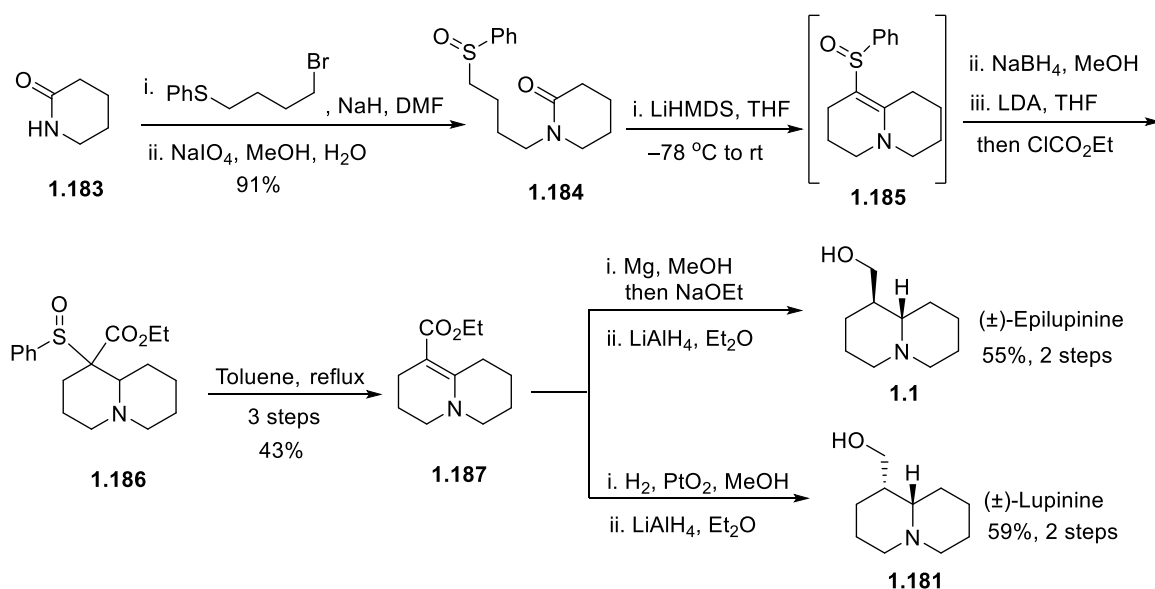


Figure 1.8: Structure of (–)-epilupinine ((–)-**1.1**) and (+)-lupinine ((+)-**1.181**) and **1.182**

1.5.1 Pohmakotr's synthesis of (±)-epilupinine and (±)-lupinine

A general synthetic route to 1-azabicycles was reported by Pohmakotr *et al.* in 2003 using α -sulfinyl carbanions for intramolecular carbon-carbon bond forming reactions.¹²² This approach relies on the capability of cyclic amides to undergo nucleophilic addition reactions. In 2008, Pohmakotr *et al.* prepared (±)-epilupinine ((±)-**1.1**) and (±)-lupinine ((±)-**1.181**) by *N*-alkylation of 2-piperidinone (**1.183**) with 4-bromobutylphenylsulfane (**Scheme 1.39**).¹²³ Subsequent oxidation of **1.167** using sodium periodate provided the sulfoxide **1.184**. Base promoted cyclisation of the sulfoxide produced **1.185**. Reduction of **1.185** using NaBH₄ and subsequent acylation using ethyl chloroformate yielded the sulfoxide **1.186** as a mixture of diastereoisomers. Elimination of sulfoxide from **1.186** afforded **1.187**, followed by reduction under appropriate conditions generated either (±)-epilupinine or (±)-lupinine.

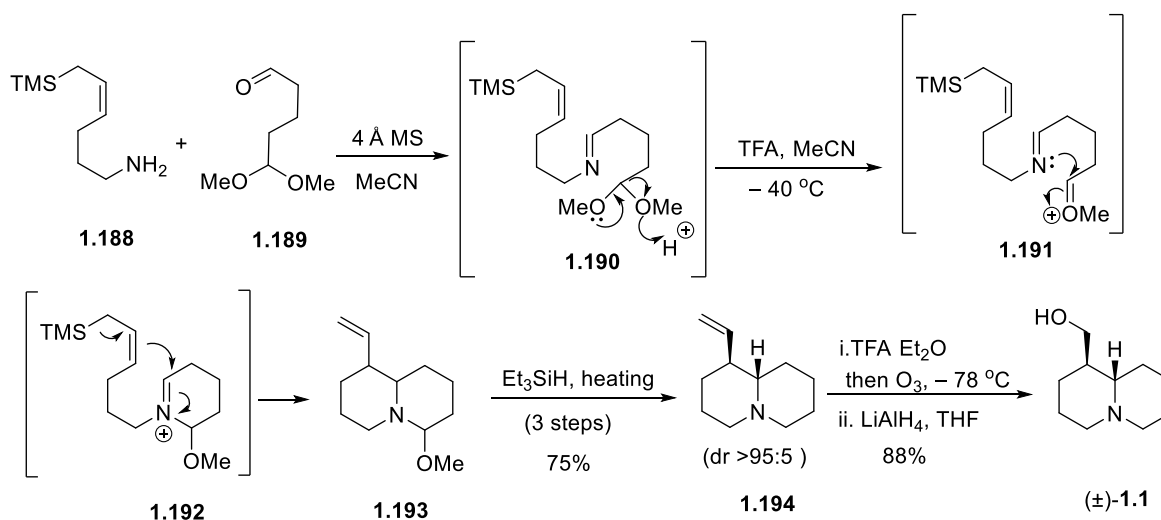


Scheme 1.39: Pohmakotr's synthesis of (\pm)-epilupinine and (\pm)-lupinine

Reduction of **1.187** with Mg in MeOH, and subsequent epimerization of the ester followed by LiAlH₄ reduction furnished (\pm)-epilupinine as a single diastereomer in 55% over two steps. Alternatively, access (\pm)-lupinine was through hydrogenation of **1.187** followed by ester reduction using LiAlH₄ to afford a single diastereomer in 59% over two steps.

1.5.2 Martin's synthesis of (\pm)-epilupinine,

Remuson reviewed *N*-acyliminium ions in the synthesis of alkaloids with a focus on products containing a piperidine ring.¹²⁴ Strategies using *N*-acyliminium ions can be very efficient and are generally attractive for their rapid formation of heterocyclic rings from acyclic precursors. A concise synthesis of (\pm)-epilupinine was developed by Martin and co-workers in 2009, which depends on the intramolecular allylation and *N*-alkylation of an imine (**Scheme 1.40**).¹²⁵

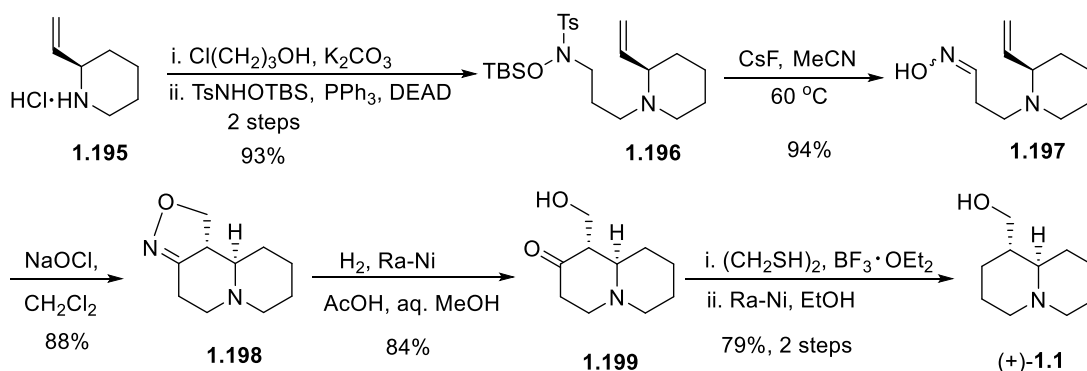


Scheme 1.40: Martin's synthesis of (\pm)-epilupinine

The synthetic approach started from the aminosilane **1.188**, which was prepared in 6 steps and 43% yield by Speckamp in 1985.^{126,127} Condensation of **1.188** with the mono protected dialdehyde **1.189** (prepared in 2 steps and 48% yield)¹²⁸ afforded the corresponding imine **1.190**. Removal the methanol group under acid conditions to afford oxonium ion **1.191**, which generated iminium ion **1.192**. Intramolecular nucleophilic addition of the allylsilane to the iminium ion **1.192** produced the bicyclic *N,O*-acetal **1.193** (not isolated). Triethylsilane (Et₃SiH) was added to the crude reaction mixture to reduce **1.193** affording **1.194**. Ozonolysis of the TFA salt of **1.194** followed by reduction of the corresponding aldehyde secured (±)-epilupinine ((±)-**1.1**). Overall, the synthesis of (±)-epilupinine was achieved in 5 steps with 66% yield from the aminosilane **1.188** (Note that an additional 6 steps were required to make **1.188**).

1.5.3 Hu and Wang's synthesis of (+)-epilupinine

A synthesis of (+)-epilupinine published in 2011 by Hu, Wang and co-workers utilised nitrile oxide cycloaddition chemistry as the pivotal step (**Scheme 1.41**).¹²⁹ The known enantiopure 2-vinyl piperidine **1.195** was used as starting point for their synthesis, which was prepared in 4 steps with 86% overall yield.¹³⁰ *N*-Alkylation of **1.195** with 3-chloropropanol and subsequent conversion of the alcohol into the *N*-tosyl-*O*-TBS hydroxyl amine derivative **1.196** was achieved using the Fukuyama procedure.¹³¹

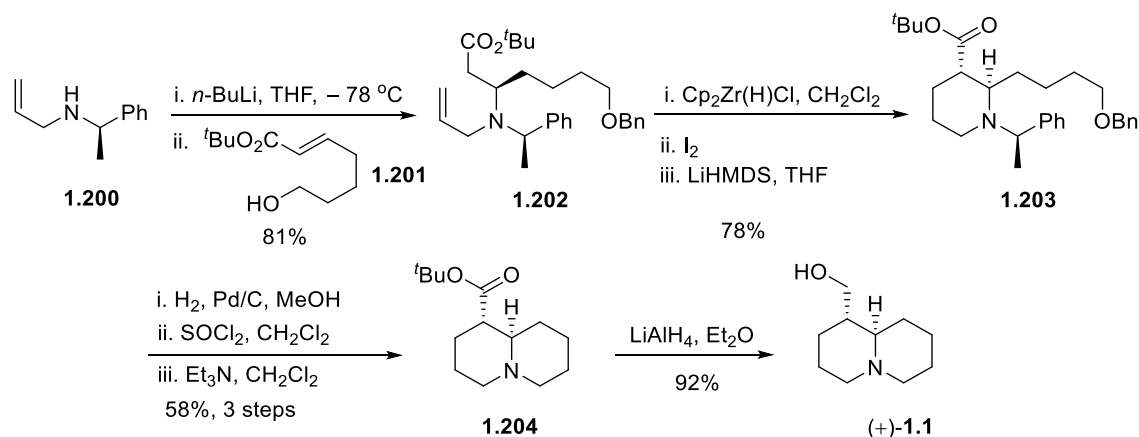


Scheme 1.41: Synthesis of (+)-epilupinine *via* an intramolecular nitrile oxide cycloaddition

Treatment of protected hydroxyl amine **1.196** with CsF generated the oxime **1.197**, which was oxidised to the nitrile oxide **1.198** using NaOCl. The intramolecular [3+2] cycloaddition provided the isoxazoline **1.198** as a single diastereomer. Reductive N-O bond cleavage followed by *in situ* hydrolysis of the resulting imine gave the intermediate aldol **1.199**. Conversion of **1.199** to (+)-epilupinine ((+)-**1.1**) was accomplished by dithiolane formation followed by desulfurisation using Raney Ni. The synthesis of (+)-epilupinine was achieved in 9 steps and in 48% overall yield from **1.195** (13 steps from commercial starting materials).

1.5.4 Szymoniak synthesis of (+)-epilupinine

In 2008, Szymoniak *et al.* published a synthetic strategy that applied a hydrozirconation / iodination / cyclization protocol for the formation of the piperidine ring in (+)-epilupinine.¹³² In 2013, the same group also reported a synthesis of (±)-lupinine by employing a hydrozirconation cyclization of a functionalized pyridine moiety.¹³³ For the synthesis of epilupinine, enantiomerically pure amine **1.200** was used as the starting material. Conjugate addition of lithiated chiral amine **1.200** to the enoate **1.201** generated **1.202** as a single diastereomer (**Scheme 1.42**).



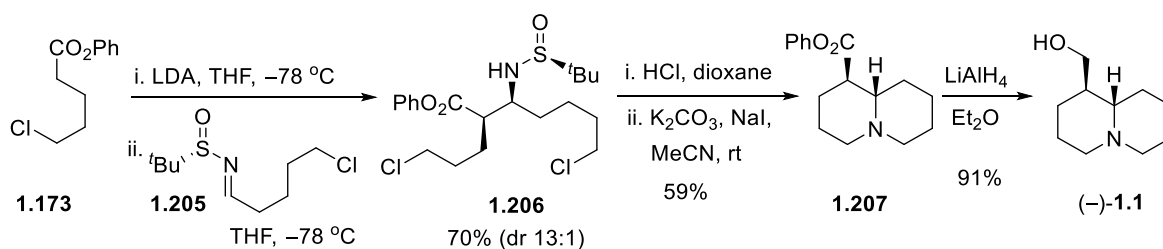
Scheme 1.42: Szymoniak synthesis of (+)-epilupinine

Hydrozirconation of the *N*-allyl group in **1.202** followed by treatment with iodine generated the corresponding primary iodide. Treatment of this iodoester intermediate with LiHMDS resulted in intramolecular alkylation of the ester enolate to provide piperidine **1.203**. This strategy was also used in the synthesis of other *trans*-2,3-disubstituted piperidines. Hydrogenolysis of **1.203** over Pd/C gave the corresponding amino alcohol, which was treated with SOCl₂ to give the corresponding primary chloride that cyclised to provide quinolizidine **1.204**. Finally, reduction of the ester **1.204** using LiAlH₄ gave (+)-epilupinine ((+)-**1.1**) in 92% yield. Overall, the synthesis involved 7 steps and proceeded in 34% yield. Additional steps were required to prepare the starting materials.

1.5.5 Brown's synthesis of (–)-epilupinine

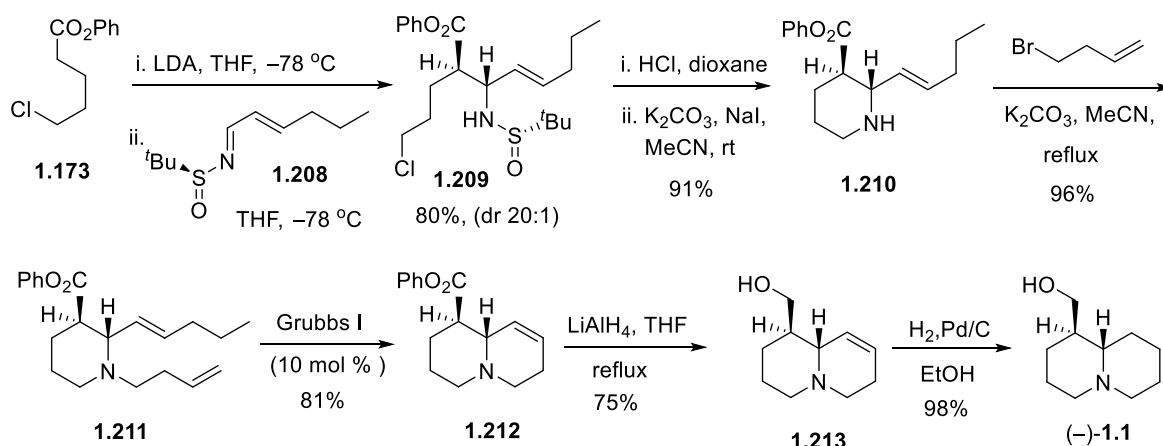
In 2013 Brown and co-workers described the use of an imino-aldol reaction approach to the synthesis of (–)-epilupinine.¹³⁴ This strategy was efficient for the fused ring systems ([5, 6], [6, 6]) with varying degrees of substitution. Methodology involving cyclization of open chain precursors, where the stereochemistry has already been established, appears more commonly in the literature. The synthesis of (–)-epilupinine was reported twice by the Brown group beginning from two

different imines.^{134,135} A stereoselective imino-aldol reaction of the enolate of phenyl 5-chloropentanoate (**1.173**) with halo imine **1.205** (Scheme 1.43) furnished *syn* imino-aldol adduct **1.206** in 70% yield and high diastereoselectivity. Deprotection of the *N*-sulfinyl auxiliary of **1.206** using conc. HCl followed by treatment with K₂CO₃ and NaI induced double cyclisation of the primary amine onto the chloroalkyl side chains to give bicycle **1.207**. The synthesis of (–)-epilupinine ((–)-**1.1**) was completed by reduction of the phenyl ester **1.207** to a primary alcohol using LiAlH₄ in just four steps and 15% overall yield.



Scheme 1.43: Brown's synthesis of (–)-epilupinine from halo imine **1.205**

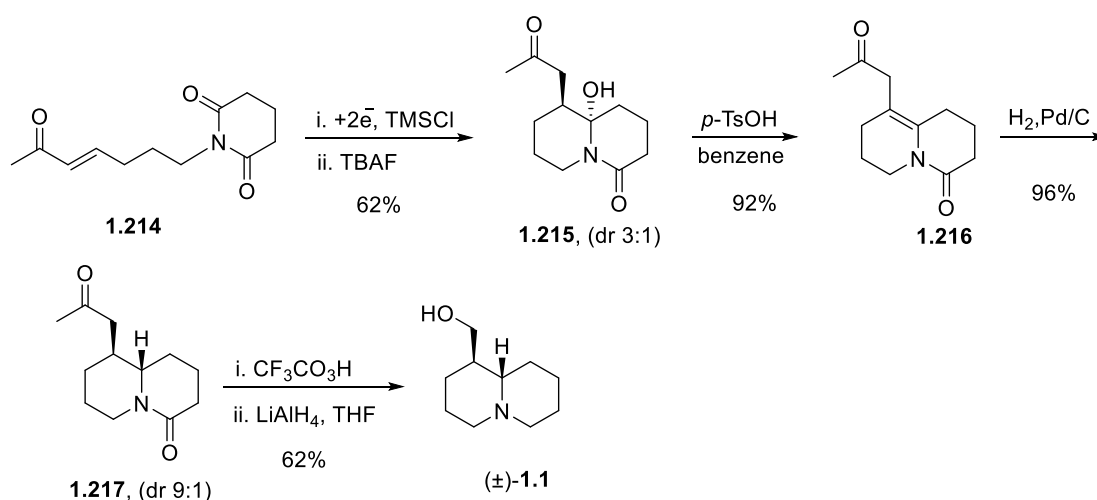
A second approach reported in a PhD thesis,¹³⁵ employed unsaturated sulfinylimine **1.208** with phenyl ester **1.173** in the presence of LDA to give *syn* imino-aldol adduct **1.209** in 80% yield and high diastereoselectivity (Scheme 1.44). Removal of *N*-sulfinyl group from *syn*-adduct **1.209** under acidic conditions and subsequent treatment with K₂CO₃ and NaI provided piperidine **1.210**. *N*-Alkylation of piperidine **1.210** with 4-bromo-1-butene afforded **1.211**, which was treated with Grubbs I catalyst to produce quinolizidine **1.212**. Reduction of ester **1.212** in the presence of LiAlH₄ gave **1.213** and hydrogenation over Pd/C completed the synthesis of (–)-epilupinine in seven steps and 39% overall yield. Although the overall yield for this route is higher, it should be noted that the earlier shorter route was not optimised.



Scheme 1.44: Walkin and Brown's synthesis of (–)-epilupinine from unsaturated imine **1.208**

1.5.6 Kise's synthesis of (±)-epilupinine *via* electroreductive coupling

In 2013 Kise *et al.* reported the synthesis of (±)-epilupinine (±)-**1.1** using an electroreductive intramolecular cyclisation as a key step (**Scheme 1.45**).¹³⁶ Electroreductive coupling of glutarimide **1.214** in the presence of chlorotrimethylsilane (TMSCl) and subsequent de-silylation with TBAF provided bicycle **1.215**. Dehydration of cyclised ester **1.215** using *p*-TsOH in refluxing benzene afforded α,β -unsaturated ketone **1.216**. Hydrogenation of **1.216** over Pd/C generated *syn* quinolizidine derivative **1.217** with good diastereoselectivity (dr 9:1). Oxidation of **1.217** under Baeyer-Villiger conditions using trifluoroacetic acid followed by reduction in the presence LiAlH₄ accessed (±)-epilupinine in six steps and in 34% overall yield from **1.214**.



Scheme 1.45: Kise's synthesis of (±)-epilupinine *via* electroreductive coupling

1.5.7 Davies's synthesis of (+)-epilupinine *via* a double reductive cyclisation protocol

A concise asymmetric synthesis of (+)-epilupinine ((+)-**1.1**) was reported by Davies *et al.* in 2016 making use of double reductive cyclisation.^{137,138} Initially (+)-epilupinine was obtained in low overall yield after several attempts through alkylation and double reductive cyclisation. However, a higher yielding synthesis of (+)-epilupinine was achieved *via* diastereoselective conjugate addition of (*R*)-**1.221** to α,β -unsaturated ester **1.220** (**Scheme 1.46**). Deprotonation of ester **1.218** using NaH and subsequent addition of but-3-enyl bromide provided ester **1.219**. Wadsworth-Emmons olefination of 5-hexenal with phosphonate **1.219** using an organomagnesium reagent as the base afforded α,β -unsaturated ester **1.220** with moderate selectivity [(*E*):(*Z*)] (dr 3:1). The (*Z*)-configuration of α,β -unsaturated ester **1.220** was not considered to be a problem because the lithium amide only undergoes conjugate addition to the (*E*)-stereoisomer. Conjugate addition of (*R*)-*N*-benzyl-*N*-(α -methylbenzyl) amide (*R*)-**1.221** to (*E*)- α,β -unsaturated ester **1.220** was followed by addition of 2,6-di-*tert*-butylphenol to generate β -amino ester **1.222** as a single diastereoisomer

Chapter 2: Results and Discussion

The development of general strategies towards bicyclic and tetracyclic lupin alkaloids using imino-aldol reactions is described in this chapter. In these strategies, imino-aldol adducts provide key backbones to access the desired lupin alkaloids (**Figure 2.1**).

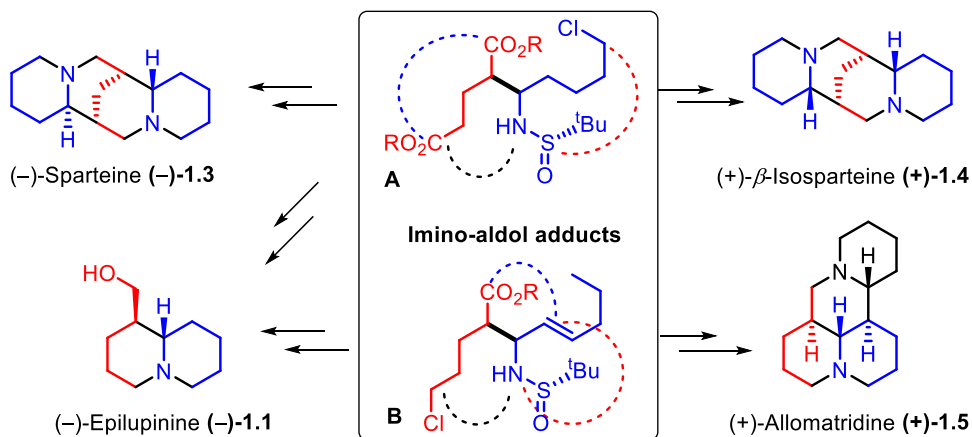


Figure 2.1: Overview of strategy towards the synthesis of lupin alkaloids

Synthetic pathways towards (+)- β -isosparteine ((+)-**1.4**), (-)-sparteine ((-)-**1.3**), (-)-epilupinine ((-)-**1.1**) and (+)-allomatridine ((+)-**1.5**) will be discussed from two different imino-aldol adducts **A** and **B**. The first strategy involves imino-aldol adduct **A** to access (+)- β -isosparteine, (-)-sparteine, and (-)-epilupinine. The second strategy investigates the use of a mono imino-aldol reaction to access (-)-epilupinine and (+)-allomatridine from imino-aldol adduct **B**.

2.1 Synthesis of the tetracyclic alkaloid (+)- β -isosparteine ((+)-**1.4**)

Our approach towards (+)- β -isosparteine ((+)-**1.4**) using a novel double imino-aldol reaction of glutaric acid diesters and imine derivatives is described in this section.

2.1.1 Retrosynthetic analysis of (+)- β -isosparteine

Our retrosynthetic analysis of (+)- β -isosparteine ((+)-**1.4**) led us to consider two approaches using two different *syn,syn* double imino-aldol adducts (**Figure 2.2** & **2.3**). The first approach involves cleavage of C-C bonds of the A and D rings in ((+)-**1.4**) (**Figure 2.2**). Ring closing metathesis (RCM) followed by hydrogenation and reduction would give (+)- β -isosparteine from tetraene **2.4**. Disconnection of *N*-homoallyl group from **2.4** and subsequent cleavage of the lactam bonds leads back to the *syn,syn* adduct **2.2**. The key intermediate is therefore double imino-aldol adduct **2.2**,

which may be obtained from two *syn*-selective imino-aldol reactions of diphenyl glutarate (**2.1**) with two equivalents of unsaturated imine **1.208**.

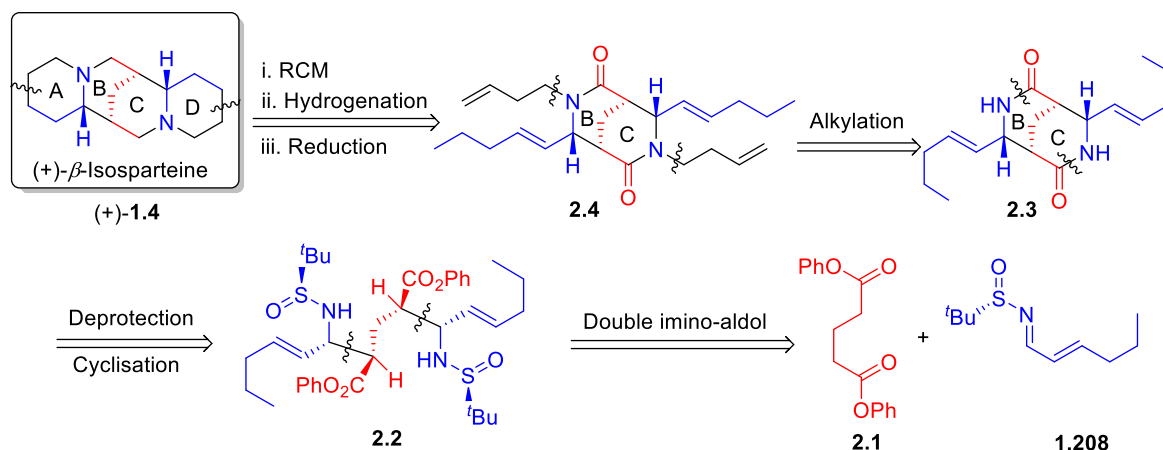


Figure 2.2: Retrosynthetic analysis of (+)- β -isosparteine from unsaturated imine **1.208**.

A shorter approach to β -isosparteine may be achieved by using halo imine **1.205** instead of unsaturated imine **1.208** (**Figure 2.3**). Cleavage of C-N bonds in (+)- β -isosparteine led back to open chain double imino-aldol adduct **2.5** (**Figure 2.3**). Formation of the B and C rings will require cyclisation of **2.5** by deprotection of the *N*-sulfinyl groups and cyclisation onto the ester groups. Double imino-aldol adduct **2.5** requires two functionalised fragments **2.1** and **1.205**. Although this approach is clearly shorter and more attractive, both routes were initially investigated in parallel.

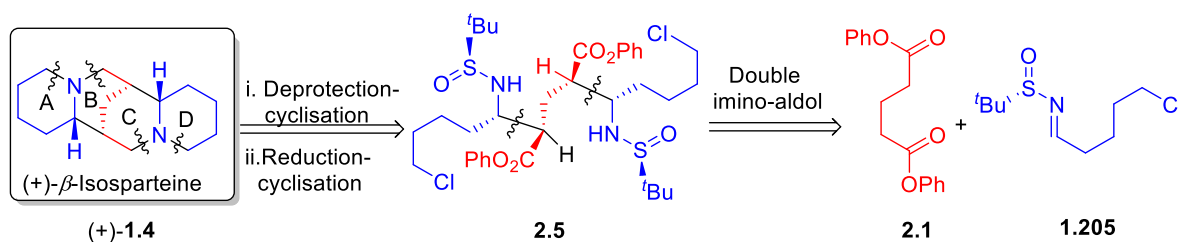
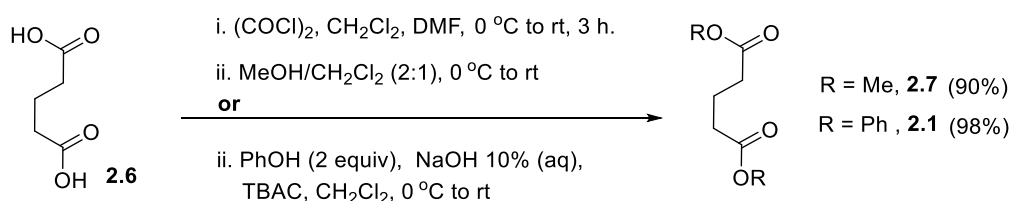


Figure 2.3: Retrosynthetic analysis of (+)- β -isosparteine from halo imine **1.205**.

2.1.2 Double imino-aldol reaction of glutarate esters

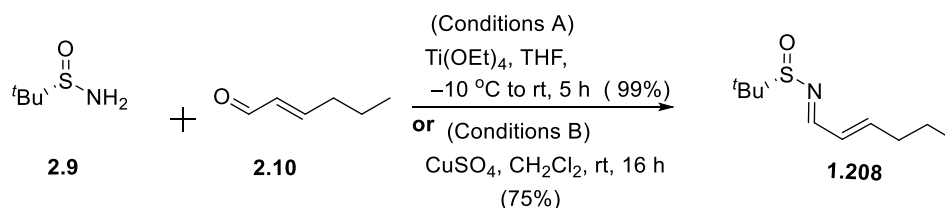
Double imino-aldol reactions of diesters of glutaric acid were investigated. Previous studies of the imino-aldol reaction by Brown and co-workers demonstrated that the choice of ester and the metal counter ion are both important in achieving high stereoselectivity.^{134,135,139} During the current work we have used two different esters to generate lithium dienolates. Diastereoselectivity and isolation

of the major diastereoisomeric double imino-aldol products will be covered in this section. Initially, suitable functional groups and chain lengths in the imine were chosen that would ultimately allow access to (+)- β -isosparteine ((+)-**1.4**). In the first instance, our goal was to achieve high diastereoselectivity in the imino-aldol reaction between sulfinyl imine and dimethyl and diphenyl esters of glutaric acid *via* the corresponding lithium dienolates. Dimethyl glutarate (**2.7**) was prepared from glutaric acid (**2.6**) using oxalyl chloride and subsequent esterification in the presence of excess methanol in 90% yield. Diphenyl glutarate (**2.1**) was prepared in high yield by reaction of the diacid chloride with two equivalents of phenol under basic conditions in the presence of the phase transfer catalyst tetrabutylammonium chloride (TBAC) (**Scheme 2.1**).



Scheme 2.1: Synthesis of diphenyl and dimethyl glutarates (**2.1** & **2.7**)

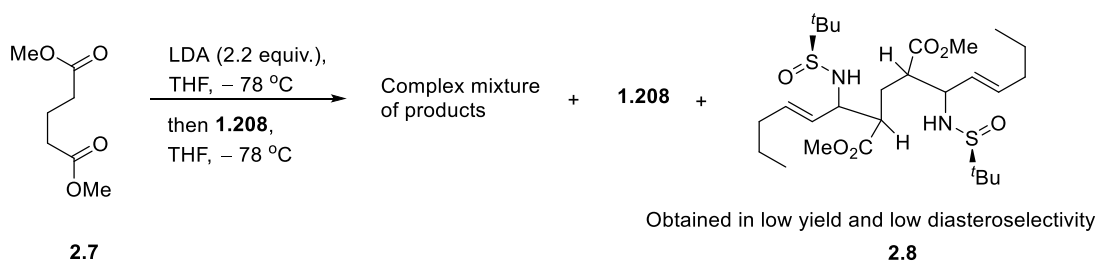
α,β -Unsaturated sulfinyl imine **1.208** was conveniently prepared from condensation of commercially available starting materials *trans*-2-hexen-1-al (**2.10**) and *tert*-butyl sulfinamide (**2.9**) using a procedure described by Raghavan *et al.* (**Scheme 2.2**). Reaction of the sulfinamide **2.9** with aldehyde **2.10** in the presence of $\text{Ti}(\text{OEt})_4$ in THF gave the required sulfinyl imine as the *trans* stereoisomer in excellent yield. A lower yield of 75% was obtained using CuSO_4 in CH_2Cl_2 .¹³⁴



Scheme 2.2: Preparation of α,β -unsaturated sulfinyl imine **1.208**

The double imino-aldol reaction of unsaturated sulfinyl imine **1.208** with dimethyl glutarate **2.7** was investigated using two equivalents of LDA to generate the dienolate in THF at $-78\text{ }^\circ\text{C}$ (**Scheme 2.3**). After 1 h of stirring at $-78\text{ }^\circ\text{C}$, the imine **1.208** was then added dropwise and stirred for 1 h. The reaction mixture was quenched by dropwise addition of aq. NH_4Cl at $-78\text{ }^\circ\text{C}$, then the crude material was purified by column chromatography to obtain the mixture of products and recovery of unsaturated imine **1.208**. The mixture of products was repeatedly purified by column chromatography to separate double imino-aldol adduct **2.8** in low yield along with a complex mixture of other products. The diastereoselectivity of double imino-aldol adduct **2.8** was found to

be low. Although the composition of the mixture of diastereoisomers of **2.8** was hard to determine by ^1H NMR spectroscopy. However, the double imino-aldol adduct **2.8** was identified by MS spectrometry and characteristic peaks present in the ^1H NMR spectrum. Based on this result, it was concluded that the use of dimethyl glutarate (**2.7**) in double imino-aldol reaction is not appropriate due to the poor stereoselectivity and low yields of **2.8**.

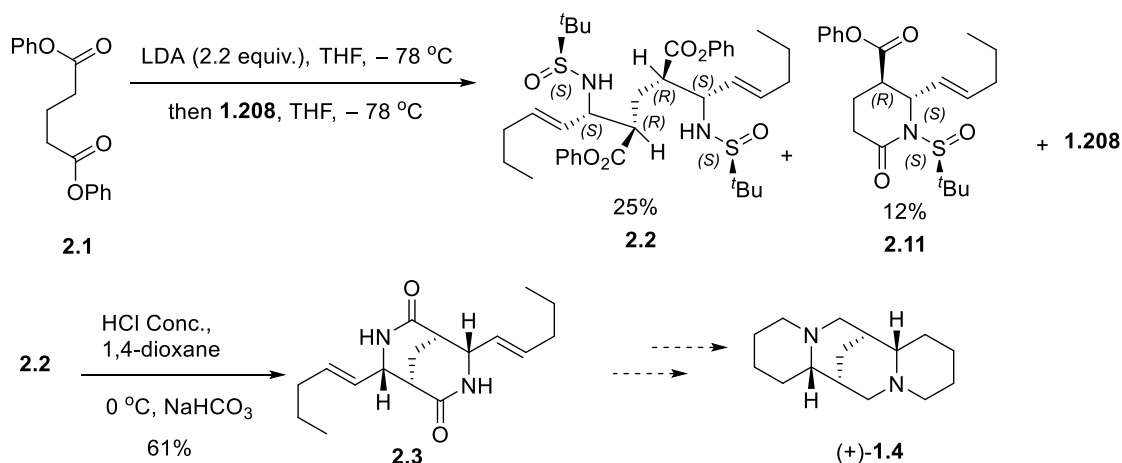


Scheme 2.3: Double imino-aldol reaction of dimethyl glutarate **2.7**

Due to the complex nature of the reaction product mixture and the difficulty in isolating any pure products, the double imino-aldol reaction of dimethyl glutarate (**2.7**) was not explored further. As anticipated from earlier studies in our laboratory, the diastereoselectivity of the double imino-aldol reaction may be significantly improved by employing diphenyl glutarate (**2.1**) in place of dimethyl glutarate (**2.7**). Therefore, diphenyl glutarate (**2.1**) was used for further studies described below.

2.1.3 Double imino-aldol reaction of diphenyl glutarate with unsaturated imine **1.208**

A diastereoselective double imino-aldol reaction was first achieved using one equivalent of diphenyl glutarate (**2.1**), two equivalents of LDA and two equivalents of imine **1.208** at $-78\text{ }^\circ\text{C}$ (**Scheme 2.4**). It was found that allowing the imino-aldol reaction mixture to warm above $-70\text{ }^\circ\text{C}$ led to partial decomposition giving phenol and recovery of starting materials following work-up. The reaction was carefully quenched by dropwise addition of aq. NH_4Cl at $-78\text{ }^\circ\text{C}$ in order to avoid decomposition of the products, and then the solution was allowed to warm to rt. The *syn,syn* diastereoisomer **2.2** was obtained as a major product of the double imino-aldol reaction in 25% yield. The mono *syn* imino-aldol adduct **2.11** was also obtained in 12% yield. Fortunately, it was possible to recrystallise the double imino-aldol product **2.2** from hexane and its absolute stereochemistry was confirmed to be *syn,syn* by single crystal X-ray (**Figure 2.4**). Other imino-aldol products were also present in the crude reaction mixture. However, no other pure diastereoisomers were isolated from this reaction.



Scheme 2.4: Diastereoselective double imino-aldol adduct of unsaturated imine **1.208**

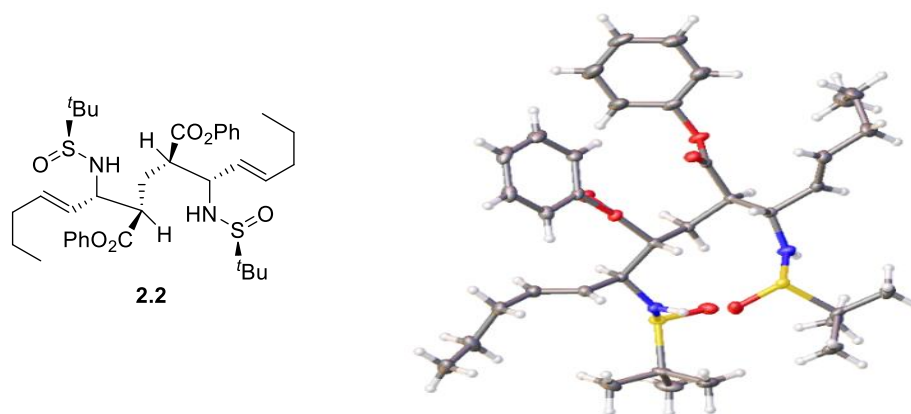


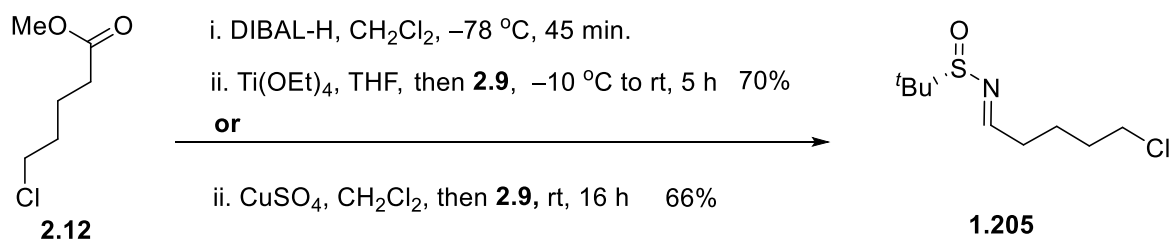
Figure 2.4: X-ray crystal structure of *syn,syn* double imino-aldol adduct **2.2**.

Deprotection and cyclisation of **2.2** using conc. HCl and subsequent neutralisation with saturated aq. NaHCO_3 gave *syn,syn* dioxo-bispidine **2.3**. Although high diastereoselectivity was achieved for the double imino-aldol adduct **2.2**, and its absolute stereochemistry was confirmed by X-ray, this route was not progressed further towards $(+)\text{-}\beta$ -isosparteine as our attention turned to the shorter route using the chloroalkyl imine **1.205**, which is discussed in the following section.

2.1.4 A concise double imino-aldol approach to the synthesis of $(+)\text{-}\beta$ -isosparteine

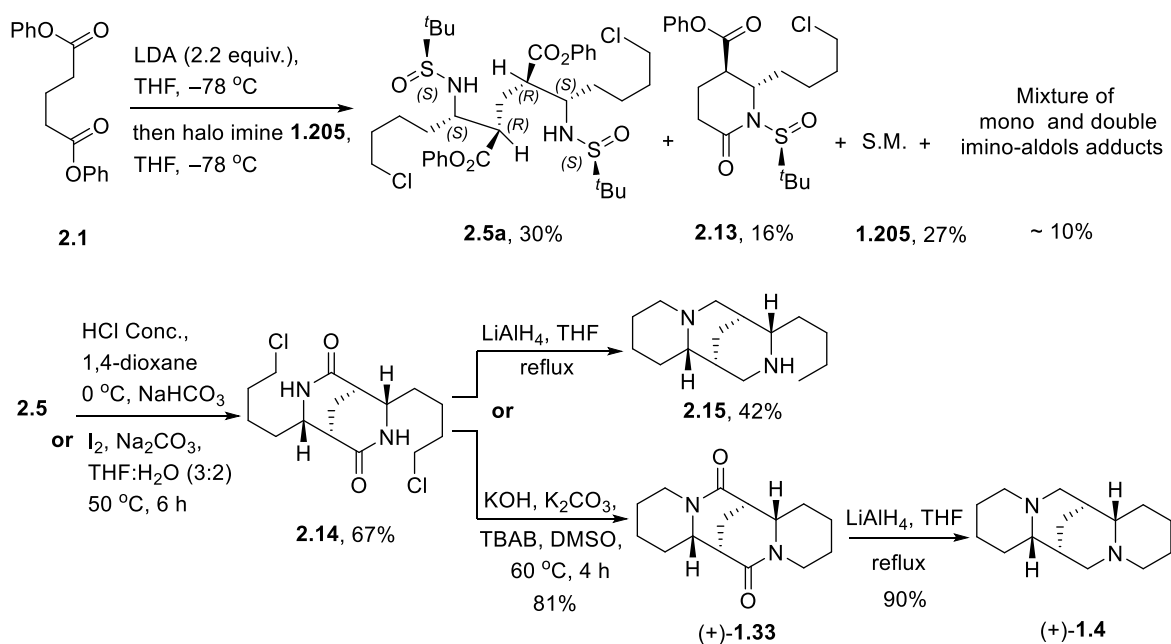
An alternative, short synthesis of $(+)\text{-}\beta$ -isosparteine was investigated from diphenyl glutarate (**2.1**) and halo imine **1.205**. The requisite *tert*-butylsulfinyl halo imine **1.205** was obtained over two steps (**Scheme 2.5**). Reduction of commercially available methyl 5-chlorovalerate (**2.12**) with DIBAL-H afforded the corresponding aldehyde, which due to its volatility, was used without purification in

the next step. Condensation of the crude aldehyde with the chiral auxiliary **2.9** in the presence of $\text{Ti}(\text{OEt})_4$ afforded halo imine **1.205** over two steps in 70% yield. Alternatively, halo imine **1.205** was formed in the presence of CuSO_4 in CH_2Cl_2 in 66% yield over two steps.



Scheme 2.5: Preparation of *tert*-butylsulfinyl halo imine **1.205**

The key double imino-aldol reaction was successfully achieved by adding two-equivalents of LDA to diphenyl glutarate (**2.1**) to form the corresponding dienolate, which was treated with halo imine **1.205** (Scheme 2.6). These conditions were adapted from the previous work conducted in Brown's group for related imino-aldol reactions. The *syn,syn* double imino-aldol adduct **2.5a** was obtained in 30% yield as a main product together with cyclised mono imino-aldol adduct **2.13** in 16% yield. In addition, a mixture of components including minor diastereomers of mono and double imino-aldol products was obtained. Although we obtained 30% yield of **2.5a**, and were able to continue the synthesis of (+)- β -isosparteine ((+)-**1.4**), we were keenly interested in optimizing the double imino-aldol reaction. This is discussed in the next section. The stereochemical determination of all the products from the imino-aldol reaction will also be discussed below.



Scheme 2.6: The total synthesis of (+)- β -isosparteine ((+)-**1.4**) from halo imine **1.205**.

The chloroalkyl side chains present in **2.5** contained the functionality required to access *syn,syn* dioxo-bispidine **2.14** after double deprotection and cyclisation. Deprotection was achieved using either conc. HCl followed by neutralising with aq. Na₂CO₃, or under basic conditions using I₂ with Na₂CO₃ in THF:H₂O (3:2) to give *syn,syn* dioxo-bispidine **2.14** in 67% yield. Reduction of dioxo-bispidine **2.14** using LiAlH₄ and final double cyclisation was expected to give access to (+)- β -isosparteine. Unfortunately, double concomitant reduction-cyclisation of bispidine **2.14** was unsuccessful due to dehalogenation of the alkyl halide side chain by LiAlH₄ giving the tricyclic derivative **2.15** as major product in 42% yield together with unidentified by-products.¹⁴⁰ At this stage, to gain selective access to (+)- β -isosparteine, either selective reduction of the lactams in **2.14** and double cyclisation is required, or cyclisation needs to be performed before reduction. Cyclisation of **2.14** was successfully carried out under basic conditions using phase transfer catalysis to provide (+)-10,17-dioxo- β -isosparteine ((+)-**1.33**) in good yield. The relative stereochemistry of dioxo- β -isosparteine was confirmed by single crystal X-ray crystallography after recrystallisation from hexane (**Figure 2.5**). (+)-10,17-Dioxo- β -isosparteine is also natural product, isolated in small quantity from *lupines sericeus* by Kinghorn *et al.* in 1982.¹⁴¹ Initially, this natural product **1.33** was identified by GC/MS, and later confirmed by semi-synthesis.

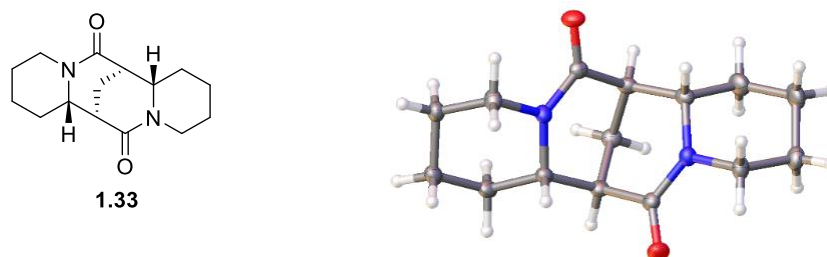
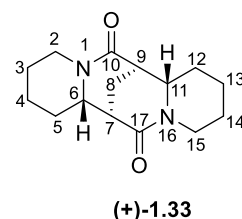


Figure 2.5: X-ray crystal structure of (+)-10,17-dioxo- β -isosparteine ((+)-**1.33**)

Finally, (+)- β -isosparteine ((+)-**1.4**) was obtained by reduction of bislactam **1.33** using LiAlH₄ under reflux in THF. The spectral and physical data for our synthetic (+)-10,17-dioxo- β -isosparteine and (+)- β -isosparteine are in excellent agreement with the values previously reported (**Table 2.1** and **Table 2.2**).^{48,76,55} The optical rotation of (+)-10,17-dioxo- β -isosparteine ((+)-**1.33**) was not recorded previously in the literature due to the lack of material, or its preparation as a racemic product.

Table 2.1. ^{13}C NMR data for (+)-10,17-dioxo- β -isosparteine ((+)-**1.33**)

Carbon	$\delta_{\text{C}}^{\text{a}}$	Lit. ⁵⁵ $\delta_{\text{C}}^{\text{b}}$
10,17	169.0	169.2
6,11	60.4	60.6
2,15	43.5	43.6
9,7	42.5	42.7
5,12	32.2	32.3
3,14	25.3	25.4
4,13	24.9	25.0
8	18.7	18.9



Physical data: m.p.= 170 – 172 °C

Lit.¹⁵ m.p.= 173 – 173.5 °C

Lit.⁵⁵ m.p.= 172 – 174 °C

Optical Rotation:

Recorded data current work:

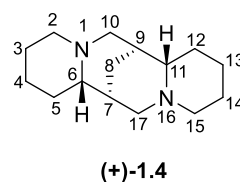
$[\alpha]_{\text{D}}^{\text{20}}$: +47.3 (c 1.5, MeOH, 23 °C)

Literature data: not reported

^a The current work: recorded in CDCl_3 at 101 MHz. ^b Recorded in CDCl_3 at 75 MHz.

Table 2.2. ^{13}C NMR data for (+)- β -isosparteine ((+)-**1.4**)

Carbon	$\delta_{\text{C}}^{\text{a}}$	Lit. ⁵⁵ $\delta_{\text{C}}^{\text{b}}$	Lit. ⁴⁸ $\delta_{\text{C}}^{\text{c}}$	Lit. ⁷⁶ $\delta_{\text{C}}^{\text{d}}$
6,11	62.8	63.0	63.3	62.8
2,15	55.2	55.3	55.9	55.1
10,17	55.0	55.1	55.7	54.9
9,7	34.5	35.6	35.6	34.4
5,12	28.8	28.8	29.4	28.6
3,14	25.5	25.6	26.4	25.4
4,13	22.7	22.8	23.6	22.6
8	19.8	20.0	20.6	19.8



Optical Rotation:

Recorded data current work:

$[\alpha]_{\text{D}}^{\text{20}}$: +15.1 (c 0.75 absolute EtOH, 23 °C)

Literature data:

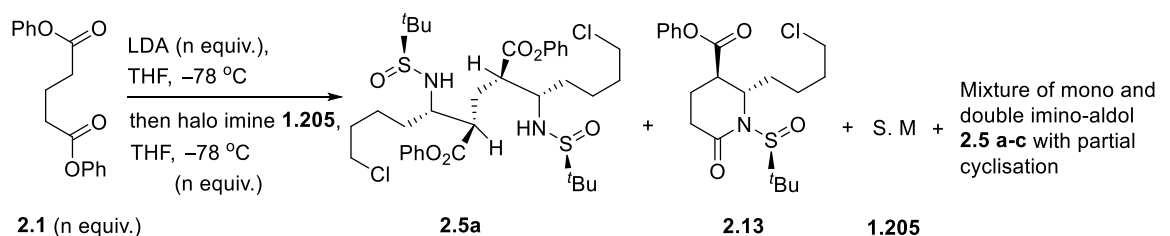
$[\alpha]_{\text{D}}^{\text{20}}$: + 15.38 (c 0.142, absolute EtOH, 21.1 °C) Lit.⁴⁸

^a The current work: recorded in CDCl_3 at 101 MHz. ^b Recorded in CDCl_3 at 75 MHz. ^c Recorded in CDCl_3 at 125 MHz. ^d Not recorded.

2.1.5 Optimisation of the double imino-aldol reaction

For optimisation of the double imino-aldol reaction to improve the yield of the double imino-aldol adduct **2.5a**, we investigated different conditions (**Table 2.3**). Unfortunately, extensive investigation of different reaction conditions only gave a small increase in yield of the *syn,syn* double imino-aldol product **2.5a**. The best conditions included using 1 equiv. of diphenyl glutarate **2.1** and 2 equiv. of halo imine **1.205** in the presence 2.2 equiv. of LDA at -80 to -78 °C, generating pure cyclised imino-aldol **2.13** in 16% yield, double imino-aldol **2.5a** in 30% yield, and recovery of starting halo imine **1.205** in 27% yield (entry 4). In addition, a complex mixture of products was obtained, which contained uncyclised-*syn* imino-aldol **2.16** and *anti* **2.17**, and a mixture of *anti,anti* **2.5b** and *syn,anti* **2.5c** double imino-aldol products. The analysis of this mixture will be discussed below.

Table 2.3. Optimisation of the double imino-aldol reaction.

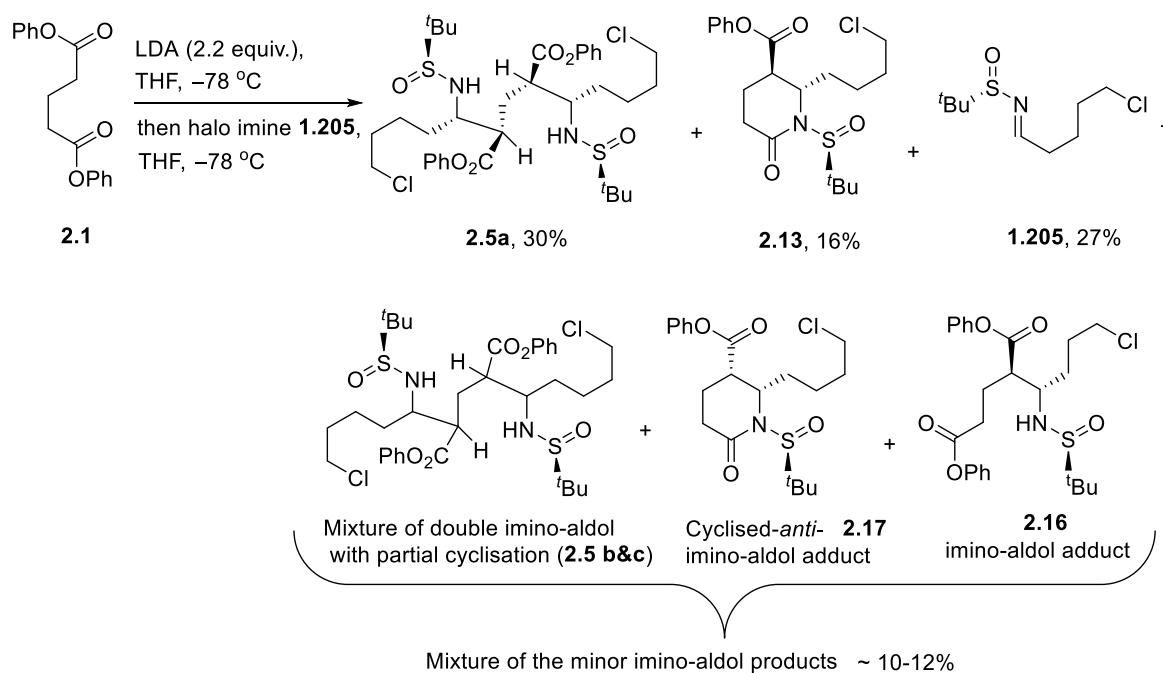


	Diester 2.1 (equiv)	Imine 1.205 (equiv)	Base and (equiv)	Temp (°C)	Double 2.5a	mono 2.13	S.M 1.205	Mixture of by products ^a
1	1.3	2	LDA (2.6)	-78	26%	22%	34%	22%
2	1	2.2	LDA (2.0)	-78	18%	34%	32%	23%
3	1	2	LDA (2.0)	-78	20%	22%	30%	26%
4	1	2	LDA (2.2)	-78	30%	16%	27%	24%
5	1	2	LDA (3.0)	-78	25%	20%	35%	27%
6	1	2	LHMDS (2.0)	-78	22%	15%	33%	22%
7	1	2	LHMDS (2.0)	-78 - -70	9%	23%	32%	23%
8	1	2	LDA (2.0)	-98 - -90	23%	18%	31%	26%
9	1	2	LDA (2.0)	-78 - -70	13%	25%	34%	26%
10	1	2	LDA (2.0) + DMPU	-78	24%	19%	30%	25%

^a The mixture contained uncyclised-*syn* imino-aldol **2.16**, cyclised-*anti* **2.17**, *anti,anti* **2.5b** and *syn,anti* **2.5c** double imino-aldol products, the yield is estimated based upon the mw. of the major components.

2.1.6 Determination of the structures and stereochemistry of the major and minor products from the double imino-aldol reaction

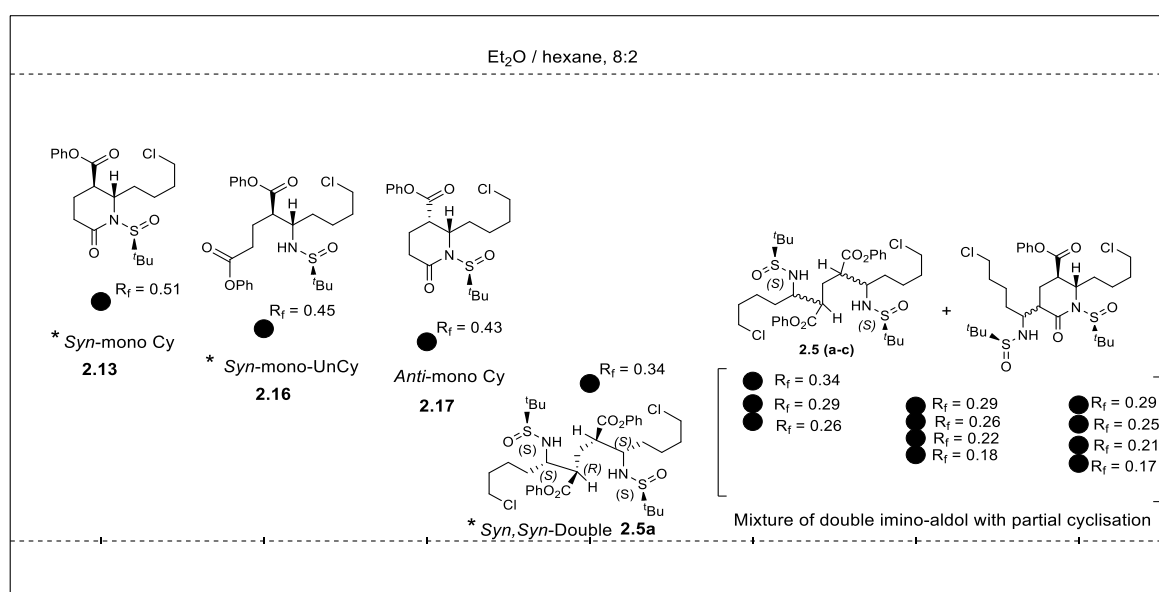
In this section, we will describe the stages of separation and structural determination of the mixture of products from the double imino-aldol reaction. The first major components **2.5a** and **2.13** were directly isolated from the double imino-aldol reaction as pure compounds together with a mixture of minor imino-aldol products (**Scheme 2.7**). The recovered imine **1.205** was also isolated as a pure compound from the reaction mixture in 27% yield.



Scheme 2.7: The major and minor products from double imino-aldol reaction

Initially, we were not able to identify all the products from the double imino-aldol reaction due to their difficult separation by column chromatography. Careful separation of the reaction mixture by column chromatography gave two groups of imino-aldol products. The first group consists of mono imino-aldol products **2.13**, **2.16** and **2.17** while the other components are double imino-aldols (**2.5a**) *syn,syn* and the mixture of (**2.5b**) *anti,anti* and (**2.5c**) *syn,anti* diastereoisomers which had also undergone partial cyclisation (**Figure 2.6**). Due to the complexity of this mixture, repeated chromatographic separation and further reactions were required to fully elucidate their structures. The imino-aldol products **2.5a** and **2.13** were separated as major components by the first column chromatography, while the remaining mixture of imino-aldol adducts was separated by repeated column chromatography (**Figure 2.6**). After purification by column chromatography eluting with Et₂O / hexane (2:8 to 9:1), almost all imino-aldol products and mixture of products were separated as follows:

The first fraction is phenol, the second is halo imine **1.205**, the third is cyclised *syn*-mono **2.13**, the fourth is *syn* imino-aldol (uncyclised) **2.16** and the fifth is cyclised *anti*-mono **2.17**. The fractions of the mono imino-aldol adducts **2.16** and **2.17** were separable by repeated column chromatography. The next fractions isolated by careful column chromatography were shown to be (**2.5a**) *syn,syn* double uncyclised imino aldol as the major fraction and the last fraction is mixture of uncyclised (**2.5b**) *anti,anti* and (**2.5c**) *syn,anti* double imino aldols, complicated due to some partial cyclisation. Since, the mixture of (**2.5b**) *anti,anti* and (**2.5c**) *syn,anti* the double imino-aldol adducts were inseparable by column chromatography, this mixture was taken forwards in the next step of the synthesis by deprotection and cyclisation (see Scheme 2.8). Further analysis of the mixture of double imino-aldols is described in the next section.



* The products of imino-aldol reaction **2.13**, **2.16** and **2.5a** were separated by careful column chromatography.

Figure 2.6: Representation of the TLC plate showing R_f values for different imino-aldol products

The structures of major imino-aldol adducts **2.5a** and **2.13** can be identified in the crude material by ¹H NMR spectroscopy (Figure 2.7 B). The inset figure A shows an expansion of characteristic peaks for the mono and double imino-aldol adducts **2.13** and **2.5a** respectively (Figure 2.7 A). From the crude ¹H NMR, it was difficult to determine the ratios of imino-aldol products due to significant overlapping signals. However, the presence of the minor products are indicated by the signals from the free N-H bonds (4-5 ppm) of double adducts **2.5a** and β -H of mono adducts **2.13** at (>4 ppm).

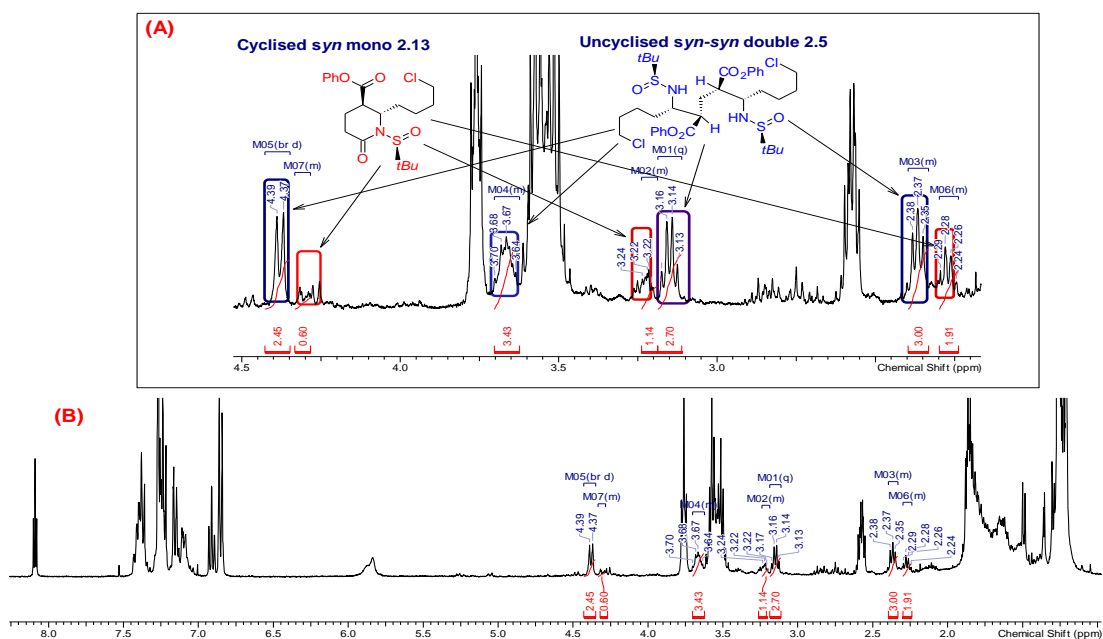


Figure 2.7: The ^1H NMR spectrum of the crude double imino-aldol reaction mixture

The mixture of mono imino-aldol products was separated to give three components; the major product was the cyclised *syn* mono imino-aldol **2.13**, initially isolated as an oil. Fortunately, on storage in the freezer **2.13** gave crystals suitable for determining the stereochemistry by single crystal X-ray (Figure 2.8). The mono *syn* imino-aldol (uncyclised) **2.16** was also present as a minor product with some small amount of cyclised *anti*-mono **2.17**. The diastereoisomer of *syn*-imino-aldol adduct **2.16** was recrystallised from hexane and its structure confirmed by single crystal X-ray (Figure 2.8).

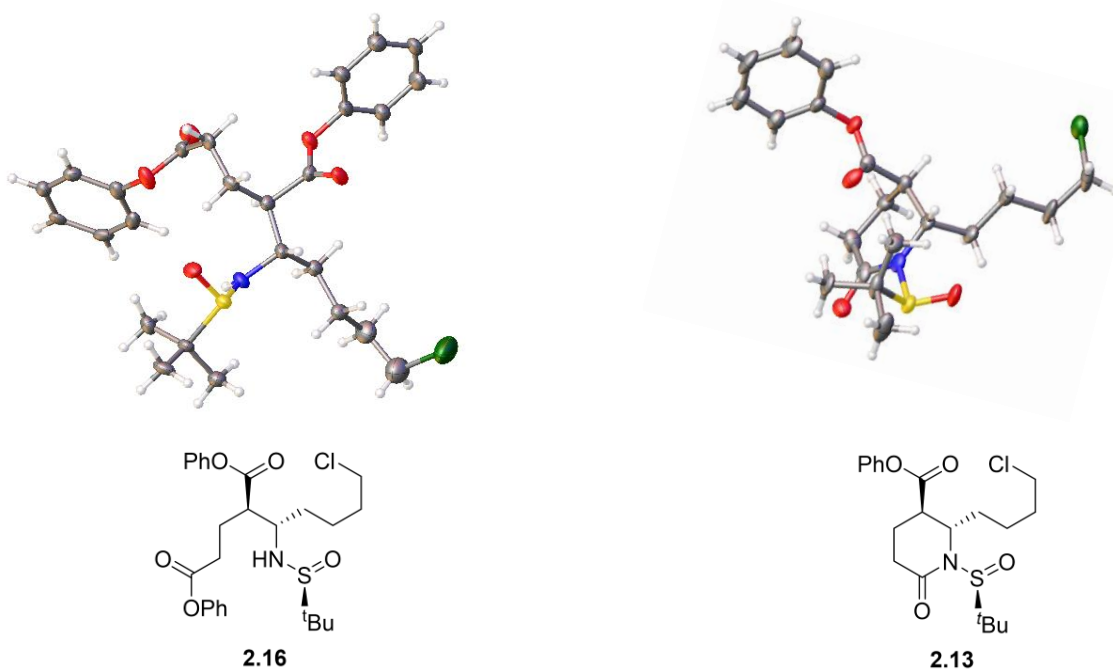


Figure 2.8: X-ray crystal structures of mono *syn* imino-aldol **2.16** and its cyclised product **2.13**

In different experiments the ratios of *syn*-mono imino-aldol **2.16** and its cyclised product **2.13** were found to vary, this can be seen by ^1H NMR spectroscopy (**Figure 2.9**). Several diagnostic chemical shifts were identified in the ^1H NMR spectra allowing identification of **2.16** and **2.13** in the crude mixtures. The N-H proton in mono imino-aldol **2.16** (labelled B) is observed as a 1 H doublet with a chemical shift of 4.20 ppm. During the course of the reaction a (dt) with chemical shift of 4.30 ppm was observed, which indicated formation of the cyclised adduct **2.13**. This ^1H NMR shift is consistent with the cyclisation of **2.16** to **2.13**, which proceeds slowly under the reaction conditions. Also, the β -methine proton of **2.16** labelled D is observed as a 1 H multiplet with a chemical shift of 3.28–3.21 ppm, and under the reaction conditions converted to (td, $J = 5.7, 2.0$ Hz, 1H) with a chemical shift of 3.21 ppm in **2.13**.

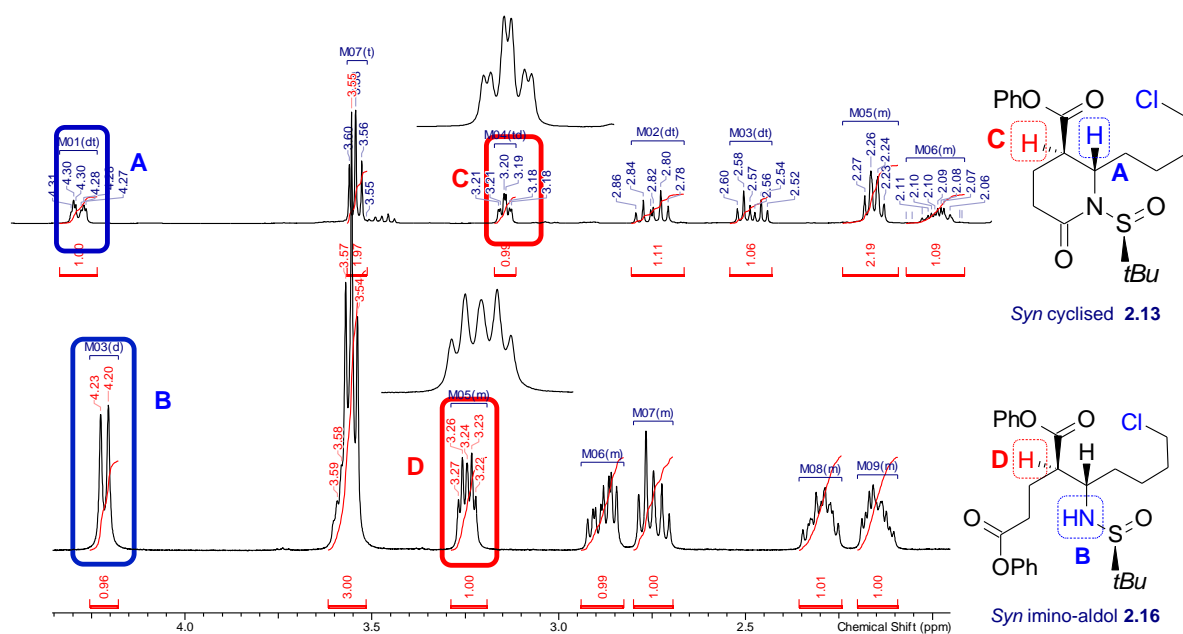
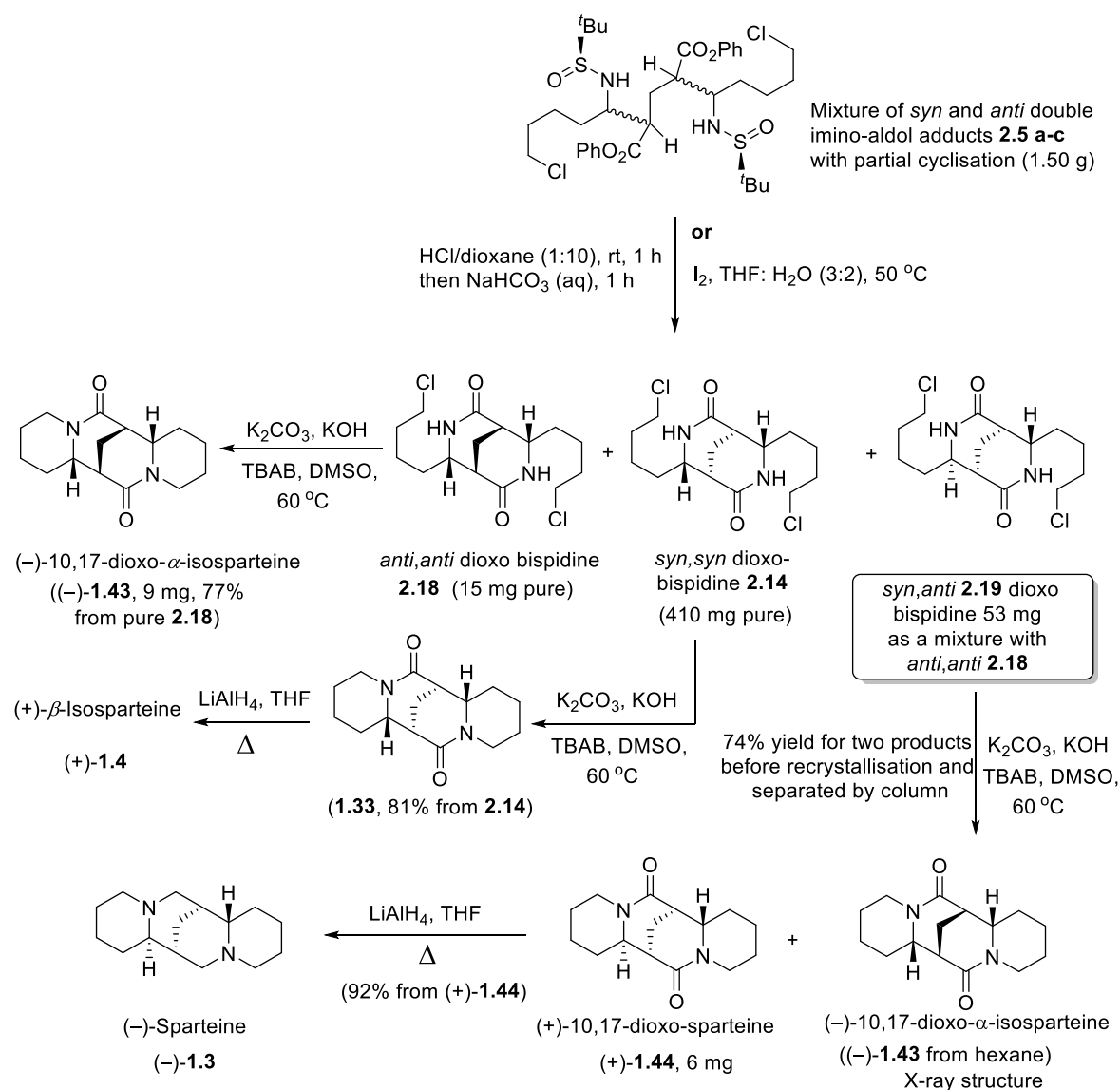


Figure 2.9: ^1H NMR spectra for mono *syn* imino-aldol **2.16** and its cyclised *syn* product **2.13**

Now that the structural and stereochemical determination of the products **2.5**, **2.13**, **2.16** and **2.17** had been achieved. Attention moved on to the complex mixture of double imino-aldol products, which will be described in the next section.

2.1.7 Determination of the remaining structures from imino-aldol reaction

Having completed the first total syntheses of (+)-10,17-dioxo- β -isosparteine (+)-**1.33** and (+)- β -isosparteine (+)-**1.4**, work began to determine the structures of the remaining products from the double imino-aldol reaction. Despite the presence of multiple products, we succeeded in determining the stereochemistry of double imino-aldol adducts by a sequence of reactions and separations described below (**Scheme 2.8**).



Scheme 2.8: Characterisation of the double imino-aldols by conversion to (-)-10,17-dioxo- α -isosparteine and (-)-sparteine.

The mixture of double imino-aldol products was collected after separation from the mono imino-aldol adducts **2.13**, **2.16** and **2.17** by careful column chromatography. The mixture of double imino-aldol products included uncyclised and partially cyclised components (*syn,syn* (**2.5a**), *anti,anti* (**2.5b**) and *syn,anti* (**2.5c**)).

Two methods for deprotection and cyclisation of the crude materials were used. The first involved deprotection of *N*-sulfinyl group of the mixture using conc. HCl followed by neutralisation with saturated aq. NaHCO₃. The second method used I₂ and THF:H₂O (3:2) (**Scheme 2.8**). Both methods gave similar results, which can be seen as three components by TLC (*eluent*: EtOAc/MeOH, 19:1) (**Figure 2.10**). Following column chromatography three fractions were separated; the first fraction is *syn,syn* dioxobispidine **2.14**, the second fraction *anti,anti* dioxobispidine **2.18** and the last fraction is *syn,anti* dioxobispidine **2.19**.

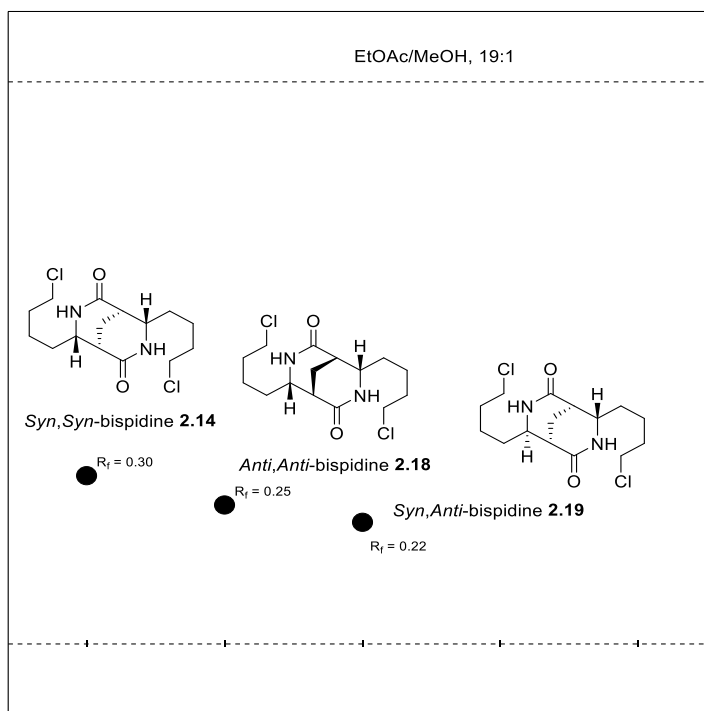


Figure 2.10: Representation of the TLC plate showing R_f values for bicycled products

Syn,syn dioxo-bispidine **2.14** and *anti,anti* dioxo-bispidine **2.18** were separated as pure diastereoisomers by careful column chromatography (silica gel, *eluent*: EtOAc/hexane 9:1 then EtOAc/MeOH, 19:1). While, *syn,anti* dioxo-bispidine **2.19** was isolated as a mixture contaminated with *anti,anti* **2.18**. Although it was not possible to separate the *anti,anti* and *syn,anti* bispidines **2.18** and **2.19** completely, cyclisation under basic conditions provided (–)-10,17-dioxo- α -isosparteine ((–)-**1.43**) as a crystalline solid from hexane. The X-ray structure confirmed the relative stereochemistry of (–)-**1.43**. Double cyclisation of the mixture of dioxo-bispidines (**2.18**, **2.19**) under the same basic conditions afforded dioxo-sparteine diastereoisomers (**1.43**, **1.44**) in ratio of (10:1), which were separated by careful column chromatography (silica gel, *eluent*: EtOAc 100% then EtOAc/MeOH, 98:2 to 95:5) giving (–)-10,17-dioxo- α -isosparteine ((–)-**1.43**) as the less polar minor fraction and (+)-10,17-dioxosparteine ((+)-**1.44**) as the more polar fraction. The dioxosparteine isomers (**1.33**, **1.43** and **1.44**) were identified by analysis of their ¹H-NMR spectra and the absolute stereochemistry of (–)-10,17-dioxo- α -isosparteine ((–)-**1.43**) was confirmed by optical rotation

(**Figure 2.11**). Finally, (–)-sparteine was obtained by reduction of (+)-10,17-dioxosparteine using LiAlH_4 .

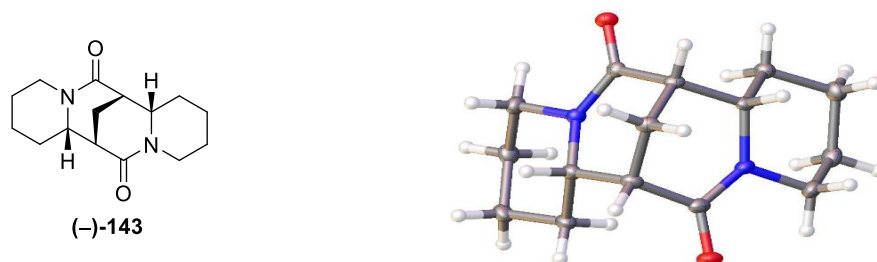


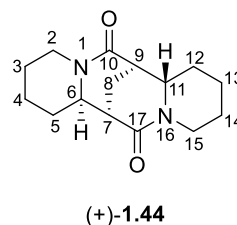
Figure 2.11: X-ray crystal structure of (–)-10,17-dioxo- α -isosparteine ((–)-**143**)

2.1.8 Determination of the absolute stereochemical assignment of sparteine isomers

The spectroscopic (^1H , ^{13}C NMR and FT-IR), and physical data for our synthetic (+)-10,17-dioxosparteine and (–)-sparteine were consistent with literature values (**Table 2.4** and **Table 2.5**).^{84,92} While optically pure 10,17-dioxo- α -isosparteine has not been previously reported in the literature, melting point values were consistent with literature (**Table 2.6**).^{15,66}

Table 2.4. ^{13}C NMR data for (+)-10,17-dioxo-sparteine ((+)-**1.44**) and recorded physical data.

Carbon	$\delta\text{C}^{\text{a}}$	Lit. ⁸⁴ $\delta\text{C}^{\text{b}}$
17	170.2	170.2
10	166.4	166.3
11	60.0	59.9
6	59.2	59.1
15	43.4	43.3
9	42.8	42.7
2	42.3	42.2
7	42.0	41.9
12	32.6	32.5
5	31.2	31.2
14	25.1	25.1
3	25.0	24.9
13	24.9	24.8
4	24.2	24.1
8	21.9	21.8



Physical data:

Recorded data: m.p. = 62 – 66 °C

Literature data: Lit.⁸⁴ m.p. = 60 – 65 °C

Optical Rotation:

Recorded data current work:

$[\alpha]_{\text{D}}: +70.3$ (c 0.6, CH_3Cl , 20 °C)

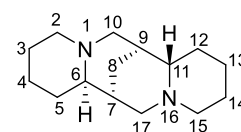
Literature data:

$[\alpha]_{\text{D}}: +72.3$ (c 1.0 in CH_3Cl , 20 °C) Lit.⁸⁴

^a The current work: recorded in CDCl_3 at 101 MHz. ^b Recorded in CDCl_3 at 75 MHz.

Table 2.5. ^{13}C NMR data for (–)-sparteine ((–)-**1.3**) and recorded physical data

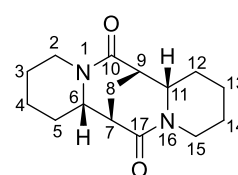
Carbon	$\delta_{\text{c}}^{\text{a}}$	Lit. ⁸⁴ $\delta_{\text{c}}^{\text{b}}$	Lit. ⁹² $\delta_{\text{c}}^{\text{c}}$
6	66.4	66.5	66.5
11	64.5	64.4	64.4
10	61.8	61.9	61.9
2	56.2	56.2	56.2
15	55.3	55.4	55.4
17	53.4	53.6	53.6
7	35.9	36.1	36.0
12	34.3	33.0	34.7
9	33.0	32.5	33.0
5	29.3	29.3	29.3
8	27.5	27.6	27.6
3	25.8	25.9	25.9
14	25.6	25.8	25.8
4	24.6	24.8	24.8
13	24.4	24.7	24.7

(–)-**1.3****Optical Rotation:***Recorded data current work:* $[\alpha]_{\text{D}}: -16.9$ (c 0.5 absolute EtOH, 20 °C)*Literature data:* $([\alpha]_{\text{D}} -18.1$ (c 1.3 in EtOH)) Lit.⁸⁴; $([\alpha]_{\text{D}} -20.4$ (c 1.3 in EtOH)) Lit.⁹²

^a The current work: recorded in CDCl_3 at 101 MHz. ^b Recorded in CDCl_3 at 75 MHz. ^c Recorded in CDCl_3 at 100.6 MHz.

Table 2.6. ^{13}C NMR data for (–)-10,17-dioxo- α -isoparteine ((–)-**1.43**) and recorded physical data

Carbon	$\delta_{\text{c}}^{\text{a}}$
10,17	167.9
6,11	58.8
2,15	42.4
7,9	41.8
5,12	31.3
3,14	25.2
8	24.4
4,13	24.3

Physical data:*Recorded data:* m.p. = 160 – 164 °C*Literature data:*Lit.^{15,66} m.p. = 159 – 160 °C**Optical Rotation:***Recorded data current work:* $[\alpha]_{\text{D}}: -58.8$ (c 1.0, MeOH, 20 °C)*Literature data:* Not recorded(–)-**1.43**

^a The current work: recorded in CDCl_3 at 101 MHz.

2.1.9 Elaboration of *syn* mono imino-aldol product towards a synthesis of (-)-sparteine

In this section, attempts to synthesise sparteine from *syn* mono imino-aldol adduct **2.16** will be described. Exploitation of the *syn* mono imino-aldol adduct **2.16** as a starting point to access (-)-sparteine requires a second imino-aldol reaction with *anti*-selectivity (**Figure 2.12**). The imino-aldol reaction requires deprotonation of adduct **2.16** in the presence of a suitable base followed by selective alkylation using halo imine to give *syn,anti* (**2.5c**) double imino-aldol. Deprotection of the sulfinyl groups and then cyclisation could give access to dioxo-sparteine **1.44**. Finally, reduction of dioxo-sparteine would complete a synthesis of sparteine.

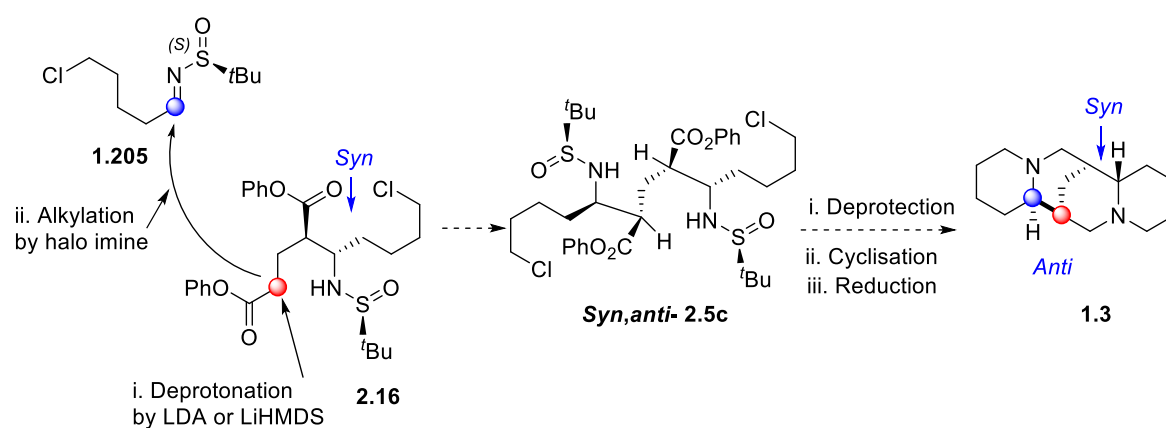
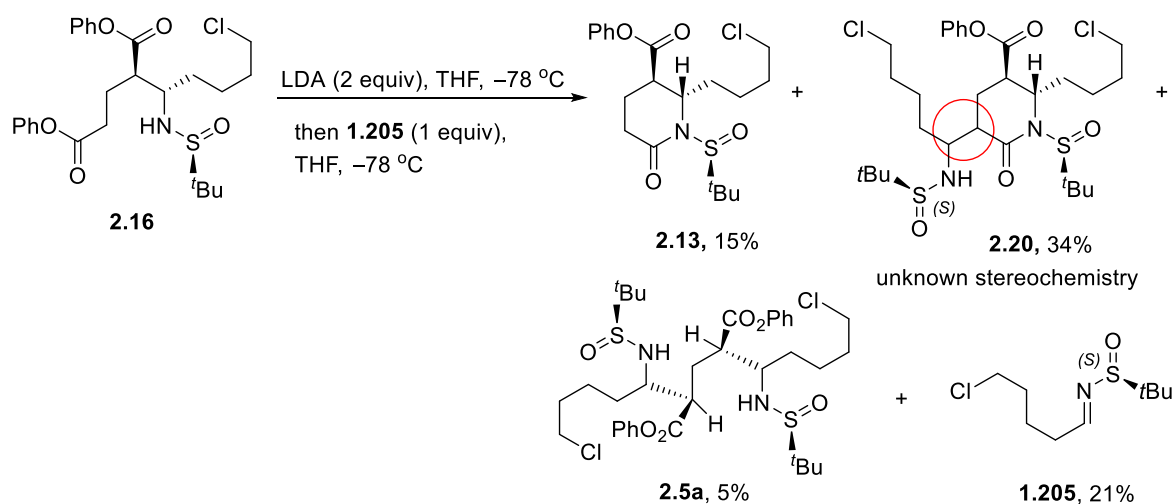


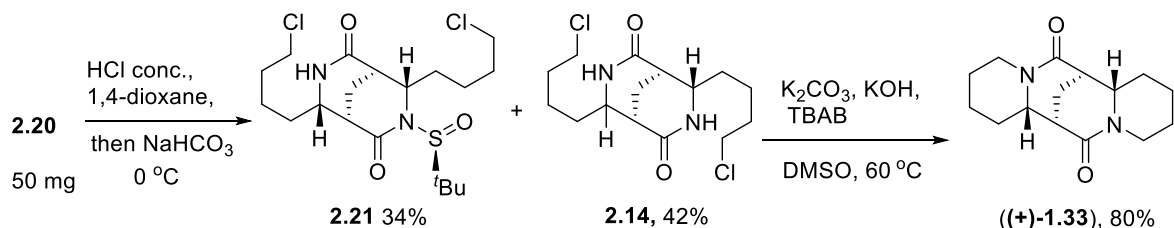
Figure 2.12: Proposed synthesis of (-)-sparteine from *syn* imino-aldol adduct **2.16**

Although *syn* imino-aldol **2.16** was only obtained as a minor product from different imino-aldol reactions in yields from 5 to 15%, we wished to use it as a starting point to access sparteine. We would need to go back and optimise the formation of **2.16** later if this route to sparteine proved to be successful. Formation of **2.23** required deprotonation of **2.16** using two equivalents of base to form the dianion followed by dropwise addition of one equivalent of halo imine **1.205** at $-78\text{ }^{\circ}\text{C}$ (**Scheme 2.9**). The crude mixture of products was separated by column chromatography giving different components which were difficult to identify. Several imino-aldol reactions were performed using LDA or LiHMDS giving different products including; cyclised-*syn* **2.13**, partially cyclised double imino-aldol **2.20**, double imino-aldol **2.5a** and recovered halo imine **1.205**. The major product **2.20** was identified firstly by mass spectrometry (MS) as a partially cyclised.



Scheme 2.9: Imino-aldol reaction of *syn* mono imino-aldol adduct **2.16**

The imino-aldol products were obtained in better yield by using LDA compared to LiHMDS. Unfortunately, we were not able to identify the stereochemistry of the double imino-aldol product **2.20** from analysis of their ^1H NMR spectra. The main double imino-aldol product **2.20** was forwarded to the next step to form bispidine by deprotection and cyclisation under acidic conditions (**Scheme 2.10**), as described below.

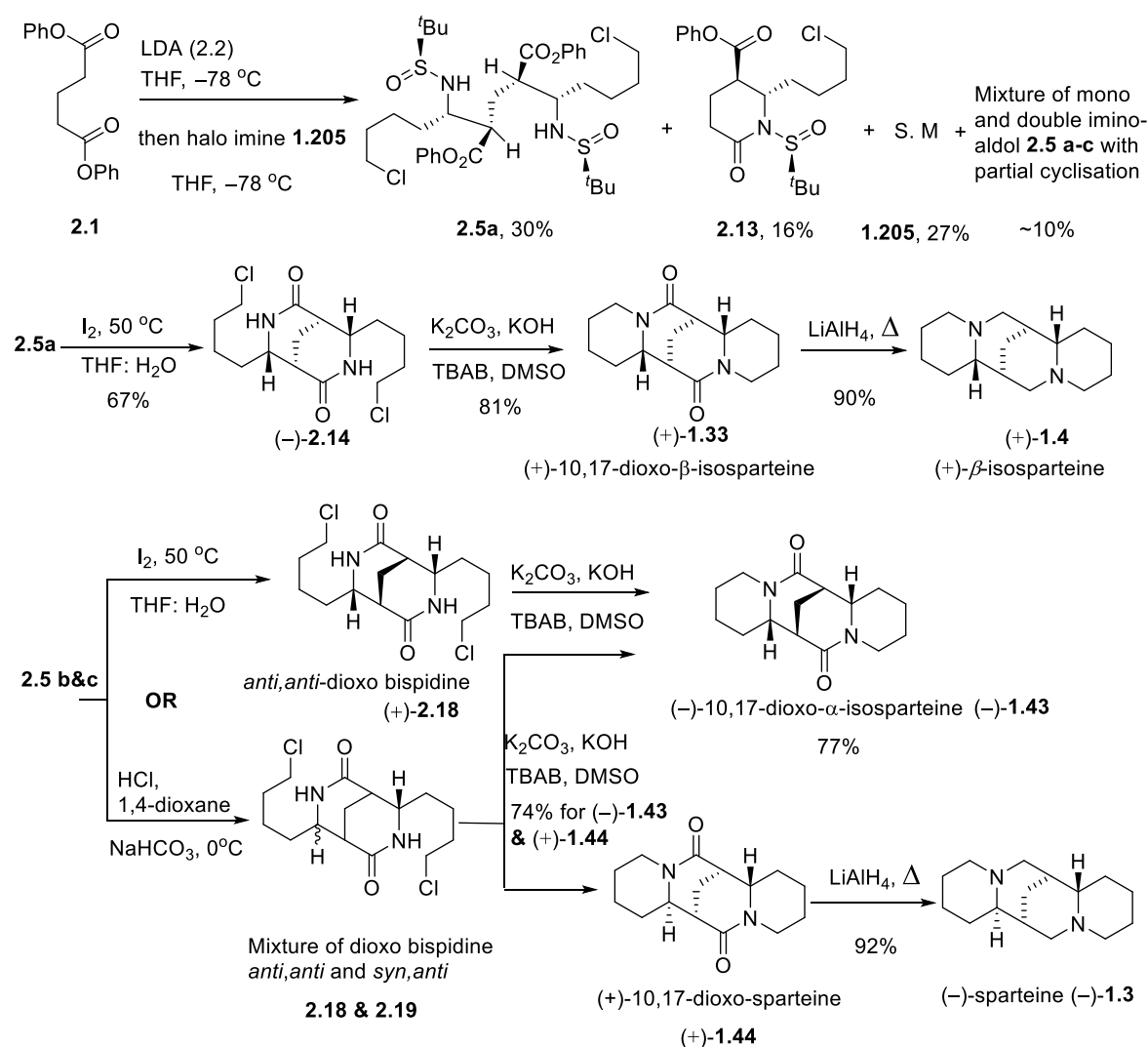


Scheme 2.10: The synthesis of (+)-10,17-dioxo- β -isosparteine from imino-aldol adduct **2.20**

Deprotection and cyclisation of the partial cyclised adduct **2.20** under acidic conditions and then NaHCO_3 afforded bispidine **2.14** and mono protected bispidine **2.21** (**Scheme 2.10**). The stereochemistry of both bispidines **2.14** and **2.21** were shown clearly by ^1H NMR. Cyclisation of both bispidines **2.14** and **2.21** under basic conditions using phase transfer catalyst TBAB gave impure dioxo- β -isosparteine. The stereochemistry of dioxo- β -isosparteine confirms the stereochemistry of the cyclised double imino-aldol adduct **2.20** and bispidine **2.14**, and it also validates the stereoselectivity assumptions regarding imino-aldol reaction of adduct **2.16**, ultimately leading to the synthesis of (+)-10,17-dioxo- β -isosparteine, rather than (+)-10,17-dioxo-sparteine (**Figure 2.12**).

2.1.10 Conclusions:

The total synthesis of (+)- β -isosparteine was achieved in 15% yield over 4 steps from halo imine **1.205** by using a diastereoselective double imino-aldol reaction (**Scheme 2.11**). The double imino-aldol reaction was carried out using diphenyl glutarate (**2.1**) and halo imine **1.205** to generate four stereocentres within double imino-aldol adduct **2.5a** with *syn,syn* relative stereochemistry in 30% yield. In addition, *syn* and *anti*-cyclised mono imino-aldol adducts (**2.13** & **2.17**), and mixture of double imino-aldol adducts (**2.5a-c**) were obtained as minor products. The stereochemistry of the minor double imino-aldol adducts (**2.5b** & **c**) have been investigated in order to determine their stereochemistry, and shown to be (*anti,anti* **2.5b** and *syn,anti* **2.5c**). The stereochemistry of *anti,anti*-product **2.5b** provides the skeleton of (+)- α -isosparteine whose stereochemistry was confirmed by single crystal X-ray after conversion to (+)-10,17-dioxo- α -isosparteine. The synthesis of (-)-sparteine from the minor product *syn,anti* diastereoisomer **2.5c** confirmed its relative and absolute stereochemistry.



Scheme 2.11: The total synthesis of (+)- β -isosparteine and (-)-sparteine

2.2 Synthesis of (–)-epilupinine from mono imino-aldol adducts of diphenyl glutarate.

The following section will discuss an approach to the synthesis of (–)-epilupinine ((–)-**1.1**) using mono imino-aldol adduct **2.13** obtained from diphenyl glutarate (**2.1**) reacting with halo imine **1.205**. The cyclised imino-aldol **2.13** was described as a minor by-product in the previous section from the double imino-aldol reaction. Here we will also discuss attempts to optimise the mono imino-aldol adducts of different side chain functionalised imines.

2.2.1 Retrosynthetic analysis of (–)-epilupinine

Our approach exploits the selective formation of the cyclised imino-aldol adduct **2.13** from diphenyl glutarate to access (–)-epilupinine by reductive cyclisation (**Figure 2.13**). A short synthesis of (–)-epilupinine requires *N*-sulfinyl deprotection of cyclised adduct **2.13** followed by reduction of lactam and ester groups and then cyclisation of the amine onto the side chain halide. The cyclised adduct **2.13** was previously obtained from double imino-aldol reaction as a minor product in low yield. This strategy first requires optimisation to favour the mono adduct **2.13** from diphenyl glutarate (**2.1**) with one equivalent of halo imine **1.205**.

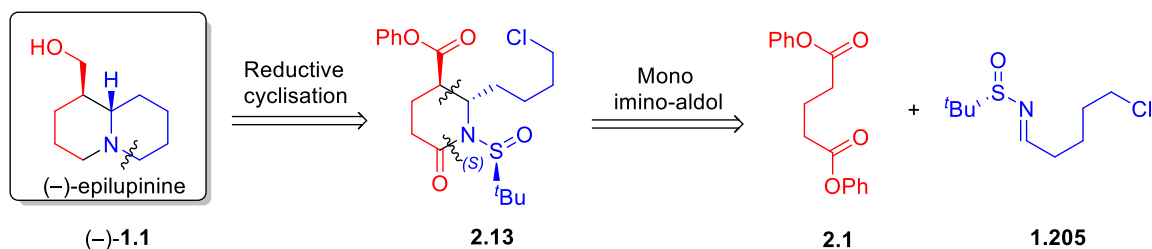


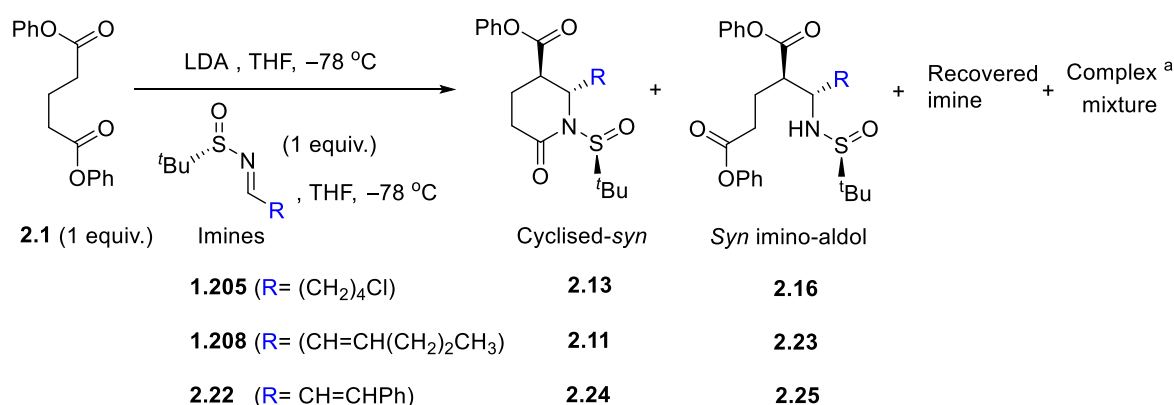
Figure 2.13: Retrosynthetic analysis of (–)-epilupinine from halo imine **1.205**

2.2.2 Optimisation of mono imino-aldol adduct formation

Our attention first focused on the synthesis of (–)-epilupinine (–)-**1.1** from mono imino-aldol product **2.13**.^{134,135} The amount of the mono imino-aldol adduct **2.13** obtained from double imino-aldol reaction was clearly not sufficient as a starting point to the synthesis of (–)-epilupinine. Different conditions and imine derivatives were investigated to obtain mono imino-aldol adducts such as **2.13** using equal amounts of diphenyl glutarate (**2.1**) and imines. The optimisation of mono imino-aldol reaction was investigated using 3 different imines with diphenyl glutarate (**2.1**) using different amounts of LDA (**Table 2.7**). Employing an equal amount of diphenyl glutarate and imine derivatives with one equivalent of LDA gave mono imino-aldol adducts in low isolated yield together with recovered imine (**entries 1, 4 & 7, Table 2.7**). We believe that the low isolated yield may be

due to side reactions as such intermolecular Claisen condensation of the mono enolate of diphenyl glutarate (**2.1**), although the keto-ester product was not observed. Therefore, the quantity of LDA was increased 2 equivalents (**entries 2, 5 & 8, Table 2.7**) leading to significantly improved yields. The dianion of diphenyl glutarate is likely to possess increased nucleophilicity, leading to more efficient reaction with imine, and also avoiding intermolecular Claisen condensation.

Table 2.7: Optimisation of mono imino-aldol reaction using different imines

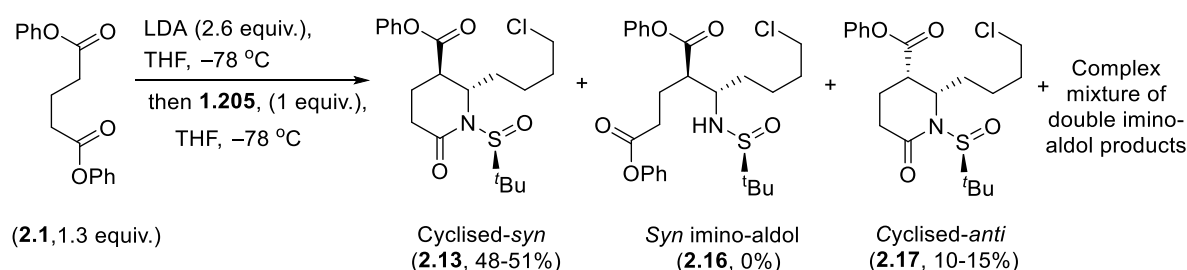


R	Entry	Amount of LDA (equiv.)	Yield of <i>syn</i> cyclised	Yield of <i>syn</i> imino-aldol	Recovered imine
	1	1.0	2.13 (21%)	2.16 (6%)	34%
	2	2.0	2.13 (40%)	2.16 (11%)	1%
	3	3.0	2.13 (38%)	2.16 (10%)	5%
	4	1.0	2.11 (20%)	2.23 (N.D.)	30%
	5	2.0	2.11 (38%)	2.23 (12%)	19%
	6	3.0	2.11 (35%)	2.23 (N.D.)	3%
	7	1.0	2.24 (19%)	2.25 (N.D.)	35%
	8	2.0	2.24 (35%)	2.25 (3%) ^b	12%
	9	3.0	2.24 (33%)	2.25 (N.D.)	5%

^a The complex mixture containing small amounts of mono *anti* imino-aldols adducts derivatives were separated by column chromatography, see details in experimental part. ^b Isolated as an impure and no assignment was reported. N.D= not determined

Small amounts of imine derivatives were recovered despite increasing the amount of LDA to 3 equivalents (**entries 3, 6 & 9, Table 2.7**). A mixture of minor products including cyclised-*anti* **2.17** and double imino-aldol products **2.5** (**a-c**) were also obtained from the reactions after careful separation by column chromatography. Although the best yield of desired product **2.13** was obtained (**entry 2, Table 2.7**), isolation of the *syn*-imino-aldol **2.16** as a minor product suggested

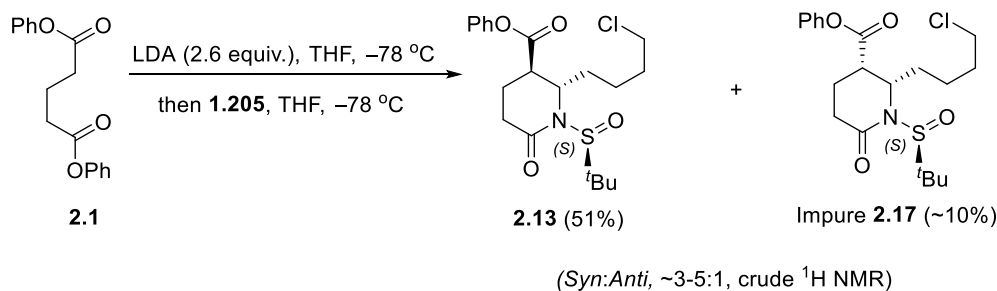
that the yield could be improved further. It was found that the amount of **2.16** could be minimised through slow addition of halo imine **1.205** by syringe pump. The best result was obtained from the mono imino-aldol reaction of halo imine **1.205** giving the highest yield of 51% of cyclised *syn* **2.13** using 2.6 equivalent of LDA at $-78\text{ }^{\circ}\text{C}$, and slow addition of imine **1.205** to the dienolate solution using a syringe pump at $-78\text{ }^{\circ}\text{C}$ (**Scheme 2.12**). Subsequently, careful quench of the reaction by keeping the temperature under $-70\text{ }^{\circ}\text{C}$, and then leaving the quenched reaction solution warm to rt. These conditions also gave cyclised-*anti* **2.17** as impure product and complex mixture of double imino-aldol products but avoided isolation of *syn* imino-aldol **2.16** and recovery of halo imine **1.205**. The yields were consistent over several experiments giving cyclised-*syn* **2.13** in 48-51% and cyclised-*anti* **2.17** in 10-15% and complex mixture of double imino-aldol products as minor components. Separation of remaining mono imino-aldol mixture was completed by careful column chromatography.



Scheme 2.12: Optimised mono imino-aldol reaction

2.2.3 Determination the diastereoselectivity of imino-aldol products

The ratio of *syn* and *anti* imino-aldols **2.13** and **2.17**, determined from the crude ^1H NMR spectra, varied under the reaction conditions between $\sim 3:1$ and $5:1$ (**Scheme 2.13**). The diastereoselectivity was improved by slow addition of imine **1.205** around the bottom of the flask wall and keeping the reaction temperature around at $-78\text{ }^{\circ}\text{C}$. However, when the reaction temperature was allowed to warm above $-70\text{ }^{\circ}\text{C}$ during the addition, the yield and the selectivity decreased.



Scheme 2.13: The diastereoselectivity of the mono imino-aldol reaction

The cyclised mono imino-aldol products were identified by comparison of their β methine protons in ^1H NMR spectra. The multiplet at 4.30 ppm corresponds to cyclised *syn*-adduct **2.13** (S_S , $2S$, $3R$) (**Figure 2.14**). The multiplet at 4.46 ppm corresponds to the minor cyclised *anti*-adduct **2.17** (S_S , $2S$, $3S$). The NH doublet for *syn* imino-aldol adduct **2.16** (S_S , $2S$, $3R$) at 4.22 ppm was not observed in ^1H NMR spectra from crude reaction mixtures obtained under the optimised conditions (**see experimental part**).

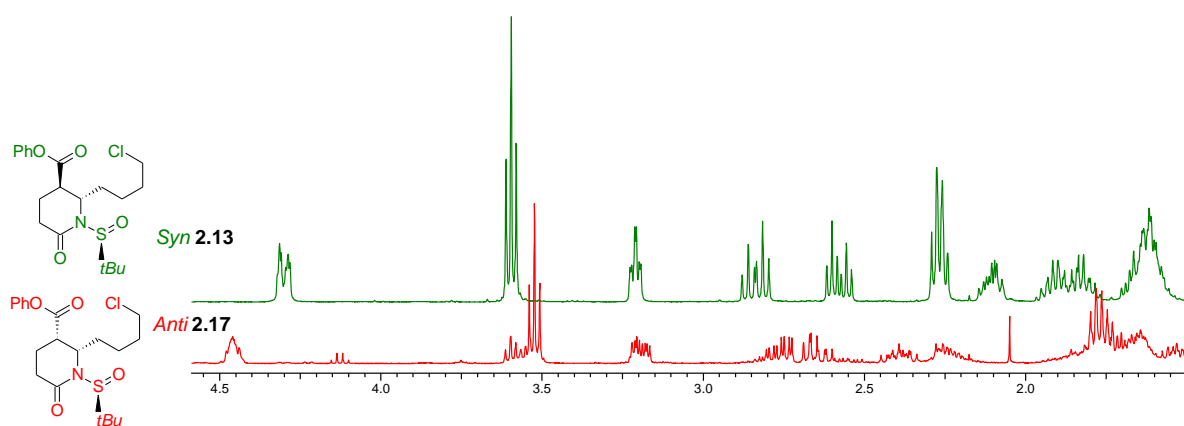
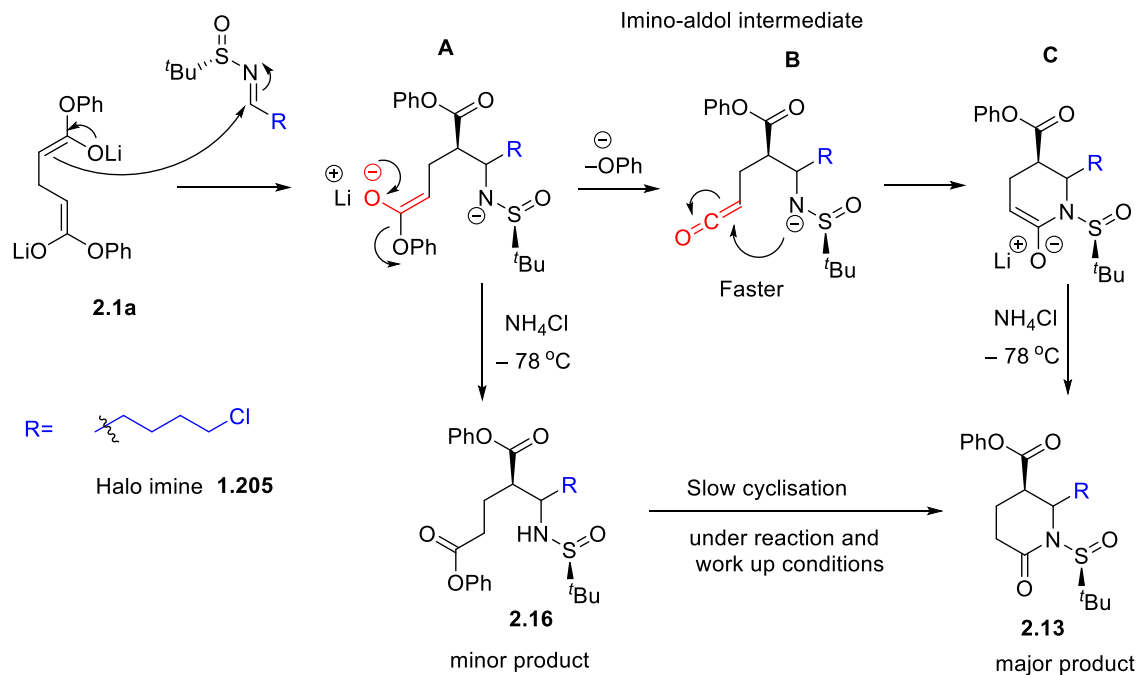


Figure 2.14: ^1H NMR (400 MHz) for cyclised *syn* and *anti*-adducts **2.13** and **2.17**

2.2.4 The mechanism of mono imino-aldol reaction

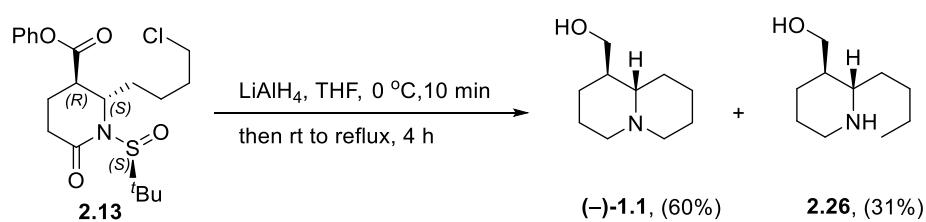
A proposed mechanistic pathway to account for the formation of the cyclised mono imino-aldol product is outlined in Scheme 2.14. The dianion of diphenyl glutarate **2.1a** undergoes an initial *syn*-selective imino-aldol reaction with the imine to give enolate intermediate **A**. The enolate **A** can convert to ketene intermediate **B** after loss of phenoxide ion. The highly reactive ketene intermediate **B** can then undergo cyclisation to form enolate lactam **C**, which gives cyclised imino-aldol adduct **2.13** upon acidic work-up. Alternatively, protonation of the enolate intermediate **A** on work-up will give the uncyclised (normal) imino-aldol **2.16**. Both **2.13** and **2.16** have been isolated and their relative amounts were dependent on the reaction conditions. Slow cyclisation of the mono imino-aldol **2.16** can also occur under reaction and work-up conditions.



Scheme 2.14: Proposed mechanism for cyclisation of imino-aldol intermediates

2.2.5 Completion of the synthesis of (–)-epilupinine from cyclised-*syn* imino-aldol **2.13**

The synthetic route to (–)-epilupinine (**1.1**) was completed by reductive cyclisation of *syn*-adduct **2.13** in refluxing LiAlH_4 giving (–)-epilupinine along with over reduced by-product **2.26** (**Scheme 2.15**). The total synthesis of (–)-epilupinine (**1.1**) was achieved over two steps in 31% overall yield from halo imine **1.205**.



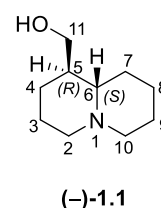
Scheme 2.15: Synthesis of (–)-epilupinine from **2.13**

2.2.6 Confirmation of the absolute stereochemistry of (–)-epilupinine

The analytical data obtained for synthetic (–)-epilupinine was in good agreement with that previously reported by us and with literature values.^{134,140,142,143} Specific rotation of epilupinine showed a negative value supporting the assigned major enantiomeric product of our imino-aldol reaction.^{140,142} Comparison of physical and ¹H and ¹³C NMR data with the reported literature values is provided in (**Table 2.8**).^{134,135,143}

Table 2.8: Comparison of recorded and literature spectroscopic data for (–)-epilupinine

assignment	Recorded δ ppm ^a	Lit. ¹³⁴ δ ppm ^b	Lit. ¹³⁵ δ ppm ^c	Lit. ¹⁴³ δ ppm ^d
C2	56.9	56.9	56.8	56.9
C3	25.1	25.0	24.9	25.0
C4	24.6	24.5	24.4	24.5
C5	44.0	43.9	43.8	43.9
C6	64.2	64.3	64.4	64.3
C7	28.2	28.2	28.1	28.2
C8	29.8	29.7	29.6	29.7
C9	25.6	25.5	25.4	25.6
C10	56.6	56.6	56.5	56.6
C11	64.8	64.5	64.4	64.6



Optical Rotation:

Recorded data current work :

$[\alpha]_D$: –31.2 (c 0.5 absolute EtOH, 20 °C)

Literature data:

lit.¹³⁴ $[\alpha]_D$: –29.2 (c 1.00, EtOH, 26 °C),

lit.¹³⁵ $[\alpha]_D$: –30.0 (c 0.90, EtOH, 22 °C)

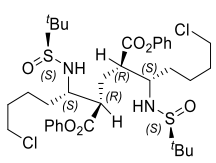
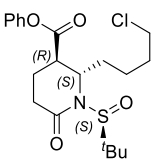
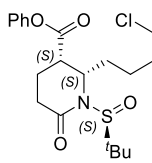
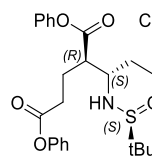
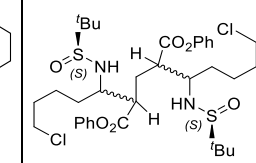
lit.¹⁴³ $[\alpha]_D$: –28.5 (c 0.72, EtOH, 27 °C)

^a The current work: recorded in CDCl₃ at 101 MHz. ^b Recorded in CDCl₃ at 100 MHz. ^c Recorded in CDCl₃ at 100 MHz. ^d Recorded in CDCl₃ at 100 MHz.

2.2.7 Comparison of the product distribution observed for the mono and double imino-aldol reactions.

Both “single” and “double” imino-aldol reaction conditions gave the same products but with different yields (**Table 2.9**). The double imino-aldol was performed by using 1 equiv. of diphenyl glutarate **1.173** with 2 equiv. of halo imine **1.205** and 2.2 equiv. of LDA at –78 °C as explained in the previous section. However, the mono imino-aldol reaction could be favoured by using 1.3 equiv. of diphenyl glutarate **1.173** with 1 equiv. of halo imine **1.205** and 2.6 equiv. of LDA at –78 °C. The yields of the different products were obtained from isolation of pure compounds, and estimation using ¹H NMR for mixed fractions (**Table 2.9**).

Table 2.9: Summary of the main identified components^a from reaction under optimised double (conditions A)^b and mono (conditions B)^c imino-aldol reactions:

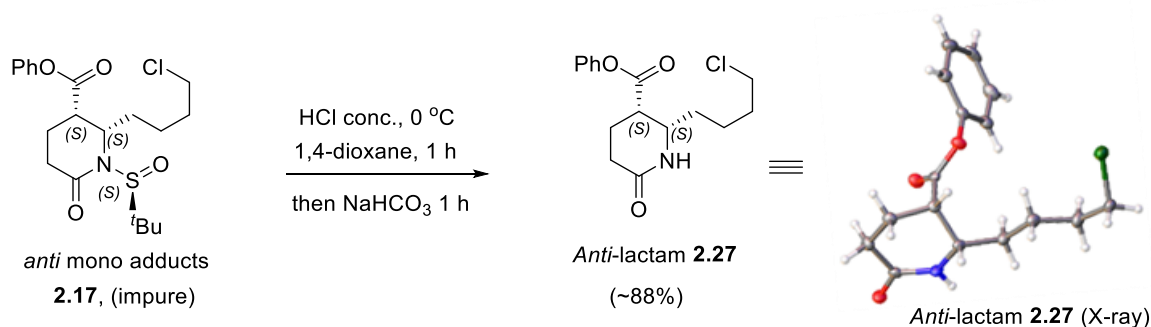
Products	 Syn,syn double imino-aldol 2.5a	 Cyclised-syn 2.13	 Cyclised-anti 2.17	 Syn imino-aldol 2.16	 Mixture of diastereoisomers ^d
Yield from conditions A	30% ^f	16% ^f	~5% ^f	~7% ^f	~10% ^e
Yield from conditions B	(2% - 15%) ^{e,f}	(38% - 51%) ^{e,f}	(3% - 13%) ^{e,f}	(0% - 15%) ^{e,f}	~5% (26 : 3 : 1) ^e

^a. Isolated purified products obtained from reactions. Other very minor components not identified.

^b. Conditions A: optimised double imino-aldol reaction conditions: 1 equiv. of **1.173** with 2 equiv. of **1.205** in 2.2 equiv. of LDA at $-78\text{ }^{\circ}\text{C}$. ^c. Conditions B: optimised mono imino-aldol reaction conditions: 1.3 equiv. of **1.173** with 1 equiv. of **1.205** in 2.6 equiv. of LDA $-78\text{ }^{\circ}\text{C}$. ^d. Unseparated mixture of diastereoisomers (*syn,anti* (**2.5c**) and *anti,anti* (**2.5b**)). ^e. Determined by ^1H NMR spectra from the crude product. ^f. Determined by column chromatography.

2.2.8 Structure determination of the minor imino-aldol products

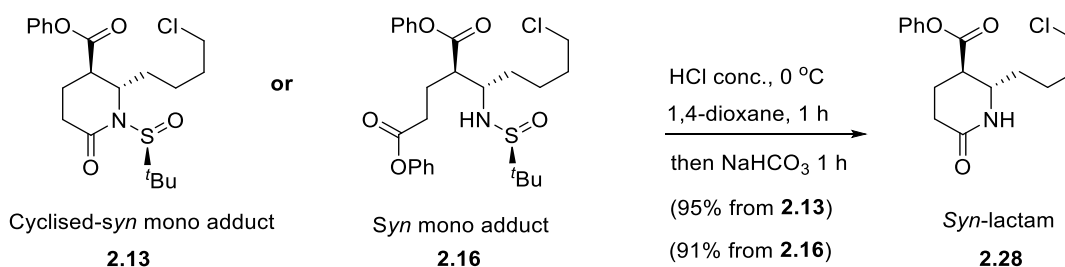
To confirm the absolute stereochemistry of cyclised-*anti* mono adduct **2.17**, we employed acidic conditions to remove the *N*-sulfinyl protection (**Scheme 2.16**). Following neutralisation with aq. NaHCO_3 , the *anti*-lactam **2.27** was obtained as a white crystalline solid. Recrystallisation from hexane gave crystals suitable for X-ray structure determination, confirming the *anti*-relationship.



Scheme 2.16: Confirmation of the structure for *anti*-lactam **2.27** by X-ray

The stereochemistry of the cyclised *syn*-imino-aldol **2.13** and the *syn*-imino-aldol **2.16** were confirmed by converting them to a common product (**Scheme 2.17**). Treatment of either compound

2.13 or **2.16** with acid led to removal of the sulfinyl-protecting group, and subsequent base treatment gave *syn*-lactam **2.28**.



Scheme 2.17: Formation of *syn*-lactam **2.28** from cyclised and imino-aldol adducts **2.13** & **2.16**

The stereochemistry of *syn*-lactam **2.28** and *anti*-lactam **2.27** were supported by analysis of their ^1H NMR spectra (**Figure 2.15**). As a result, the mixture of diastereoisomers present in the imino-aldol reaction can be identified from the crude ^1H NMR spectra (**Figure 2.15**). Inspection of the α H and β H multiplet for the diastereomers of lactam *syn* (*R,S*) and *anti* (*S,S*) at 2.69 and 3.22 ppm respectively show a clear difference. In addition, the NH lactam signal for *syn* (*R,S*) and *anti* (*S,S*) show a broad peaks at 6.8 and 6.0 ppm, respectively. The identification of the double imino-aldol adducts **2.5** (a-c) was described in the previous section (**Scheme 2.8**).

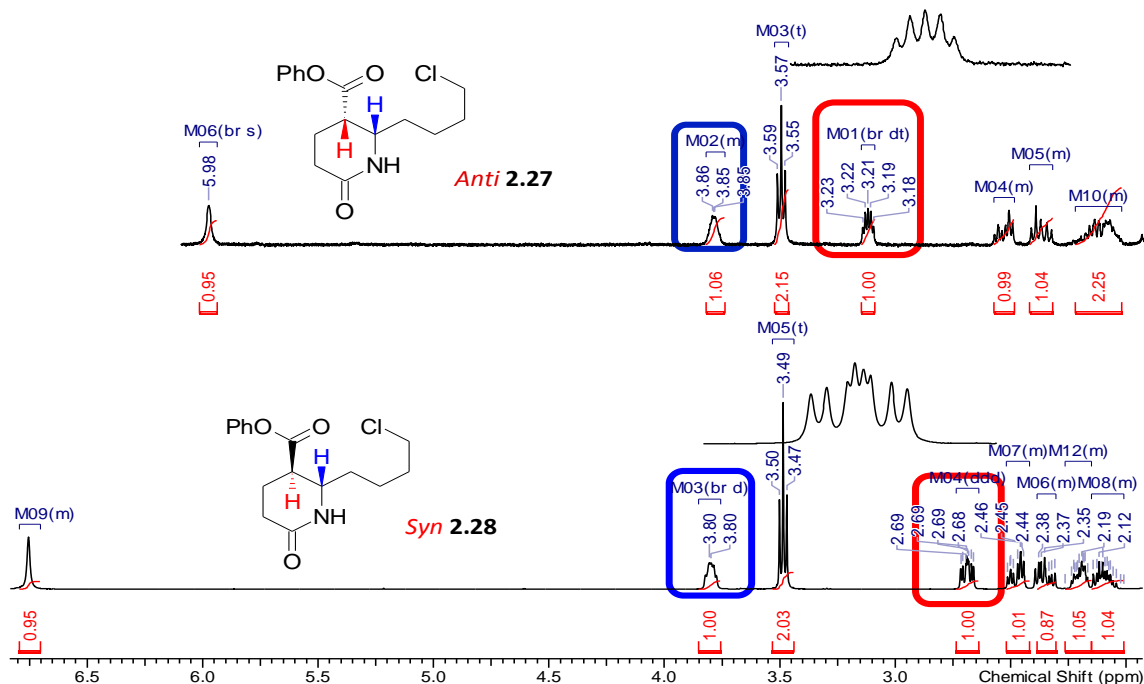
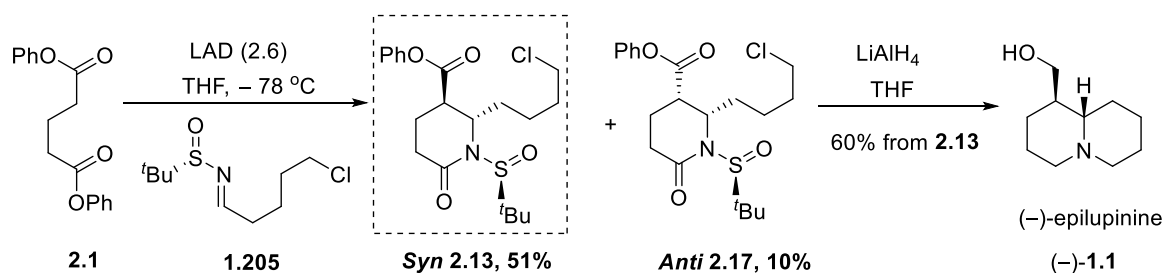


Figure 2.15: ^1H NMR (400 MHz) for comparison of *syn*- and *anti*-mono imino-aldol adducts

2.2.9 Conclusion:

The mono imino-aldol reaction was carried out by using diphenyl glutarate (**2.1**) with halo imine **1.205** to produce cyclised *syn* imino-aldol **2.13** in 51% yield. The impure *anti*-imino-aldol **2.17** was obtained as the main by-product in 10% yield (**Scheme 2.18**). Minor products from the mono imino-aldol reaction were identified to be *syn,syn*, *anti,anti* and *syn,anti* double imino-aldol adducts. The stereochemistry of *anti* imino-aldol **2.17** was determined by deprotection of the sulfinyl group and cyclisation to give *anti*-lactam **2.27**. The structure of the *anti*-lactam was confirmed by X-ray structure determination. A total synthesis of (-)-epilupinine ((-)-**1.1**) was accomplished over two steps from halo imine **1.205** in 31% overall yield by reducing the **2.13** and cyclisation of alkyl halide in the presence of LiAlH₄. The mono imino-aldol adduct **2.13** may provide a useful intermediate for the synthesis of (-)-sparteine and other nitrogen-containing bicyclic natural products, and our progress in this direction will be discussed later.



Scheme 2.18: The total synthesis of (-)-epilupinine ((-)-**1.1**) from halo imine **1.205**

2.3 RCM approach to the total synthesis of (–)-epilupinine from 5-chlorovalerate and an unsaturated imine

2.3.1 Retrosynthetic analysis of (–)-epilupinine

This approach will use ring closing metathesis (RCM) to access the quinolizidinone **2.30**, and *syn*-selective imino-aldol reaction between phenyl ester **1.173** and an unsaturated imine **1.208** (Figure 2.16). The retrosynthesis of (–)-epilupinine ((–)-**1.1**) requires hydrogenation and reduction of quinolizidinone **2.30**. Disconnection carbonyl-amine bond of **2.29**, and the piperidine **1.210** C-N bond leads back to imino-aldol adduct **1.209**. The imino-aldol product **1.209** can be formed from two functionalised fragments **1.173** and **1.208** to be brought together in a diastereoselective imino-aldol reaction.

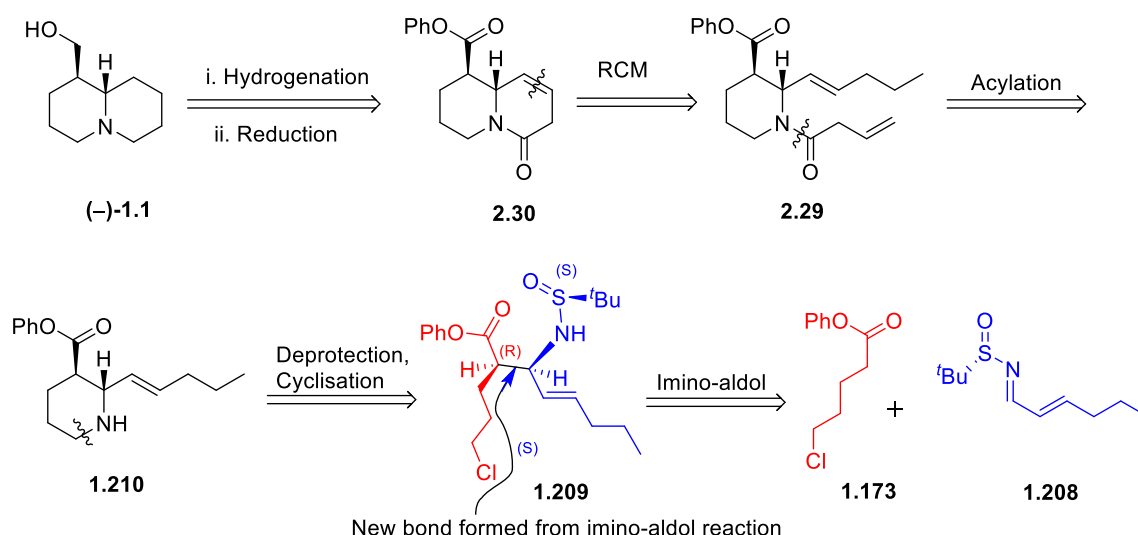
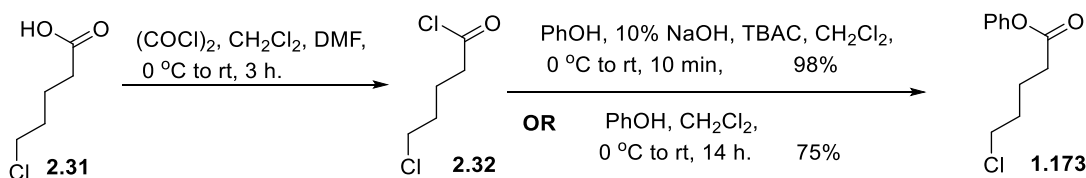


Figure 2.16: Retrosynthetic analysis of (–)-epilupinine

2.3.2 Towards the synthesis of (–)-epilupinine

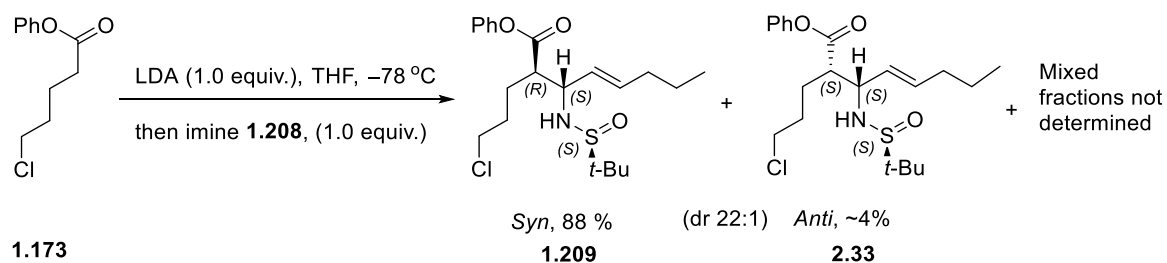
5-Chlorovaleric acid (**2.31**) was used as a commercially available starting material which was converted to the acid chloride **2.32** using oxalyl chloride and (Scheme 2.19). The crude acid chloride **2.32** was esterified with phenol to afford phenyl 5-Chlorovalerate (**1.173**) in 75% yield. A more efficient synthesis of phenyl ester **1.173** used equimolar amounts of phenol and acyl chloride **2.32** under phase-transfer catalysis (PTC) conditions, giving the product in near quantitative yield and shorter reaction time.²⁵



Scheme 2.19: Synthesis of phenyl 5-chlorovalerate (**1.173**)

2.3.3 Imino-aldol reaction of unsaturated imine 1.208

The imino-aldol reaction conditions optimised within the Brown group were applied using the lithium enolate of ester **1.173** (Scheme 2.20). Addition of the lithium enolate to unsaturated sulfinyl imine **1.208** provided imino-aldol **1.209** with high diastereocontrol (dr 22:1, ^1H NMR of the crude reaction mixture). It was essential that the reaction was quenched at -78°C . If allowed to warm to rt prior to quench, none of the desired product was isolated. In addition, a 1:1 stoichiometry of LDA to phenyl ester **1.173** provided the best result. The desired *syn*-product **1.209** was isolated by column chromatography on silica gel in 88% yield. In addition, the minor diastereomer (*S,S*) **2.33** was obtained in ~4% and 8% of mixed fractions were also isolated. The stereochemical outcome can be rationalised using a Zimmerman-Traxler type six-membered transition state model (Figure 2.17), where reaction of the *E*-enolate from the *Re* face of the sulfinyl imine gives the major product. The *E*-enolate is known to favour the *syn* product for phenyl esters.¹⁴⁴



Scheme 2.20: Synthesis of imino-aldol adducts.

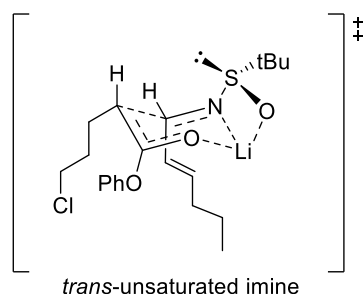


Figure 2.17: Proposed Zimmerman-Traxler transition state model for the imino-aldol reaction leading to the major *syn* product.¹⁴⁵

2.3.4 Total synthesis of (-)-epilupinine from imino-aldol 1.208

The synthesis of (-)-epilupinine was proposed through two pathways, starting from *syn* imino-aldol **1.209** (Figure 2.18). The first pathway **A** via lactam derivative **2.35**, requires initial acylation of **1.209** to form **2.34**, while the second pathway **B** requires, firstly preparation of piperidine intermediate **1.210** and then acylation of **2.29** to access (-)-epilupinine *via* RCM.

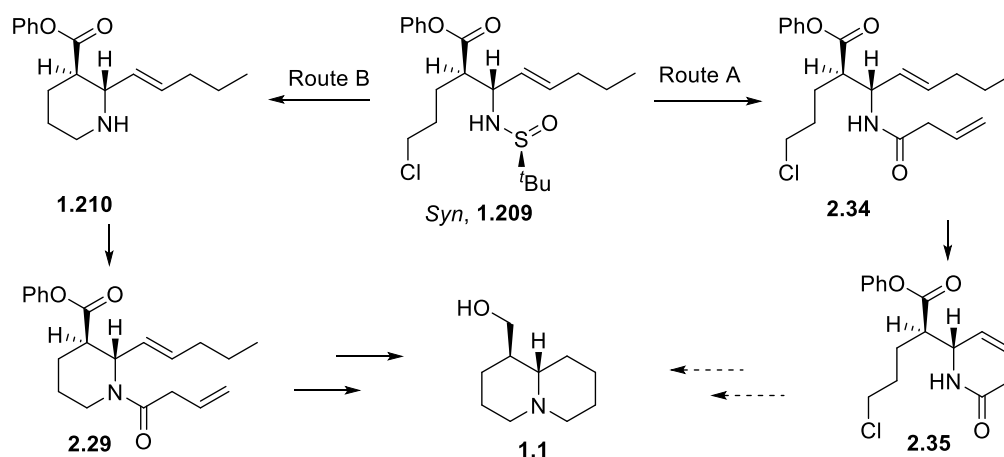
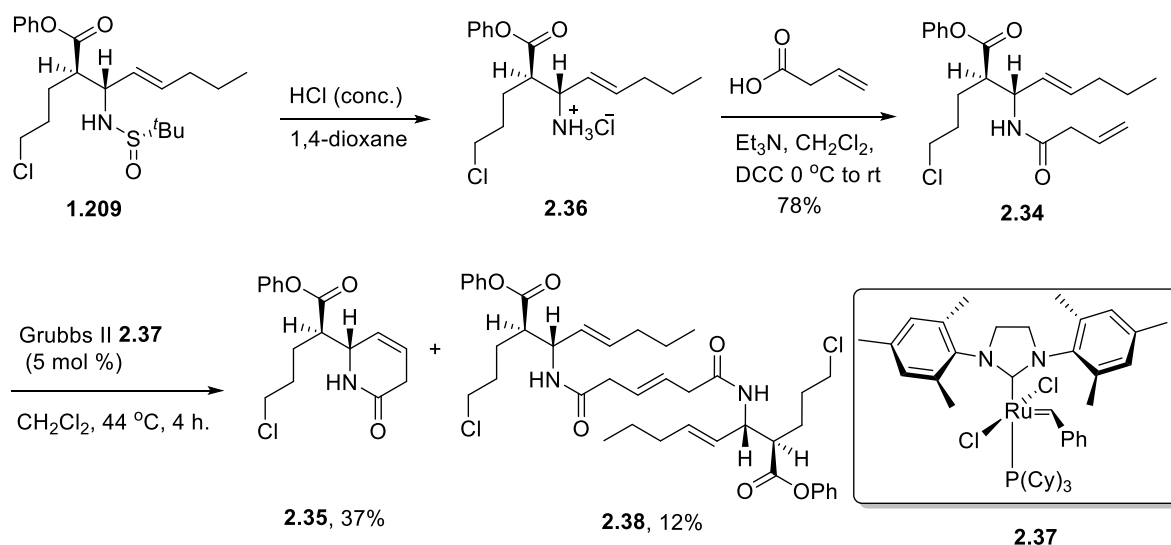


Figure 2.18: Proposed routes towards the synthesis of (-)-epilupinine

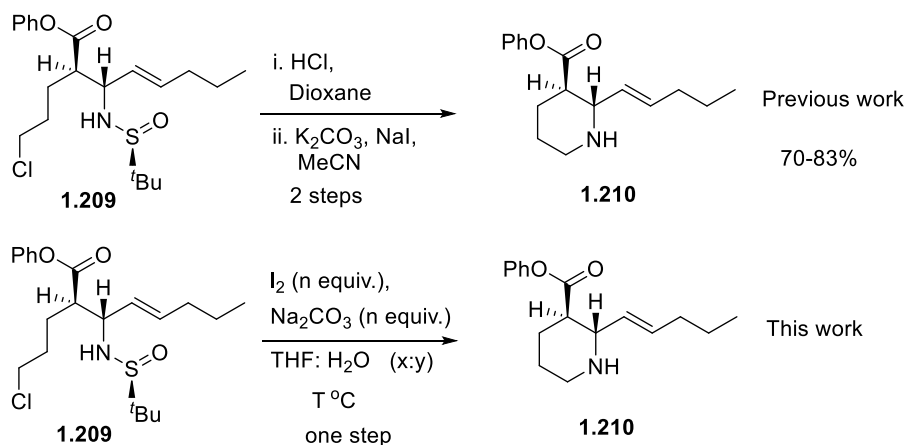
The first pathway to the synthesis of (-)-epilupinine started by removal of the *N*-sulfinyl group from *syn*-adduct **1.209** under acidic conditions, providing amine salt **2.36**, which was followed by acylation to obtain amide **2.34** in 78% yield over two steps (Scheme 2.21). RCM using Grubbs II catalyst (**2.37**) gave two products; the desired unsaturated δ -lactam **2.35** as the major product in 37% yield and dimer **2.38** as a minor product in 12% yield. This approach was not continued due to the relatively low yield of the desired product **2.38**.



Scheme 2.21: Approach to synthesis of (-)-epilupinine *via* lactam intermediate **2.35**.

An alternative synthetic pathway to access (–)-epilupinine, proceeding *via* piperidine intermediate **1.210** was investigated. Piperidine **1.210** was prepared by two methods, firstly removal *N*-sulfinyl group from **1.209** using 3 equiv. of conc. HCl (~36 %) at 0 °C in dioxane, and subsequent cyclisation in the presence of K₂CO₃ and catalytic NaI gave 83% over two steps. An alternative method was investigated by deprotection-cyclisation using molecular iodine under basic conditions. Initially, the reaction was carried out using I₂ and Na₂CO₃ for 24 h giving the amine salt **2.36** in 90% (**entry 1, Table 2.10**), while increasing the amount of Na₂CO₃ and heating in the presence of I₂ in a mixture of THF and H₂O gave the piperidine intermediate **1.210** directly (**entries 4&5, Table 2.10**). The best conditions used excess of base with I₂ at 50 °C giving piperidine **1.210** in high yield and short reaction time in one-step compared to the two-step procedure described below. Piperidine **1.210** was recrystallised from *n*-hexane to provide the pure product in 95% yield as a white solid.

Table 2.10: Optimisation and the deprotection-cyclisation reaction of the *syn*-adduct. **1.209**.

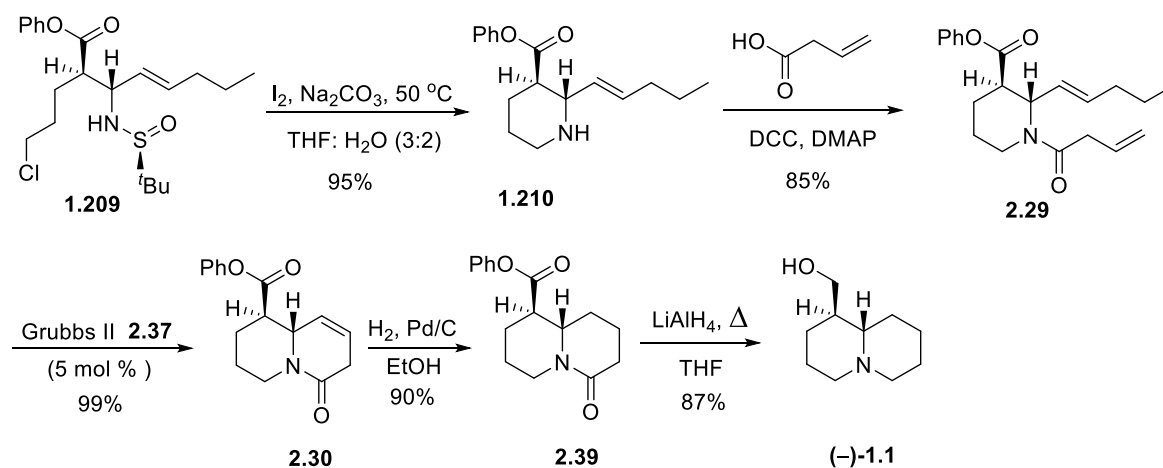


Entry	THF:H ₂ O	Na ₂ CO ₃ equiv.	I ₂ equiv.	NaI	T °C	Reaction time	Yield of 1.210
1	1:1	3	2.5	-	rt	I ₂ , Na ₂ CO ₃ , 24 h	- *
2	1:1	5	2.0	0.1	rt	I ₂ , Na ₂ CO ₃ 1 h, then NaI, 18 h	90%
3	2:1	12	1.5	-	rt	I ₂ 1 h, then Na ₂ CO ₃ , 18 h	88%
4	4:1	12	1.0	-	50	I ₂ 1 h, then Na ₂ CO ₃ , 18 h	90%
5	3:2	12	2.0	-	50	I ₂ 2 h, then Na ₂ CO ₃ , 6 h	95%

*The amine salt **2.36** was obtained in 90% yield.

Piperidine **1.210** was acylated with 3-butenic acid using *N,N'*-dicyclohexylcarbodiimide (DCC) to give β,γ -unsaturated amide **2.29** in 85% yield (**Scheme 2.22**). RCM of **2.29** using Grubbs I was

unsuccessful even at high loading of the Grubbs catalyst I and long reaction time (30 h). However, RCM of **2.29** using Grubbs catalyst II (**2.37**) afforded the unsaturated quinolizidinone **2.30** in excellent yield. Quinolizidinone **2.30** was recrystallised from hexane and its stereochemistry was confirmed by single crystal X-ray crystallography (**Figure 2.19**). The unsaturated quinolizidinone **2.30** was hydrogenated over Pd/C to give quinolizidinone **2.39**, and finally reduction of **2.39** using LiAlH₄ furnished (-)-epilupinine ((-)-**1.1**) in 87% yield.



Scheme 2.22: The total synthesis of (-)-epilupinine

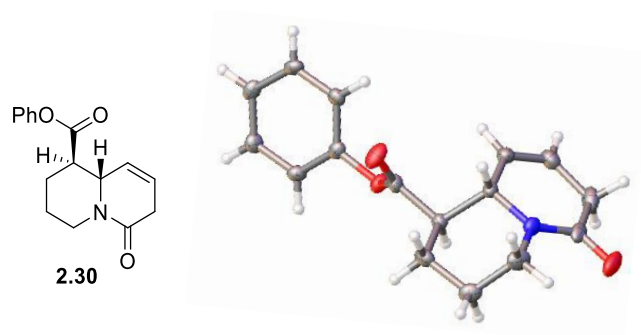
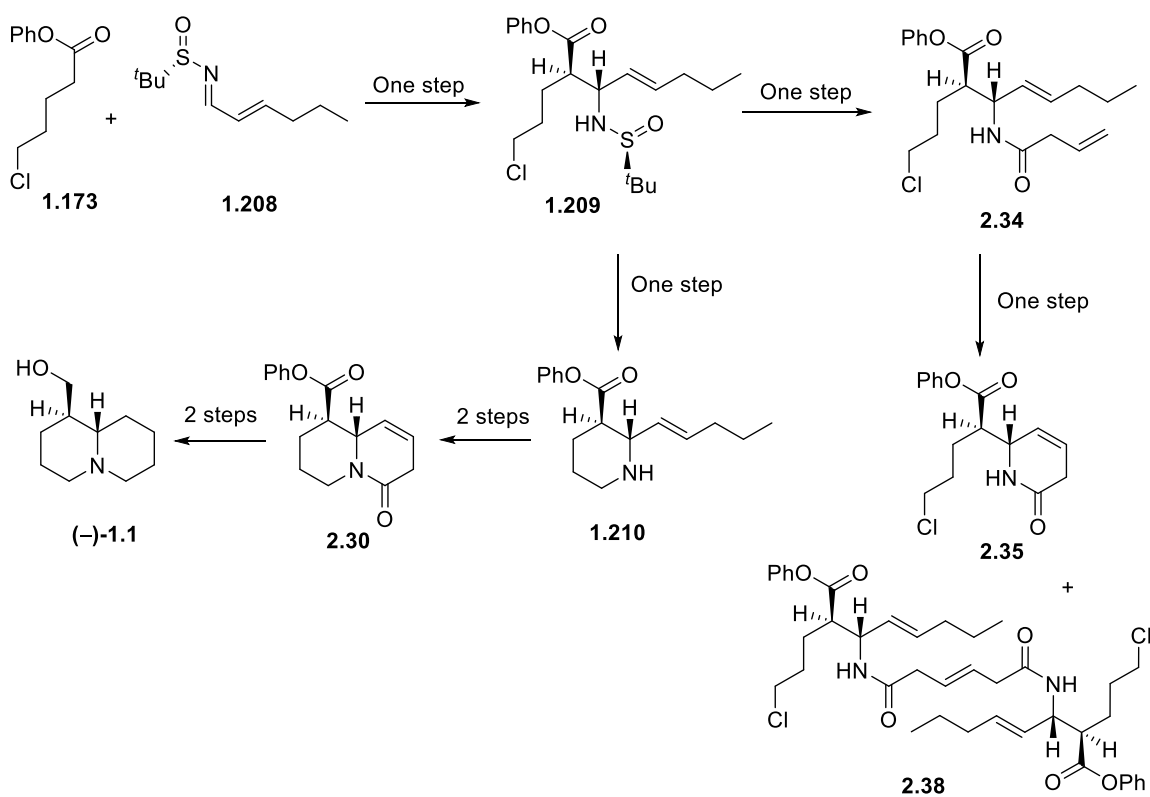


Figure 2.19: X-ray crystal structure of the unsaturated quinolizidinone **2.30**

Although we were delighted to have completed a short total synthesis of (-)-epilupinine, our interest in this relatively long route was derived from the ability to introduce a functionalised quinolizidine system **2.30** that could be used in the synthesis of other lupin alkaloids. These efforts will be described in the following section. Although the synthesis of (-)-epilupinine is similar to our previous synthesis (**Scheme 1.44**),¹³⁵ the overall yield of (-)-epilupinine was increased from 39% in seven steps compared to previous work,^{134,135} now achieving 55% in six steps from the unsaturated imine **1.208**.

2.3.5 Conclusions:

The total synthesis of (-)-epilupinine was achieved in 55% overall yield over six steps from unsaturated imine **1.208** by using a RCM approach (**Scheme 2.23**). *Syn*-selective of imino-aldol reaction was provided **1.209** with high diastereocontrol (*dr* 22:1). Initially, deprotection and acylation of *syn* imino-aldol adduct **1.209** gave an intermediate **2.34** followed by ring-closing metathesis. Although this gave the desired unsaturated lactam **2.35**, cross-metathesis also occurred leading to a by-product **2.38**. Several reaction conditions have been explored for deprotection and cyclisation of imino-aldol adduct **1.209** giving the piperidine **1.210** in 95%. The stereochemistry of quinolizidinone **2.30** was confirmed by single crystal X-ray crystallography. The functionalised quinolizidine system was converted to (-)-epilupinine in two further steps.



Scheme 2.23: Overview of the total synthesis of (-)-epilupinine from unsaturated imine **1.208**

2.4 Towards the synthesis of (+)-allomatridine and (-)-sparteine

A synthesis of (+)-allomatridine ((+)-**1.139**) was reported by Brown and co-workers, from an imino-aldol intermediate and using *N*-acyliminium ion cyclisation as a key step (Scheme 1.38).¹⁰⁹ Our plan in this section is to progress a new cyclisation strategy for the synthesis of (+)-allomatridine, starting from *syn* imino-aldol adduct **1.209** (Figure 2.20, route A). Tricyclic imide **2.45** will be a key intermediate to access (+)-allomatridine. A synthetic route to (-)-sparteine (route B) will also be investigated starting from cyclised *syn* imino-aldol **2.13**, which was described in the previous section (Scheme 2.13). Sulfinyl piperidine **2.13** can be used to generate an imide intermediate **2.46** to access (-)-sparteine ((-)-**1.3**) by using *N*-acyliminium ion cyclisation approach.

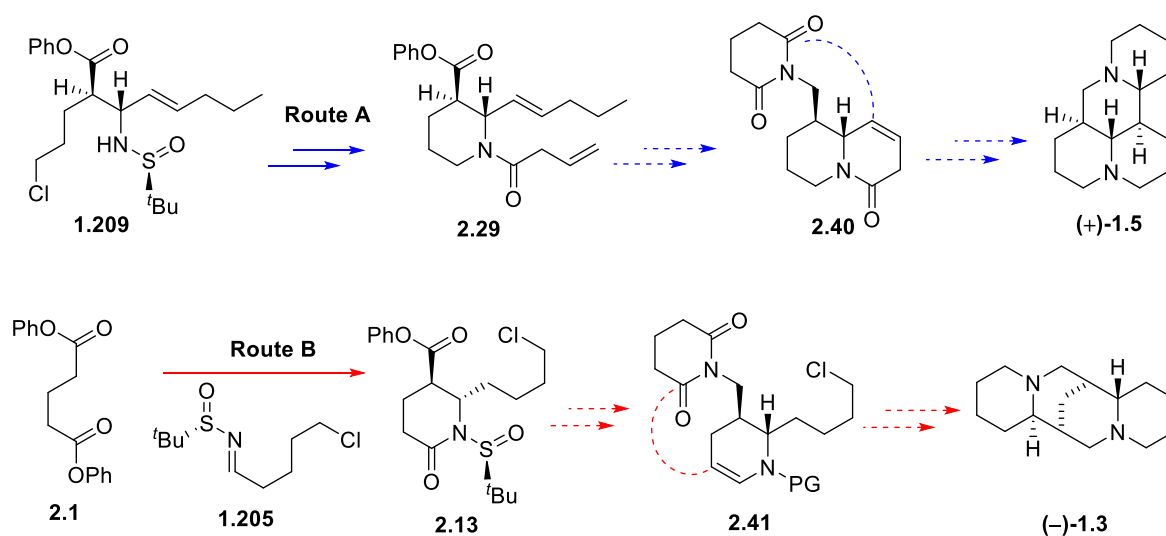


Figure 2.20: Routes towards (+)-allomatridine ((+)-**1.5**) and (-)-sparteine ((-)-**1.3**) from piperidine and quinolizidine intermediates

2.4.1 Retrosynthetic analysis of (+)-allomatridine

Our approach to the synthesis of (+)-allomatridine ((+)-**1.5**) was designed to exploit β,γ -unsaturated amide **2.29** which was previously prepared during our synthesis of (-)-epilupinine (Scheme 2.22). RCM of intermediate **2.29** followed by selective reduction of ester will provide the corresponding alcohol **2.42** (Figure 2.21). Mitsunobu reaction of alcohol **2.42** with glutarimide will give tricyclic imide **2.40**. Selective reduction of imide **2.40** will give intermediate **2.43**, which can be cyclised using Brønsted acid, basic conditions, or reduction under acidic conditions using Mannich-type or *N*-acyliminium ion cyclisation. (+)-Allomatridine will be generated by hydrogenation and reduction at a late stage.

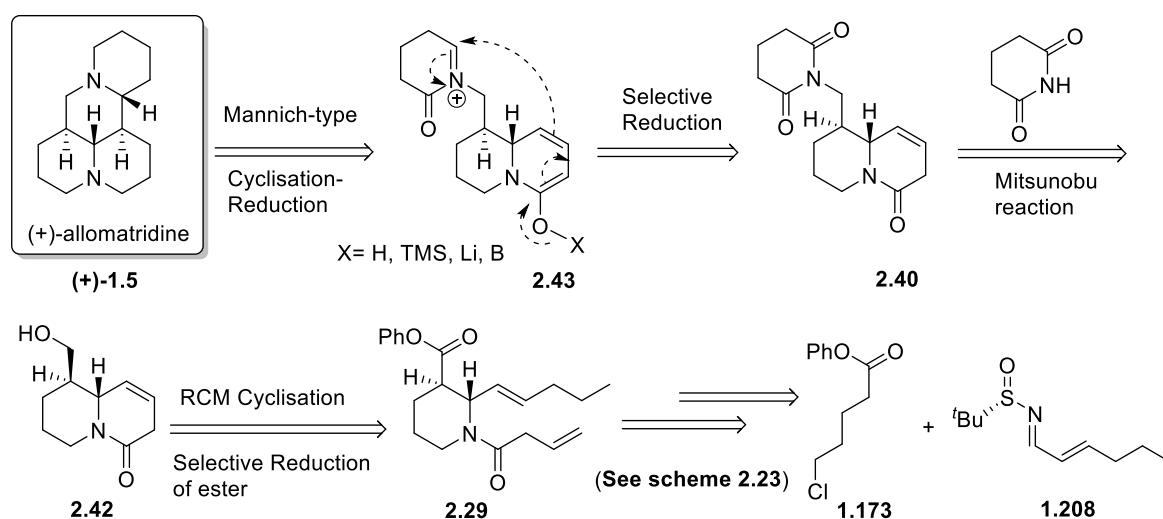
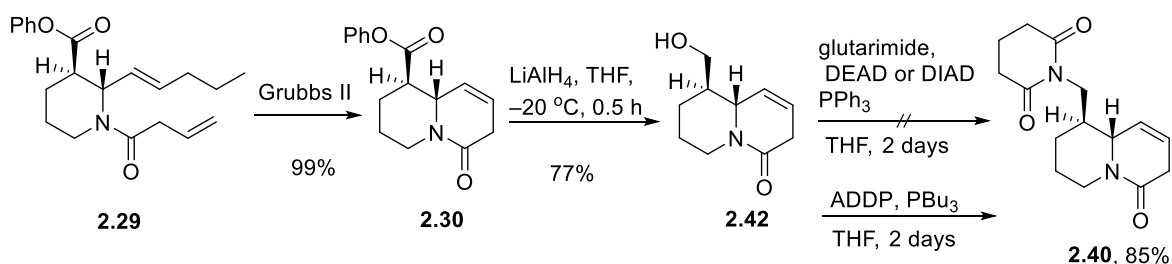


Figure 2.21: Retrosynthetic analysis of (+)-allomatridine ((+)-1.5)

2.4.1.1 The synthesis of a tricyclic imide intermediate towards (+)-allomatridine

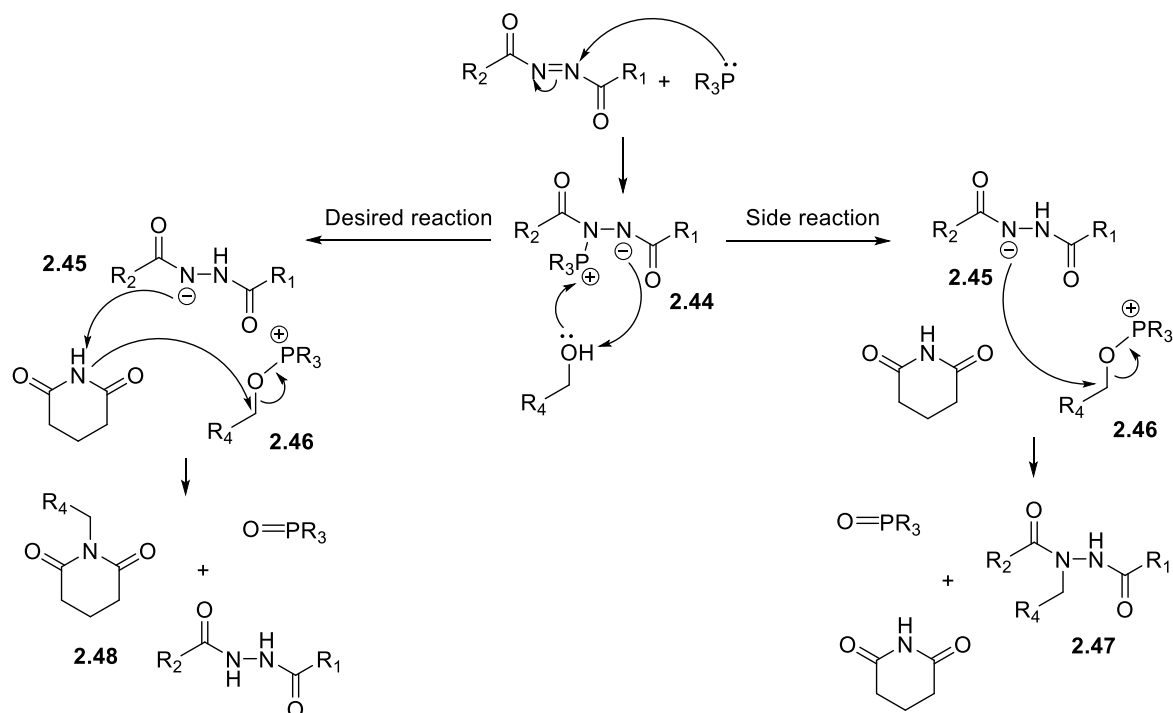
The attempted synthesis of (+)-allomatridine started from the intermediate **2.29** which was used previously during the synthesis of (–)-epilupinine (Scheme 2.22). There are two pathways leading to tricyclic imide **2.40**; the first route involved cyclisation of **2.29** using Grubbs II catalyst to provide quinolizidinone **2.30** (Scheme 2.24). Selective reduction of ester **2.30** using LiAlH_4 at $-20\text{ }^\circ\text{C}$ for 30 min gave the corresponding alcohol **2.42**. Mitsunobu reaction with glutarimide was unsuccessful in the presence of DEAD and triphenylphosphine. Several attempts to couple glutarimide with primary alcohol **2.47**, under different Mitsunobu conditions failed.



Scheme 2.24: A first pathway toward the synthesis of tricyclic imide **2.40**

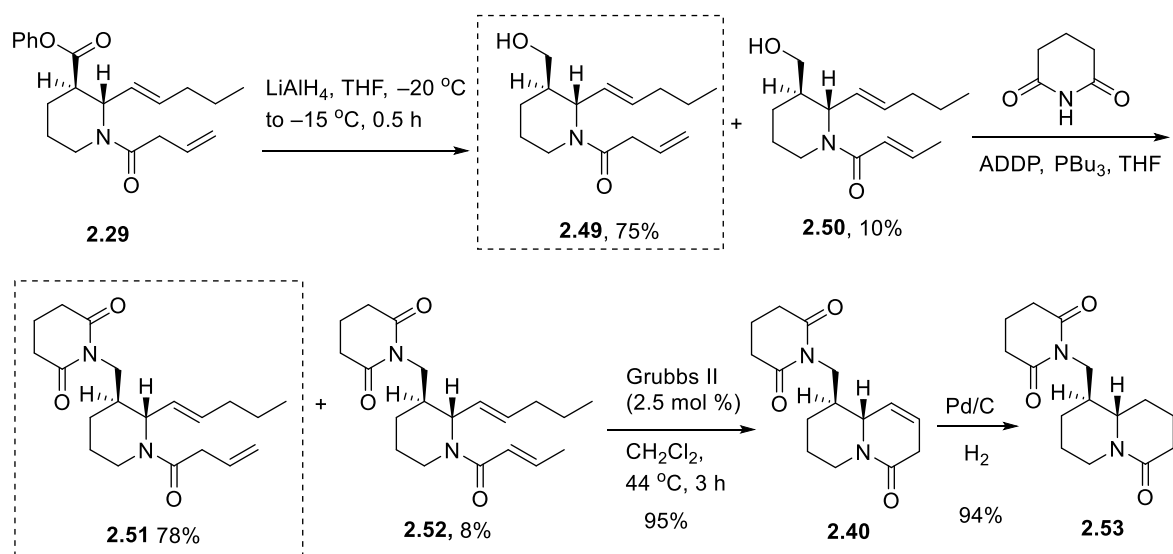
Both DIAD and DEAD were applied to this transformation, but none of the desired product was obtained in the reaction and quantitative recovery of alcohol **2.42** was observed. In this case, both DIAD and DEAD were not efficient in deprotonating the acidic hydrogen,¹⁴⁶ due to attack of the hydrazo anion **2.45** on the alkoxyphosphonium **2.46** directly to afford alkylated hydrazine derivative **2.47** as the by-product (Scheme 2.25). However, using strong electron donating groups such as are present in 1,1'-(azodicarbonyl) dipiperidine (ADDP)¹⁴⁷ and Bu_3P in the modified Mitsunobu reaction under more concentrated conditions successfully generated imide **2.40** in high yield (Scheme 2.24). Using ADDP increases reactivity of phosphonium intermediate **2.44** in order to facilitate the

nucleophilic attack of alcohol, and increase its basicity in the intermediate **2.45**, and to be more efficient in deprotonating the acidic hydrogen of glutarimide to form **2.48** (Scheme 2.25).



Scheme 2.25: Proposed mechanism of the Mitsunobu reaction.

The second pathway begins from selective reduction of ester **2.29** using LiAlH_4 to give the corresponding alcohol **2.49** (Scheme 2.26). Partial isomerisation of the β,γ -unsaturated alcohol **2.49** was obtained under the reaction conditions to give α,β -unsaturated alcohol **2.50** as by-product in 10% yield. Mitsunobu reaction of alcohol **2.49** with glutarimide in the presence of ADDP provided the corresponding imide **2.51**.



Scheme 2.26: Alternative pathway toward the synthesis of tricyclic imide **2.40**

The undesired α,β -unsaturated amide **2.52** was also formed from partial isomerisation of β,γ -unsaturated amide **2.51**. Although partial transformation into the corresponding α,β -unsaturated amide **2.52** was observed, RCM of β,γ -unsaturated amide **2.51** afforded the tricyclic imide **2.40** in 95% yield. The stereochemistry of tricyclic imide **2.40** was confirmed by single crystal X-ray structure determination (**Figure 2.22**). Hydrogenation of tricyclic imide **2.40** led to form (-)-10-oxo-lamprolobine **2.53** in 94% yield (**Scheme 2.26**).

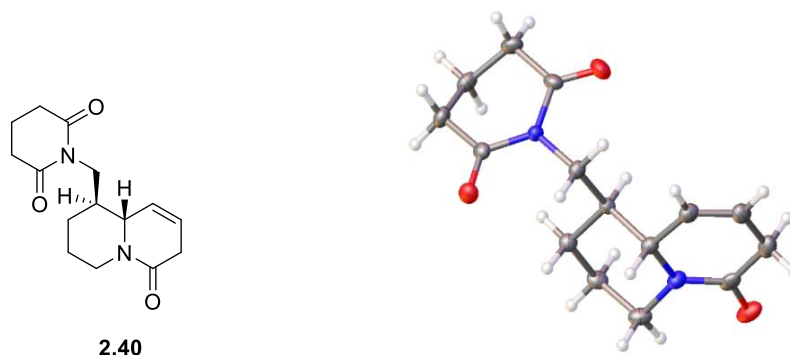
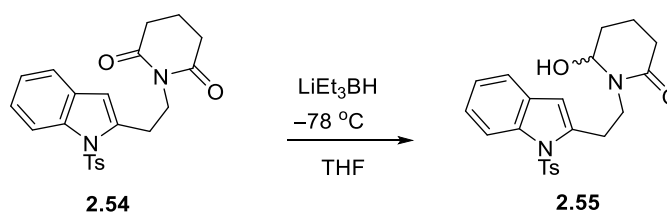


Figure 2.22: X-ray crystal structure of tricyclic imide **2.40**

The first route is clearly preferred, as it avoids the undesired isomerisation that complicated the second approach and gives the desired tricyclic intermediate **2.40** in good overall yield. With the tricyclic imide **2.40** in hand, we explored its use as a key intermediate for the *N*-acyliminium ion cyclisation. Cyclisation of tricyclic imide **2.40** was attempted using several different approaches, followed by hydrogenation and reduction to access (+)-allomatridine ((+)-**1.5**), and these efforts are described in the next section.

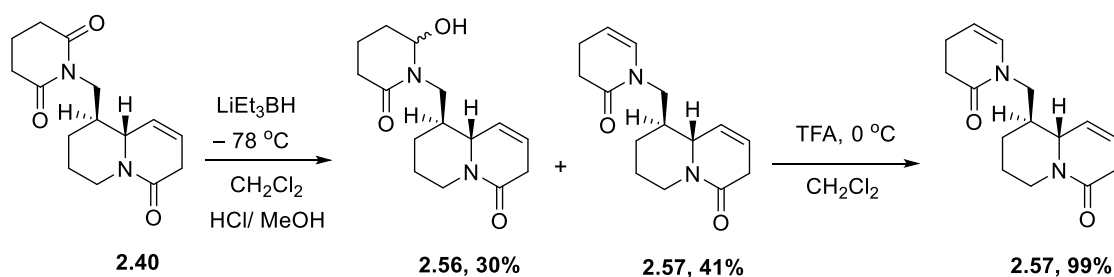
2.4.1.2 Efforts towards the synthesis of (+)-allomatridine

The final cyclisation towards the synthesis of (+)-allomatridine ((+)-**1.5**) focused on establishing a suitable *N*-acyliminium ion precursor (**Scheme 2.28**). Utilising a procedure adapted from Grigg and co-workers (**Scheme 2.27**),¹⁴⁸ selective reduction of the tricyclic imide **2.40** was achieved to provide hydroxylactam **2.56** and enamide **2.57** using LiEt_3BH at $-78\text{ }^\circ\text{C}$ in CH_2Cl_2 (**Scheme 2.28**).



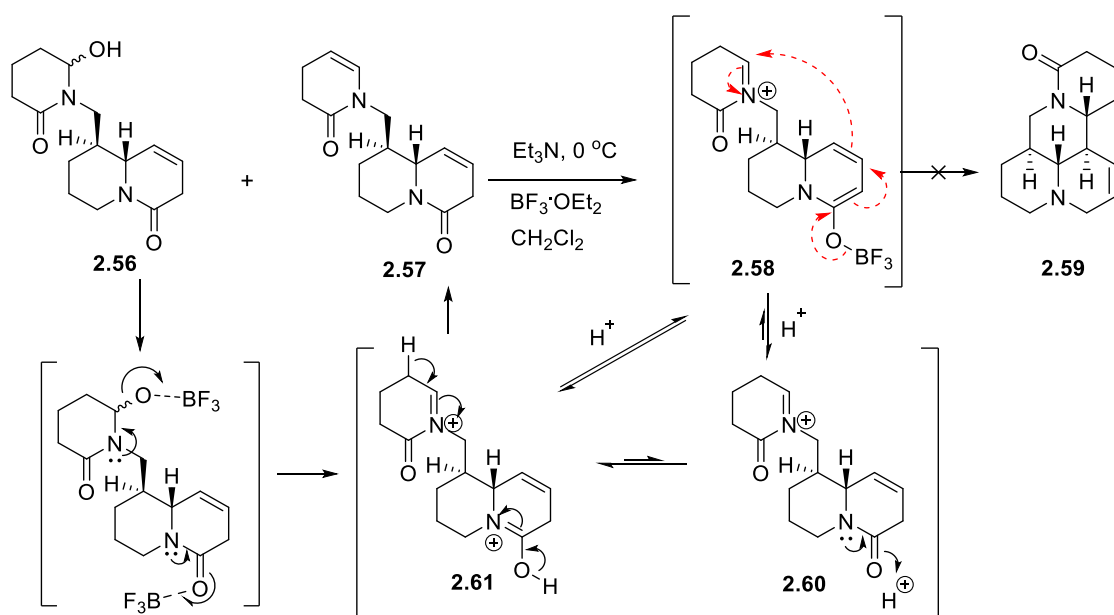
Scheme 2.27: Grigg's selective reduction of imide

Subsequent, attempted *N*-acyliminium ion cyclisation of **2.56** and **2.57** in the presence of TFA in CH₂Cl₂ resulted only the tricyclic enamide **2.57**, even after extended reaction periods.



Scheme 2.28: Selective reduction of tricyclic imide

In an attempt to induce cyclisation *via* enolisation-Mannich-type cyclisation, we used Et₃N in the presence of a Lewis acid at 0 °C. Even after extended reaction time at rt cyclisation products were not observed, and only tricyclic enamide **2.57** was obtained (**Scheme 2.29**). We could infer that the desired reactive *N*-acyliminium ion **2.58** was being formed under the reaction conditions, but the cyclisation was not taking place. Instead of undergoing cyclisation, the intermediate *N*-acyliminium eliminated to give the enamide **2.57** (during the reaction or upon work-up). A proposed mechanism is shown below. Due to the failure of these attempted Mannich cyclisation, we considered different approaches towards cyclisation.



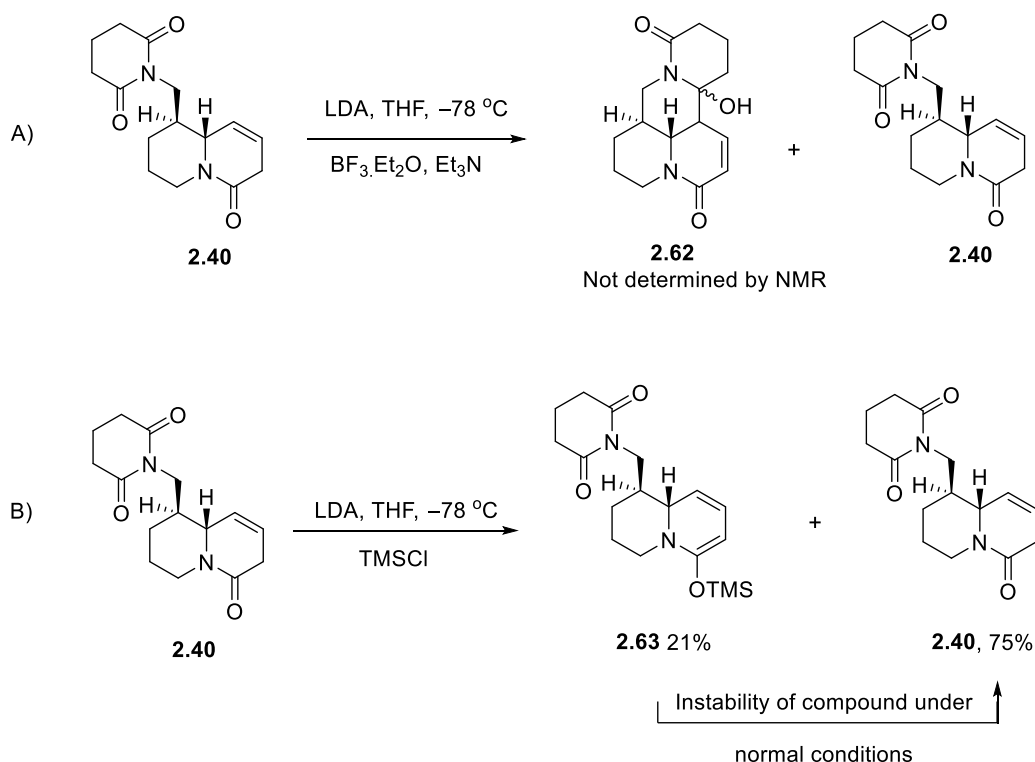
Scheme 2.29: Mannich cyclisation of iminium ion from tricyclic imide

2.4.1.3 Further attempts to cyclise tricyclic intermediates

It is worthwhile to mention here the numerous experiments that went into establishing the above sequence of reactions. In the beginning, we attempted to use LDA to deprotonate the amide followed by aldol type condensation by activation of the imide carbonyl using Lewis acid (**Scheme**

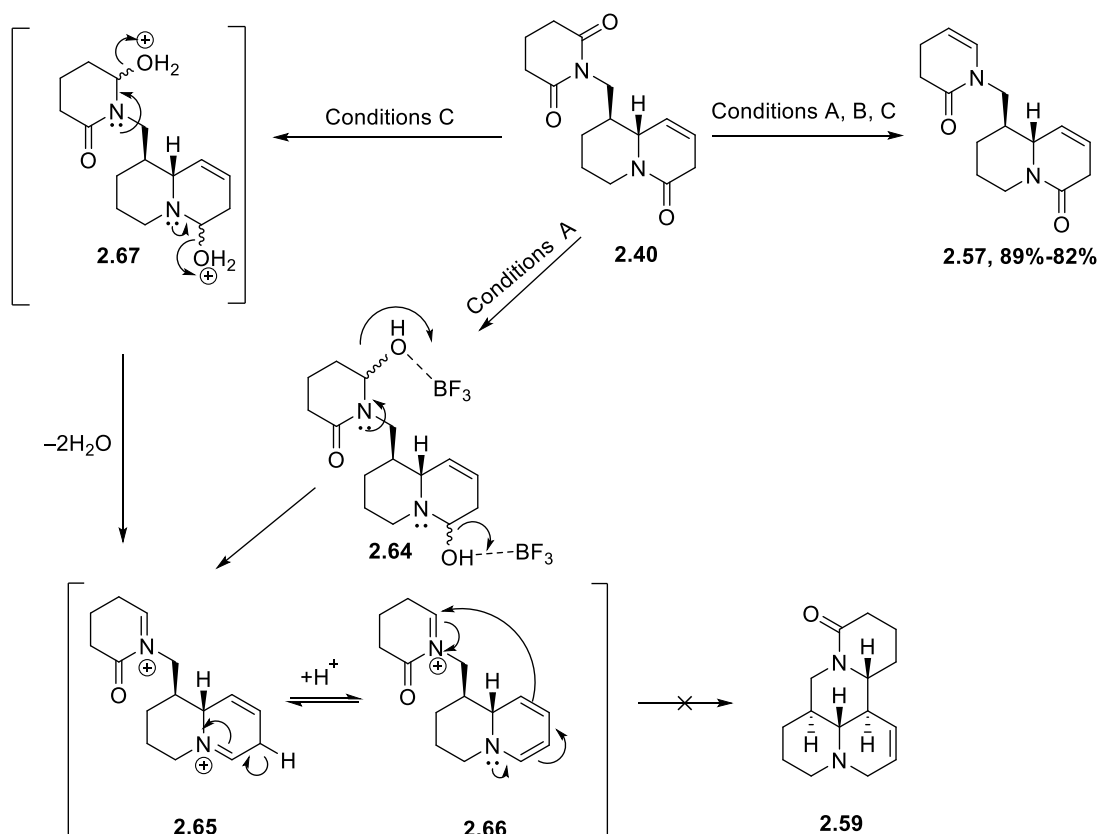
2.30, A). This procedure was not effective and gave tricyclic imide **2.40** as the major product. A small amount (~1 mg) of a compound tentatively assigned to be the tetracycle **2.62** was obtained.

However, evidence for this structure only came from mass spectrometry. We attempted alternative methods for cyclisation by aldol condensation using LDA again to deprotonate the amide, trapping the enolate with trimethylsilyl chloride (TMSCl) to form silyl enol ether **2.63** (**Scheme 2.30, B**). Only partial conversion was obtained due to instability of silyl enol ether **2.63**, with recovery of tricyclic imide **2.40**. No further reaction was attempted of silyl enol ether **2.63** due to its instability and conversion to the tricyclic imide **2.40**.



Scheme 2.30: Attempts to cyclisation of tricyclic imide **2.40** using LDA

Efforts turned toward reduction of both the imide and amide groups present in tricycle **2.40** followed by Mannich-type cyclisation (**Scheme 2.31**). First DIBAL-H (conditions **A**) were investigated to generate bishydroxyl lactam **2.64**, followed by addition of Lewis acid $\text{BF}_3 \cdot \text{OEt}_2$ for activation to form diiminium cation **2.65**. Under these conditions, the allomatridine precursor **2.40** was not obtained, but tricyclic enamide **2.57** was observed. Under basic conditions **B**, using an excess of DIBAL-H to form bishydroxyl lactam **2.65** followed by addition of Lewis acid and Et_3N also failed to access **2.57**.



Conditions A DIBAL-H (3 equiv.) $\text{BF}_3 \cdot \text{OEt}_2$, CH_2Cl_2 -78°C , rt 24 h

Conditions B DIBAL-H (6 equiv.) Et_3N , $\text{BF}_3 \cdot \text{OEt}_2$, CH_2Cl_2 -78°C , then 0°C , rt 24 h

Conditions C DIBAL-H (3-6 equiv.) aq. HCl 1N, CH_2Cl_2 -78°C , to -60°C , rt 24 h

Scheme 2.31: Attempts to access tetracycle **2.59** via *N*-acyliminium ion from tricyclic imide **2.40**

Finally, reduction of **2.40** followed by acidic conditions (conditions **C**) for dehydration of **2.67** only gave tricyclic enamide **2.57** in 89% – 82% yield for conditions **A**, **B** or **C**. It is possible that this general strategy could succeed under the right conditions, and with a suitable precursor. However, no further investigation of this route was carried out due to lack of time.

2.4.2 Retrosynthetic analysis of (–)-sparteine

We proposed an asymmetric synthesis of (–)-sparteine using the previously described imino aldol products. (–)-Sparteine possesses two stereochemical relationships: *syn* (*S,S*) and *anti* (*R,S*). The *syn* relationship is present in mono cyclised imino-aldol **2.13**. To build *anti* relationship might be achieved by *N*-acyliminium ion cyclisation of an intermediate **2.70** (Figure 2.23). Deprotection of mono imino-aldol adduct **2.13** followed by re-protection using Cbz group will provide **2.68**. Reduction of ester imide **2.68** will give the corresponding alcohol enamide, and subsequent Mitsunobu reaction in the presence of glutramide will afford **2.69**. Selective reduction of imide **2.69**

followed by cyclisation of intermediate **2.70** via *N*-acyliminium ion will establish tricyclic cation **2.71**. Reduction of iminium ion of **2.71** and then deprotective cyclisation, will generate oxo-sparteine **1.6** followed by reduction of amide **1.6** to access (–)-sparteine (–)-**1.3**.

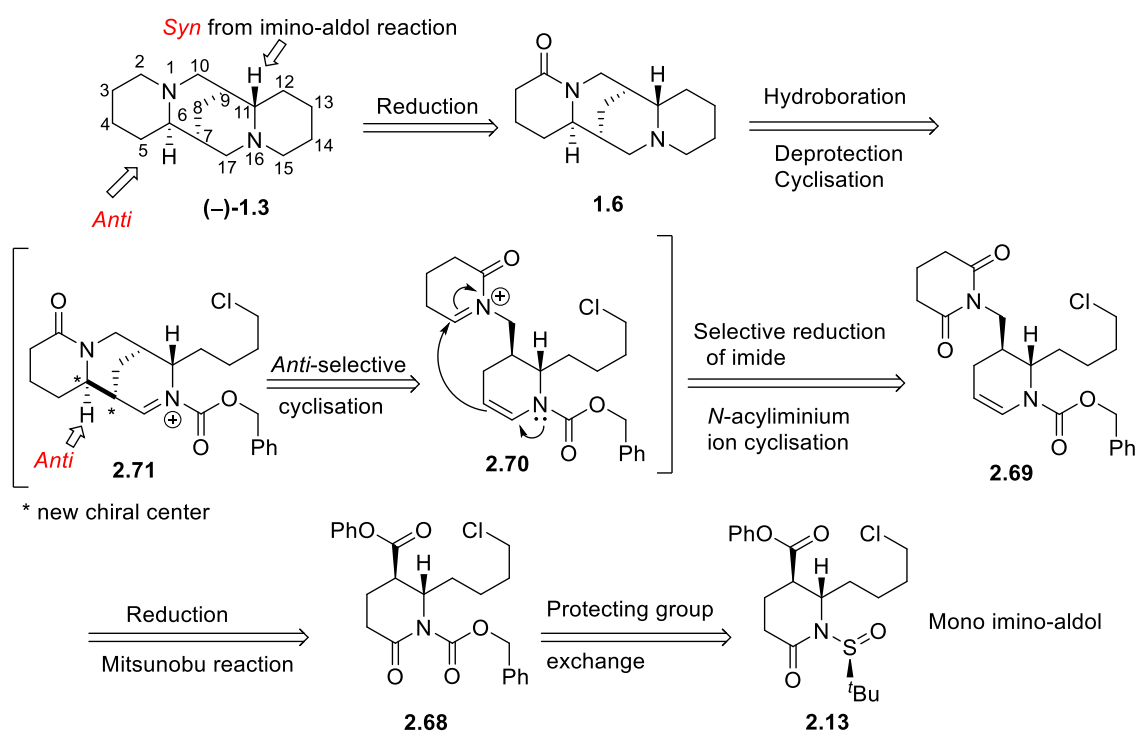


Figure 2.23: Retrosynthetic analysis of (–)-sparteine over *N*-acyliminium ion cyclisation

2.4.2.1 Towards a stereocontrolled synthesis of (–)-sparteine

The mono imino-aldol reaction to give cyclised-*syn* mono **2.13** was described in section 2.2. Our plan to synthesise (–)-sparteine requires a stereocontrolled *N*-acyliminium ion cyclisation to generate the *syn,anti*-product **1.53** (**Figure 2.24**). The *syn*-stereochemistry is present in the intermediate **2.13**, while the *anti*-stereochemistry **2.71** may be achieved by *N*-acyliminium ion cyclisation (**Figure 2.23**). Previous work by Bohlmann *et al.* reported a similar cyclisation to give (±)-sparteine, which suggested a chair transition state cyclisation *via an* iminium ion intermediate (**Figure 2.24**).⁷⁰ The cyclised *syn* imino-aldol adduct **2.13** was used as starting point to access (–)-sparteine.

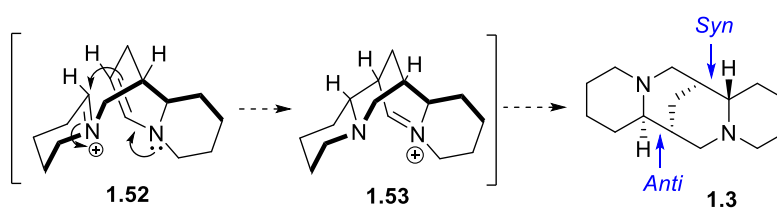
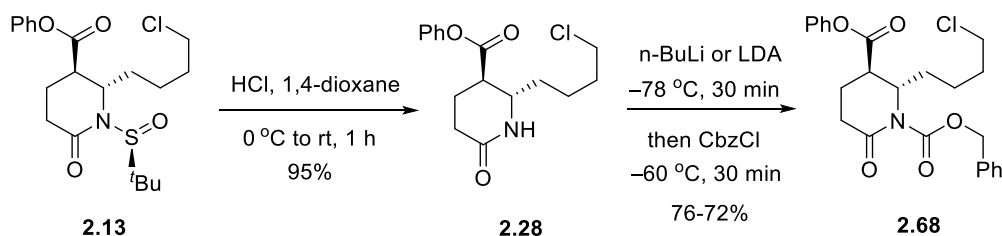


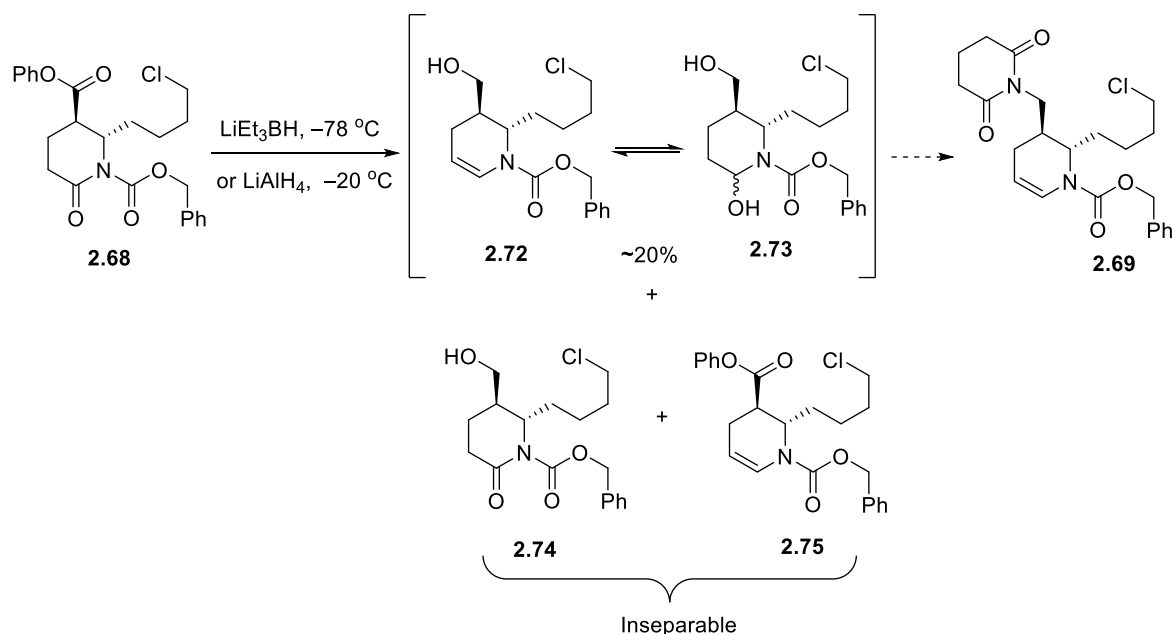
Figure 2.24: Bohlmann's reported synthesis of (±)-sparteine

However, sulfinyl auxiliary group in **2.13** proved to be unstable under a variety of conditions attempted cyclisation. Therefore, we replaced the *N*-sulfinyl auxiliary group with a more stable protecting group. Deprotection of *N*-sulfinyl auxiliary of **2.13** under acidic conditions followed by re-protection of *syn*-lactam **2.28** using LDA or *n*-BuLi with benzyl chloroformate (CbzCl) gave imide **2.68** (Scheme 2.32).



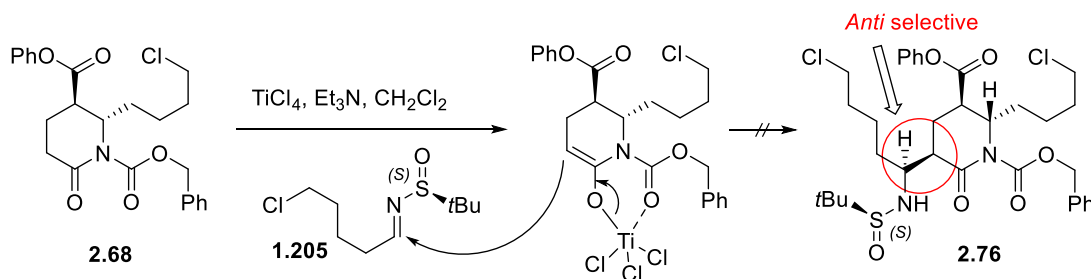
Scheme 2.32: The early stages towards the synthesis of (–)-sparteine

In our proposed approach to the synthesis of (–)-sparteine, we planned to introduce a new ring *via* reduction of the ester imide **2.68** followed by treatment of alcohol enamide **2.72** with glutarimide under Mitsunobu conditions to give imide **2.69** (Scheme 2.33). The reduction of ester imide **2.68** gave the product **2.72** and equilibrium with hemiaminal **2.73**, and a mixture of alcohol imide **2.74** and enamide **2.75** were identified only by mass spectrometry (MS). In addition, the selective reduction of the ester group in **2.68** using different reducing agents was not possible due to the reactivity of the imide towards the reducing agent. Although this procedure was not satisfactory to produce the desired product **2.72** in good yield, we thought that the corresponding alcohol **2.74** could undergo Mitsunobu coupling with glutarimide later to access (–)-sparteine by *N*-acyliminium cyclisation approach. Unfortunately, insufficient time was available to optimise the reduction.



Scheme 2.33: Failed attempt to synthesise the key intermediate imide **2.69**

At this point, we proposed an alternative way to prepare *anti*-adduct **2.76** using soft enolisation of **2.68** in the presence of Lewis acid to perform an imino-aldol reaction with halo imine **1.205** to access (-)-sparteine (**Scheme 2.34**).

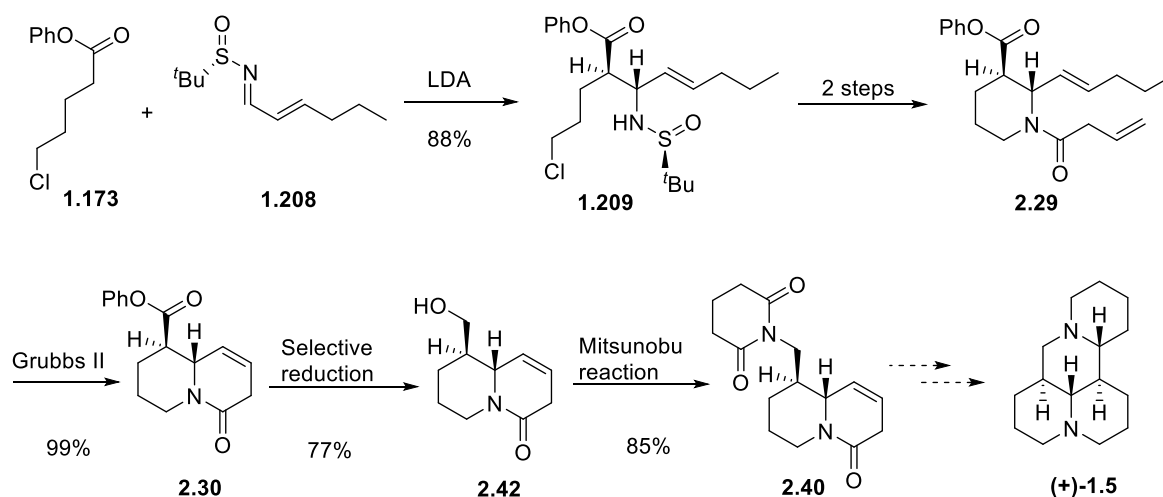


Scheme 2.34: Proposed an alternative way using soft enolisation of **2.68**

Unfortunately, the soft enolisation of **2.68** was not successful under Lewis acid conditions to achieve *anti*-selective addition. By this stage in the project, we were not able to further investigate the introduction of the new ring due to time constraints, and could not pursue the synthesis further. It also became clear that the substrate **2.68** used in this route also had the same underlying problems in terms of selective reduction of the imide and ester groups needed for the synthesis of (-)-sparteine.

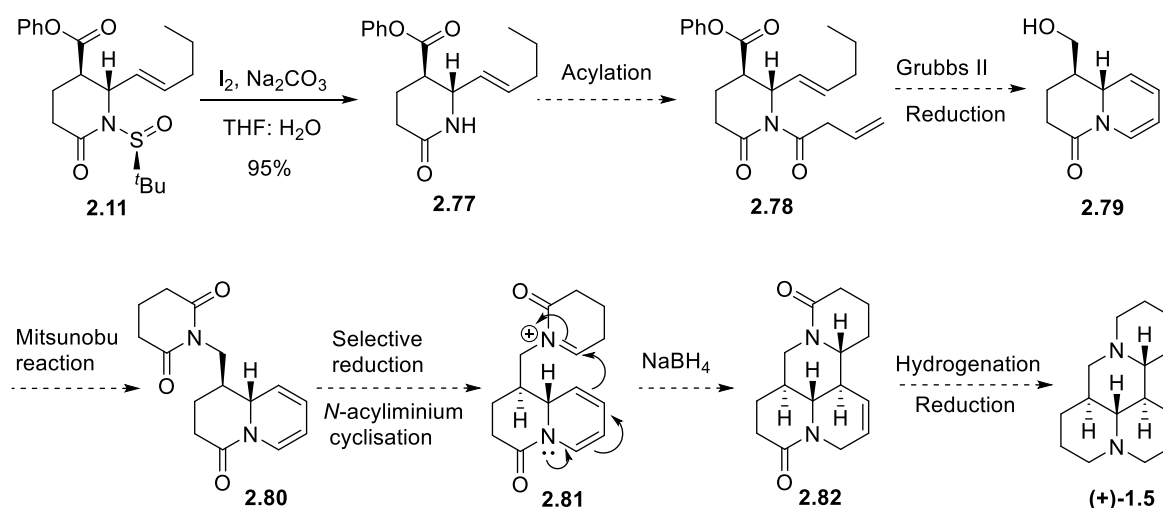
2.4.3 Conclusions and future work:

Two approaches towards the syntheses of (+)-allomatridine and (-)-sparteine are described in this section. The attempted synthesis of (+)-allomatridine started from an imino-aldol reaction between an unsaturated imine **1.208** and phenyl ester **1.173** to give the intermediate **2.29** (**Scheme 2.35**). In a modified synthetic route, we were able to form a tricyclic imide **2.40** from the hydroxy quinolizidinone **2.42** as a precursor for *N*-acyliminium cyclisation. The structure of enamide intermediate **2.40** was confirmed by single crystal X-ray crystallography. Different cyclisation conditions were attempted for *N*-acyliminium cyclisation towards allomatridine, but all of them failed at the stage of the final cyclisation. However, the *N*-acyliminium cyclisation approach to allomatridine could still be viable under appropriate conditions, and using a suitable precursor.



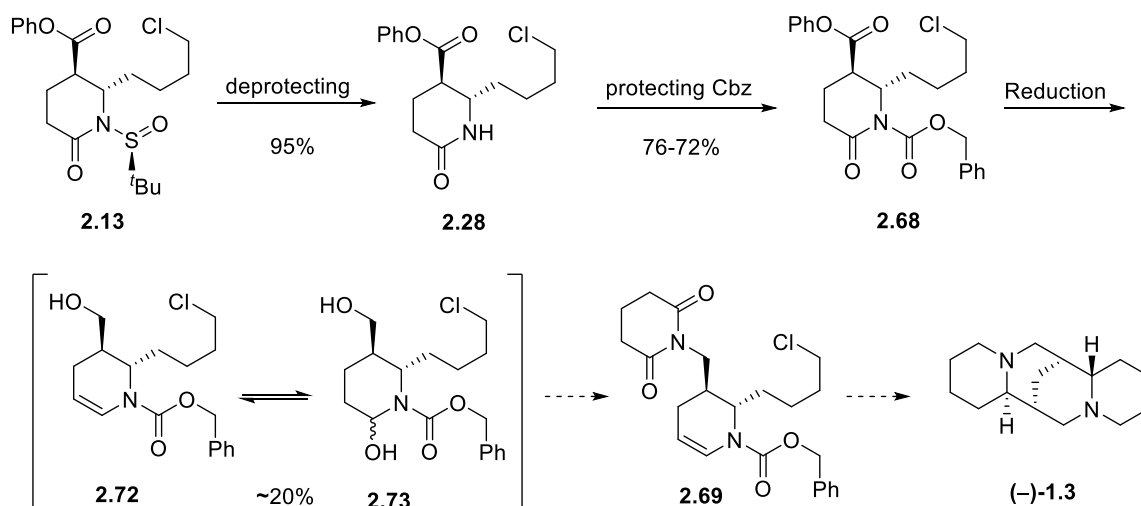
Scheme 2.35: Towards the synthesis of (+)-allomatridine ((+)-1.5)

Toward the synthesis of (+)-allomatridine ((+)-1.5) using mono imino-aldol **2.11** as starting point (**Scheme 2.36**) to access a key intermediate of tricyclic imide **2.80**. Deprotection of **2.11** gave unsaturated lactam **2.77** following by acylation with 3-butenoic acid could give **2.78**. RCM of **2.78**, and subsequent reduction could form bicyclic **2.79**. Mitsunobu reaction of hydroxy quinolizidinone **2.79** with glutarimide could afford **2.80**. Selective reduction of imide **2.80** followed by *N*-acyliminium cyclisation of **2.81** could generate tetracycle **2.82**. Finally, hydrogenation and reduction of **2.82** could furnish to (+)-allomatridine ((+)-1.5).



Scheme 2.36: Alternative approach towards the synthesis of (+)-allomatridine ((+)-1.5)

The *N*-acyliminium cyclisation approach to sparteine was investigated from an advanced intermediate at the stage of the cyclisation of imide enamide **2.69** (Scheme 2.37). *Syn*-lactam **2.28** was used as starting point for synthetic route to sparteine, where **2.28** was obtained from mono imino-aldol reaction of halo imine **1.205** and diphenyl glutarate (**2.1**). Several reductive conditions were attempted to reduce the ester imide **2.68** to hydroxy enamide **2.72**. However, reduction of **2.68** gave a mixture of the desired hydroxy enamide **2.72** and equilibrium with hemiaminal **2.73**, also the minor products **2.74** and **2.75** were identified only by mass spectrometry (MS). Attempted intermolecular imino-aldol reaction of **2.68** with a sulfinyl imine **1.205** was also unsuccessful.



Scheme 2.37: Attempted route towards the synthesis of (-)-sparteine (-)-**1.3**

Chapter 3: Experimental Details

3.1 General Methods

Chemicals were purchased from Sigma-Aldrich, Fisher Scientific, Alfa Aesar, Fluorochem or Apollo Scientific. All air/moisture sensitive reactions were carried out under an inert atmosphere, in oven-dried or flame dried glassware. The solvent THF (from Na/benzophenone), MeCN, CH₂Cl₂ (from CaH₂) were distilled before use, and where appropriate, other reagents and solvents were purified using standard techniques. TLC was performed on aluminium-precoated plates coated with silica gel 60 containing F₂₅₄ indicator; visualised under UV light (254 nm) and/or by staining with anisaldehyde, ninhydrin, potassium permanganate or vanillin. Flash column chromatography was proceeded using; high purity silica gel, Geduran[®], pore size 60 Å, 230 - 400 mesh particle size, purchased from Merck. Fourier-transform infrared (FT-IR) spectra are reported in wavenumbers (cm⁻¹).

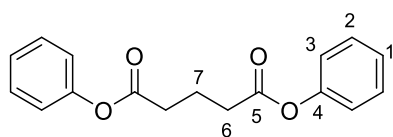
¹H NMR and ¹³C NMR spectra were recorded in CDCl₃, DMSO-*d*₆, solutions (purchased from Cambridge Isotope Laboratories, Inc.) at 298 K using Bruker DPX400, AVII400, AVIHD400 (400 and 100 MHz respectively) and at 353 K using Bruker AVII400 (400 and 101 MHz respectively) or Bruker AVIHD500 (500 and 125 MHz respectively) spectrometers. Chemical shifts values (δ) are reported in ppm relative to residual chloroform (δ 7.27 ppm for ¹H, δ 77.00 ppm for ¹³C), dimethyl sulfoxide (δ 2.50 ppm for ¹H, δ 39.51 ppm for ¹³C). All spectra were reprocessed using ACD/Labs software version: 12.1. Coupling constants (*J*) were recorded in Hz. The following abbreviations for the multiplicity of the peaks 100 are s (singlet), d (doublet), t (triplet), q (quartet), quin (quintet), sxt (sextet), br (broad), and m (multiplet).

Melting points were obtained using a Gallenkamp Electrothermal apparatus and are uncorrected. Electrospray (ESI) low resolution mass spectra were recorded on a Waters TQD quadrupole spectrometer.

Compounds containing a α,β - and β,γ -unsaturated amide and dioxo-bispidine exhibited broadening of peaks in ¹H NMR and some of the peaks were not observed in ¹³C NMR due to restricted rotation. To aid interpretation of the spectra for selected compounds variable temperature NMR experiments at T = 353 K and 373 K were conducted.

3.2 Procedures and Characterisation Data

3.2.1 Diphenyl glutarate (**2.1**)



$C_{17}H_{16}O_4$
Mol Wt: 284.31

Method A: Following the procedure described by Watkin.¹³⁵

To a solution of glutaric acid (**2.6**, 0.216 g, 15.5 mmol) in CH_2Cl_2 (20 mL) at 0 °C under Ar was added anhydrous DMF (0.10 mL, 1.3 mmol) followed by oxalyl chloride (1.64 mL, 19.4 mmol) dropwise. The reaction mixture was stirred at 0 °C for 1 h and then was allowed to warm to rt. The reaction was stirred at rt for 3 h. Upon completion the reaction mixture was concentrated *in vacuo* giving colourless oil. To the neat acid chloride at rt under Ar was added phenol (1.60 g, 17.1 mmol) in one portion with CH_2Cl_2 (20 mL) and the solution was stirred for 14 h. The reaction mixture was quenched with saturated aq. $NaHCO_3$ (20 mL). The phases were separated and the aqueous phase extracted with CH_2Cl_2 (3 × 10 mL). The organics were combined, washed with 10% K_2CO_3 (50 mL), dried ($MgSO_4$) and concentrated *in vacuo*. The desired product was isolated by column chromatography (silica gel, *eluent* gradient: EtOAc/Hexane 1:9 → 3:7) yielding the title diphenyl glutarate (**2.1**) as a colourless oil (2.43 g, 11.4 mmol, 73% yield). Physical and spectroscopic data are consistent with reported values.¹⁴⁸

Method B: Following the procedure described by Simion *et al.*,¹⁴⁹

To a solution of glutaric acid (**2.6**, 1.92 g, 14.5 mmol) in CH_2Cl_2 (18.7 mL) at 0 °C under Ar was added DMF (500 μ L, 6.45 mmol) followed by oxalyl chloride (3.00 mL, 36.2 mmol) dropwise over 15 min. The reaction mixture was stirred at 0 °C for 1 h, and allowed to warm to rt. After 3 h the solution was re-cooled to 0 °C.

In a separate flask, a solution of phenol (2.73 g, 29.0 mmol) was dissolved in 10% aqueous NaOH (38.6 mL) and a solution of tetrabutylammonium chloride (TBAC) (800 mg, 2.90 mmol) in CH_2Cl_2 (9.6 mL) was added. The resulting mixture was cooled to 0 °C and the solution of diacyl chloride (prepared above) was added in one portion. The reaction mixture was stirred vigorously at 0 °C for 10 min and was then poured onto ice water (50 mL). The organic layer was separated and the aqueous layer was extracted with Et_2O (3 × 50 mL). The combined organic extracts were washed with brine, dried (Na_2SO_4), and the solvent was removed *in vacuo*. The resulting golden syrup was

purified by column chromatography (silica gel, hexane/EtOAc, 9:1) to afford the title diester **2** as a white solid, which was recrystallised from benzene (4.05 g, 14.2 mmol, 98%). Physical and spectroscopic data are consistent with reported values.^{148,149}

M.P. 46 – 47 °C. (Lit.¹⁴⁹ 45 – 46 °C)

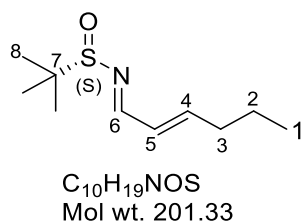
FT-IR (neat) ν_{\max} 3068, 3041, 2945, 1749, 1591, 1491, 1195, 1124 cm^{-1} .

¹H NMR (400 MHz, CDCl_3) δ 7.40 (4H, t, $J = 7.8$ Hz, 2 x **H**₂), 7.28 – 7.23 (2H, m, 2 x **H**₁), 7.12 (4H, d, $J = 7.8$ Hz, 2 x **H**₃), 2.75 (4H, t, $J = 7.3$ Hz, 2 x **H**₆), 2.22 (2H, quin, $J = 7.3$ Hz, **H**₇) ppm.

¹³C NMR (100 MHz, CDCl_3) δ 171.4 (2 x **C**₅), 150.6 (2 x **C**₄), 129.4 (4 x **C**₂), 125.8 (2 x **C**₁), 121.5 (4 x **C**₃), 33.2 (2 x **C**₆), 20.0 (**C**₇) ppm.

LRMS (ESI⁺) m/z 307.2 [**M**+Na]⁺.

3.2.2 (–)-(S)-N-((1E,2E)-Hex-2-en-1-ylidene)-2-methylpropane-2-sulfonamide (1.208)



Method A: Following the procedure described by Cutter.¹³⁴

To a solution of (S)-tertbutylsulfonamide (**2.9**, 1.21 g, 10.0 mmol) in CH_2Cl_2 (20 mL) at 40 °C under Ar were added CuSO_4 (6.38 g, 40.0 mmol) and *trans*-2-hexen1-al (**2.10**) (0.98 g, 10 mmol). After 20 h the reaction was filtered through a pad of celite and the residue washed with EtOAc (3 × 10 mL). The organic phases were combined and the solvent removed *in vacuo*. The crude material was purified by column chromatography (silica gel, *eluent* gradient: EtOAc/*n*-hexane 1:19 → 3:17) to afford the title compound as a yellow oil (1.51 g, 7.50 mmol, 75%). Physical and spectroscopic data are consistent with reported values.¹³⁵

Method B: Following the procedure described by Raghaven *et al.*¹⁵⁰

To a solution of (*S*)-tertbutylsulfonamide (**2.9**, 3.27 g, 27.0 mmol) and *trans*-2-hexen-1-al (**2.10**, 4.80 mL, 40.5 mmol) in THF (30 mL) at 0 °C under N₂ was added Ti(OEt)₄ (9.00 mL, 42.9 mmol) dropwise turning the solution yellow. The reaction was stirred for 1 h and additional Ti(OEt)₄ (6 mL, 28.58 mmol) was added dropwise at 0 °C. The reaction was monitored by TLC (*eluent*: EtOAc/ Hexane 1:4) and upon completion was poured onto brine (100 mL). The reaction was stirred rapidly for 5 min and filtered through a sintered funnel. The filter cake was washed with hot EtOAc (4 × 50 mL) and the phases separated. The aqueous layer was extracted with EtOAc (2 × 30 mL), the organics combined, washed with brine (2 × 30 mL), dried (MgSO₄) and concentrated *in vacuo*. The title compound was isolated by column chromatography (silica gel, *eluent*: EtOAc/*n*-hexane 1:4) as a pale yellow oil (5.40 g, 26.8 mmol, 99%). Physical and spectroscopic data are consistent with reported values.¹³⁵

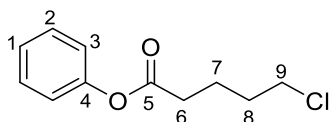
FT-IR (neat) ν_{\max} 2959 (m), 2929 , 2871 , 1639 , 1579 , 1171 , 1079 cm⁻¹.

¹H NMR (400 MHz, CDCl₃) δ 8.07 (1H, d, *J* = 9.0 Hz, **H₆**), 6.38 (1H, m, **H₄**), 6.32 (1H, m, **H₅**), 2.24 (2H, q, *J* = 6.8 Hz, **H₃**), 1.42 (2H, sxt, *J* = 7.3 Hz, **H₂**), 1.09 (9H, s, **H₈**), 0.84 (3H, t, *J* = 7.4 Hz, **H₁**) ppm

¹³C NMR (100 MHz, CDCl₃) δ 164.8 (**C₆**), 151.1 (**C₄**), 128.6 (**C₅**), 56.8 (**C₇**), 34.7 (**C₅**), 22.1 (**C₃**), 21.2 (**C₈**), 13.4 (**C₁**) ppm.

LRMS (ESI⁺) *m/z* 202.2 [M+H]⁺.

3.2.3 Phenyl 5-chloropentanoate (**1.173**)



$C_{11}H_{13}ClO_2$
Mol wt. 212.67

Method A: Following the procedure described by Watkin.¹³⁵

To a solution of 5-chlorovaleric acid (**2.31**, 0.216 g, 15.5 mmol) in CH_2Cl_2 (20 mL) at 0 °C under Ar was added anhydrous DMF (0.100 mL, 1.30 mmol) followed by oxalyl chloride (1.64 mL, 19.4 mmol) dropwise. The reaction mixture was stirred at 0 °C for 1 h and then was allowed to warm to rt. The reaction was stirred at rt for 3 h. Upon completion the reaction mixture was concentrated *in vacuo* giving colourless oil. To the neat crude acid chloride **2.32** at rt under Ar was added phenol (1.60 g, 17.0 mmol) in one portion with CH_2Cl_2 (20 mL) and stirred for 14 h. The reaction mixture was quenched with saturated aq. $NaHCO_3$ (20 mL). The phases were separated and the aqueous phase extracted with CH_2Cl_2 (3 × 10 mL). The organics were combined, washed with 10% K_2CO_3 (50 mL), dried ($MgSO_4$) and concentrated *in vacuo*. The desired product was isolated by column chromatography (silica gel, *eluent*: EtOAc/Hexane 1:9 → 3:7) yielding the title compound **1.173** as a colourless oil (2.43 g, 11.4 mmol, 73% yield). Physical and spectroscopic data are consistent with reported values.¹³⁵

Method B:

Following the procedure B described for the synthesis of **2.1**, 5-chlorovaleric acid (**2.31**, 5.40 g, 39.5 mmol) afforded the title compound (8.25 g, 38.8 mmol, 98%) as a colourless oil. Physical and spectroscopic data are consistent with reported values.¹³⁵

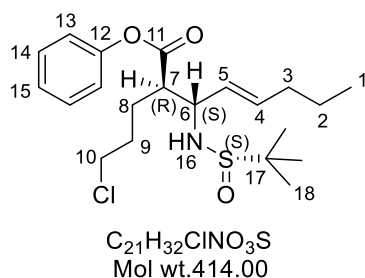
FT-IR (neat) ν_{max} 2957, 1754, 1593, 1492, 1192, 1121 cm^{-1} .

1H NMR (400 MHz, $CDCl_3$) δ 7.39 (2H t, $J = 7.3$ Hz, **H₂**), 7.25 (1H, m, **H₁**), 7.09 (2H, d, $J = 7.9$ Hz, **H₃**), 3.66 – 3.56 (2H, m, **H₉**), 2.67 – 2.58 (2H, m, **H₆**), 1.99 – 1.88 (4H, m, **H₇** & **H₈**) ppm.

^{13}C NMR (100 MHz, $CDCl_3$): δ 171.2 (**C₅**), 150.4 (**C₄**), 129.1 (2 × **C₂**), 125.5 (**C₁**), 121.2 (2 × **C₃**), 44.1 (**C₉**), 33.1 (**C₆**), 31.4 (**C₈**) ppm.

LRMS (ESI⁺) m/z 213.1 [$M^{35}Cl+H$]⁺, 215.1 [$M^{37}Cl+H$]⁺.

**3.2.4 Phenyl (2*R*,3*S*,*E*)-3-(((*S*)-tert-butylsulfinyl)amino)-2-(3-chloropropyl)oct-4-enoate
(1.209)**



Following the general procedure described by Cutter.¹³⁴

To a solution of LDA (7.20 mL, 0.9 M in THF, 4.48 mmol) at $-78\text{ }^{\circ}\text{C}$ under Ar was added to solution of phenyl 5-chloropentanoate (**1.173**, 1.35 g, 6.47 mmol) in THF (50 mL) dropwise over 45 min. The reaction was stirred for 30 min at $-78\text{ }^{\circ}\text{C}$ then a solution of sulfinylimine **1.208** (1.00 g, 4.98 mmol) in THF (5 mL) was added dropwise over 10 min. The reaction was stirred at $-78\text{ }^{\circ}\text{C}$ for 1 h and quenched with sat. NH_4Cl (25 mL) dropwise. The reaction was allowed to warm to rt with rapid stirring. The phases were separated and the aqueous layer extracted with EtOAc (3 \times 20 mL) and Et_2O (3 \times 20 mL). The organic phases were combined and washed with brine (12.5 mL), dried (Na_2SO_4) and concentrated *in vacuo*. The crude was purified by column chromatography (silica gel, *eluent* gradient EtOAc/hexane 1:9 \rightarrow 1:1) yielding the major diastereomer **1.209** (*R,S*) as a yellow oil (1.81 g, 4.38 mmol, 88 %), the minor diastereomer (*S,S*) **2.33** was isolated as a yellow oil (120 mg, 0.290 mmol, 1%), and the mixed fractions as a yellow oil (116 mg, 5%). Physical and spectroscopic data are consistent with reported values.¹³⁵

Data for major product (2*R*,3*S*,*E*)- 1.209:

FT-IR (neat) ν_{max} 3190, 2959, 2929, 2870, 1752, 1191, 1161, 1129, 1054 cm^{-1} .

^1H NMR (400 MHz, CDCl_3) δ 7.39 (2H, t, $J = 7.6$ Hz, H_{14}), 7.25 (1H, m, H_{15}), 7.06 (2H, d, $J = 7.8$ Hz, H_{13}), 5.81 (1H, m, H_4), 5.48 (1H, dd, $J = 15.3, 8.3$ Hz, H_5), 4.11 (1H, m, H_6), 3.94 (1H, d, $J = 4.2$ Hz, H_{16}), 3.59 (2H, m, H_{10}) 2.94 (1H, dt, $J = 9.4, 4.7$ Hz, H_7), 2.12 – 2.04 (2H, m, H_3), 2.04 – 1.8 (4 H, m, H_8 & H_9), 1.44 (2H, sxt, $J = 7.3$, H_2), 1.23 (9H, s, H_{18}), 0.91 (3H t, $J = 7.4$ Hz, H_1) ppm.

^{13}C NMR (101 MHz, CDCl_3) δ 171.8 (C_{11}), 150.3 (C_{12}), 136.4 (C_4), 129.5 (2 \times C_{14}), 126.5 (C_5), 126.1 (C_{15}), 121.4 (2 \times C_{13}), 58.7 (C_6), 55.6 (C_{17}), 50.4 (C_7), 44.3 (C_{10}), 34.3 (C_3), 30.3 (C_9), 25.9 (C_8), 22.6 (C_{18}), 22.1 (C_2), 13.6 (C_1) ppm.

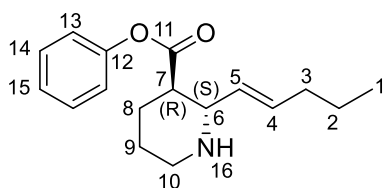
LRMS (ESI⁺) m/z 414.25 [M³⁵Cl+H]⁺, 416.2 [M³⁷Cl+H]⁺, 436.13 [M³⁵Cl+Na]⁺, 438.3 [M³⁷Cl+Na]⁺.

Selected data for minor product (2S,3S,E)- 2.33:

¹H NMR (400 MHz, CDCl₃) δ 7.40 (2H, t, J = 7.7 Hz, **H**₁₄), 7.25 (1H, m, **H**₁₅), 7.08 (2H, d, J = 7.8 Hz, **H**₁₃), 5.79 (1H, m, **H**₄), 5.41 (1H, dd, J = 15.3, 7.6 Hz, **H**₅), 4.20 – 4.01 (2H, m, **H**₆ & **H**₁₆), 3.61 (2H, t, J = 5.0 Hz, **H**₁₀), 2.83 (1H, m, **H**₇), 2.09 (2H, q, J = 6.9 Hz, **H**₃), 2.02 – 1.91 (4H, m, **H**₈ & **H**₉), 1.50 – 1.37 (2H, m, **H**₂), 1.22 (9H, s, **H**₁₈), 0.92 (3H, t, J = 7.3 Hz, **H**₁) ppm.

¹³C NMR (100 MHz, CDCl₃) δ 172.5 (**C**₁₁), 150.3 (**C**₁₂), 135.4 (**C**₄), 129.6 (2 x **C**₁₄), 128.2 (**C**₅), 126.2 (**C**₁₅), 121.4 (2 x **C**₁₃), 58.9 (**C**₆), 55.8 (**C**₁₇), 50.1 (**C**₇), 44.3 (**C**₁₀), 34.3 (**C**₃), 30.2 (**C**₉), 26.5 (**C**₈), 22.7 (**C**₁₈), 22.2 (**C**₂), 13.6 (**C**₁) ppm.

3.2.5 Phenyl (2S,3R)-2-((E)-pent-1-en-1-yl)piperidine-3-carboxylate (1.210)



C₁₇H₂₃NO₂
Mol wt. 273.37

Method A:

Following the procedure described by Watkin.¹³⁵

To a solution of imino-aldol adduct (**1.209**, 1.30 g, 3.14 mmol) in 1,4-dioxane (52 mL) at 0 °C was added conc. HCl (2.30 mL of ~36%, 9.42 mmol) dropwise. The mixture was stirred under Ar for 2 h. The reaction mixture was concentrated *in vacuo*. The crude material was dissolved in MeCN (52 mL) then K₂CO₃ (2.35 g, 15.7 mmol) and NaI (0.010 g, 0.10 mmol) were added portionwise. The resulting bright yellow solution was stirred at rt for 16 h, and then the solvent was removed *in vacuo*. The crude was re-dissolved in EtOAc/H₂O (1:1, 100 mL). The organic phases were separated. The aqueous phase was extracted with Et₂O (3 x 10 mL) and EtOAc (3 x 10 mL). The combined organic phases were washed with H₂O (20 mL) and brine (20 mL), dried (MgSO₄) and concentrated *in vacuo* to yield a white solid. The crude was passed through a plug of alumina (*eluent*: EtOAc) to

give the title piperidine **1.210** as a white solid (0.800 g, 2.92 mmol, 93%). The material was recrystallised from *n*-hexane to give pale yellow needles. Physical and spectroscopic data are consistent with reported values.¹³⁵

Method B:

Following the procedure described by Chen *et al.*¹⁵¹

To a solution of imino-aldol adduct (**1.209**, 130 mg, 0.310 mmol) in THF/H₂O (3:2, 6 mL) at rt was added I₂ (160 mg, 0.63 mmol). The reaction mixture was heated at 50 °C under Ar for 2 h before Na₂CO₃ (800 mg, 7.54 mmol) was added portionwise. The resulting dark brown solution was stirred at 50 °C for 4 h over which time it become light brown. The reaction mixture was diluted with H₂O (5 mL). After removal of THF *in vacuo*, aqueous saturated Na₂S₂O₃ (0.100 mL) was added. The resulting mixture was extracted with Et₂O (3 x 5 mL) and the combined organic phases were washed with brine (20 mL), dried (Na₂SO₄) and concentrated *in vacuo* to yield a white solid. The crude was passed through a plug of alumina (*eluent*: EtOAc) to give the title piperidine **1.210** as a white solid (82 mg, 0.30 mmol, 95%). Physical and spectroscopic data are consistent with reported values.¹

M.P. 89 – 94 °C.

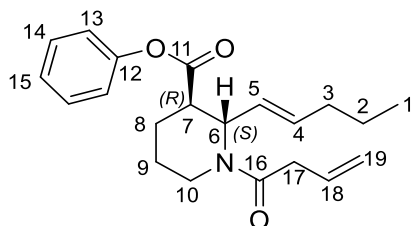
FT-IR (neat) ν_{\max} 3238, 2934, 2861, 2809, 1747, 1190, 1161, 1123 cm⁻¹.

¹H NMR (400 MHz, CDCl₃) δ 7.36 (2H, t, *J* = 7.6 Hz, **H**₁₄), 7.21 (1H, m, **H**₁₅), 7.01 (2H, d, *J* = 7.6 Hz, **H**₁₃), 5.76 (1H, dt, *J* = 15.4, 7.1 Hz, **H**₄), 5.51 (1H, dd, *J* = 15.4, 7.8 Hz, **H**₅), 3.34 (1H, dd, *J* = 9.5, 8.3 Hz, **H**₆), 3.12 (1H, dt, *J* = 11.8, 1.9 Hz, **H**₇), 2.76 (1H, td, *J* = 12.1, 2.5 Hz, **H**_{10ax}), 2.50 (1H, ddd, *J* = 11.8, 10.0, 3.7 Hz, **H**_{10eq}), 2.17 (1H, m, **H**_{8eq}), 2.03 (2H, q, *J* = 7.0 Hz, **H**₃), 1.85 – 1.67 (2H, m, **H**_{8ax} & **H**_{9ax}), 1.65 – 1.45 (2H, m, **H**₁₆ & **H**_{9eq}), 1.40 (2H, sxt, *J* = 7.4 Hz, **H**₂), 0.89 (3H, t, *J* = 7.4 Hz, **H**₁) ppm.

¹³C NMR (100 MHz, CDCl₃) δ 172.8 (**C**₁₁), 150.6 (**C**₁₂), 133.5 (**C**₄), 130.7 (**C**₅), 129.3 (**C**₁₄), 125.7 (**C**₁₅), 121.5 (**C**₁₃), 61.1 (**C**₆), 49.3 (**C**₇), 46.2 (**C**₁₀), 34.4 (**C**₃), 28.1 (**C**₈), 24.9 (**C**₉), 22.2 (**C**₂), 13.6 (**C**₁) ppm.

LRMS (ESI⁺) *m/z* 274.23 [M+H]⁺.

3.2.6 Phenyl (2*S*,3*R*)-1-(but-3-enoyl)-2-((*E*)-pent-1-en-1-yl)piperidine-3-carboxylate (**2.29**)



$C_{21}H_{27}NO_3$
Mol Wt: 341.45

To a solution of 3-butenic acid (0.40 mL, 4.60 mmol) in CH_2Cl_2 (30 mL) was added DCC (61 mg, 1.72 mmol), then the reaction mixture was stirred at 0 °C for 15 min under Ar. To the reaction mixture was added a solution of piperidine (**1.210**, 600 mg, 2.20 mmol) in CH_2Cl_2 (25 mL) at 0 °C over 15 min. The resulting mixture was stirred at rt for 4 h. The mixture was washed with water, sat. aq. $NaHCO_3$, brine (25 mL), dried over ($MgSO_4$) and concentrated *in vacuo* to give **2.21** as an oil. Purification by column chromatography (silica gel, *eluent* gradient: EtOAc/hexane 1:19 → 3:7) yielded the title amide **2.29** as light yellow oil (640 mg, 1.88 mmol, 85%).

FT-IR (neat) ν_{max} 2957, 2928, 2870, 1751, 1632, 1492, 1192 cm^{-1} .

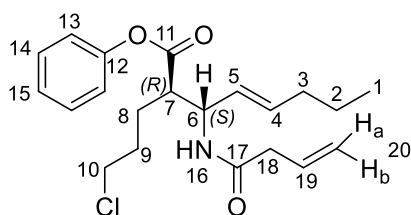
1H NMR (500 MHz, $DMSO-d_6$, T= 373 K) δ 7.41 (2H, t, $J = 7.5$ Hz, H_{14}), 7.25 (1H, m, H_{15}), 7.10 (2H, d, $J = 8.1$ Hz, H_{13}), 5.91 (1H, ddt, $J = 17.1, 10.4, 6.5$ Hz, H_{18}), 5.66–5.56 (2H, m, H_5 & H_4), 5.04–5.11 (2H, m, H_{19}), 4.00 (1H, br s, H_6), 3.18 (2H, d, $J = 6.5$ Hz, H_{17}), 3.1–3.03 (1H, m, H_7), 2.97 (2H, m, H_{10}), 2.03–2.13 (3H, m, H_{8eq} & H_3), 1.85–1.95 (1H, m, H_{8ax}), 1.56–1.73 (2H, m, H_9), 1.43 (2H, sxt, $J = 7.3$ Hz, H_2), 0.91 (3H, t, $J = 7.3$ Hz, H_1) ppm.

^{13}C NMR (125 MHz, $CDCl_3$, T= 373 K) δ 171.1 (C_{11}), 168.9 (C_{16}), 150.4 (C_{12}), 132.2 (C_{11}), 132.1 (C_4), 129.0 (C_{14}), 127.1 (C_{18}), 125.3 (C_{15}), 121.1 (C_{13}), 116.4 (C_{19}), 51.9 (C_6), 42.9 (C_7), 39.5 (C_{10}), 37.4 (C_{17}), 33.3 (C_3), 21.4 (C_9), 21.2 (C_8), 20.8 (C_2), 12.8 (C_1) ppm.

LRMS (ESI^+) m/z 342.13 [$M+H$] $^+$.

HRMS (ESI^+) for $C_{21}H_{27}NNaO_3^+$ [$M+Na$] $^+$, calculated 364.18883; found 364.18888.

3.2.7 Phenyl (2*R*,3*S*,*E*)-3-(but-3-enamido)-2-(3-chloropropyl)oct-4-enoate (2.34)



C₂₁H₂₈ClNO₃
Mol Wt: 377.91

Method A: Following the procedure described by Cropper *et al.*¹⁵²

To a solution of 3-butenic acid (0.200 g, 2.32 mmol) in CH₂Cl₂ (2.5 mL) was added 3 drops of DMF. The mixture was cooled to 0 °C, and oxalyl chloride (0.220 mL, 2.55 mmol) was added dropwise. The reaction mixture was stirred for 15 min, before being allowed to warm to rt, then stirred at rt for 3 h.

In a separate flask, to a solution of the imino-aldol adduct (**1.209**, 0.480 g, 1.16 mmol) in 1,4-dioxane (4.5 mL) was added conc. HCl (0.85 mL of ~36%, 3.48 mmol) under Ar. The reaction mixture was stirred for 1 h at rt. The solvent was removed *in vacuo* to give the crude amine **2.36** as its HCl salt.

The amine salt **2.36** was dissolved in CH₂Cl₂ (4 mL), and cooled to 0 °C under Ar. To this solution was added Et₃N (0.650 mL, 4.65 mmol), followed by the dropwise addition of the freshly prepared acid chloride at 0 °C. The mixture reaction was allowed to warm to rt and stirred for 16 h, before it was quenched by dropwise addition of H₂O (5 mL) and CH₂Cl₂ (5 mL) at 0 °C. The organic layer was separated, and the aqueous layer extracted with CH₂Cl₂ (3 x 5 mL). The combined organic solution was washed with aq. NaHCO₃, water (10 mL) and brine (10 mL), and then dried (MgSO₄). The solvent was evaporated *in vacuo*. The crude material was purified by column chromatography (silica gel, *eluent*: Et₂O/CH₂Cl₂, 1:9) to give the title compound **2.34** as a light yellow oil (243 mg, 0.640 mmol, 55%).

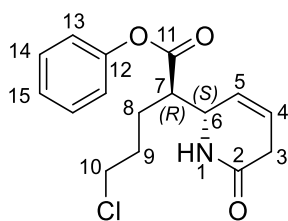
Method B:

To a solution imino-aldol adduct (**1.209**, 0.660 g, 1.59 mmol) in 1,4-dioxane (17 mL) under Ar was added conc. HCl (1.17 mL of ~36%, 4.77 mmol) dropwise. The reaction mixture was stirred for 1 h then concentrated *in vacuo*. The amine salt **2.36** was dissolved in CH₂Cl₂ (50 mL) and Et₃N (0.300 mL, 1.90 mmol) was added dropwise at 0 °C.

In a separate flask, to a solution of vinylacetic acid (0.160 ml, 1.90 mmol) in CH₂Cl₂ (20 mL) was added DCC (0.700 g, 3.19 mmol). After 15 min, to this solution was added the solution of the amine **2.36** dropwise at 0 °C over 30 min. The resulting mixture was stirred at rt for 4 h. The organic layers were washed with water, saturated aq. NaHCO₃, brine (50 mL), and dried (MgSO₄), then concentrated *in vacuo* to give crude amide **2.34**. Purification by column chromatography (silica gel, *eluent* EtOAc/Hexane, 1:19 → 2:8) gave the title compound as a white solid (470 mg, 1.24 mmol, 78%).

M.P.	47 – 49 °C
FT-IR (neat)	ν_{\max} 3336, 2963, 2924, 2860, 1747, 1638, 1520, 1158 cm ⁻¹ .
¹H NMR	(500 MHz, CDCl ₃) δ 7.39 (2H, t, J = 7.4 Hz, H₁₄), 7.25 (1H, m, H₁₅), 7.05 (2H, d, J = 7.4 Hz, H₁₃), 6.11 (1H, d, J = 8.3 Hz, H₁₆), 5.98 – 5.88 (1H, m, H₁₉), 5.80 – 5.67 (1H, m, H₅), 5.51 (1H, m, H₄), 5.24 (1H, d, J = 1.0 Hz, H_{20a}), 5.22 (1H, dd, J = 6.9, 1.0 Hz, H_{20b}), 4.81 (1H, m, H₆), 3.64 – 3.54 (2H, m, H₁₀), 3.03 (2H, d, J = 7.0 Hz, H₁₈), 2.88 (1H, dt, J = 8.7, 5.3 Hz, H₇), 2.04 (2H, q, J = 7.1 Hz, H₃), 2.0 – 1.73 (4H, m, H₈ & H₉), 1.41 (2H, sxt, J = 7.4 Hz, H₂), 0.89 (3H, t, J = 7.4 Hz, H₁) ppm.
¹³C NMR	(125 MHz, CDCl ₃) δ 171.5 (C₁₁), 169.3 (C₁₇), 150.0 (C₁₂), 134.7 (C₄), 130.8 (C₁₉), 129.2 (C₁₄), 125.8 (C₅), 125.4 (C₁₅), 121.1 (C₁₃), 119.8 (C₂₀), 52.0 (C₆), 48.8 (C₇), 44.2 (C₁₀), 41.4 (C₁₈), 34.1 (C₃), 30.0 (C₉), 25.5 (C₈), 21.8 (C₂), 13.3 (C₁) ppm.
LRMS	(ESI ⁺) m/z 378.1 [M ³⁵ Cl+H] ⁺ , 380.1 [M ³⁷ Cl+H] ⁺ .
HRMS	(ESI ⁺) for C ₂₁ H ₂₈ ClNNaO ₃ ⁺ [M+Na] ⁺ , calculated 400.1650; found 400.1649.

3.2.8 Phenyl (*R*)-5-chloro-2-((*S*)-6-oxo-1,2,5,6-tetrahydropyridin-2-yl)pentanoate (**2.35**)



$C_{16}H_{18}ClNO_3$
Mol.Wt: 307.77

Following the procedure described by Miller.¹⁵³

To a solution of amide (**2.34**, 100 mg, 0.264 mmol) in degassed CH_2Cl_2 (900 mL) was added Grubbs's II catalyst (20 mg, 0.024 mmol, 10 mol %) under Ar. The reaction mixture was heated at 44 °C for 3 h over which time the dark red solution turned dark brown in colour. The solvent was removed *in vacuo* to afford dark brown oil. The crude was purified by column chromatography (silica gel, *eluent* gradient: EtOAc/Hexane 1:9 → 7:3) yielding the title lactam **2.35** as a tan solid (30 mg, 0.097 mmol, 37%), and **2.30** as a tan solid (22 mg, 0.03 mmol, 12%).

Data for major product **2.35**:

FT-IR (neat) ν_{max} 3212, 3044, 2920, 2850, 1748, 1661, 1591, 1189 cm^{-1} .

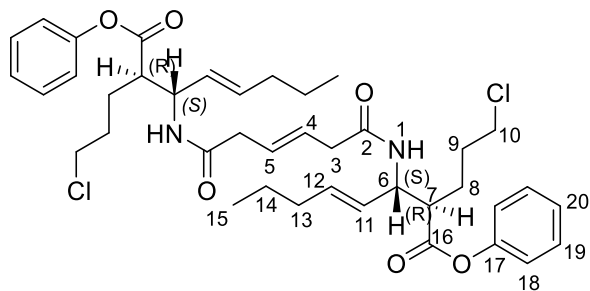
1H NMR (500 MHz, $CDCl_3$) δ 7.40 (2H, t, $J = 7.3$ Hz, **H**₁₄), 7.27 (1H, m, **H**₁₅), 7.10 – 7.06 (2H, m, **H**₁₃), 6.64 (1H, br, **H**₁), 5.97 (1H, dtd, $J = 10.1, 3.5, 1.9$ Hz, **H**₄), 5.69 (1H, ddq, $J = 10.1, 3.4, 1.9$ Hz, **H**₅), 4.57 (1H, m, **H**₆), 3.63 – 3.55 (2H, m, **H**₁₀), 3.03 – 2.95 (2H, m, **H**₃), 2.83 – 2.76 (1H, m, **H**₇), 2.09 – 1.80 (4H, m, **H**₈ & **H**₉) ppm.

^{13}C NMR (125 MHz, $CDCl_3$) δ 172.2 (**C**₁₁), 169.3 (**C**₂), 150.1 (**C**₁₂), 129.6 (**C**₁₄), 126.3 (**C**₄), 124.9 (**C**₅), 122.6 (**C**₁₅), 121.2 (**C**₁₃), 54.9 (**C**₆), 49.4 (**C**₇), 44.3 (**C**₁₀), 31.2 (**C**₃), 30.5 (**C**₉), 23.9 (**C**₈) ppm.

LRMS (ESI⁺) m/z 308 [$M^{35}Cl + H$]⁺, 310.1 [$M^{37}Cl + H$]⁺.

HRMS (ESI⁺) for $C_{16}H_{18}ClNaO_3$ ⁺ [$M + Na$]⁺, calculated 330.0867; found 330.0861.

3.2.9 Diphenyl 3,3'-(((*E*)-hex-3-enedioyl)bis(azanediyl))(2*R*,2'*R*,3*S*,3'*S*,4*E*,4'*E*)-bis(2-(3-chloropropyl) oct-4-enoate) (2.38)



$C_{40}H_{52}Cl_2N_2O_6$
Mol.Wt: 727.76

Data for minor product 2.38:

FT-IR (neat) ν_{\max} 3283, 2956, 2921, 2851, 1743, 1647, 1636, 1521, 1195 cm^{-1} .

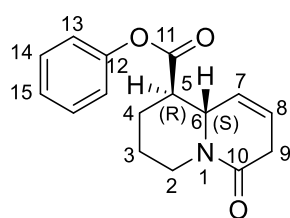
1H NMR (400 MHz, $CDCl_3$) δ 7.39 (4H, t, $J = 7.6$ Hz, 2 x H_{19}), 7.27 – 7.21 (2H, m, 2 x H_{20}), 7.05 (4H, d, $J = 7.7$ Hz, 2 x H_{18}), 6.25 (2H, d, $J = 8.8$ Hz, 2 x H_1), 5.80 – 5.68 (4H, m, H_4 & H_5 & 2 x H_{12}), 5.50 (2H, dd, $J = 7.5, 15.3$ Hz, 2 x H_{11}), 4.78 (2H, q, $J = 7.7$ Hz, 2 x H_6), 3.65 – 3.53 (4H, m, 2 x H_{10}), 2.99 (4H, d, $J = 5.3$ Hz, 2 x H_3), 2.88 (2H, dt, $J = 8.7, 5.4$ Hz, 2 x H_7), 2.08 – 2.01 (4H, m, 2 x H_{13}), 2.00 – 1.74 (8H, m, 2 x H_8 & H_9), 1.41 (4H, sxt, $J = 7.3$ Hz, 2 x H_{14}), 0.90 (6H, t, $J = 7.3$ Hz, 2 x H_{15}) ppm.

^{13}C NMR (101 MHz, $CDCl_3$) δ 171.8 (2 x C_{16}), 169.8 (2 x C_2), 150.4 (2 x C_{17}), 135.0 (2 x C_{12}), 129.5 (4 x C_{19}), 128.3 (2 x C_{11}), 126.1 (2 x C_{20}), 125.9 (C_4 & C_5), 121.4 (4 x C_{18}), 52.6 (2 x C_6), 49.2 (2 x C_7), 44.5 (2 x C_{10}), 40.0 (2 x C_3), 34.4 (2 x C_{13}), 30.2 (2 x C_9), 29.7 (C_{8a}), 25.9 (C_{8b}), 22.1 (2 x C_{14}), 13.7 (2 x C_{15}) ppm.

LRMS (ESI⁺) m/z 727.4 [$M^{35}Cl + H$]⁺, 729.2 [$M^{37}Cl + H$]⁺.

HRMS (ESI⁺) for $C_{40}H_{52}Cl_2N_2NaO_6^+$ [$M + Na$]⁺, calculated 749.3095; found 749.3092.

3.2.10 Phenyl (1*R*,9*aS*)-6-oxo-1,3,4,6,7,9*a*-hexahydro-2*H*-quinolizine-1-carboxylate (**2.30**)



$C_{16}H_{17}NO_3$
Mol.Wt: 271.32

Following the procedure described for the synthesis of **2.35**, amide (**2.29**, 330 mg, 0.966 mmol) and Grubbs's II catalyst (41 mg, 0.048 mmol, 5 mol %) afforded the title compound **2.30** (260 mg, 0.958 mmol, 99%) as a white solid.

M.P. 108 – 109 °C

FT-IR (neat) ν_{max} 3521, 2944, 2858, 2354, 1742, 1628, 1470 cm^{-1} .

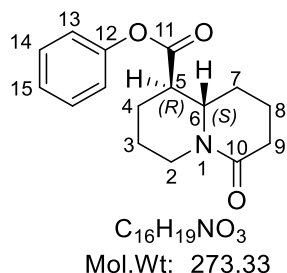
1H NMR (500 MHz, $CDCl_3$) δ 7.41 (2H, t, $J = 7.5$ Hz, **H₁₄**), 7.27 (1H, tt, $J = 7.4, 1.1$ Hz, **H₁₃**), 7.27 (1H, m, **H₁₅**), 5.89 – 5.81 (2H, m, **H₇** & **H₈**), 4.97 (1H, ddt, $J = 13.2, 4.2, 2.0$ Hz, **H₆**), 4.21 (1H, dt, $J = 10.5, 2.7$ Hz, **H_{2eq}**), 3.02 (2H, dd, $J = 4.1, 1.2$ Hz, **H₉**), 2.61 – 2.53 (2H, m, **H_{2ax}** & **H₅**), 2.38 – 2.32 (1H, m, **H_{4eq}**), 1.98 – 1.82 (2H, m, **H_{3eq}** & **H_{4ax}**), 1.60 (1H, m, **H_{3ax}**) ppm.

^{13}C NMR (126 MHz, $CDCl_3$) δ 171.8 (**C₁₁**), 166.0 (**C₁₀**), 150.2 (**C₁₂**), 129.5 (**C₁₄**), 126.1 (**C₇**), 123.6 (**C₈**), 122.6 (**C₁₅**), 121.3 (**C₁₃**), 58.9 (**C₆**), 50.1 (**C₇**), 41.9 (**C₂**), 31.6 (**C₉**), 29.1 (**C₄**), 24.0 (**C₃**) ppm.

LRMS (ESI⁺) m/z 372 [M+H]⁺.

HRMS (ESI⁺) for $C_{16}H_{17}NNaO_3^+$ [M+Na]⁺, calculated 294.1101; found 294.1105.

3.2.11 Phenyl (1*R*,9*aS*)-6-oxooctahydro-2*H*-quinolizine-1-carboxylate (**2.39**)



Following the procedure described by Watkin.¹³⁵

To a solution of **2.30** (83 mg, 0.306 mmol) in EtOH (10 mL) was added 5 wt % Pd/C (22 mg, 0.09 mmol) and the reaction mixture was placed under an H₂ atmosphere. The reaction was stirred at rt for 16 h, filtered through celite, washing with EtOH (5 × 5 mL) and the solvent removed *in vacuo*. The crude material was purified by column chromatography (silica gel, *eluent*: EtOAc/hexane 9:1) to give the title compound **2.39** as a white solid (76 mg, 0.278 mmol, 90%).

M.P. 51 – 53 °C.

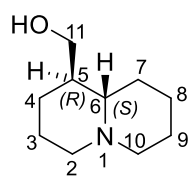
FT-IR (neat) ν_{max} 2921, 2854, 1744, 1621, 1184, 1127 cm⁻¹.

¹H NMR (400 MHz, CDCl₃) δ 7.44 – 7.35 (2H, m, **H**₁₄), 7.26 (1H, m, **H**₁₅), 7.07 (2H, d, *J* = 8.4 Hz, **H**₁₃), 4.88 (1H, m, **H**₆), 3.66 – 3.56 (1H, m, **H**₅), 2.61 – 2.33 (4H, m, **H**₂ & **H**₉), 2.32 – 2.14 (2H, m, **H**_{4eq} & **H**_{8eq}), 1.95 – 1.63 (5H, m, **H**_{3eq}, **H**_{4ax}, **H**_{8ax} & **H**₇), 1.52 (1H, m, **H**_{3ax}) ppm.

¹³C NMR (101 MHz, CDCl₃) δ 172.0 (**C**₁₁), 169.4 (**C**₁₀), 150.2 (**C**₁₂), 129.5 (**C**₁₄), 126.1 (**C**₁₅), 121.2 (**C**₁₃), 57.5 (**C**₆), 49.6 (**C**₅), 42.1 (**C**₂), 32.8 (**C**₉), 28.8 (**C**₇), 27.9 (**C**₄), 23.9 (**C**₃), 18.6 (**C**₈) ppm.

LRMS (ESI⁺) *m/z* 374.1 [M+H]⁺.

HRMS (ESI⁺) for C₁₆H₂₀NO₃⁺ [M+H]⁺, calculated 274.1438; found 274.1436.

3.2.12 ((1*R*,9*aS*)- Octahydro-2*H*-quinolizin-1-yl)methanol/ (-)-epilupinine ((-)**1.1**)

$C_{10}H_{19}NO$
Mol Wt: 169.27

Following the procedure described by Koly *et al.*¹⁴³

To a solution of (**2.39**, 35 mg, 0.128 mmol) in THF (4 mL) at 0 °C a solution of $LiAlH_4$ (0.770 mL of 1M in THF, 0.770 mmol) was added dropwise. The reaction mixture was stirred for 15 min, and then heated at reflux for 2 h. the reaction mixture was cooled to 0 °C and saturated aq. Na_2SO_4 (0.2 mL) was added carefully and was stirred for further 30 min at rt. The mixture was diluted with THF (5 mL), and the suspension was filtered through celite and washed with THF (3 x 5 mL). The solvent was removed *in vacuo*. Purification by column chromatography on basic alumina (*eluent* gradient: $CHCl_3/MeOH$, 19:1 → 9:1) gave (-)-epilupinine (**1.1**, 19 mg, 0.112 mmol, 87%). Physical and spectroscopic data were consistent with reported values.^{135,143}

The spectrographic data for the synthetic material closely matched those reported for the natural products epilupinine.

M. P. 79 – 81 °C.

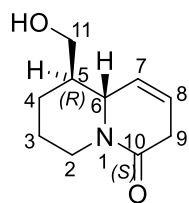
$[\alpha]_D$ -31.2 (c 0.5, EtOH, 20 °C), lit.¹⁴³ -28.0 (c 0.72, EtOH, 26 °C)

FT-IR (neat) ν_{max} 3209, 2925, 2856, 2805, 2758, 2676, 1465, 1442, 1070 cm^{-1} .

1H NMR (400 MHz, $CDCl_3$) δ 3.67 (1H, dd, $J = 10.8, 3.6$ Hz, **H_{11a}**), 3.59 (1H, dd, $J = 10.8, 5.8$ Hz, **H_{11b}**), 2.87 – 2.76 (2H, m, **H_{2eq}** & **H_{10ax}**), 2.11 – 1.95 (2H, m, **H_{2ax}** & **H_{10eq}**), 1.93 – 1.75 (3H, m, **H₅**, **H₆** & **OH**), 1.70 (2H, tdd, $J = 9.8, 6.4, 3.3$ Hz, **H₇**), 1.64 – 1.56 (2H m, **H₃**), 1.49 – 1.36 (2H, m, **H₉**), 1.34 – 1.13 (4H, m, **H₄** & **H₈**) ppm.

^{13}C NMR (101 MHz, $CDCl_3$) δ 64.8 (**C₁₁**), 64.2 (**C₆**), 56.9 (**C₂**), 56.6 (**C₁₀**), 44.0 (**C₅**), 29.8 (**C₈**), 28.2 (**C₇**), 25.6 (**C₉**), 25.1 (**C₃**), 24.6 (**C₄**) ppm

LRMS (ESI⁺) m/z 170.2 [**M+H**]⁺.

3.2.13 (9R,9aS)-9-(Hydroxymethyl)-3,6,7,8,9,9a-hexahydro-4H-quinolizin-4-one (2.42)

$C_{10}H_{15}NO_2$
Mol Wt: 181.24

Following the procedure described by Gallagher *et al.*¹⁵⁴

To a solution of **2.30** (50 mg, 0.200 mmol) in THF (0.85 mL) was added a solution $LiAlH_4$ (0.100 mL of 1.0 M in THF, 0.1 mmol) dropwise. The reaction mixture was stirred at $-15\text{ }^\circ\text{C}$ for 15 min then quenched by careful addition of 1 M NaOH (0.100 mL). The suspension was filtered through celite and washed with THF (3×5 mL), dried (Na_2SO_4) and the solvent was removed *in vacuo*. Purification by flash column chromatography (silica gel, *eluent*: EtOAc/MeOH, 95:5) gave the desired alcohol **2.42** (28 mg, 0.155 mmol, 77 %) as a white solid.

M. P. 89 – 91 $^\circ\text{C}$.

FT-IR (neat) ν_{max} 3242, 2998, 2918, 2857, 1608, 1488, 1446, 1071 cm^{-1} .

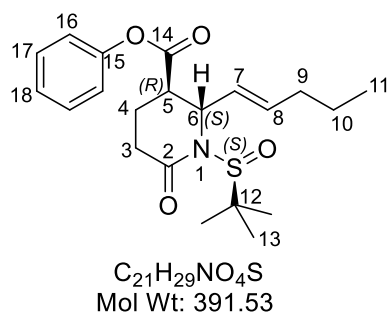
$^1\text{H NMR}$ (400 MHz, $CDCl_3$) δ 5.96 (1H, tdd, $J = 10.3, 3.7, 1.8$ Hz, **H₈**), 5.76 (1H, dtd, $J = 10.4, 3.4, 1.3$ Hz, **H₇**), 4.86 (1H, m, **H₅**), 3.83 (1H, m, **H₆**), 3.77 – 3.60 (2H, m, **H₁₁**), 2.98 – 2.90 (2H m, **H₉**), 2.45 (1H, dt, $J = 12.6, 2.9$ Hz, **H_{2ax}**), 2.06 (1H, br s, **OH**), 1.94 – 1.70 (2H m, **H_{3ax}** & **H_{4eq}**), 1.64 – 1.44 (3H, m, **H_{2eq}**, **H_{3eq}** & **H_{4ax}**) ppm.

$^{13}\text{C NMR}$ (101 MHz, $CDCl_3$) δ 166.2 (**C₁₀**), 123.5 (**C₇**), 122.0 (**C₈**), 64.0 (**C₁₁**), 60.2 (**C₇**), 46.4 (**C₅**), 42.5 (**C₂**), 31.6 (**C₉**), 28.4 (**C₄**), 25.0 (**C₃**) ppm.

LRMS (ESI $^+$) m/z 182.2 $[M+H]^+$.

HRMS (ESI $^+$) for $C_{10}H_{15}NNaO_2^+$ $[M+Na]^+$, calculated 204.0995; found 204.0994.

3.2.14 Phenyl (2*S*,3*R*)-1-((*S*)-tert-butylsulfinyl)-6-oxo-2-((*E*)-pent-1-en-1-yl)piperidine-3-carboxylate (2.11**)**



To a solution of LDA (0.61 mL of 0.8 M, 0.49 mmol) at $-78\text{ }^\circ\text{C}$ under N_2 was added to solution of diphenyl glutarate (**2.1**, 140 mg, 0.49 mmol) in THF (7.6 mL) dropwise over 15 min. The reaction was stirred at $-78\text{ }^\circ\text{C}$ for 1 h, then a solution of sulfinylimine (**1.208**, 100 mg, 0.50 mmol) in THF (0.5 mL) was added dropwise over 5 min. The reaction was stirred at $-78\text{ }^\circ\text{C}$ for 1.5 h before it was quenched by dropwise addition of saturated aq. NH_4Cl (10 mL). The reaction was allowed to warm to rt with rapid stirring. The phases were separated, and the aqueous layer was extracted with EtOAc (3 \times 5 mL) and Et_2O (3 \times 5 mL). The organic phases were combined and washed with brine (2.5 mL), dried (Na_2SO_4) and concentrated *in vacuo*. The crude material was purified by column chromatography (silica gel, *eluent* gradient: EtOAc/hexane 1:9 \rightarrow 8:2) to give the title compound **2.11** as the major product as a colourless oil (38 mg, 0.097 mmol, 20%) and mixture imino-aldol product \sim 28%, which were not characterised, and recovered sulfinylimine (**1.208**, 30 mg, 0.149 mmol, 30%).

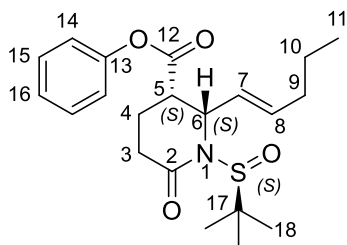
Following the procedure described above for 2 equivalents of LDA (1.24 mL of 0.8 M, 0.980 mmol), diphenyl glutarate (**2.1**, 140 mg, 0.490 mmol) and sulfinylimine (**1.208**, 100 mg, 0.500 mmol) afforded the title cyclised *syn* imino-aldol (**2.11**, 73 mg, 0.186 mmol, 38%), and uncyclised imino-aldol (**2.23**, 30 mg, 0.060 mmol, 12%). and recovered sulfinylimine (**1.208**, 19 mg, 0.094 mmol, 19%). In addition, impure cyclised *anti* imino-aldol (9 mg) was obtained; see selected its data below.

FT-IR (neat) ν_{max} 2959, 2927, 2871, 1754, 1658, 1492, 1136 cm^{-1} .

$^1\text{H NMR}$ (400 MHz, CDCl_3) δ 7.44 – 7.37 (2H, m, **H**₁₇), 7.26 (1H, m, **H**₁₈), 7.12 – 7.07 (2H, m, **H**₁₆), 5.69 – 5.59 (1H, m, **H**₈), 5.55 (1H, dd, $J = 15.4, 4.2$ Hz, **H**₇), 4.93 (1H, br s, **H**₆), 3.18 (1H, td, $J = 4.7, 2.1$ Hz, **H**₅), 2.83 (1H, m, **H**_{3a}), 2.57 (1H, dt, $J = 18.0, 5.5$ Hz, **H**_{3b}), 2.27 – 2.17 (2H, m, **H**_{4a} & **H**_{9a}), 2.14 – 2.04 (2H, m, **H**_{4b} & **H**_{9b}), 1.48 – 1.38 (2H, m, **H**₁₀), 1.23 (9H, s, **H**₁₃), 0.92 (3H, t, $J = 7.3$ Hz, **H**₁₁) ppm.

¹³C NMR	(101 MHz, CDCl ₃) δ 173.5 (C ₁₄), 170.9 (C ₂), 150.3 (C ₁₅), 132.7 (C ₈), 130.7 (C ₇), 129.6 (C ₁₇), 126.2 (C ₁₈), 121.1 (C ₁₆), 62.4 (C ₁₂), 53.6 (C ₆), 43.4 (C ₅), 34.1 (C ₉), 30.6 (C ₃), 22.5 (C ₁₃), 22.4 (C ₁₀), 22.2 (C ₄), 13.6 (C ₁₁) ppm.
LRMS	(ESI ⁺) <i>m/z</i> 392.1 [M+H] ⁺ , 413.9 [M+Na] ⁺ , 805.3 [2M+Na] ⁺
HRMS	(ESI ⁺) for C ₂₁ H ₂₉ NNaO ₄ S ⁺ [M+Na] ⁺ , calculated 414.1710; found 414.1708.

3.2.15 Phenyl (2*S*,3*S*)-1-((*S*)-tert-butylsulfinyl)-6-oxo-2-((*E*)-pent-1-en-1-yl)piperidine-3-carboxylate



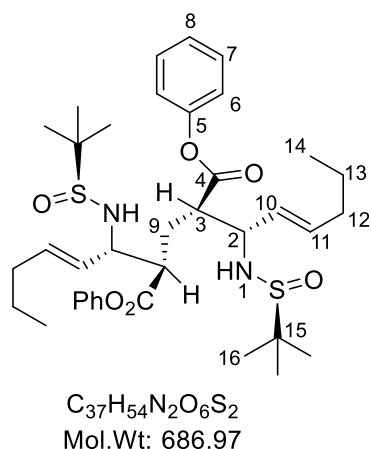
C₂₁H₂₉NO₄S
Mol. Wt: 391.53

Selected data for impure cyclised *anti* imino-aldol:

FT-IR (neat)	ν_{\max} 2966, 2945, 2876, 1745, 1663, 1491, 1162 cm ⁻¹ .
¹H NMR	(400 MHz, CDCl ₃) δ 7.44 – 7.35 (2H, m, H ₁₅), 7.29 – 7.25 (1H, m, H ₁₆), 7.06 (2H, d, <i>J</i> = 7.7 Hz, H ₁₄), 5.77 – 5.67 (1H, m, H ₈), 5.48 (1H, dd, <i>J</i> = 15.3, 5.1 Hz, H ₇), 4.97 (1H, t, <i>J</i> = 3.9 Hz, H ₆), 3.20 (1H, dt, <i>J</i> = 12.5, 4.5 Hz, H ₅), 2.75 – 2.65 (1H, m, H _{3eq}), 2.62 – 2.50 (1H, m, H _{9ax}), 2.28 (1H, tt, <i>J</i> = 13.4, 8.8 Hz, H _{4ax}), 2.18 – 2.10 (1H, m, H _{4eq}), 2.06 (2H, q, <i>J</i> = 7.0 Hz, H ₉), 1.41 (3H, qd, <i>J</i> = 14.5, 7.3, Hz, H ₁₀), 1.30 (9H, s, H ₁₈), 0.89 (3H, t, <i>J</i> = 7.4 Hz, H ₁₁) ppm.
¹³C NMR	(101 MHz, CDCl ₃) δ 172.4 (C ₁₂), 169.3 (C ₂), 150.3 (C ₁₃), 135.7 (C ₈), 129.5 (2 x C ₁₅), 126.2 (C ₇), 125.7 (C ₁₆), 121.2 (C ₁₄), 62.4 (C ₁₇), 52.8 (C ₆), 44.3 (C ₅), 34.3 (C ₉), 30.9 (C ₃), 22.7 (C ₁₈), 22.1 (C ₁₀), 17.9 (C ₄), 13.5 (C ₁₁) ppm.
LRMS	(ESI ⁺) <i>m/z</i> 392.2 [M+H] ⁺ .

3.2.16 Diphenyl (2*R*,4*R*)-2,4-bis((*S*,*E*)-1-(((*S*)-tert-butylsulfinyl)amino)hex-2-en-1-yl)pentanedioate (**2.2**)

Double imino-aldol conditions from unsaturated imine **1.208**.



To a solution of LDA (1.50 mL of 0.85 M in THF, 1.30 mmol) at $-78\text{ }^{\circ}\text{C}$ under N_2 was added a solution of diphenyl glutarate (**2.1**, 370 mg, 1.30 mmol) in THF (10 mL) dropwise over 15 min. The reaction was stirred at $-78\text{ }^{\circ}\text{C}$ for 1 h. A second portion of LDA (1.5 mL of 0.85 M in THF, 1.30 mmol) at $-78\text{ }^{\circ}\text{C}$ was added dropwise. The reaction was stirred at $-78\text{ }^{\circ}\text{C}$ for 1 h, and a solution of sulfinylimine **1.208** (400 mg, 2.00 mmol) in THF (2 mL) was added dropwise over 15 min. The reaction was stirred for 1 h and quenched at $-78\text{ }^{\circ}\text{C}$ by dropwise addition of saturated aq. NH_4Cl (10 mL). The reaction was allowed to warm to rt with rapid stirring. The phases were separated and the aqueous layer extracted with EtOAc (3 \times 5 mL) and Et_2O (3 \times 5 mL). The organic phases were combined and washed with brine (2.5 mL), dried (Na_2SO_4) and concentrated *in vacuo*. The crude material was purified by column chromatography (silica gel, *eluent* gradient: EtOAc/hexane 1:9 \rightarrow 8:2) to give the title compound **2.32** as the major product (228 mg, 0.330 mmol, 25%) and mixture of other imino-aldol products \sim 30%, which were not characterised. The double imino-aldol adduct **2.2** was recrystallised from *n*-hexane to give white needles.

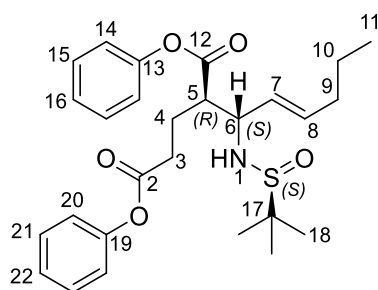
M.P. 123 – 127 $^{\circ}\text{C}$

FT-IR (neat) ν_{max} 3174, 2958, 2927, 2871, 1751, 1667, 1592, 1190, 1049 cm^{-1} .

$^1\text{H NMR}$ (400 MHz, $CDCl_3$) δ 7.38 (4H, t, $J = 7.6$ Hz, 2 \times **H₇**), 7.27 – 7.22 (2H, m, 2 \times **H₈**), 7.09 (4H, d, $J = 7.6$ Hz, 2 \times **H₆**), 5.81 (2H, dt, $J = 15.3, 6.7$ Hz, 2 \times **H₁₁**), 5.47 (2H, dd, $J = 15.3, 8.4$ Hz, 2 \times **H₁₀**), 4.19 – 4.12 (2H, m, 2 \times **H₂**), 3.98 (2H, d, $J = 3.8$ Hz, 2 \times **H₁**), 3.04 (2H, br dt, $J = 7.9, 6.1$ Hz, 2 \times **H₃**), 2.20 (2H, dd, $J = 7.7, 6.6$ Hz, **H₉**), 2.07 (4H, q, $J = 7.0$ Hz, 2 \times **H₁₂**), 1.42 (4H, sxt, $J = 7.3$ Hz, 2 \times **H₁₃**), 1.23 (18H, s, 2 \times **H₁₆**), 0.91 (6H, t, $J = 7.3$ Hz, 2 \times **H₁₄**) ppm.

¹³C NMR	(100 MHz, CDCl ₃) δ 171.6 (2 x C ₄), 150.3 (2 x C ₅), 136.5 (2 x C ₁₁), 129.5 (2 x C ₇), 126.8 (2 x C ₁₀), 126.1 (2 x C ₈), 121.5 (2 x C ₆), 59.1 (2 x C ₂), 55.7 (2 x C ₁₅), 48.6 (2 x C ₃), 34.3 (2 x C ₁₂), 27.5 (C ₉), 22.7 (2 x C ₁₆), 22.1 (2 x C ₁₃), 13.6 (2 x C ₁₄) ppm.
LRMS	(ESI ⁺) <i>m/z</i> 687.2 [M+H] ⁺ .
HRMS	(ESI ⁺) for C ₃₇ H ₅₄ N ₂ NaO ₆ S ₂ ⁺ [M+Na] ⁺ , calculated 709.3315; found 709.3309.

3.2.17 Diphenyl (*R*)-2-((*S,E*)-1-(((*S*)-*tert*-butylsulfinyl)amino)hex-2-en-1-yl)pentanedioate (2.23)

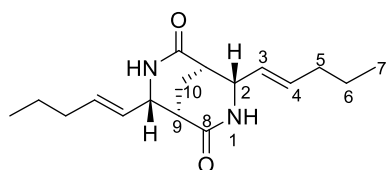


C₂₇H₃₅NO₅S
Mol. Wt: 485.64

Data for uncyclised *syn* imino-aldol 2.23:

FT-IR (neat)	ν_{\max} 2964, 2877, 2835, 1745, 1665, 1493, 1163 cm ⁻¹ .
¹H NMR	(400 MHz, CDCl ₃) δ 7.40 (4H, q, <i>J</i> = 7.3 Hz, H ₁₅), 7.32 – 7.21 (2H, m, H ₁₆), 7.17 – 7.03 (4H, m, H ₁₄), 5.86 (1H, dt, <i>J</i> = 15.2, 6.8 Hz, H ₈), 5.53 (1H, br dd, <i>J</i> = 15.3, 8.2 Hz, H ₇), 4.19 (1H, dt, <i>J</i> = 8.5, 4.5 Hz, H ₆), 4.05 (1H, d, <i>J</i> = 3.9 Hz, H ₁), 3.08 (1H, dt, <i>J</i> = 9.9, 4.8 Hz, H ₅), 2.90 – 2.66 (2H, m, H ₃), 2.32 – 2.15 (2H, m, H ₄), 2.11 (2H, q, <i>J</i> = 6.9 Hz, H ₉), 1.46 (2H, dq, <i>J</i> = 14.7, 7.4 Hz, H ₁₀), 1.25 (9H, s, H ₁₈), 0.94 (3H, t, <i>J</i> = 7.4 Hz, H ₁₁) ppm.
¹³C NMR	(101 MHz, CDCl ₃) δ 171.7 (C ₁₂), 171.1 (C ₂), 150.5 (C ₁₃), 150.2 (C ₁₉), 136.5 (C ₇), 129.5 (2 x C ₁₅), 129.4 (2 x C ₂₁), 126.5 (C ₈), 126.1 (C ₁₆), 125.8 (C ₂₂), 121.5 (2 x C ₂₀), 121.4 (2 x C ₁₄), 58.7 (C ₆), 55.6 (C ₁₇), 50.1 (C ₅), 34.30 (C ₉), 32.0 (C ₃), 23.6 (C ₄), 22.6 (C ₁₈), 22.07 (C ₁₀), 13.6 (C ₁₁) ppm.
LRMS	(ESI ⁺) <i>m/z</i> 486.2 [M+H] ⁺ .

**3.2.18 (1R,4S,5R,8S)-4,8-di ((E)-Pent-1-en-1-yl)-3,7-diazabicyclo[3.3.1]nonane-2,6-dione
(2.3)**



$C_{17}H_{26}N_2O_2$
Mole Wt: 290.41

To a solution of double imino-aldol adduct (**2.2**, 100 mg, 0.150 mmol) in 1,4-dioxane (2.2 mL) at 0 °C was added conc. HCl (0.210 mL of ~36%, 0.87 mmol) dropwise, then the mixture was stirred for 2 h under Ar. The reaction mixture was concentrated *in vacuo*. The crude was dissolved in EtOAc (2 mL) and saturated aq. NaHCO₃ (1 mL) at 0 °C was added dropwise. The phases were separated and the aqueous phase was extracted with Et₂O (3 × 3 mL), H₂O (3 × 3 mL) and the organic combined solution was washed with brine (2 × 3 mL), dried (MgSO₄) and the solvent was removed *in vacuo*. The crude material was purified by column chromatography (silica gel, *eluent*: EtOAc/hexane 9:1 then EtOAc/MeOH 19:1) to give the title compound **2.3** as a pale yellow oil (26 mg, 0.089 mmol 61%).

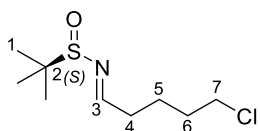
FT-IR (neat) ν_{\max} 3444, 2924, 1655, 1464, 1023, 1004 cm⁻¹.

¹H NMR (500 MHz, DMSO-*d*₆, T= 373 K) δ 7.48 (2H, m, 2 x **H**₁), 5.64 (1H, td, *J* = 6.6, 1.3 Hz, **H**_{3a}), 5.61 (1H, td, *J* = 6.5, 1.3 Hz, **H**_{3b}), 5.54 (1H, dt, *J* = 5.1, 1.2 Hz, **H**_{4a}), 5.51 (1H, dt, *J* = 5.1, 1.2 Hz, **H**_{4b}), 3.97 (2H, dd, *J* = 4.7, 3.6 Hz, 2 x **H**₂), 3.01 (4H, br, 2 x **H**₉), 2.38 – 2.34 (2H, m, **H**₁₀), 2.08 – 2.00 (4H, m, 2 x **H**₅), 1.41 (4H, sxt, *J* = 7.3 Hz, 2 x **H**₆), 0.90 (6H, t, *J* = 7.3 Hz, 2 x **H**₇) ppm.

¹³C NMR (125 MHz, DMSO-*d*₆, T= 373 K) δ 170.3 (2 x **C**₈), 131.1 (2 x **C**₄), 130.3 (2 x **C**₃), 55.6 (2 x **C**₂), 40.0 (2 x **C**₉), 32.9 (2 x **C**₅), 21.2 (2 x **C**₆), 15.3 (**C**₁₀), 12.7 (2 x **C**₇) ppm.

LRMS (ESI⁺) *m/z* 290.9 [M+H]⁺, 581.2 [2M+H]⁺.

HRMS (ESI⁺) for C₁₇H₂₆N₂NaO₂⁺ [M+Na]⁺, calculated 313.1886; found 313.1895.

3.2.19 (-)-(S)-N-[(1E)-5-Chloropentylidene]-2-methylpropane-2-sulfonamide (1.205)

C₉H₁₈ClNOS
Mol. Wt. : 223.76

Following a modified procedure from Cutter *et al.*,¹³⁴ to a solution of methyl-5-chloropentanoate (**2.12**, 1.90 mL, 13.3 mmol, 1.0 equiv) in CH₂Cl₂ (40 mL) at -78 °C was added a solution of DIBAL-H (14.6 mL of 1 M in CH₂Cl₂, 14.6 mmol, 1.1 equiv) dropwise over 10 min. The reaction mixture was stirred at -78 °C for 30 min. The reaction was quenched with saturated aqueous Rochelle's salt solution (50 mL). The suspension was filtered and extracted with CH₂Cl₂ (3 x 100 mL). The combined organic layers were washed with brine (25 mL), dried (MgSO₄) and the solvent was removed *in vacuo* to give 5-chloropentanal as a yellow oil (1.45 g, 12.0 mmol, 90%). The crude material was used in the subsequent reaction without further purification. ¹H NMR spectroscopic data were consistent with reported values.⁴ **¹H NMR** (400 MHz, CDCl₃) δ 9.77 (t, *J* = 1.5 Hz, 1H), 3.55 (t, *J* = 6.2, 2H), 2.52 – 2.45 (m, 2H), 1.85 – 1.74 (m, 4H) ppm. **¹³C NMR** (101 MHz, CDCl₃) δ 201.8, 44.4, 42.9, 31.7, 19.3 ppm. Following a procedure described by Ellman *et al.*,¹⁵⁵ (S)-2-methylpropane-2-sulfonamide (**2.9**, 1.48 g, 12.2 mmol, 1.2 equiv) was dissolved in dry CH₂Cl₂ (20 mL) before anhydrous CuSO₄ (7.66 g, 48.0 mmol, 4.0 equiv) was added in one portion followed by 5-chloropentanal (1.45 g, 12.0 mmol, 1.0 equiv). The reaction mixture was heated at 40 °C for 24 h then filtered through celite and washed with CH₂Cl₂. The solvent was removed *in vacuo* and the crude reaction mixture was purified by column chromatography (SiO₂, hexane/EtOAc, 3:1) to afford the title sulfinylimine **1.205** as a mobile pale yellow oil (2.08 g, 9.30 mmol, 77%). Physical and spectroscopic data are consistent with the reported values.^{134,135}

FT-IR (neat) ν_{\max} 2957, 2868, 1622, 1456, 1078 cm⁻¹.

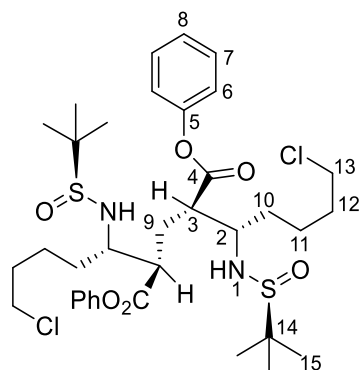
¹H NMR (500 MHz, CDCl₃) δ 8.09 (1H, t, *J* = 4.5 Hz, **H₃**), 3.57 (2H, t, *J* = 6.1 Hz, **H₇**), 2.57 (2H, td, *J* = 6.9, 4.5 Hz, **H₄**), 1.90 – 1.77 (4H, m, **H₅** & **H₆**), 1.20 (9H, s, **H₁**) ppm.

¹³C NMR (101 MHz, CDCl₃) δ 168.7 (**C₃**), 56.6 (**C₂**), 44.4 (**C₇**), 35.2 (**C₄**), 31.9 (**C₆**), 22.7 (**C₅**), 22.3 (**C₁**) ppm.

LRMS (ESI⁺) *m/z* 224.3 [M³⁵Cl+H]⁺, 226.3 [M³⁷Cl+H]⁺.

3.2.20 Diphenyl (2*R*,4*R*)-2,4-bis((*S*)-1-(((*S*)-*tert*-butylsulfinyl)amino)-5-chloropentyl) pentanedioate (2.5a).

Double imino-aldol conditions from halo imine 1.205.



$C_{35}H_{52}Cl_2N_2O_6S_2$
Mol Wt: 731.83

To a solution of LDA (4.90 mL of 1.0 M in THF/hexane, 4.90 mmol) in THF (20 mL) at $-78\text{ }^{\circ}\text{C}$ under Ar was added a solution of diphenyl glutarate (**2.1**, 635 mg, 2.23 mmol) in THF (5 mL) dropwise. The reaction was stirred at $-78\text{ }^{\circ}\text{C}$ for 1 h, and then a solution of sulfinylimine (**1.205**, 1.00 g, 4.47 mmol) in THF (5 mL) was added dropwise over 10 min at $-78\text{ }^{\circ}\text{C}$. After 1 h, the reaction was quenched at $-78\text{ }^{\circ}\text{C}$ by dropwise addition of saturated aq NH_4Cl (12 mL) over 30 min. The reaction was allowed to warm to rt with rapid stirring for 30 min. The phases were separated and the aqueous layer extracted with EtOAc (3 \times 15 mL). The organic phase was combined, washed with brine (2 \times 10 mL), dried (Na_2SO_4) and concentrated *in vacuo*. The crude material was purified by column chromatography (silica gel, *eluent* gradient: EtOAc/hexane, 2:8 \rightarrow 8:2) affording several fractions: *Fraction 1* ($R_f = 0.51$, $\text{Et}_2\text{O}/\text{hexane}$, 8:2) contained the pure cyclised mono *syn* imino-aldol **2.13** as off-white solid (149 mg, 0.36 mmol, 16%); *Fraction 2* ($R_f = 0.45$, $\text{Et}_2\text{O}/\text{hexane}$, 8:2) contained *syn*-uncyclised mono imino-aldol **2.16** as a white solid (71 mg, 0.14 mmol, 6 %); *Fraction 3* ($R_f = 0.43$, $\text{Et}_2\text{O}/\text{hexane}$, 8:2) contained cyclised-*anti*- **2.17** as a an impure yellow oil (50 mg, 0.12 mmol, 5%); *Fraction 4* ($R_f = 0.34$, $\text{Et}_2\text{O}/\text{hexane}$, 8:2) contained the pure *syn,syn* double imino-aldol product **2.5a** as a colourless viscous syrup (488 mg, 0.66 mmol, 30%); *Fraction 5* ($R_f = 0.34\text{--}0.18$, $\text{Et}_2\text{O}/\text{hexane}$, 8:2) contained unseparated mixture of double imino-aldol products (see below) as a yellow oil (168 mg).^a Sulfinylimine **1.205** ($R_f = 0.64$, 270 mg, 1.2 mmol, 27%) was also recovered.

Data for *syn, syn* double imino-aldol adduct 2.5a:

$[\alpha]_D$ +29 (*c* 1.8, MeOH, 24 °C)

FT-IR (neat) ν_{\max} 3356, 2971, 2925, 1751, 1592, 1456, 1190, 1163, 1045 cm^{-1} .

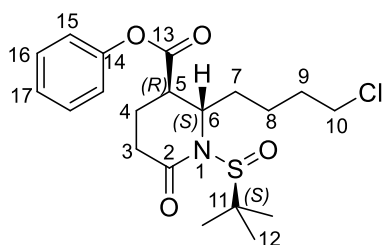
^1H NMR (400 MHz, CDCl_3) δ 7.39 (4H, t, $J = 7.6$ Hz, 2 x H_7), 7.26 – 7.22 (2H, m, 2 x H_8), 7.18 (4H, d, $J = 7.6$ Hz, 2 x H_6), 4.25 (2H, d, $J = 8.1$ Hz, 2 x H_1), 3.72 – 3.63 (2H, m, 2 x H_2), 3.52 (4H, $J = 6.3$ Hz, 2 x H_{13}), 3.17 (2H, q, $J = 6.3$ Hz, 2 x H_3), 2.40 – 2.31 (2H, m, 2 x H_9), 1.88 – 1.59 (12H, m, 2 x H_{10} , H_{11} & H_{12}), 1.26 (18H, s, 2 x H_{15}) ppm.

^{13}C NMR (100 MHz, CDCl_3) δ 172.4 (2 x C_4), 150.3 (2 x C_5), 129.5 (2 x C_7), 126.2 (2 x C_8), 121.6 (2 x C_6), 58.4 (2 x C_2), 56.4 (2 x C_{14}), 48.2 (2 x C_3), 44.7 (2 x C_{13}), 33.4 (2 x C_{10}), 32.1 (2 x C_{12}), 27.3 (C_9), 23.2 (2 x C_{11}), 22.9 (2 x C_{15}) ppm.

LRMS (ESI⁺) m/z 753.4 [$\text{M}^{35}\text{Cl}+\text{Na}$]⁺, 755.4 [$\text{M}^{37}\text{Cl}+\text{Na}$]⁺.

HRMS (ESI⁺) for $\text{C}_{35}\text{H}_{52}^{35}\text{Cl}_2\text{N}_2\text{NaO}_6\text{S}_2^+$ [$\text{M}+\text{Na}$]⁺, calculated 753.2536; found 753.2520.

3.2.21 Phenyl (2*S*,3*R*)-1-((*S*)-tert-butylsulfinyl)-2-(4-chlorobutyl)-6-oxopiperidine-3-carboxylate (2.13)



$\text{C}_{20}\text{H}_{28}\text{ClNO}_4\text{S}$
Mol Wt: 413.96

Data for cyclised mono *syn* imino-aldol 2.13: Slow evaporation of a solution of **2.13** in CHCl_3 gave crystals suitable for X-ray structure determination.

$[\alpha]_D$ -74 (*c* 2.1, MeOH, 24 °C)

M.P. 56 – 58 °C

FT-IR (neat) ν_{\max} 2960, 2929, 2866, 1753, 1660, 1492, 1163 cm^{-1} .

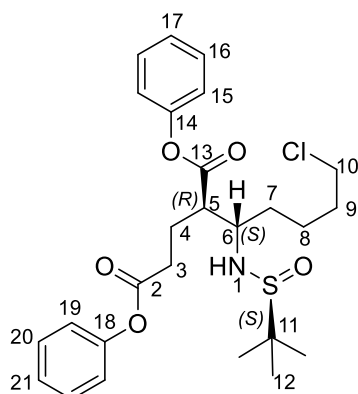
$^1\text{H NMR}$ (400 MHz, CDCl_3) δ 7.43 – 7.37 (2H, m, H_{16}), 7.30 – 7.23 (1H, m, H_{17}), 7.09 (2H, d, $J = 7.5$ Hz, H_{15}), 4.30 (1H, dt, $J = 10.5, 2.4$ Hz, H_6), 3.60 (2H, t, $J = 6.4$ Hz, H_{10}), 3.21 (1H, td, $J = 5.7, 2.0$ Hz, H_5), 2.84 (1H, dt, $J = 17.8, 7.7$ Hz, $\text{H}_{3\text{eq}}$), 2.58 (1H, dt, $J = 17.9, 6.5$ Hz, $\text{H}_{3\text{ax}}$), 2.30 – 2.23 (2H, m, H_4), 2.16 – 2.06 (1H, m, $\text{H}_{7\text{a}}$), 1.96 – 1.76 (2H, m, H_9), 1.71 - 1.55 (3H, m, $\text{H}_{7\text{b}}$ & H_8), 1.22 (9H, s, H_{12}) ppm.

$^{13}\text{C NMR}$ (100 MHz, CDCl_3) δ 173.1 (C_{13}), 171.6 (C_2), 150.3 (C_{14}), 129.6 (C_{16}), 126.2 (C_{17}), 121.0 (C_{15}), 62.3 (C_{11}), 53.0 (C_6), 44.7 (C_5), 40.9 (C_{10}), 36.9 (C_7), 31.5 (C_3), 30.8 (C_9), 23.2 (C_8), 22.4 (C_{12}), 19.3 (C_4) ppm.

LRMS (ESI^+) m/z 436.2 [$\text{M}^{35}\text{Cl}+\text{Na}$] $^+$, 438.2 [$\text{M}^{37}\text{Cl}+\text{Na}$] $^+$.

HRMS (ESI^+) for $\text{C}_{20}\text{H}_{28}^{35}\text{ClNNaO}_4\text{S}^+$ [$\text{M}+\text{Na}$] $^+$, calculated 436.1320; found 436.1324.

3.2.22 Diphenyl (*R*)-2-((*S*)-1-(((*S*)-*tert*-butylsulfinyl)amino)-5-chloropentyl)pentanedioate (2.16)



$\text{C}_{26}\text{H}_{34}\text{ClNO}_5\text{S}$
Mol Wt: 508.07

Data for uncyclised mono *syn* imino-aldol 2.16: recrystallisation from hexane and EtOAc gave crystals suitable for X-ray structure determination.

M.P. 93 – 96 °C

$[\alpha]_D$ +31 (c 1.5, MeOH, 20 °C)

FT-IR (neat) ν_{max} 3322, 2991, 2928, 2869, 1739, 1591, 1483, 1454, 1236, 1184, 1049 cm^{-1} .

¹H NMR (400 MHz, CDCl₃) δ 7.40 (4H, m, 2 x H₁₆ & H₂₀), 7.30 – 7.20 (2H, m, H₁₇ & H₂₁), 7.12 (4H, t, *J* = 8.5 Hz, 2 x H₁₅ & H₁₉), 4.22 (1H, d, *J* = 8.5 Hz, H₁), 3.62 – 3.51 (3H, m, H₆ & H₁₀), 3.28 – 3.21 (1H, m, H₅), 2.93 – 2.83 (1H, m, H_{3a}), 2.77 (1H, s, H_{3b}), 2.36 – 2.23 (1H, m, H_{4a}), 2.2 – 2.09 (1H, m, H_{4b}), 1.90 – 1.50 (6H, m, H₇, H₈ & H₉), 1.26 (9H, s, H₁₂) ppm.

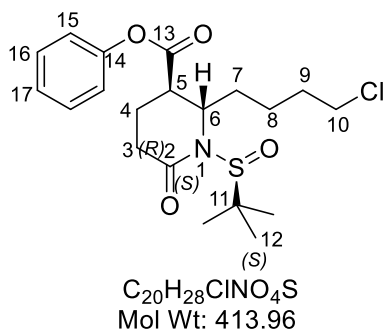
¹³C NMR (100 MHz, CDCl₃) δ 172.1 (C₁₃), 171.40 (C₂), 150.6 (C₁₄), 150.2 (C₁₈), 129.6 (C₁₆), 129.4 (C₂₀), 126.3 (C₁₇), 125.9 (C₂₁), 121.5 (C₁₅), 121.5 (C₁₉), 58.4 (C₆), 56.3 (C₁₄ & C₁₈), 49.8 (C₅), 44.70 (C₁₀), 32.4 (C₃), 32.0 (C₇), 31.9 (C₉), 23.7 (C₄), 23.5 (C₈), 22.8 (C₁₂) ppm.

LRMS (ESI⁺) *m/z* 508.2 [M³⁵Cl+H]⁺, 510.2 [M³⁷Cl+H]⁺.

HRMS (ESI⁺) for C₂₆H₃₅³⁵ClNO₅S⁺ [M+H]⁺, calculated 508.1919; found 508.1923; for C₂₆H₃₄³⁵ClNNaO₅S⁺ [M+Na]⁺, calculated 530.1738; found 530.1740.

3.2.23 Phenyl (2*S*,3*R*)-1-((*S*)-*tert*-butylsulfinyl)-2-(4-chlorobutyl)-6-oxopiperidine-3-carboxylate (**2.13**).

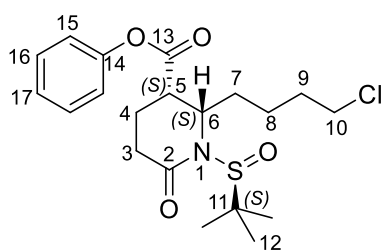
Prepared under conditions optimised to favour mono imino-aldol products.



To a solution of LDA (7.0 mL of 1.0 M in THF/hexane, 7.00 mmol) in THF (15 mL) at –78 °C under Ar was added a solution of diphenyl glutarate (**2.1**, 991 mg, 3.48 mmol) in THF (14 mL) dropwise. The reaction was stirred at –78 °C for 1 h, and then a solution of sulfinylimine (**1.205**, 650 mg, 2.90 mmol) in THF (3 mL) was added dropwise using a syringe pump at –78 °C. After addition was complete, the reaction mixture was maintained at this temperature for 1 h, then quenched by dropwise addition of saturated aq NH₄Cl (14 mL) over 30 min at –78 °C. The reaction was allowed to warm to rt with rapid stirring. After 30 min, the phases were separated and the aqueous layer extracted with EtOAc (3 × 15 mL). The organic phases were combined, washed with brine (2 x 10 mL), dried (Na₂SO₄) and concentrated *in vacuo*. The major components of the crude material were

syn- and *anti*-cyclised mono imino-aldol products **2.13** and **2.17** (3:1), respectively see crude spectrta in appendix part. The crude material was purified by column chromatography (silica gel, *eluent* gradient: EtOAc/hexane, 2:8 → 1:1) affording several fraction: *Fraction 1* ($R_f = 0.51$, Et₂O/hexane, 8:2) contained the pure cyclised mono *syn* imino-aldol **2.13** as off-white solid (615 mg, 1.49 mmol, 51%); *Fraction 2* ($R_f = 0.43$, Et₂O/hexane, 8:2) contained *anti*-cyclised **2.17** as an impure yellow oil (163 mg, 0.390 mmol, 13%); *Fraction 3* ($R_f = 0.34 - 0.18$, Et₂O/hexane, 8:2) contained unseparated mixture of double imino-aldol products as yellow oil (44 mg).

Data for cyclised mono *syn* imino-aldol **2.13** are consistent with those reported above.

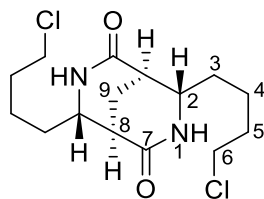


C₂₀H₂₈ClNO₄S
Mol Wt: 413.96

Selected data for impure cyclised mono *anti* imino-aldol **2.17**:

- FT-IR (neat)** ν_{\max} 2962, 2873, 2930, 2866, 1751, 1661, 1492, 1164 cm⁻¹.
- ¹H NMR** (400 MHz, CDCl₃) δ 7.44 – 7.38 (2H, m, **H**₁₆), 7.26 – 7.19 (1H, m, **H**₁₇), 7.13 – 7.07 (2H, m, **H**₁₅), 4.49 – 4.42 (1H, m, **H**₆), 3.52 (2H, t, $J = 6.5$ Hz, **H**₁₀), 3.19 (1H, ddd, $J = 12.6, 5.7, 3.6$ Hz, **H**₅), 2.81 – 2.72 (1H, m, **H**_{3eq}), 2.70 – 2.59 (1H, m, **H**_{3ax}), 2.47 – 2.32 (1H, m, **H**_{4eq}), 2.29 – 2.17 (1H, m, **H**_{3ax}), 1.83 – 1.61 (6H, m, **H**₇, **H**₈ & **H**₉), 1.32 – 1.28 (9H, m,) ppm.
- ¹³C NMR** (100 MHz, CDCl₃) δ 171.9 (**C**₁₃), 169.7 (**C**₂), 150.2 (**C**₁₄), 129.6 (2 x **C**₁₆), 126.3 (**C**₁₇), 121.1 (2 x **C**₁₅), 62.4 (**C**₁₁), 51.3 (**C**₆), 44.5 (**C**₅), 44.0 (**C**₁₀), 33.3 (**C**₃), 32.4 (**C**₉), 30.6 (**C**₇), 24.0 (**C**₈), 23.2 (**C**₁₂), 22.8 (**C**₄) ppm.
- LRMS** (ESI⁺) m/z 436.2 [**M**³⁵Cl+Na]⁺, 438.2 [**M**³⁷Cl+Na]⁺.

**3.2.24 (1R,4S,5R,8S)-4,8-bis (4-Chlorobutyl)-3,7-diazabicyclo [3.3.1] nonane-2,6-dione
(2.14)**



$C_{15}H_{24}Cl_2N_2O_2$
Mol Wt: 335.27

Method A: under basic conditions

To a solution of double imino-aldol adduct (**2.5a**, 400 mg, 0.550 mmol) in THF/ H₂O (3:2, 11 mL) at rt was added I₂ (555 mg, 2.18 mmol). The reaction mixture was heated at 50 °C under Ar. After 1 h, then Na₂CO₃ (463 mg, 4.36 mmol) was added portionwise. The resulting dark brown mixture lightened in colour. After 1 h, the mixture was allowed to cool to rt, then diluted with H₂O (5 mL). After removal of THF under reduced pressure, EtOAc (10 mL) was added, followed by dropwise addition of an aqueous saturated solution of Na₂S₂O₃ until the solution became colourless. The resulting mixture was extracted with EtOAc (3 x 10 mL) and the combined organic phase was washed with brine (2 x 10 mL), dried (Na₂SO₄) and concentrated *in vacuo* to yield a white solid. Purification by column chromatography (silica gel, *eluent*: EtOAc/hexane 9:1 then EtOAc/MeOH, 9:1) afforded the title bispidine **2.14** as a white solid (124 mg, 0.370 mmol, 67%).

Method B: under acidic conditions

To a solution of double imino-aldol adduct (**2.5a**, 50 mg, 0.068 mmol) in 1,4-dioxane (1.1 mL) at 0 °C was added conc. HCl (0.100 mL of ~36%, 0.410 mmol) dropwise and then stirred for 2 h under Ar. The reaction mixture was concentrated *in vacuo*. The crude was dissolved in EtOAc (2 mL) and saturated aq. NaHCO₃ was added dropwise at 0 °C. The phases were separated and aqueous phase was extracted with Et₂O (3 x 3 mL), H₂O (3 x 3 mL). The combined organics solution were washed with brine (2 x 3 mL), dried (MgSO₄) the solvent was removed *in vacuo*. The crude material was purified by column chromatography (silica gel, *eluent*: EtOAc/hexane 9:1 then EtOAc/MeOH, 19:1) to give the title compound **2.14** as a white solid (15 mg, 0.048 mmol, 66%). The material was recrystallised from EtOH to give white fluffy solid.

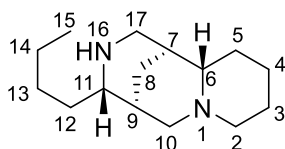
M.P. 270 – 273 °C

[α]_D –50.3 (c 1.5, MeOH, 24 °C)

FT-IR (neat) ν_{max} 3356, 2972, 2927, 1653, 1541, 1456, 1045 cm⁻¹.

¹H NMR	(400 MHz, CDCl ₃) δ 8.29 (2H, br s, 2 x H ₁), 3.56 (6H, t, <i>J</i> = 5.4 Hz, 2 x H ₂ & H ₆), 2.54 (2H, br, 2 x H ₉), 2.03 (2H, br, 2 x H ₈), 1.87 – 1.77 (4H, m, 2 x H ₅), 1.76 – 1.47 (8H, m, 2 x H ₃ & H ₄) ppm.
¹³C NMR	(101 MHz, CDCl ₃) δ 173.5 (2 x C ₇), 55.3 (2 x C ₂), 44.6 (2 x C ₆), 39.2 (2 x C ₈), 34.8 (2 x C ₃), 32.0 (2 x C ₅), 23.3 (C ₉), 16.6 (2 x C ₄) ppm.
LRMS	(ESI ⁺) <i>m/z</i> 335.2 [M ³⁵ Cl+H] ⁺ , 337.2 [M ³⁷ Cl+H] ⁺ .
HRMS	(ESI ⁺) for C ₁₅ H ₂₄ Cl ₂ N ₂ NaO ₂ ⁺ [M+Na] ⁺ , calculated 357.1107; found 357.1100.

3.2.25 (1*S*,4*S*,5*S*,11*aS*)-4-Butyldecahydro-2*H*-1,5-methanopyrido[1,2-*a*][1,5]diazocine (**2.15**)



C₁₅H₂₈N₂
Mol Wt: 236.40

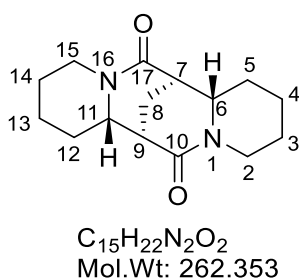
Following the procedure described by Nagao *et al.*,¹⁴⁰ to a solution of **2.14**, 16 mg, 0.050 mmol) in THF (0.3 mL) at 0 °C was added a solution of LiAlH₄ (0.150 ml of 1 M in THF, 0.150 mmol), dropwise. The reaction mixture was stirred at rt for 3 h, then heated under reflux for 3 h. Reaction progress was monitored by TLC (*eluent*: EtOAc/MeOH/NH₄OH 8:1.5:0.5). The mixture was allowed to cool to 0 °C, then it was diluted with Et₂O (1 mL), and quenched by careful addition of 30% NaOH (0.5 mL) and water (0.5 mL). The suspension was stirred at rt for 30 min then filtered through celite and washed with 10% Et₃N in THF (3 × 5 mL), dried (Na₂SO₄) and the solvent was removed *in vacuo*. Purification by column chromatography (silica gel, *eluent*: EtOAc/hexane 9:1 then EtOAc/MeOH, 8:2) gave sparteine derivative **2.15** as a pale yellow (5 mg, 0.021 mmol, 42%).

FT-IR (neat) ν_{\max} 2923, 2853, 1733, 1457, 1377, 1260, cm⁻¹.

¹H NMR (400 MHz CDCl₃) δ 3.27 (1H, dd, *J* = 11.1, 6.5 Hz, **H**_{17eq}), 2.99 (1H, dd, *J* = 13.1, 2.9 Hz, **H**_{10eq}), 2.85 – 2.76 (1H, m, **H**_{2eq}), 2.68 – 2.56 (2H, m, **H**₁₁ & **H**₁₆), 2.55 – 2.41 (2H, m, **H**₆ & **H**_{17ax}), 2.34 – 2.13 (2H, m, **H**_{2ax} & **H**_{10ax}), 1.84 – 1.50 (7H, m, **H**₈, **H**₉, **H**₁₂ & **H**₁₃), 1.47 – 1.18 (9H, m, **H**₃, **H**₄, **H**₅, **H**₇ & **H**₁₄), 0.91 (3H, br t, *J* = 7.0 Hz, **H**₁₅)

¹³C NMR	(101 MHz, CDCl ₃) δ 63.0 (C ₁₁), 58.4 (C ₆), 56.0 (C ₁₀), 55.2 (C ₂), 54.7 (C ₁₇), 47.4 (C ₉), 34.9 (C ₁₂), 34.5 (C ₇), 32.1 (C ₅), 30.8 (C ₈), 25.5 (C ₃), 25.5 (C ₄), 22.9 (C ₁₄), 21.1 (C ₁₃), 14.1 (C ₁₅) ppm.
LRMS	(ESI ⁺) <i>m/z</i> 237.1 [M+H] ⁺ .
HRMS	(ESI ⁺) for C ₁₅ H ₂₉ N ₂ ⁺ [M+H] ⁺ , calculated 237.2325; found 237.2326.

3.2.26 (+)-10,17-Dioxo-β-isosparteine ((+)-1.33)



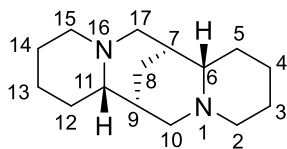
Following a modified procedure from Bogdal;¹⁵⁶ to a solution of halo dioxobispidine (**2.14**, 100 mg, 0.300 mmol) in DMSO (3 mL) was added K₂CO₃ (205 mg, 1.490 mmol), and KOH (84 mg, 1.490 mmol) portionwise, followed by TBAB (20 mg, 0.060 mmol). The reaction mixture was heated at 60 °C for 4 h. The mixture was cooled to rt and extracted with EtOAc (5 x 10 mL), washing with iced water (5 x 5 mL). The organic phase was dried (MgSO₄), and the solvent was removed using a high vacuum pump. The title bislactam (+)-**1.33** was obtained as a white solid (64 mg, 0.240 mmol, 81%). Physical and spectroscopic data are consistent with the reported values.⁵⁵

M.P.	170 – 172 °C (Lit. ⁵⁵ 172 – 174 °C for racemate).
[α]_D	+47.3 (c 1.5, MeOH, 23 °C)
FT-IR (neat)	<i>v</i> _{max} 2928, 2850, 1628, 1458, 1436, 1356, 1269, 1211 cm ⁻¹ .
¹H NMR	(400 MHz, CDCl ₃) δ 4.71 (2H, ddt, <i>J</i> = 13.1, 4.0, 1.8 Hz, H _{2eq} & H _{15eq}), 3.58 – 3.46 (2H, m, H ₆ & H ₁₁), 2.58 (2H, t, <i>J</i> = 3.0 Hz, H _{2ax} & H _{15ax}), 2.45 (2H, td, <i>J</i> = 13.0, 2.7 Hz, H ₇ & H ₉), 2.10 (2H, t, <i>J</i> = 3.0 Hz, H ₈), 2.01 – 1.89 (2H m, H _{5a} & H _{12a}), 1.77 – 1.53 (8H, m,), 1.46 – 1.32 (2H, m,) ppm.
¹³C NMR	(101 MHz, CDCl ₃) δ 169.0 (C ₁₀ & C ₁₇), 60.4 (C ₆ & C ₁₁), 43.5 (C ₂ & C ₁₅), 42.5 (C ₇ & C ₉), 32.2 (C ₅ & C ₁₂), 25.3 (C ₃ & C ₁₄), 24.9 (C ₄ & C ₁₃), 18.7 (C ₈) ppm.

LRMS (ESI⁺) m/z 363.3 [M+H]⁺

HRMS (ESI⁺) for C₁₅H₂₃N₂O₂⁺ [M+H]⁺, calculated 263.1754; found 263.1757.

3.2.27 (+)- β -Isosparteine ((+)-**1.4**)



C₁₅H₂₆N₂
Mol. Wt: 234.39

Following the procedure of Hermet *et al.*;⁸⁴ to a solution of bislactam (**1.33**, 30 mg, 0.11 mmol) in THF (1 mL) at 0 °C under N₂ was added LiAlH₄ (1.00 mL, 1 M in THF, 1.00 mmol) dropwise. The resulting suspension was heated at reflux for 4 h. After cooling to rt, the suspension was diluted with Et₂O (10 mL) and excess solid hydrated sodium sulfate was added portionwise until effervescence ceased. The suspension was stirred for 30 min at rt during which it became pale grey. The solids were removed by filtration through celite and the filter cake was washed with CH₂Cl₂-MeOH (9:1, 40 mL). The filtrate and combined washing were dried (NaSO₄) and concentrated *in vacuo* to access (+)- β -isosparteine ((+)-**1.4**, 24 mg, 0.100 mmol, 90%) as a colourless oil. Physical and spectroscopic data are consistent with the reported values.^{48,55}

[α]_D +15.1 (c 0.75 absolute EtOH, 23 °C), Lit.⁴⁸ +15.38 (c 0.142 absolute EtOH, 21.1 °C)

FT-IR (neat) ν_{\max} 2924, 2850, 1443, 1354, 1130 cm⁻¹.

¹H NMR (400 MHz, CDCl₃) δ 3.02 (2H, dd, $J = 10.9, 6.7$ Hz, **H**_{10eq}), 2.80 (dt, $J = 12.7, 2.0$ Hz, 2H, **H**_{2eq}), 2.45 (2H, td, $J = 12.6, 2.6$ Hz, **H**_{2ax}), 2.26 (2H, dt, $J = 11.7, 2.5$ Hz, **H**_{6ax}), 2.17 (2H, dd, $J = 10.8, 2.9$ Hz, **H**_{10ax}), 1.82 – 1.74 (2H, m, **H**_{4eq}), 1.71 – 1.50 (8H, m, **H**_{3eq}, **H**_{5eq}, **H**_{7ax} & **H**₈), 1.44 – 1.32 (4H, m, **H**_{3ax} & **H**_{5ax}), 1.25 – 1.20 (m, 2H, **H**_{4ax}) ppm.

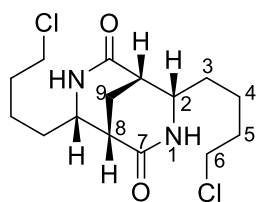
¹³C NMR (101 MHz, CDCl₃) δ 62.8 (2 x **C**₆), 55.2 (2 x **C**₂), 55.0 (2 x **C**₉), 34.5 (2 x **C**₇), 28.8 (2 x **C**₅), 25.5 (2 x **C**₄), 22.7 (2 x **C**₃), 19.8 (**C**₈) ppm.

LRMS (ESI⁺) m/z 235.2 [M+H]⁺.

HRMS (ESI⁺) for C₁₅H₂₇N₂⁺ [M+H]⁺, calculated 235.2169; found 235.2168.

3.2.28 (1S,4S,5S,8S)-4,8-bis(4-Chlorobutyl)-3,7-diazabicyclo[3.3.1]nonane-2,6-dione (2.18)

Complex mixture of double imino-aldol products isolated from double and mono imino-aldol reactions.



$C_{15}H_{24}Cl_2N_2O_2$
Mol Wt: 335.27

To a solution of a mixture of double imino-aldol adduct (**2.5a-c**, 1.50 g, 2.050 mmol) in 1,4-dioxane (41 mL) at 0 °C was added conc. HCl (4 mL of ~36%, 16.4 mmol) dropwise and then the mixture was stirred at rt for 1 h under Ar. The reaction mixture was basified by the dropwise addition of saturated aq. NaHCO₃ at 0 °C, then stirred at rt for 1 h. The phases were separated and the aqueous phase was extracted with EtOAc (3 × 25 mL), washing with saturated aq. NaHCO₃ (3 × 20 mL). The combined organic solutions were washed with brine (2 × 25 mL), dried (NaSO₄) the solvent was removed *in vacuo*. The crude material contained three diastereomers (*anti,anti:syn,anti:syn,syn*). The mixture of diastereomers was purified by repeated column chromatography (silica gel, *eluent*: EtOAc/MeOH 98:2 then EtOAc/MeOH, 19:1) to provide the first diastereomer *anti,anti* dioxo-bispidine (**2.18**), followed quickly by *syn,anti* dioxo-bispidine (**2.19**) as a second diastereomer, and later, the third diastereomer *syn,syn* dioxo-bispidine (**2.14**). The *syn,syn* dioxo-bispidine (**2.14**) was obtained as a white solid (410 mg, 1.220 mmol). The *anti,anti* dioxo-bispidine (**2.18**) was also obtained as a white solid (15 mg, 0.040 mmol). The mixture of *anti,anti* and *syn,anti* dioxo-bispidines was obtained as a white solid (53 mg, 0.160 mmol).

Data for *anti,anti* dioxo-bispidine (2.18):

M.P. 133 – 135 °C.

[α]_D +21.4 (c 1.5, MeOH, 20 °C)

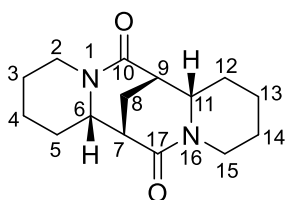
FT-IR (neat) ν_{\max} 3199, 2944, 1661, 1418, 1317, 1066 cm⁻¹.

¹H NMR (400 MHz, CDCl₃) δ 5.97 (2H, s, 2 x **H**₁), 3.54 – 3.43 (6H, m, 2 x **H**₂ & **H**₆), 2.69 (2H, br d, *J* = 3.3 Hz, 2 x **H**₉), 2.12 (2H, t, *J* = 3.1 Hz, 2 x **H**₈), 1.82 – 1.56 (8H, m, 2 x **H**_{4a}, **H**_{3a} & **H**₅), 1.52 – 1.44 (2H, m, **H**_{4b}), 1.40 – 1.27 (2H, m, **H**_{3b}) ppm.

^{13}C NMR (101 MHz, CDCl_3) δ 169.5 (2 x C_7), 56.3 (2 x C_2), 44.6 (2 x C_6), 38.7 (2 x C_8), 33.3 (2 x C_3), 32.2 (2 x C_5), 27.2 (C_9), 23.1 (2 x C_4) ppm.

LRMS (ESI^+) m/z 335.2 [$\text{M}^{35}\text{Cl}+\text{H}$] $^+$, 337.2 [$\text{M}^{37}\text{Cl}+\text{H}$] $^+$.

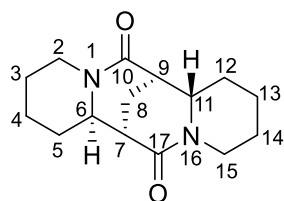
3.2.29 (7S,7aS,14S,14aS)-Dodecahydro-6H,13H-7,14-methanodipyrido[1,2-a:1',2'-e][1,5]diazocine-6,13-dione, (-)-10,17-dioxo- α -isosparteine ((-)-1.43)



$\text{C}_{15}\text{H}_{22}\text{N}_2\text{O}_2$
Mol.Wt: 262.353

Following a modified procedure from Bogdal,¹⁵⁶ to a solution containing a mixture of *anti,anti* and *syn,anti* dioxo-bispidines (**2.18** & **2.19**, 50 mg, 0.150 mmol) in DMSO (2 mL) was added K_2CO_3 (100 mg, 0.720 mmol), and KOH (40 mg, 0.710 mmol) portionwise, followed by TBAB (10 mg, 0.030 mmol). The reaction mixture was heated at 60 °C for 6 h. The mixture was cooled to rt and extracted with EtOAc (5 x 10 mL), and iced water (5 x 5 mL). The organic phase was dried (NaSO_4), and the solvent was removed under high vacuum. The mixture of *anti,anti* and *syn,anti* bislactams were obtained as a white solid (29 mg, 0.110 mmol, 74%). The mixture was recrystallised from hexane. Careful separation of the needles provided (-)-10,17-dioxo- α -isosparteine ((-)-**1.43**), 9 mg, 0.030 mmol).

Alternatively, purification of the mixture of diastereomers by column chromatography (silica gel, *eluent*: EtOAc/MeOH 98:2 then EtOAc/MeOH, 19:1) provided the first diastereomer (+)-10,17-dioxo-sparteine (**1.44**, 7 mg, 0.026 mmol), followed by (-)-10,17-dioxo- α -isosparteine ((-)-**1.43**) as a white solid (11 mg, 0.042 mmol). Physical and spectroscopic data for (+)-**1.44** are consistent with the reported values.⁸⁴

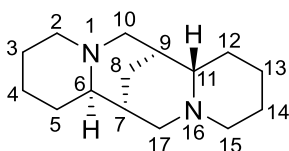
Data for (–)-10,17-dioxo- α -isosparteine ((–)-1.43):**M.P.** 160 – 164 °C. $[\alpha]_D$ –58.8 (c 1.0, MeOH, 20 °C)**FT-IR (neat)** ν_{\max} 2922, 2850, 1632, 1427, 1361, 1263, 1112 cm^{-1} . **^1H NMR** (400 MHz, CDCl_3) δ 4.74 (2H, ddt, $J = 13.3, 4.1, 2.0$ Hz, $\text{H}_{2\text{eq}}$ & $\text{H}_{15\text{eq}}$), 3.33 (2H, ddd, $J = 12.0, 5.1, 2.4$ Hz, H_6 & H_{11}), 2.85 – 2.81 (2H, m, $\text{H}_{2\text{ax}}$ & $\text{H}_{15\text{ax}}$), 2.46 (2H, td, $J = 13.1, 3.0$ Hz, H_7 & H_9), 2.06 (2H, t, $J = 3.1$ Hz, H_8), 2.04 – 1.97 (2H, m, $\text{H}_{5\text{a}}$ & $\text{H}_{12\text{a}}$), 1.92 – 1.84 (2H, m, $\text{H}_{4\text{a}}$ & $\text{H}_{13\text{a}}$), 1.77 – 1.69 (2H, m, $\text{H}_{3\text{a}}$ & $\text{H}_{14\text{a}}$), 1.46 – 1.13 (6H, m, $\text{H}_{3\text{b}}$, $\text{H}_{4\text{b}}$, $\text{H}_{5\text{b}}$, $\text{H}_{12\text{b}}$, $\text{H}_{13\text{b}}$ & $\text{H}_{14\text{b}}$) ppm **^{13}C NMR** (101 MHz, CDCl_3) δ 167.9 (C_{10} & C_{17}), 58.8 (C_6 & C_{11}), 42.4 (C_2 & C_{15}), 41.8 (C_7 & C_9), 31.3 (C_5 & C_{12}), 25.2 (C_3 & C_{14}), 24.4 (C_8), 24.3 (C_4 & C_{13}) ppm.**LRMS** m/z 263.2 $[\text{M}+\text{H}]^+$.**HRMS** (ESI⁺) for $\text{C}_{15}\text{H}_{23}\text{N}_2\text{O}_2^+$ $[\text{M}+\text{H}]^+$, calculated 263.1754; found 263.1755.**3.2.30 (7R,7aR,14R,14aS)-Dodecahydro-6H,13H-7,14-methanodipyrido[1,2-a:1',2'-e][1,5]diazocine-6,13-dione, (+)-10,17-dioxo-sparteine ((+)-1.44)**
 $\text{C}_{15}\text{H}_{22}\text{N}_2\text{O}_2$
 Mol.Wt: 262.353
Data for (+)-10,17-dioxo-sparteine ((+)-1.44):**M.P.** 62 – 66 °C. $[\alpha]_D$ +70.3 (c 0.6, CH_3Cl , 20 °C), Lit⁸⁴ +72.3 (c 1.0 in CH_3Cl , 20 °C)**FT-IR (neat)** ν_{\max} 2922, 2850, 1632, 1427, 1361, 1263, 1112 cm^{-1} . **^1H NMR** (400 MHz, CDCl_3) δ 4.79 – 4.70 (2H, m, $\text{H}_{2\text{eq}}$ & $\text{H}_{15\text{eq}}$), 3.56 (1H, dd, $J = 11.7, 2.0$ Hz, H_{11}), 3.37 (1H, ddd, $J = 11.8, 5.2, 2.6$ Hz, H_6), 2.80 – 2.75 (1H, m, H_7), 2.62 (br

s, 1H **H**₉), 2.53 – 2.41 (2H, m, **H**_{2ax} & **H**_{15ax}), 2.22 (1H, ddd, *J* = 13.0, 4.0, 2.0 Hz, **H**_{8eq}), 1.99 – 1.91 (3H, m, **H**₅, **H**_{8ax}), 1.90 – 1.83 (1H, m, **H**_{3a}), 1.76 – 1.57 (5H, m, **H**_{3b}, **H**_{4a}, **H**₁₂ & **H**_{14a}), 1.45 – 1.33 (3H, m, **H**_{4b}, **H**_{13a} & **H**_{14b}), 1.24 – 1.19 (1H, m, **H**_{13b}) ppm.

¹³C NMR (101 MHz, CDCl₃) δ 170.2 (**C**₁₇), 166.4 (**C**₁₀), 60.0 (**C**₁₁), 59.2 (**C**₆), 43.4 (**C**₁₅), 42.8 (**C**₉), 42.3 (**C**₂), 42.0 (**C**₇), 32.6 (**C**₁₂), 31.2 (**C**₅), 25.1 (**C**₁₄), 25.0 (**C**₃), 24.9 (**C**₁₃), 24.2 (**C**₄), 21.9 (**C**₈) ppm.

LRMS *m/z* 263.2 [M+H]⁺.

3.2.31 (-)-sparteine ((-)-1.3)



C₁₅H₂₆N₂
Mol.Wt: 234.39

Following the procedure of Hermet *et al.*;⁸⁴ to a solution of (+)-10,17-dioxo-sparteine ((+)-**1.44**, 6 mg, 0.023 mmol) in THF (1 mL) at 0 °C under N₂ was added a solution of LiAlH₄ (0.14 mL of 1.0 M, 0.14 mmol) dropwise. The resulting suspension was heated at reflux for 6 h. After cooling to rt, the suspension was diluted with Et₂O (10 mL) and excess solid hydrated sodium sulfate was added portionwise until effervescence ceased. The suspension was stirred for 30 min at rt during which it became pale grey. The solids were removed by filtration through celite and the filter cake was washed with CH₂Cl₂-MeOH (9:1) (20 mL). The filtrate and combined washing were dried (Na₂SO₄) and concentrated *in vacuo* to access (-)-sparteine ((-)-**1.3**, 5 mg, 0.021 mmol, 92%) as a yellow oil. Physical and spectroscopic data are consistent with the reported values.⁸⁴

[α]_D -16.9 (c 0.5 absolute EtOH, 20 °C), Lit.⁸⁴ (-18.1 (c 1.3 in EtOH)), Lit⁹² -20.4 (c 1.3 in EtOH).

FT-IR (neat) ν_{max} 2922, 2850, 1632, 1427, 1361, 1263, 1112 cm⁻¹.

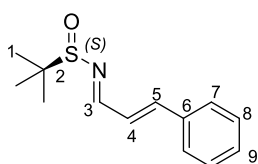
¹H NMR ¹H NMR (400 MHz, CDCl₃) δ 2.81 (1H, br d, *J* = 11.4 Hz, **H**_{15eq}), 2.77 – 2.65 (2H, m, **H**_{2eq} & **H**_{17eq}), 2.54 (1H, br d, *J* = 10.0 Hz, **H**_{10eq}), 2.36 (1H, br dd, *J* = 10.2, 2.1 Hz, **H**_{17ax}), 2.11 – 1.91 (5H, m, **H**_{2ax}, **H**_{8eq}, **H**_{10ax}, **H**₁₁ & **H**_{15ax}), 1.89 – 1.81 (1H, m, **H**₇),

1.77 – 1.66 (3H, m, **H**_{4eq}, **H**₆ & **H**_{13eq}), 1.66 – 1.43 (6H, m, **H**₃, **H**₉, **H**_{12ax} & **H**₁₄), 1.42 – 1.19 (5H, m, **H**_{4ax}, **H**₅, **H**_{12eq} & **H**_{13ax}), 1.07 (1H, d, *J* = 12.0 Hz, **H**_{8ax}) ppm.

¹³C NMR (101 MHz, CDCl₃) δ 66.4 (**C**₆), 64.4 (**C**₁₁), 61.8 (**C**₁₀), 56.2 (**C**₂), 55.3 (**C**₁₅), 53.4 (**C**₁₇), 35.9 (**C**₇), 34.3 (**C**₁₂), 33.0 (**C**₉), 29.3 (**C**₅), 27.5 (**C**₈), 25.8 (**C**₃ & **C**₁₄), 24.6 (**C**₄), 24.4 (**C**₁₃) ppm.

LRMS *m/z* 235.2 [M+H]⁺.

3.2.32 2-Methyl-N-((1E,2E)-3-phenylallylidene)propane-2-sulfonamide (2.22)



C₁₃H₁₇NOS
Mol Wt: 235.35

To a solution of (*S*)-tertbutylsulfonamide (**2.9**, 2.5 g, 20.7 mmol) and cinnamaldehyde (3.12 mL, 24.75 mmol) in THF (30 mL) at 0 °C under N₂ was added Ti(OEt)₄ (4.50 mL, 18.8 mmol) dropwise turning the solution yellow. The reaction was stirred for 1 h and additional Ti(OEt)₄ (2.50 mL, 9.51 mmol) was added dropwise at 0 °C. The reaction was monitored by TLC (eluent: EtOAc/ hexane 1:4) and upon completion for 4 h. The reaction mixture was poured onto brine (100 mL). The reaction was stirred rapidly for 5 min and filtered through a sintered funnel. The filter cake was washed with hot EtOAc (4 × 25 mL) and the phases separated. The aqueous layer was extracted with EtOAc (2 × 20 mL), the organics combined, washed with brine (2 × 20 mL), dried (MgSO₄) and concentrated *in vacuo*. The title compound **2.22** was isolated by column chromatography (silica gel, eluent: EtOAc/*n*-hexane 1:4) as a pale yellow oil (4.02 g, 17.0 mmol, 82%). Physical and spectroscopic data are consistent with reported values.¹⁵⁷

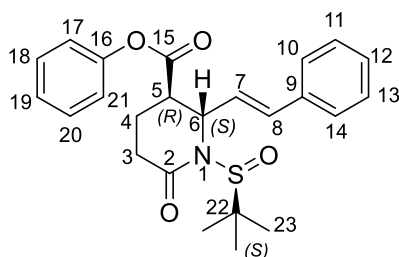
FT-IR (neat) ν_{\max} 1622, 1578, 1565, 1151, 1075, 749, 686 cm⁻¹.

¹H NMR (400 MHz, CDCl₃) δ 8.39 (1H, d, *J* = 9.2 Hz, **H**₃), 7.58 – 7.52 (2H, m, **H**₇), 7.45 – 7.36 (3H, m, **H**₈ & **H**₉), 7.23 (1H, d, *J* = 16.0 Hz, **H**₅), 7.14 – 7.06 (1H, m, **H**₄), 1.25 (9H, s, **H**₁) ppm.

¹³C NMR (101 MHz, CDCl₃) δ 163.8 (C₃), 146.3 (C₅), 135.0 (C₆), 130.2 (C₉), 128.9 (2 x C₇), 127.9 (2 x C₈), 125.6 (C₄), 57.5 (C₂), 22.5 (C₁) ppm.

LRMS (ESI+) *m/z* 236.2 [M+H]⁺.

3.2.33 Phenyl (2*R*,3*R*)-1-((*S*)-tert-butylsulfinyl)-6-oxo-2-((*E*)-styryl) piperidine-3-carboxylate (2.24)



C₂₄H₂₇NO₄S
Mol. Wt: 425.54

To a solution of LDA (2.93 mL of 2.0 M in THF, 5.860 mmol) at -78 °C under Ar was added a solution of diphenyl glutarate (**2.1**, 832 mg, 2.930 mmol) in THF (22.5 mL) dropwise over 15 min. The reaction was stirred at -78 °C for 1 h, and then a solution of phenyl imine (**2.22**, 530 mg, 2.250 mmol) in THF (2.5 mL) at -78 °C was added dropwise over 5 min. The reaction was stirred at between -78 and -70 °C for 1 h, and quenched by dropwise addition of saturated aq. NH₄Cl (9 mL). The reaction was allowed to warm to rt with rapid stirring for 30 min. The phases were separated and the aqueous layer extracted with EtOAc (3 × 15 mL). The organic phases were combined, dried (Na₂SO₄) and concentrated *in vacuo*. The crude mixture of diastereomers were purified by column chromatography (silica gel, *eluent* gradient: Et₂O/hexane, 2:8 → 7:2) to provide the first diastereomer (cyclised mono *syn* imino-aldol **2.24**), as a colourless oil (400 mg, 0.940 mmol, 41%). The second diastereomer was the cyclised mono *anti* imino-aldol, which was isolated impure in low quantity. The uncyclised *syn* imino-aldol **2.25** was instable with no assignment recorded.

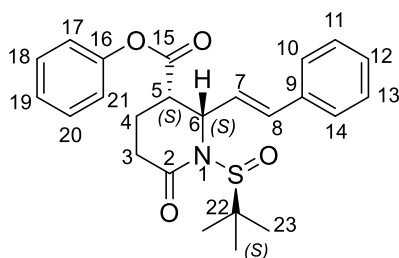
FT-IR (neat) ν_{\max} 2958, 2925, 2876, 1757, 1660, 1496, 1471, 1136 cm⁻¹.

¹H NMR (400 MHz, CDCl₃) δ 7.45 – 7.38 (4H, m, H₁₁, H₁₃, H₁₈ & H₂₀), 7.35 – 7.29 (2H, m, H₁₀ & H₁₄), 7.29 – 7.25 (2H, m, H₁₂ & H₁₉), 7.16 – 7.11 (2H, m, H₁₇ & H₂₁), 6.55 (1H, dd, *J* = 16.0, 1.3 Hz, H₈), 6.29 (1H, dd, *J* = 16.0, 4.8 Hz, H₇), 5.17 – 5.13 (1H, m, H₆), 3.31 (1H, td, *J* = 4.7, 2.1 Hz, H₅), 2.94 – 2.83 (1H, m, H_{3eq}), 2.69 – 2.59 (1H, m, H_{3ax}), 2.31 – 2.24 (2H, m, H₄), 1.27 (9H, s, H₂₃) ppm.

¹³C NMR (100 MHz, CDCl₃) δ 173.2 (C₂), 170.6 (C₁₅), 150.2 (C₁₆), 135.7 (C₉), 131.2 (C₈), 130.1 (C₇), 129.5 (C₁₈ & C₂₀), 128.5 (C₁₁ & C₁₃), 128.0 (C₁₂), 126.6 (C₁₀ & C₁₄), 126.2 (C₁₉), 121.0 (C₁₇ & C₂₁), 62.5 (C₂₂), 53.9 (C₆), 43.5 (C₅), 30.6 (C₃), 22.5 (3 × C₂₃), 18.8 (C₄) ppm.

LRMS (ESI⁺) *m/z* 448.2 [M+Na]⁺.

3.2.34 Phenyl (2*S*,3*S*)-1-((*S*)-tert-butylsulfinyl)-6-oxo-2-((*E*)-styryl)piperidine-3-carboxylate.



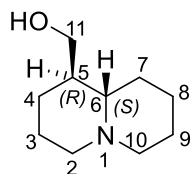
C₂₄H₂₇NO₄S
Mol. Wt: 425.54

Selected data for impure cyclised *anti* mono imino-aldol:

¹H NMR (400 MHz, CDCl₃) δ 7.45 – 7.31 (8H, m, H₁₀, H₁₁, H₁₂, H₁₃, H₁₄, H₁₅, H₁₈, H₁₉ & H₂₀), 7.07 (2H, br d, *J* = 7.7 Hz, H₁₇ & H₂₁), 6.67 – 6.60 (1H, m, H₈), 6.28 – 6.20 (1H, m, H₇), 5.18 (1H, dd, *J* = 5.1, 4.2 Hz, H₆), 3.32 (1H, dt, *J* = 12.4, 4.5 Hz, H₅), 2.83 – 2.73 (1H, m, H_{3eq}), 2.70 – 2.58 (1H, m, H_{3ax}), 2.39 – 2.28 (1H, m, H_{4eq}), 2.26 – 2.17 (1H, m, H_{4ax}), 1.39 – 1.30 (9H, m, H₂₃) ppm.

3.2.35 ((1*R*,9*aS*)- Octahydro-2*H*-quinolizin-1-yl)methanol

Preparation of (–)-epilupinine ((–) 1.1) from *syn*-mono imino-aldol adduct 2.13

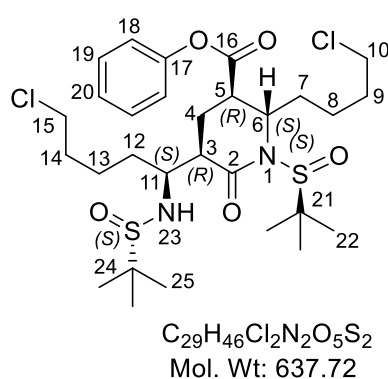


C₁₀H₁₉NO
Mol Wt: 169.27

Following a modified procedure from Nagao *et al.*,¹⁴⁰ to a solution of **2.13**, 55 mg, 0.133 mmol) in THF (1.0 mL) at 0 °C was added a solution of LiAlH₄ (0.150 ml of 1 M in THF, 0.150 mmol), dropwise. The reaction mixture was stirred at rt for 1 h, then heated under reflux for 3 h. Reaction progress

was monitored by TLC (*eluent*: EtOAc/MeOH/NH₄OH 8:1.5:0.5). The mixture was allowed to cool to 0 °C, then it was diluted with Et₂O (1 mL), and quenched by careful addition saturated aq. Na₂SO₄ (0.5 mL). The suspension was stirred at rt for 30 min then filtered through celite and washed with EtOAc (3 × 5 mL), dried (Na₂SO₄) and the solvent was removed *in vacuo*. Purification by column chromatography (silica gel, *eluent*: EtOAc/hexane 9:1 then EtOAc/MeOH, 8:2) gave (–)-epilupinine ((–)-**1.1**) as a white solid (13.5 mg, 0.080 mmol, 60%). Data for (–)-epilupinine are consistent with those reported above.

3.2.36 Phenyl (2*S*,3*R*)-1-((*S*)-tert-butylsulfinyl)-5-((*R*)-1-(((*S*)-tert-butylsulfinyl)amino)-5-chloropentyl)-2-(4-chlorobutyl)-6-oxopiperidine-3-carboxylate (**2.20**)

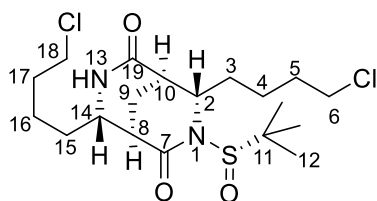


To a solution of LDA (0.80 mL of 1.0 M in THF/hexane, 0.800 mmol) in THF (10 mL) at –78 °C under Ar was added a solution of mono *syn*-imino-aldol (unsyclised) (**2.16**, 200 mg, 0.390 mmol) in THF (2.5 mL) dropwise. The reaction was stirred at –78 °C for 1 h, and then a solution of sulfinylimine **1.205** (85 mg, 0.380 mmol) in THF (2.5 mL) was added dropwise over 10 min at –78 °C. After 1 h, the reaction was quenched at –78 °C by dropwise addition of saturated aq NH₄Cl (10 mL) over 10 min. The reaction was allowed to warm to rt with rapid stirring for 30 min. The phases were separated and the aqueous layer extracted with EtOAc (3 × 10 mL). The organic phase was combined, washed with brine (2 × 5 mL), dried (Na₂SO₄) and concentrated *in vacuo*. The crude material was purified by column chromatography (silica gel, *eluent* gradient: EtOAc/hexane, 2:8 → 8:2) affording several fractions: *Fraction 1* (R_f = 0.64, Et₂O/hexane, 8:2) contained sulfinylimine **1.205** (18 mg, 0.080 mmol, 21%) was recovered; *Fraction 2* (R_f = 0.51, Et₂O/hexane, 8:2) contained cyclised mono *syn* imino-aldol **2.13** as off-white solid (24 mg, 0.057 mmol, 15%); *Fraction 3* (R_f=0.34, Et₂O/hexane, 8:2) contained impure *syn-syn* double imino-aldol **2.5a** as a yellow oil (15 mg, 0.020 mmol, 5 %); *Fraction 4* (R_f = 0.26, Et₂O/hexane, 8:2) contained partial cyclised of double imino-aldol **2.20** as a pale yellow oil (82 mg, 0.130 mmol, 34%) recorded as unknown stereochemistry.

Selected data for partial cyclised double imino-aldol **2.20**:

- FT-IR (neat)** ν_{\max} 3322, 2991, 2928, 2869, 1739, 1591, 1483, 1454, 1236, 1184, 1049 cm^{-1} .
- ^1H NMR** (400 MHz, CDCl_3) δ 7.37 – 7.44 (2H, m, 2 x H_{19}), 7.27 (1H, m, H_{20}), 7.02 – 7.09 (2H, m, 2 x H_{18}), 4.20 – 4.28 (1H, m, H_6), 4.06 (1H, d, $J = 8.3$ Hz, H_{23}), 3.55 – 3.62 (4H, m, H_{10} & H_{15}), 3.35 – 3.43 (1H, m, H_{11}), 3.16 – 3.24 (1H, m, H_5), 2.88 (1H, ddd, $J = 11.9, 5.9, 3.1$ Hz, H_3), 2.23 – 2.35 (2H, m, H_4), 1.66 – 2.01 (12H, m, $\text{H}_7, \text{H}_8, \text{H}_9, \text{H}_{12}, \text{H}_{13}$ & H_{14}), 1.21 (18H, d, $J = 5.4$ Hz, H_{22} & H_{25}) ppm.
- ^{13}C NMR** (100 MHz, CDCl_3) δ 175.1 (C_{16}), 172.1 (C_2), 150.3 (C_{17}), 129.7 (2 x C_{19}), 126.3 (C_{20}), 121.0 (2 x C_{18}), 61.6 (C_{24}), 59.4 (C_{11}), 56.3 (C_{21}), 51.3 (C_6), 45.3 (C_3), 44.8 (C_{15}), 44.7 (C_{10}), 42.5 (C_5), 39.0 (C_{12}), 34.1 (C_7), 32.1 (C_{14}), 31.4 (C_9), 27.3 (C_4), 24.0 (C_{13}), 22.9 (C_8), 22.8 (C_{25}), 22.3 (C_{22}) ppm.
- LRMS** (ESI^+) m/z 637.4 [$\text{M}^{35}\text{Cl}+\text{H}$] $^+$, 639.3 [$\text{M}^{37}\text{Cl}+\text{H}$] $^+$.
- HRMS** (ESI^+) for $\text{C}_{29}\text{H}_{47}^{35}\text{Cl}_2\text{N}_2\text{O}_5\text{S}_2^+$ [$\text{M}+\text{H}$] $^+$, calculated 637.2299; found 639.2298; for $\text{C}_{29}\text{H}_{46}^{35}\text{Cl}_2\text{N}_2\text{NaO}_5\text{S}_2^+$ [$\text{M}+\text{Na}$] $^+$, calculated 659.2118; found 659.2117.

3.2.37 (1R,4S,5R,8S)-3-((R)-tert-Butylsulfinyl)-4,8-bis(4-chlorobutyl)-3,7-diazabicyclo [3.3.1] nonane-2,6-dione (2.21)



$\text{C}_{19}\text{H}_{32}\text{Cl}_2\text{N}_2\text{O}_3\text{S}$
Mol Wt: 339.44

Following the procedure described for the synthesis of **2.14**, method B; partial double imino-aldol adduct (**2.20**, 50 mg, 0.0784 mmol) afforded the title *syn,syn*-dioxo-bispidine **2.14** (11 mg, 0.0328 mmol, 42%) and mono protection bispidine **2.21** (9 mg, 0.0265 mmol, 34%).

Data for *syn,syn*-dioxo-bispidine **2.14** are consistent with those reported above.

Data for mono protection bispidine 2.21:

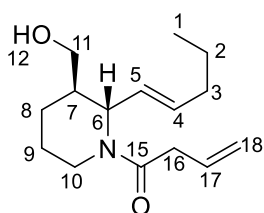
FT-IR (neat) ν_{\max} 3356 2972, 2927, 1653, 1541, 1456, 1045 cm^{-1} .

¹H NMR (400 MHz, CDCl₃) δ 8.03 (2H, br s, **H**₁₃), 4.02 (1H, m, **H**₂), 3.62 – 3.48 (5H, m, **H**₁₂ & 2 x **H**₆), 2.80 (1H, br s, **H**_{9a}), 2.70 (1H, brs, **H**_{9b}), 2.35 – 2.16 (2H, m, **H**₈ & **H**₁₀), 2.08 (1H, m, **H**_{5a}), 1.91 – 1.71 (5H, m, 2 x (**H**₃, **H**₁₇) & **H**_{5b}), 1.70 – 1.46 (6H, m, 2 x (**H**₄ & **H**₁₅) & **H**₁₆) 1.23 – 1.19 (9H, m, **H**₁₂) ppm.

¹³C NMR (100 MHz, CDCl₃) δ 173.3 (**C**₁₉), 171.7 (**C**₇), 63.9 (**C**₁₁), 56.9 (**C**₂), 46.4 (**C**₁₄), 44.6 (**C**₁₈), 44.5 (**C**₆), 41.8 (**C**₈), 38.8 (**C**₁₀), 35.0 (**C**₁₅), 34.0 (**C**₃), 31.9 (**C**₁₇), 31.6 (**C**₅), 23.4 (**C**₉), 23.3 (**C**₄), 22.7 (**C**₁₂), 16.2 (**C**₁₆) ppm.

LRMS (ESI⁺) *m/z* 461.3 [M³⁵Cl+Na]⁺, 463.4 [M³⁷Cl+Na]⁺, 879.5 [2M³⁵Cl+H]⁺, 381.3 [2M³⁷Cl+H]⁺, 901.5 [2M³⁵Cl+Na]⁺, 903.5 [2M³⁷Cl+Na]⁺.

3.2.38 1-((2*S*,3*R*)-3-(Hydroxymethyl)-2-((*E*)-pent-1-en-1-yl)piperidin-1-yl)but-3-en-1-one (2.49)



C₁₅H₂₅NO₂
Mol Wt: 251.37

To a solution of ester amide **2.21** (600 mg, 1.76 mmol) in THF (20 mL) at –10 °C LiAlH₄ (1M solution in THF 0.88 mL, 0.88 mmol) was added dropwise. The reaction mixture was stirred at –10 °C to –5 °C for 30 min. The reaction mixture was cooled to 0 °C and saturated aq. Na₂SO₄ (3 mL) was added carefully and was stirred for further 30 min at rt. The mixture was diluted with CH₂Cl₂ (20 mL), and the suspension was filtered through celite and washed with CH₂Cl₂ (3 x 10 mL). The solvent was removed *in vacuo*. Purification by column chromatography on basic alumina (EtOAc /MeOH, 19:1 → 9:1) gave the title compound **249** (332 mg, 1.32 mmol, 75%). Also it was isolated small quantity of α,β -unsaturated hydroxyl amide **2.50** (43 mg, 0.17 mmol, 10%)

Selected data for mixture of rotamers **2.49**:

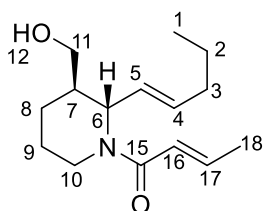
FT-IR (neat) ν_{\max} 3042, 2962, 2883, 2910, 2856, 1741, 1661, 1492, 1164 cm⁻¹.

¹H NMR (400 MHz, CDCl₃) δ 6.05 – 5.83 (2H, m, 2 x **H**₁₇), 5.59 – 5.38 (4H, m, 2 x **H**₄ & **H**₅), 5.34 – 5.22 (1H, m, **H**_{6'}), 5.19 – 5.05 (4H, m, 2 x **H**₁₈), 4.62 – 4.52 (1H, m, **H**_{6''}), 4.48 – 4.36 (1H, m, **H**_{16'a}), 3.72 – 3.38 (5H, m, 2 x **H**₁₁ & **H**_{10'eq}), 3.37 – 3.08 (6H, m, **H**_{10'ax}, **H**_{10''}, **OH**_{12'} & **H**_{16''}), 3.01 (1H, br s, **H**_{12''}) 2.77 – 2.59 (1H, m, **H**_{16'b}), 2.00 (4H, q, *J* = 6.9 Hz, 2 x **H**₃), 1.97 – 1.67 (4H, m, 2 x **H**₅, **H**_{8'} & **H**_{9'}), 1.55 – 1.31 (10H, m, **H**₂, **H**_{8''}, & **H**_{9''}), 0.86 (6H, t, *J* = 7.3 Hz, **H**₁) ppm.

¹³C NMR (101 MHz, CDCl₃) δ 171.3, 170.9 (**C**₁₅), 133.2, 132.5 (**C**₄), 132.2, 131.3 (**C**₁₇), 127.9, 127.5 (**C**₅), 117.8, 117.4 (**C**₁₈), 62.4, 62.1 (**C**₁₁), 54.2, 49.8 (**C**₆), 41.7 (**C**₁₀), 40.6, 39.4 (2 x **C**₇), 38.9, (**C**₁₀), 38.2, 36.9 (**C**₁₆), 34.4, 34.3 (**C**₃), 22.2 (2 x **C**₂), 21.6, 21.5 (**C**₉), 20.8, 20.4 (**C**₈), 13.5 (2 x **C**₁) ppm.

LRMS (ESI⁺) *m/z* 274.2 [**M**³⁵Cl+Na]⁺, 276.2 [**M**³⁷Cl+Na]⁺.

3.2.39 (E)-1-((2S,3R)-3-(Hydroxymethyl)-2-((E)-pent-1-en-1-yl)piperidin-1-yl)but-2-en-1-one (2.50)



C₁₅**H**₂₅**NO**₂
Mol Wt: 251.37

Data for α,β-unsaturated hydroxyl amide 2.50:

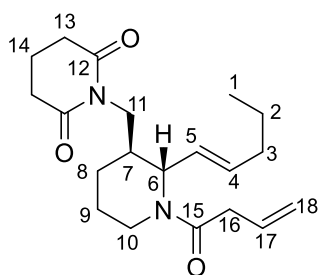
FT-IR (neat) *v*_{max} 3043, 2964, 2883, 2913, 2849, 1745, 1663, 1492, 1164 cm⁻¹.

¹H NMR (400 MHz, CDCl₃) δ 6.94 – 6.80 (1H, br dd, *J* = 14.3, 6.7 Hz, **H**₁₇), 6.27 (1H, dd, *J* = 15.0, 1.6 Hz, **H**₁₆), 5.64 – 5.41 (2H, m, **H**₄ & **H**₅), 5.25 – 5.06 (1H, m, **H**₆), 3.76 – 3.12 (4H, m, **H**₁₀ & **H**₁₁), 2.09 – 1.98 (2H, m, **H**₃), 1.87 (3H, br d, *J* = 6.4 Hz, **H**₁₈), 1.94 – 1.81 (1H, m, **H**₇), 1.58 – 1.41 (4H, m, **H**₈ & **H**₉), 1.39 (2H, sxt, *J* = 7.3 Hz, **H**₂), 0.89 (3H, t, *J* = 7.4 Hz, **H**₁) ppm.

¹³C NMR (101 MHz, CDCl₃) δ 167.4 (C₁₅), 142.1 (C₁₇), 133.2 (C₄), 127.9 (C₅), 121.5 (C₁₆), 62.1 (C₁₁), 49.8 (C₆), 41.8 (C₇), 34.5 (C₁₀), 33.0 (C₃), 25.4 (C₉), 24.7 (C₈), 22.3 (C₂), 18.2 (C₁₈), 13.6 (C₁) ppm.

LRMS (ESI⁺) *m/z* 274.3 [M³⁵Cl+Na]⁺, 276.3 [M³⁷Cl+Na]⁺.

3.2.40 1-(((2*S*,3*S*)-1-(But-3-enoyl)-2-((*E*)-pent-1-en-1-yl)piperidin-3-yl)methyl)piperidine-2,6-dione (2.51)



C₂₀H₃₀N₂O₃
Mol Wt: 346.47

To a solution of alcohol (**2.49**, 385 mg, 1.53 mmol) in anhydrous THF (10 mL) was added glutarimide (190 mg, 1.68 mmol), ADDP (424 mg, 1.68 mmol) and PBU₃ (415 μL, 1.68 mmol). The solution turned bright orange on addition of ADDP, and off-yellow after 5 min upon addition of PBU₃. The solution was stirred for 2 days, then quenched by the addition of H₂O (8 mL). The phases were separated, and the aqueous layer extracted with EtOAc (3 x 10 mL). The mixture was acidified with 2M HCl (1 mL) in order to aid separation. The combined organic extract was washed with 2M HCl (40 mL), brine (40 mL), dried (MgSO₄) then concentrated *in vacuo* to afford the crude product as a colourless oil. Purification by chromatography (silica gel, 40:60 EtOAc / hexane) afforded the title compound **2.51** as a colourless oil (415 mg, 1.20 mmol, 78%) and the product of partial isomerisation of α,β-unsaturated amide (**2.52**, 41 mg, 0.12 mmol, 8%).

Data for β,γ-unsaturated amide 2.51:

FT-IR (neat) ν_{\max} 2974, 2893, 2922, 2859, 1755, 1668, 1495, 1174 cm⁻¹.

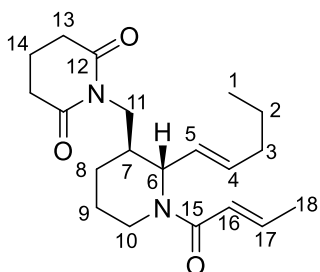
¹H NMR (400 MHz, CDCl₃) δ 5.94 (1H, br s, H₅), 5.47 – 5.38 (1H, m, H₄), 5.38 – 5.28 (1H, m, H₁₇), 5.10 (2H, d, *J* = 14.2 Hz, H₁₈), 4.53 – 4.22 (1H, m, H₆), 4.03 – 3.45 (3H, m, H_{10eq} & H₁₁), 3.31 – 2.95 (3H, m, H_{10ax} & H₁₆), 2.62 (4H, br t, *J* = 6.1 Hz, 2 x H₁₃),

2.34 – 2.12 (1H, m, **H**₇), 2.01 – 1.88 (4H, m, **H**₃ & **H**₁₄), 1.78 – 1.47 (2H, **H**_{8eq} & **H**_{9eq}), 1.43 – 1.21 (4H, m, **H**_{8ax}, **H**_{9ax} & **H**₂), 0.83 (3H, q, $J = 7.5$ Hz, **H**₁) ppm.

¹³C NMR (101 MHz, CDCl₃) δ 172.6 (**C**₁₂), 169.9 (**C**₁₅), 132.6 (**C**₄), 131.6 (**C**₅), 127.4 (**C**₁₇), 117.4 (**C**₁₈), 57.0 (**C**₆), 41.3 (**C**₁₀), 40.0 (**C**₁₁), 39.0 (**C**₁₆), 34.90 (**C**₇), 34.3 (**C**₃), 32.80 (2 × **C**₁₃), 22.1 (**C**₂), 21.6 (**C**₉), 20.6 (**C**₈), 17.01 (**C**₁₄), 13.49 (**C**₁) ppm. The ¹³C NMR spectrum was complicated by the presence of rotamers only selected peaks are reported.

LRMS (ESI⁺) m/z 347.3 [M + H]⁺.

3.2.41 1-(((2*S*,3*S*)-1-((*E*)-But-2-enoyl)-2-((*E*)-pent-1-en-1-yl)piperidin-3-yl)methyl)piperidine-2,6-dione (**2.52**)



C₂₀H₃₀N₂O₃
Mol Wt: 346.47

Data of unclear α,β -unsaturated amide **2.52**:

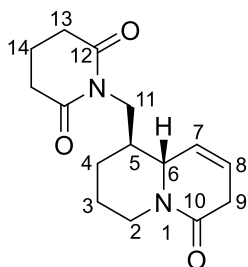
FT-IR (neat) ν_{\max} 2974, 2894, 2924, 2856, 1752, 1668, 1485, 1171 cm⁻¹.

¹H NMR (400 MHz, CDCl₃) δ 6.89 – 6.76 (1H, m, **H**₁₇), 6.27 (1H, br d, $J = 14.9$ Hz, **H**₁₆), 5.52 – 5.43 (1H, m, **H**₄), 5.41 – 5.33 (1H, m, **H**₅), ~5.20 – 5.08 (missing **H**₆), 4.03 – 3.68 (2H, m, **H**₁₁), 2.66 (4H, t, $J = 6.5$ Hz, **H**₁₃), ~3.60 (missing **H**₁₀), 2.00 (2H, q, $J = 7.5$ Hz, **H**₃) 1.97 – 1.91 (2H, m, **H**₁₄), 1.86 (3H, dd, $J = 6.8, 1.4$ Hz, **H**₁₈), 1.84 – 1.54 (3H, m, **H**₇, **H**_{8a} & **H**_{9a}), 1.48 – 1.28 (4H, m, **H**₂, **H**_{8b} & **H**_{9b}), 0.87 (3H, t, $J = 7.3$ Hz, **H**₁) ppm. The ¹H NMR spectrum was complicated by the presence of rotamers only selected peaks are reported, additional broad signals.

¹³C NMR (101 MHz, CDCl₃) δ 172.7 (2 × **C**₁₂, **C**₁₅), 140.8 (**C**₁₇), 132.8 (**C**₄), 127.7 (**C**₅), 122.2 (**C**₁₆), 58.0 (**C**₆), 44.6 (**C**₁₀), 40.7 (**C**₇ & **C**₁₁), 34.4 (**C**₃), 32.9 (2 × **C**₁₃), 31.6 (**C**₇) 22.2 (**C**₂), 21.3 (**C**₉), 20.4 (**C**₈), 18.2 (**C**₁₈), 17.1 (**C**₁₄), 13.6 (**C**₁) ppm.

LRMS (ESI⁺) m/z 347.2 [M + H]⁺.

3.2.42 1-(((1S,9aS)-6-Oxo-1,3,4,6,7,9a-hexahydro-2H-quinolizin-1-yl)methyl)piperidine-2,6-dione (2.40)



$C_{15}H_{20}N_2O_3$
Mol Wt: 276.34

To a solution of **2.51** (400 mg, 1.15 mmol) in degassed CH_2Cl_2 was added Grubbs II pre-catalyst (25 mg, 0.029 mmol, 2.5 mol%) in one portion and the reaction heated under reflux for 4 h. The reaction mixture was concentrated *in vacuo* to give a viscous darck brown oil. The residue was partitioned between sat. aq. K_2CO_3 (30 mL) and EtOAc (20 mL). The phases were separated and the aqueous phase extracted with EtOAc (3 × 20 mL). The crude material was extracted with EtOAc (2 × 30 mL), the organic phases combined, dried (Na_2SO_4) and concentrated *in vacuo*. The crude material was purified by column chromatography (silica gel, *eluent*: 35% $NH_4OH/MeOH/CH_2Cl_2$ 1:10:190) to give the title compound **2.40** as a white solid (303 mg, 1.10 mmol, 95%). Recrystallisation with hexane gave fine needles.

Alternatively, **2.40** was prepared from hydroxy quinolisidine **2.42** following the procedure described for the synthesis of **2.51**; alcohol (**2.42**, 230 mg, 1.27 mmol), glutarimide (157 mg, 1.39 mmol), ADDP (350 mg, 1.39 mmol) and PBu_3 (345 μ L, 1.39 mmol); to afforded the title tricyclic imide (**2.40**, 298 mg, 1.08 mmol, 85%) as a white solid.

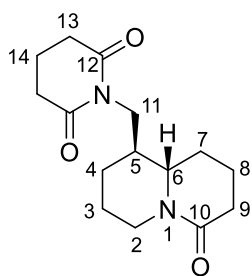
FT-IR (neat) ν_{max} 3041, 2925, 2853, 2832, 2791, 2723, 1734, 1722, 1668 cm^{-1} .

1H NMR (400 MHz, $CDCl_3$) δ 5.89 (1H, ddt, $J = 10.3, 3.6, 1.8$, Hz, H_7), 5.84 – 5.76 (1H, m, H_8), 4.83 (1H, dt, $J = 2.1, 13.0$ Hz, H_{2eq}), 3.87 – 3.79 (2H, m, H_{11}), 3.69 – 3.62 (1H, m, H_6), 2.97 – 2.91 (2H, m, H_9), 2.66 (4H, t, $J = 6.5$ Hz, H_{13}), 2.40 (1H, td, $J = 12.8, 2.6$ Hz, H_{2ax}), 1.94 (2H, quin, $J = 6.6$ Hz, H_{14}), 1.89 – 1.77 (1H, m, H_5), 1.71 – 1.57 (2H, m, H_{3eq} & H_{4eq}), 1.46 – 1.33 (1H, m, H_{3ax}), 1.32 – 1.19 (1H, m, H_{4ax})

¹³C NMR (101 MHz, CDCl₃) δ 172.68 (2 x C₁₂), 165.94 (C₁₀), 123.07 (C₇), 122.61 (C₈), 61.68 (C₆), 42.40 (C₂ & C₁₁), 40.84 (C₅), 32.84 (C₁₃), 31.64 (C₉), 28.43 (C₄), 24.69 (C₃), 17.04 (C₁₄) ppm.

LRMS (ES⁺) *m/z* 347.2 [M + H]⁺.

3.2.43 1-(((1S,9aS)-6-Oxo-octahydro-2H-quinolizin-1-yl)methyl)piperidine-2,6-dione (2.53), (-)-10-oxo-Lamprolobine



C₁₅H₂₂N₂O₃
Mol Wt: 278.35

To a solution of **2.40** (50 mg, 1.160 mmol) in EtOH (5 mL) was added 5 wt% Pd/C (10 mg, 0.130 mmol) and placed under an H₂ atmosphere. The reaction was stirred at rt for 16 h, filtered through celite, washing with EtOH (5 × 5 mL) and the solvent removed *in vacuo*. The crude material was purified by column chromatography (silica gel, *eluent*: 35% NH₄OH/MeOH/CH₂Cl₂ 1:20:180) to give the title compound **2.53** (48 mg, 1.140 mmol, 94%).

M.P. 133 – 135 °C.

[α]_D -15.9 (c 0.5, CHCl₃, 21°C).

FT-IR (neat) ν_{max} 2925, 2844, 2805, 2739, 1734, 1721, 1670 cm⁻¹.

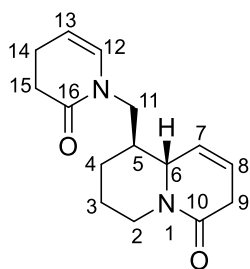
¹H NMR (400 MHz, CDCl₃) δ 4.79 (1H, br d, *J* = 13.1 Hz, H_{2eq}), 3.77 (1H, br d, *J* = 7.0 Hz, H_{11eq}), 3.74 – 3.67 (1H, m, H_{11ax}), 3.16 – 3.02 (1H, m, H₆), 2.67 (4H, t, *J* = 6.4 Hz, H₁₃), 2.47 – 2.22 (3H, m, H_{2ax} & H₉), 2.20 – 2.09 (1H, m, H₅), 2.01 – 1.80 (4H, m, H_{4eq}, H_{8eq} & H₁₄), 1.77 – 1.67 (2H, m, H_{3ax} & H_{7ax}), 1.58 – 1.50 (1H, m, H_{8ax}), 1.35 – 1.15 (3H, m, H_{3eq}, H_{4ax} & H_{7eq}) ppm.

¹³C NMR (101 MHz, CDCl₃) δ 172.71 (2 x C₁₂), 169.30 (C₁₀), 60.13 (C₆), 42.44 (C₂), 41.14 (C₁₁), 40.94 (C₅), 32.87 (2 x C₁₃), 32.75 (C₉), 28.21 (C₇), 27.24 (C₄), 24.60 (C₃), 18.80 (C₈), 17.12 (C₁₄) ppm.

LRMS (ESI⁺) 279.3 [M+H]⁺.

HRMS: (ESI⁺) for C₁₅H₂₃N₂O₃ [M+H]⁺, calculated 279.1704; found 279.1703, for C₁₅H₂₂N₂NaO₃ [M+Na]⁺, calculated 301.1520; found 301.1523.

3.2.44 (9S,9aS)-9-((2-Oxo-3,4-dihydropyridin-1(2H)-yl)methyl)-3,6,7,8,9a-hexahydro-4H-quinolizin-4-one (2.57)



C₁₅H₂₀N₂O₂
Mol Wt: 260.34

To a stirred solution of imide (**2.40**, 25 mg, 0.410 mmol) in CH₂Cl₂ (1.5 mL) at -78 °C under N₂ was added a solution of LiEt₃BH (0.90 mL of 1.0 M in THF, 0.900 mmol) dropwise. The resulting mixture was stirred at -78 °C for 3 h, then it was allowed to warm to -20 °C and a solution of HCl (0.75 mL of 2.0 M in EtOH, 1.570 mmol) was added dropwise. The mixture was allowed to warm to rt and stirred for 1 h before quenching with sat. aq. NaHCO₃ (1.5 mL) and concentrated *in vacuo*. Purification by column chromatography (silica gel, *eluent*: 35% NH₄OH/MeOH/EtOAc 2:8:90) afforded the title tricyclic enamide (**2.57**, 12 mg, 0.12 mmol, 41%) as a yellow oil, and tricyclic hydroxy lactam (**2.56**, 8 mg, 0.120 mmol, 30%) as an inseparable mixture of two diastereoisomers *dr* ~ 1:1.

Data for tricyclic enamid 2.57:

FT-IR (neat) ν_{\max} 2935, 2858, 2842, 2771, 2743, 1738, 1721, 1668, 1578 cm⁻¹.

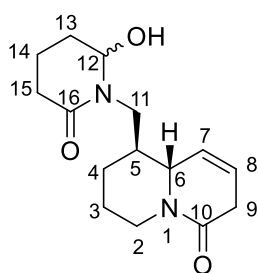
¹H NMR (400 MHz, CDCl₃) δ 5.96 (1H, dt, *J* = 7.7, 1.5 Hz, H₁₂), 5.94 – 5.88 (1H, m, H₇), 5.84 – 5.78 (1H, m, H₈), 5.22 – 5.15 (1H, m, H₁₃), 4.88 (1H, ddt, *J* = 12.9, 4.1, 1.9 Hz, H_{2eq}), 3.71 – 3.64 (1H, m, H₆), 3.64 – 3.56 (1H, m, H_{11a}), 3.52 – 3.43 (1H, m, H_{11b}), 2.99 – 2.94 (2H, m, H₉), 2.56 – 2.50 (2H, m, H₁₅), 2.43 (1H, td, *J* = 12.9, 2.7 Hz,

H_{2ax}), 2.36 – 2.28 (2H, m, H_{14}), 1.87 – 1.79 (m, 1H, H_{4eq}), 1.78 – 1.67 (2H, m, H_{3eq} & H_5), 1.51 – 1.43 (1H, m, H_{3eq}), 1.38 – 1.30 (1H, m, H_{4ax}) ppm.

^{13}C NMR (101 MHz, $CDCl_3$) δ 169.7 (C_{16}), 166.0 (C_{10}), 129.9 (C_{12}), 123.2 (C_7), 122.8 (C_8), 106.6 (C_{13}), 61.5 (C_6), 47.4 (C_{11}), 43.7 (C_5), 42.6 (C_2), 31.7 (C_9), 31.4 (C_{15}), 28.8 (C_4), 24.8 (C_3), 20.2 (C_{14}) ppm.

LRMS (ESI⁺) m/z 261.2 [M + H]⁺.

3.2.45 (9S,9aS)-9-((2-Hydroxy-6-oxopiperidin-1-yl)methyl)-3,6,7,8,9,9a-hexahydro-4H-quinolizin-4-one (2.56)



$C_{15}H_{22}N_2O_3$
Mol Wt: 278.35

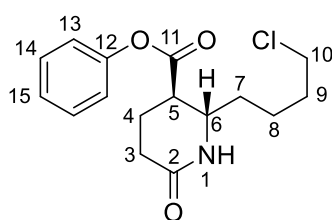
Data for tricyclic hydroxy lactam 2.56:

FT-IR (neat) ν_{max} 3047, 2946, 2854, 2840, 2761, 2742, 1735, 1720, 1670, 1568 cm^{-1} .

1H NMR (400 MHz, $CDCl_3$) δ 5.94 – 5.75 (4H, m, 2 x H_7 & H_8), 4.98 (1H, br t, $J = 3.1$ Hz, $H_{12'}$), 4.91 (1H, br t, $J = 3.0$ Hz, $H_{12''}$), 4.89 – 4.86 (1H, m, $H_{2'eq}$), 4.86 – 4.82 (1H, m, $H_{2''eq}$), 3.98 (1H, dd, $J = 13.6, 10.2$ Hz, $H_{11'a}$), 3.81 (1H, dd, $J = 13.7, 5.5$ Hz, $H_{11'b}$), 3.76 – 3.69 (1H, m, H_6'), 3.67 – 3.59 (1H, m, H_6''), 3.27 (1H, dd, $J = 13.6, 4.6$ Hz, $H_{11''b}$), 3.18 (1H dd, $J = 13.6, 9.4$ Hz, $H_{11''a}$), 2.98 – 2.92 (4H, m, 2 x H_9), 2.57 – 2.30 (6H, m, 2 x H_{2ax} & H_{15}), 2.11 – 1.89 (7H, m, $H_{5'}$, $H_{14'}$ & 2 x H_{13}), 1.79 – 1.64 (7H, m, $H_{5''}$, $H_{14''}$, $H_{3'}$ & $H_{4'}$), 1.50 – 1.30 (4H, m, $H_{3''}$ & $H_{4''}$) ppm.

^{13}C NMR (101MHz, $CDCl_3$) δ 170.6 (2 x C_{10}), 166.1 (2 x C_{16}), 123.0 (2 x C_7), 122.8 (2 x C_8), 81.5 (C_{12a}), 78.5 (C_{12b}), 62.1 (C_6'), 61.7 (C_6''), 47.5 (2 x $C_{11'}$), 43.7 ($C_{11''}$), 43.4 (C_5'), 42.9 (C_5''), 42.7 (C_2'), 42.6 (C_2''), 32.4 ($C_{15'}$), 32.3 ($C_{15''}$), 31.7 (2 x C_9), 31.0 (2 x C_{13}), 29.4 ($C_{4'}$), 28.6 ($C_{4''}$), 24.9 (2 x C_3), 15.7 (2 x C_{14}) ppm.

LRMS (ESI⁺) m/z 279.2 [M + H]⁺.

3.2.46 Phenyl (2*S*,3*R*)-2-(4-chlorobutyl)-6-oxopiperidine-3-carboxylate (**2.28**)

$C_{16}H_{20}ClNO_3$
Mol Wt: 309.79

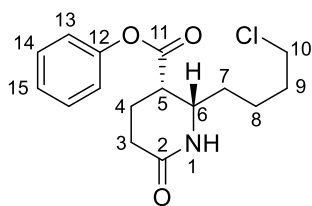
To a solution of cyclised *syn* imino-aldol adduct (**2.13**, 350 mg, 0.850 mmol) in THF/H₂O (3:2, 20 mL) at rt was added I₂ (430 mg, 1.70 mmol) and Na₂CO₃ (1.08 g, 10.20 mmol) portionwise. The reaction mixture was heating at 50 °C under Ar and stirred for 2 h. The resulting dark brown solution became light brown. The reaction mixture was diluted with H₂O (10 mL). After removal of THF *in vacuo*, an aqueous saturated Na₂S₂O₃ (0.100 mL) was added. The resulting aqueous mixture was extracted with Et₂O (3 x 10 mL) and the combined organic phase was washed with brine (20 mL), dried (Na₂SO₄) and concentrated *in vacuo* to yield a white solid. The crude was passed through a plug of alumina (*eluent*: EtOAc) to give the title compound *syn* lactam **2.28** as a white solid (251 mg, 0.810 mmol, 95%).

FT-IR (neat) ν_{\max} 3134, 2951, 2857, 2844, 2772, 2742, 1725, 1670, 1567, 1546 cm⁻¹.

¹H NMR (400 MHz, CDCl₃) δ 7.41 (2H, t, J = 7.3 Hz, **H**₁₄), 7.31 – 7.23 (1H, m, **H**₁₅), 7.08 (2H, d, J = 7.9 Hz, **H**₁₃), 6.45 (1H br s, **H**₁), 3.93 – 3.84 (1H, m, **H**₆), 3.57 (2H, t, J = 6.4 Hz, **H**₁₀), 2.77 (1H, ddd, J = 10.2, 8.5, 3.7 Hz, **H**₅), 2.62 – 2.51 (1H, m, **H**_{3ax}), 2.50 – 2.39 (1H, m, **H**_{4eq}), 2.35 – 2.11 (2H m, **H**_{3eq} & **H**_{4ax}), 1.91 – 1.76 (2H, m, **H**₉), 1.76 – 1.51 (4H, m, **H**₇ & **H**₈) ppm.

¹³C NMR (101 MHz, CDCl₃) δ 171.4 (**C**₂), 171.2 (**C**₁₁), 150.2 (**C**₁₂), 129.6 (2 x **C**₁₄), 126.2 (**C**₁₅), 121.2 (2 x **C**₁₃), 53.7 (**C**₆), 44.5 (**C**₅), 44.1 (**C**₁₀), 34.7 (**C**₇), 32.0 (**C**₃), 29.8 (**C**₉), 23.5 (**C**₄), 22.1 (**C**₈) ppm.

LRMS (ESI⁺) m/z 310.2 [M + H]⁺.

3.2.47 Phenyl (2S,3S)-2-(4-Chlorobutyl)-6-oxopiperidine-3-carboxylate (2.27)

$C_{16}H_{20}ClNO_3$
Mol Wt: 309.79

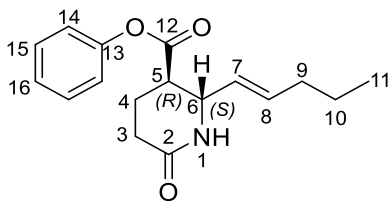
To a solution of cyclised *anti* imino-aldol adduct (**2.16**, 40 mg, 0.100 mmol) in 1,4-dioxane (10 mL) at 0 °C was added conc. HCl (1.00 mL of ~36%, 0.40 mmol) dropwise and the mixture was stirred at rt for 1 h under Ar. The reaction mixture was basified by the dropwise addition of sat. aq. NaHCO₃ at 0 °C, and stirring was continued at rt for 1 h. The phases were separated and the aqueous phase was extracted with EtOAc (3 × 15 mL), washing with saturated aq. NaHCO₃ (3 × 10 mL). The combined organic solution was washed with brine (2 × 25 mL), dried (NaSO₄) the solvent was removed *in vacuo*. The crude was passed through a plug of alumina (*eluent*: EtOAc) to give the title *anti* lactam **2.27** as a white solid (27 mg, 0.87 mmol, 87%). Recrystallisation with CHCl₃/ Et₂O 1:4 gave fine needles.

FT-IR (neat) ν_{\max} 3136, 2953, 2860, 2847, 2770, 2741, 1724, 1670, 1567, 1545 cm⁻¹.

¹H NMR (400 MHz, CDCl₃) δ 7.46 – 7.36 (2H, m, **H**₁₄), 7.33 – 7.28 (1H, m, **H**₁₅), 7.07 (2H, d, $J = 7.8$ Hz, **H**₁₃), 5.98 (1H, br s, **H**₁), 3.89 – 3.82 (1H, m, **H**₆), 3.57 (2H, t, $J = 6.4$ Hz, **H**₁₀), 3.23 – 3.18 (1H, m, **H**₅), 2.68 – 2.59 (1H, m, **H**_{3eq}), 2.53 – 2.43 (1H, m, **H**_{4eq}), 2.34 – 2.14 (2H, m, **H**_{3ax} & **H**_{4ax}), 1.89 – 1.79 (2H, m, **H**₉), 1.72 – 1.61 (4H, m, **H**₇ & **H**₈) ppm.

¹³C NMR (101 MHz, CDCl₃) δ 171.05 (**C**₂), 169.96 (**C**₁₁), 150.18 (**C**₁₂), 129.61 (**C**₂ × **C**₁₄), 126.24 (**C**₁₅), 121.24 (2 × **C**₁₃), 53.25 (**C**₆), 44.46 (**C**₅), 42.35 (**C**₁₀), 32.34 (**C**₇), 32.06 (**C**₃), 29.27 (**C**₉), 23.34 (**C**₄), 20.29 (**C**₈) ppm.

LRMS (ESI⁺) m/z 310.3 [M + H]⁺.

3.2.48 Phenyl (2*S*,3*R*)-6-oxo-2-((*E*)-pent-1-en-1-yl)piperidine-3-carboxylate (2.77)


$C_{17}H_{21}NO_3$
Mol Wt: 287.36

Following the procedure described for the synthesis of **2.28**, imino-aldol adduct (**2.11**, 130 mg, 0.33 mmol) afforded the title compound unsaturated lactam (**2.77**, 86 mg, 0.30 mmol, 91%).

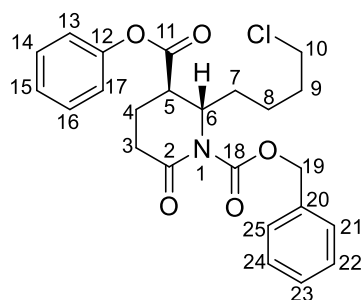
M.P. 88 – 90 °C.

FT-IR (neat) ν_{\max} 3238, 2934, 2861, 2809, 1747, 1190, 1161, 1123 cm^{-1} .

1H NMR (400 MHz, $CDCl_3$) δ 7.39 (2H, t, $J = 7.3$ Hz, **H₁₅**), 7.27 – 7.23 (1H, m, **H₁₆**), 7.06 – 7.00 (2H, m, **H₁₄**), 5.81 (1H, dtd, $J = 15.2, 6.8, 0.7$ Hz, **H₇**), 5.74 (1H, s br, **H₁**), 5.46 (1H, ddt, $J = 15.3, 7.9, 1.5$ Hz, **H₈**), 4.29 (1H, t, $J = 8.4$ Hz, **H₆**), 2.76 (1H, ddd, $J = 10.7, 8.9, 3.5$ Hz, **H₅**), 2.62 – 2.53 (1H, m, **H_{3eq}**), 2.50 – 2.40 (1H, m, **H_{4eq}**), 2.32 – 2.13 (2H, m, **H_{3ax}** & **H_{4ax}**), 2.06 (2H, td, $J = 7.2, 5.9$ Hz, **H₉**), 1.42 (2H, sxt, $J = 7.4$ Hz, **H₁₀**), 0.91 (3H, t, $J = 7.3$ Hz, **H₁₁**) ppm.

^{13}C NMR (101 MHz, $CDCl_3$) δ 170.9 (**C₂**), 170.5 (**C₁₂**), 150.3 (**C₁₃**), 135.9 (**C₇**), 129.5 (2 x **C₁₅**), 128.4 (**C₈**), 126.1 (2 x **C₁₆**), 121.2 (2 x **C₁₄**), 57.2 (**C₆**), 45.7 (**C₅**), 34.1 (**C₉**), 29.9 (**C₃**), 23.5 (**C₁₀**), 22.0 (**C₄**), 13.6 (**C₁₁**) ppm.

LRMS (ESI⁺) m/z 288.23 [M+H]⁺.

3.2.49 1-Benzyl 3-phenyl (2S,3R)-2-(4-chlorobutyl)-6-oxopiperidine-1,3-dicarboxylate (2.68)

$C_{24}H_{26}ClNO_5$
Mol Wt: 443.92

Following a modified procedure from Han *et al.*,¹⁵⁸ to a solution of *n*-BuLi (0.700 mL of 1.0 M in THF, 0.700 mmol) in THF (15 mL) at -78 °C under N_2 was added a solution of *syn* lactam (**2.28**, 200 mg, 0.650 mmol) in THF (14 mL) dropwise. The mixture was stirred at -78 °C for 30 min, and then benzyl chloroformate (1.49 mL, 9.930 mmol) was added dropwise over 5 min. The yellow suspension was stirred at -60 °C for 30 min. The reaction was quenched by the addition of aq NH_4Cl (10 mL). The layers were separated and the aqueous layer extracted with EtOAc (3 x 10 mL). The combined organic extract was washed with brine (100 mL), dried ($MgSO_4$) and concentrated *in vacuo* to yield a yellow oil. Purification by chromatography (silica gel, EtOAc/hexane 5:95) afforded the title compound **2.68** as a pale yellow oil (208 mg, 0.470 mmol, 72%).

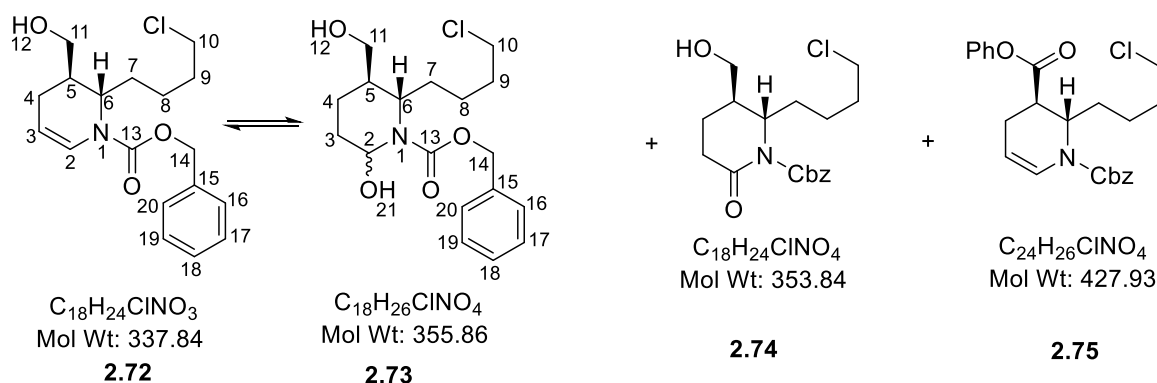
FT-IR (neat) ν_{max} 2938, 2871, 2819, 1735, 1720, 1678, 1542, 1164, 1133 cm^{-1} .

1H NMR (400 MHz, $CDCl_3$) δ 7.36 – 7.14 (8H, m, H_{14} , H_{15} , H_{16} , H_{21} , H_{22} , H_{23} , H_{24} & H_{25}), 6.92 – 6.86 (2H, m, H_{13} & H_{17}), 5.26 – 5.19 (2H, m, H_{19}), 4.93 (1H, ddd, $J = 8.3, 6.2, 1.9$ Hz, H_6), 3.45 (2H, t, $J = 6.4$ Hz, H_{10}), 3.04 – 2.99 (1H, m, H_5), 2.76 (1H, dq, $J = 9.0, 7.7$ Hz, H_{3eq}), 2.56 – 2.45 (1H, m, H_{3ax}), 2.35 – 2.25 (1H, m, H_{4eq}), 2.21 – 2.10 (1H, m, H_{4ax}), 1.83 – 1.68 (3H m, H_7 & H_{9a}), 1.64 – 1.42 (3H, m, H_8 & H_{9b}) ppm.

^{13}C NMR (101 MHz, $CDCl_3$) δ 171.0 (C_{11}), 170.6 (C_2), 154.0 (C_{18}), 150.3 (C_2), 135.2 (C_{12}), 129.5 (C_{20}), 128.5 (C_{14} & C_{16}), 128.3 (C_{22} & C_{24}), 128.0 (C_{24}), 126.1 (C_{21} & C_{25}), 121.2 (C_{13} & C_{17}), 68.7 (C_{19}), 56.5 (C_6), 44.5 (C_{10}), 41.1 (C_5), 34.3 (C_9), 31.8 (C_7), 31.4 (C_3), 23.2 (C_8), 19.1 (C_4) ppm.

LRMS (ESI+) m/z 444.3 (100%) [$M+H^+$] $^+$, 466.3 (100%) [$M+Na$] $^+$.

HRMS: (ESI $^+$) for $C_{24}H_{26}ClN_2NaO_5$ [$M+Na$] $^+$, calculated 466.1393; found 466.1392.



Following a modified procedure from Han *et al.*,¹⁵⁸ to a stirred solution of **2.68** (100 mg, 0.225 mmol) in CH_2Cl_2 (1.0 mL) at $-78^\circ C$ under N_2 was added $LiEt_3BH$ (0.250 mL of 1.0 M in THF, 0.250 mmol) dropwise. The resulting mixture was stirred for 1 h, then was allowed to warm to $0^\circ C$ and the solution was quenched by careful addition of aq. Na_2SO_4 (1.00 mL). The suspension was filtered through celite, washing with THF (3×5 mL), dried (Na_2SO_4) and the solvent was removed *in vacuo*. Purification by flash column chromatography (silica gel, *eluent*: EtOAc/MeOH, 95:5) gave the products: (**2.72**, 14 mg, 0.044 mmol, 20%) and equilibrium with hemiaminal (**2.73**, 17 mg, 0.048 mmol, 21%), and inseparable alcohol imide (**2.74**, LRMS (ESI+) m/z 354.3 [$M^{35}Cl+H^+$]⁺, 356.3 [$M^{37}Cl+H^+$]⁺, and enamide (**2.75**, LRMS (ESI+) m/z 338.3 [$M^{35}Cl+H^+$]⁺, 340.3 [$M^{37}Cl+H^+$]⁺).

Alternative reduction of **2.68**, using $LiAlH_4$ (0.23 mL of 1.0 M in THF, 0.225 mmol) was added dropwise to a solution of **2.68** (100 mg, 0.225 mmol) in CH_2Cl_2 (1.00 mL) at $-20^\circ C$ under N_2 . The resulting mixture was stirred for 30 min, then was allowed to warm to $0^\circ C$ and the solution was quenched by careful addition of aq. Na_2SO_4 (1.00 mL). The suspension was filtered through celite, washing with THF (3×5 mL), dried (Na_2SO_4) and the solvent was removed *in vacuo*. Purification by flash column chromatography (silica gel, *eluent*: EtOAc/MeOH, 95:5) gave the products: (**2.72**, 13 mg, 0.038 mmol, 17%) and equilibrium with hemiaminal (**2.73**, 16 mg, 0.045 mmol, 20%), and inseparable alcohol imide (**2.74**, LRMS (ESI+) m/z 354.3 [$M^{35}Cl+H^+$]⁺, 356.3 [$M^{37}Cl+H^+$]⁺, and enamide (**2.75**, LRMS (ESI+) m/z 338.3 [$M^{35}Cl+H^+$]⁺, 340.3 [$M^{37}Cl+H^+$]⁺).

^{13}C NMR data for hydroxyl enamide **2.72** was not reported due to instability of compound, only data for hemiaminal **2.73** are reported.

Selected data for hydroxyl enamide **2.72**:

FT-IR (neat) ν_{max} 3089, 2938, 2871, 2819, 1720, 1542, 1164, 1133 cm^{-1} .

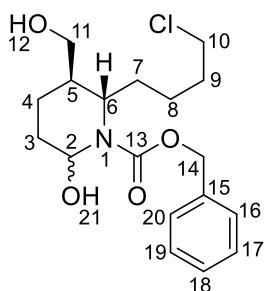
1H NMR (400 MHz, $CDCl_3$) δ 7.40 – 7.33 (5H, m, **H**₁₆, **H**₁₇, **H**₁₈, **H**₁₉ & **H**₂₀), 6.80 – 6.64 (1H, m, **H**₂), 5.28 – 5.13 (2H, m, **H**₁₄), 4.89 – 4.74 (1H, m, **H**₃), 4.42 – 4.27 (1H, m, **H**₆), 3.56 – 3.39 (4H, m, **H**₁₀ & **H**₁₁), 2.26 – 2.14 (1H, m, **H**_{4eq}), 2.09 – 1.96 (1H, m, **H**₅),

1.93 – 1.76 (m, 3H, **H**₇ & **H**₁₂), 1.75 – 1.59 (3H, m, **H**_{4ax} & **H**₉), 1.50 – 1.39 (2H, m, **H**₈) ppm.

LRMS (ESI+) m/z 338.3 [M³⁵Cl+H⁺]⁺, 340.3 [M³⁷Cl+H⁺]⁺, 360.3 [M³⁵Cl+Na]⁺ 362.3 [M³⁷Cl+Na]⁺.

HRMS: (ESI⁺) for C₁₈H₂₄ClNNO₃ [M+Na]⁺, calculated 360.1330; found 360.1337.

3.2.50 Benzyl (2*S*,3*R*)-2-(4-chlorobutyl)-6-hydroxy-3-(hydroxymethyl)piperidine-1-carboxylate **2.73**



C₁₈H₂₆ClNO₄
Mol Wt: 355.86

2.73

Selected data for two diastereoisomers of hemiaminal **2.73**:

FT-IR (neat) ν_{\max} 3168, 3088, 2938, 2871, 2819, 1723, 1542, 1164, 1132 cm⁻¹.

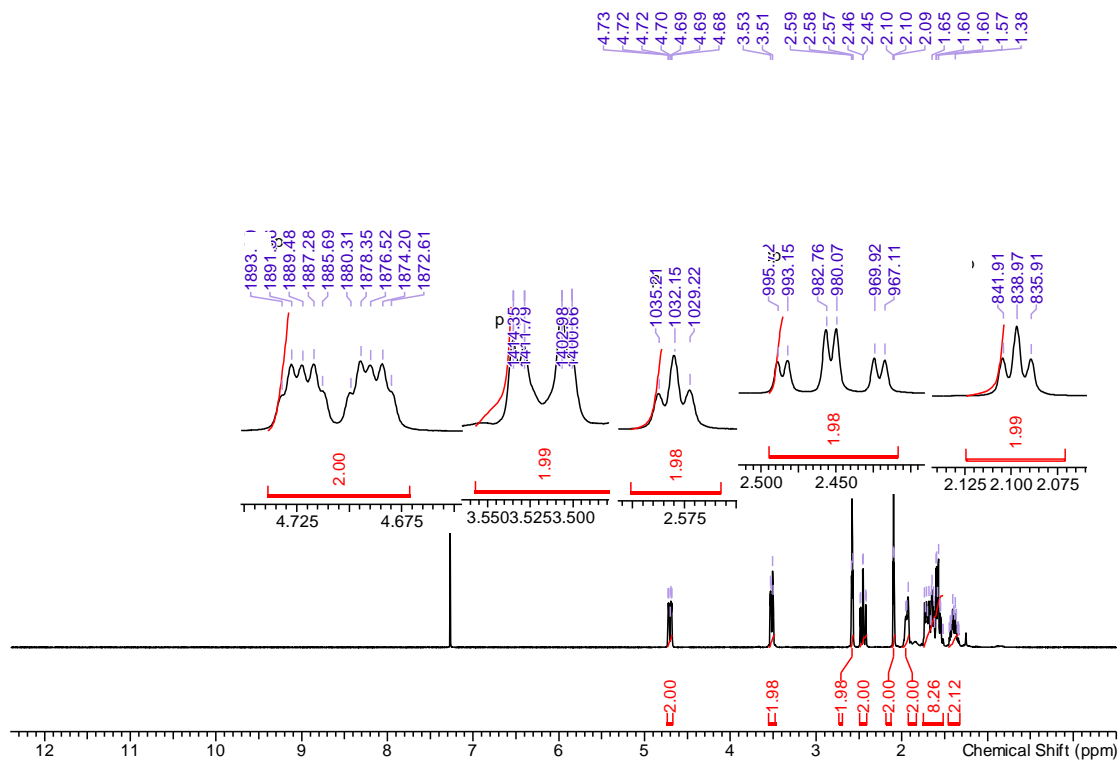
¹H NMR (400 MHz, CDCl₃) δ 7.39 – 7.32 (10H, m, 2 x **H**₁₆, **H**₁₇, **H**₁₈, **H**₁₉ & **H**₂₀), 5.18 (1H, d, J = 2.3 Hz, **H**_{2'}), 5.15 – 5.05 (4H, m, 2 x **H**₁₄), 4.72 – 4.66 (m, 1H, **H**_{6'}), 4.59 – 4.43 (m, 2H, **H**_{2''}), 4.05 – 3.96 (m, 1H, **H**_{6''}), 3.86 – 3.77 (m, 1H, **H**_{11'a}), 3.58 (br d, J = 11.1 Hz, 3H, **H**_{11'b} & **H**_{11''}), 3.51 (m, 4H, 2 x **H**₁₀), 3.34 (dd, J = 10.4, 11.4 Hz, 1H, **H**_{5'}), 3.11 – 3.06 (d, J = 5.7 Hz, 1H, **H**₂₁), 2.60 (d, J = 3.2 Hz, 1H, **H**₁₂), 2.02 – 1.27 (m, 27H, **H**_{5''}, 2 x **H**₃, **H**₄, **H**₇, **H**₈ & **H**₉) ppm.

¹³C NMR (101 MHz, CDCl₃) δ 156.3 (**C**₁₃), 136.5, 136.4 (**C**₁₅), 128.6 (**C**_{17'} & **C**_{19'}), 128.5 (**C**_{16'} & **C**_{20'}), 128.2, 128.1 (**C**₁₈), 128.1 (**C**_{17''} & **C**_{19''}), 128.0 (**C**_{16''} & **C**_{20''}), 95.8, 91.4 (**C**₂), 67.8, 66.8 (**C**₁₄), 66.8, 62.4 (**C**₁₁), 52.0, 51.5 (**C**₆), 44.7, 44.7 (**C**₁₀), 39.7, 39.5 (**C**₅), 32.3, 32.2 (**C**₉), 32.1, 31.9 (**C**₇), 31.7, 29.7 (**C**₃), 23.5, 23.2 (**C**₈), 23.1, 19.2 (**C**₄) ppm.

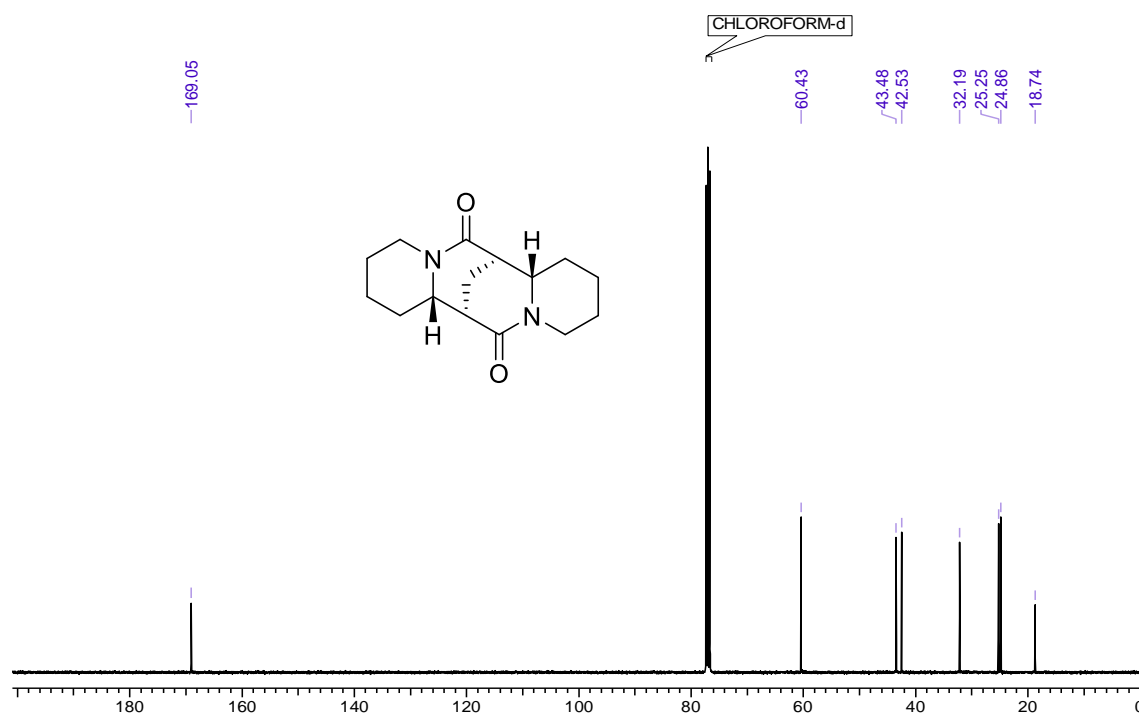
HRMS: (ESI⁺) for C₁₈H₂₆ClNNO₄ [M+Na]⁺, calculated 378.1445; found 378.1443.

Appendix A Selected NMR Spectra

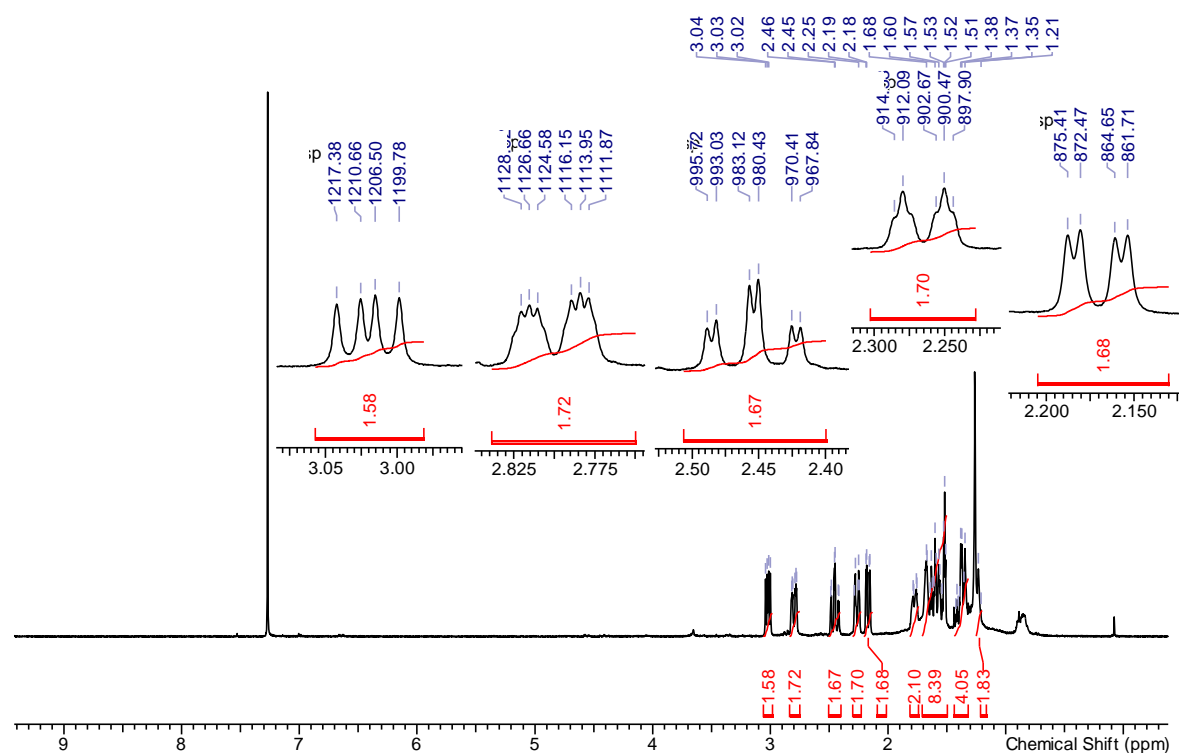
A.1.1 ^1H (400 MHz) spectrum of (+)-10,17-Dioxo- β -isosparteine ((+)-1.33) (CDCl_3)



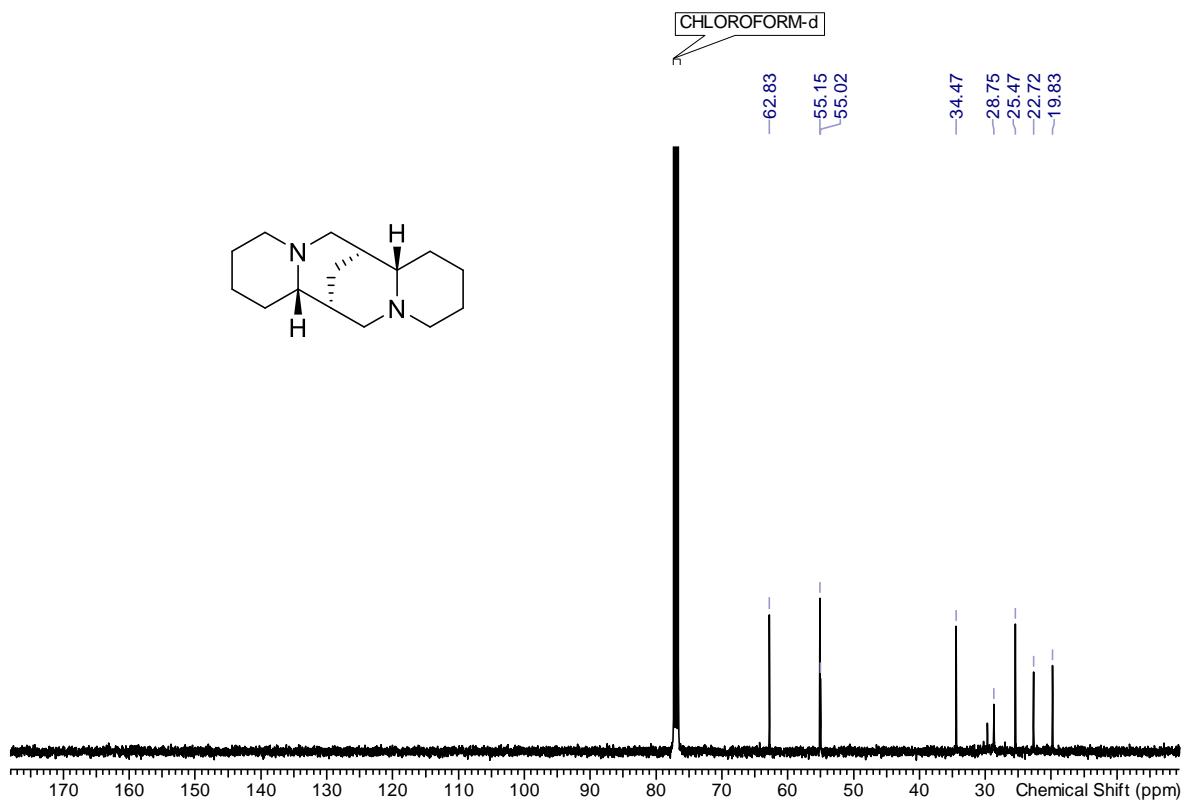
A.1.2 ^{13}C NMR (101 MHz) spectrum of (+)-10,17-Dioxo- β -isosparteine ((+)-1.33) (CDCl_3)

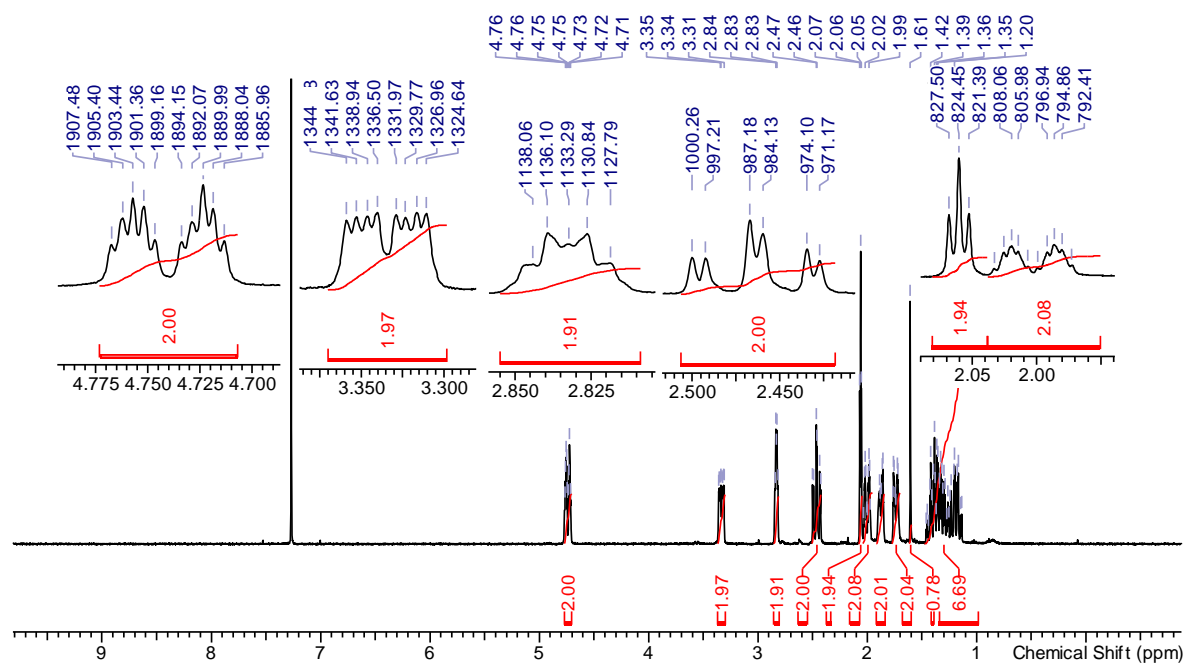
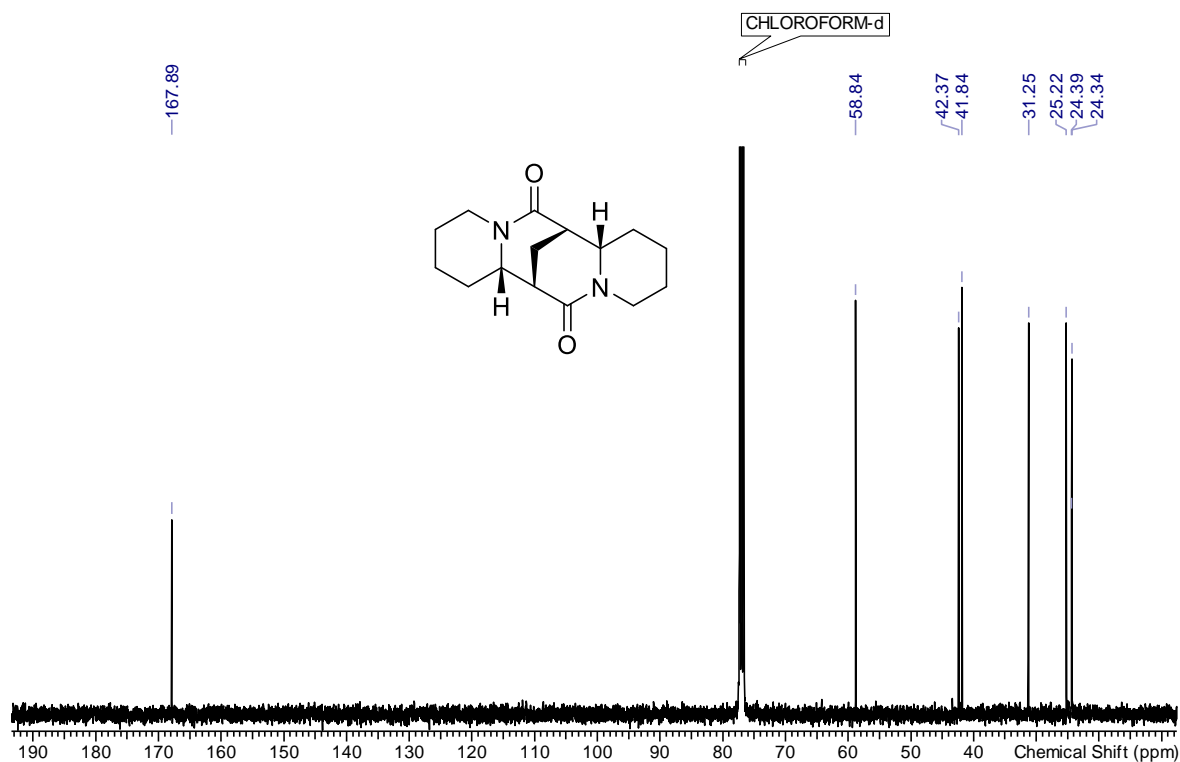


A.1.3 ^1H (400 MHz) spectrum of (+)- β -Isosparteine ((+)-1.4) (CDCl_3)

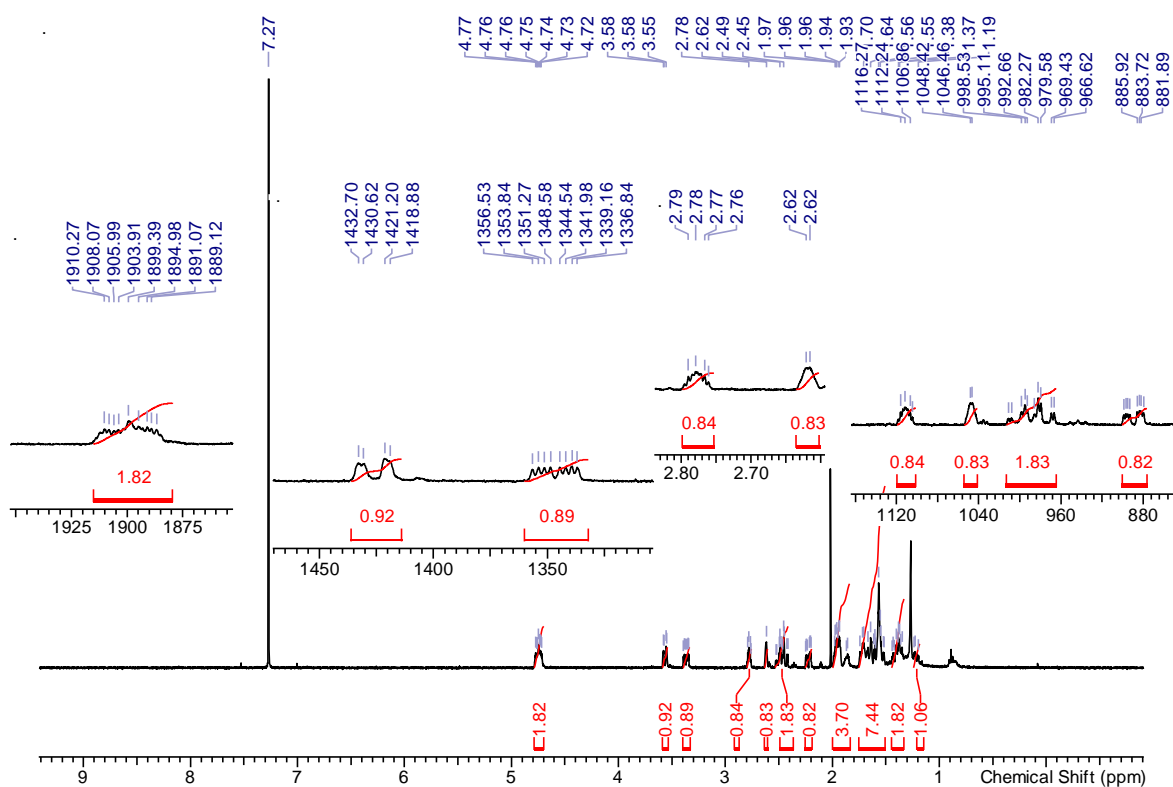


A.1.4 ^{13}C NMR (101 MHz) spectrum of (+)- β -isosparteine ((+)-1.4) (CDCl_3)

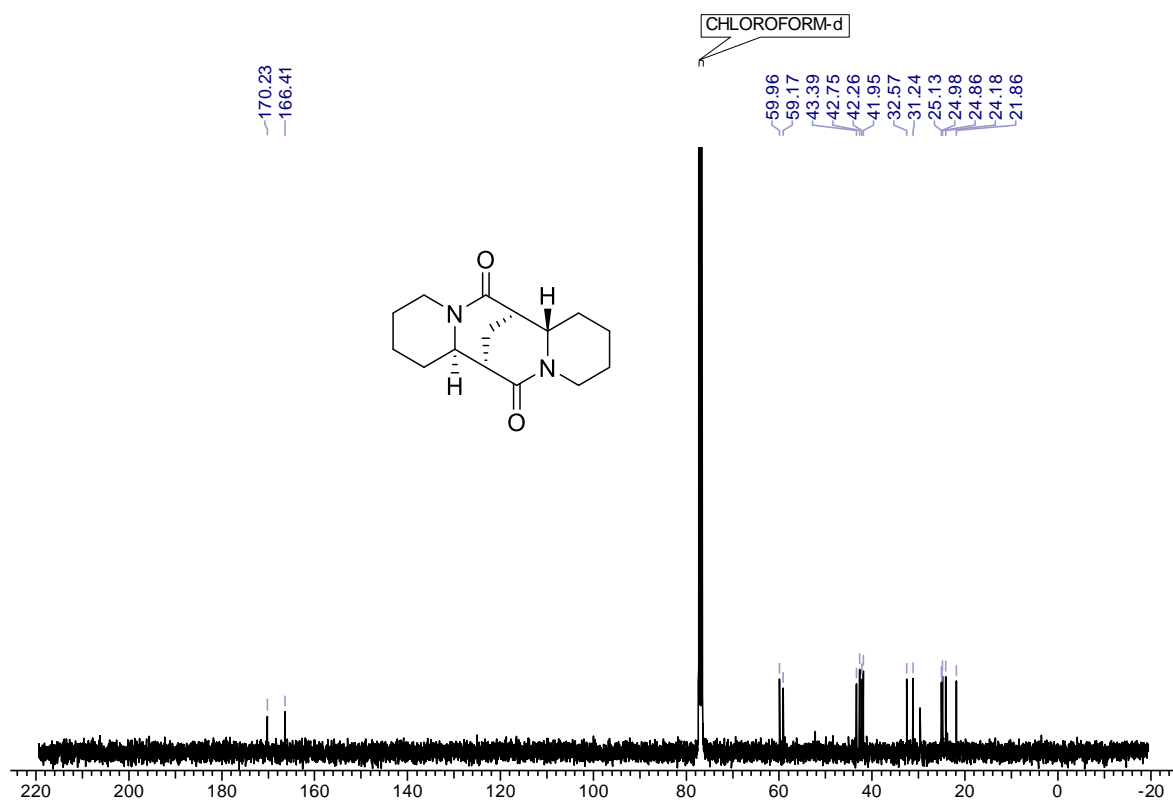


A.1.5 ^1H (400 MHz) spectrum of (–)-10,17-dioxo- α -isosparteine ((–)-1.43) (CDCl_3)

A.1.6 ^{13}C NMR (101 MHz) spectrum of (–)-10,17-dioxo- α -isosparteine ((–)-1.43) (CDCl_3)


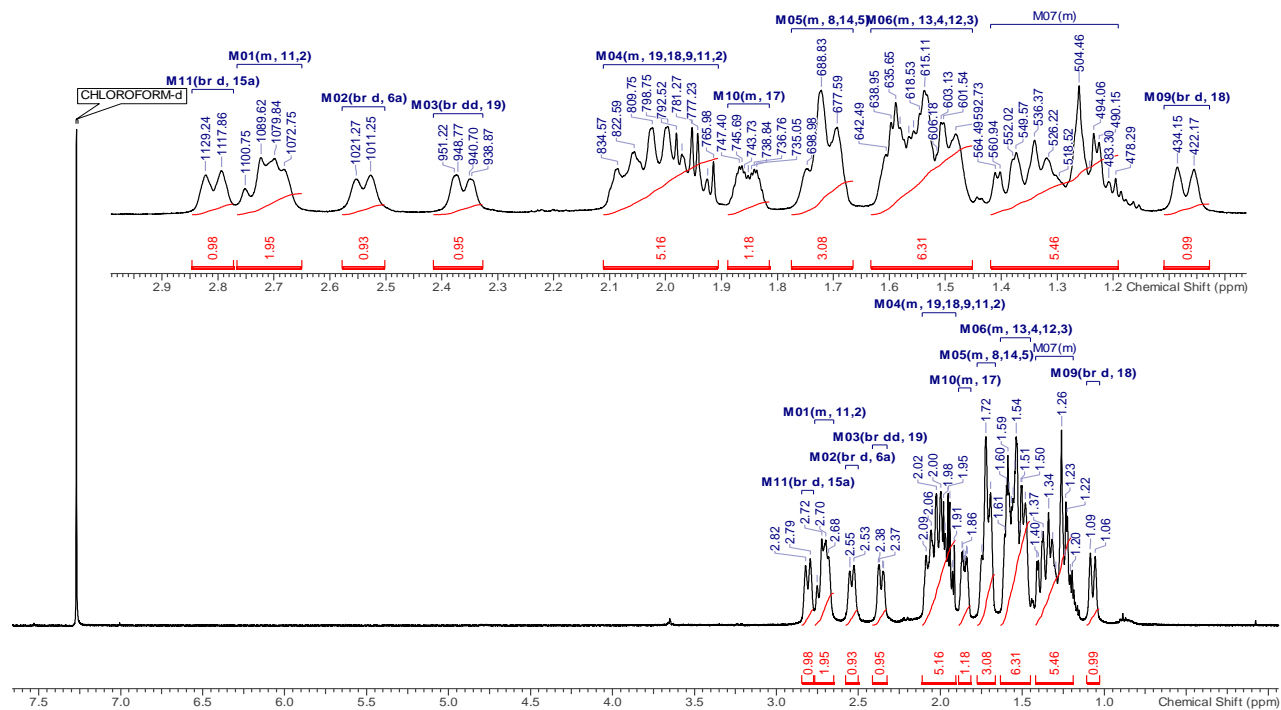
A.1.7 ^1H (400 MHz) spectrum of (+)-10,17-dioxo-sparteine ((+)-1.44) (CDCl_3)



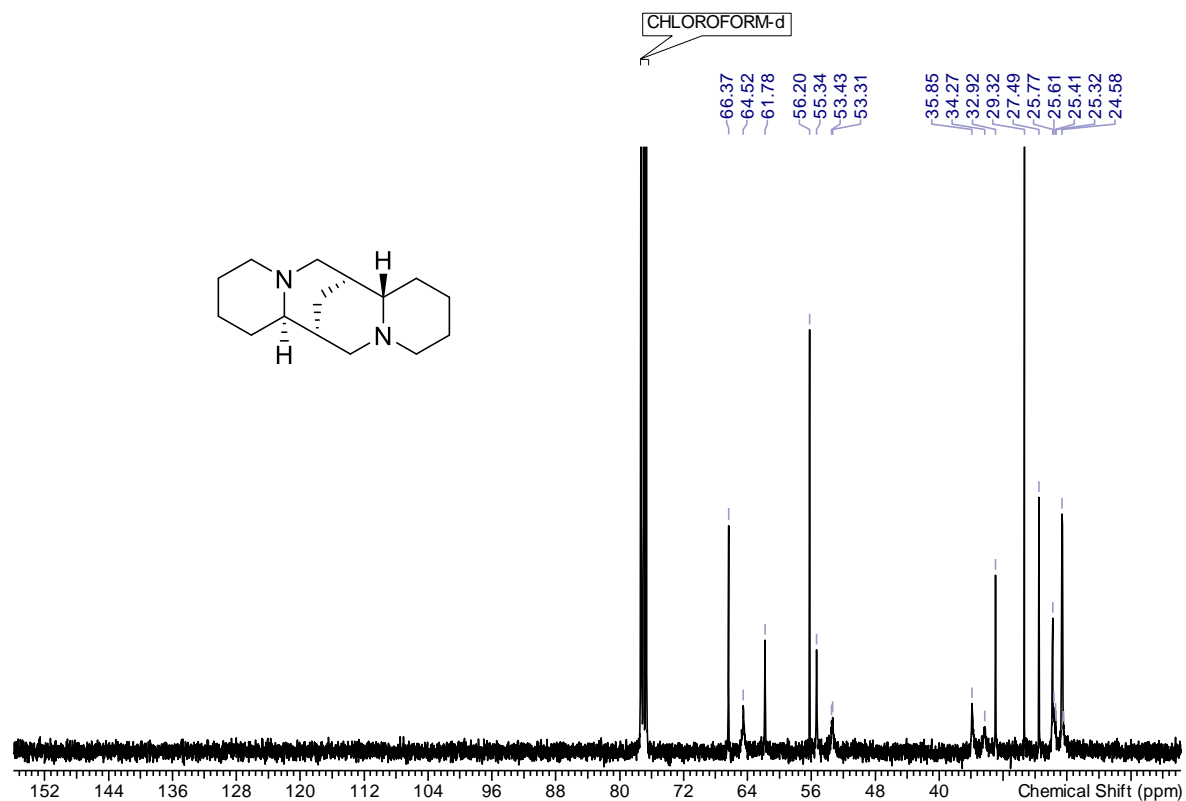
A.1.8 ^{13}C NMR (101 MHz) spectrum of (+)-10,17-dioxo-sparteine ((+)-1.44) (CDCl_3)



A.1.9 ^1H (400 MHz) spectrum of (-)-sparteine ((-)-1.3) (CDCl_3)

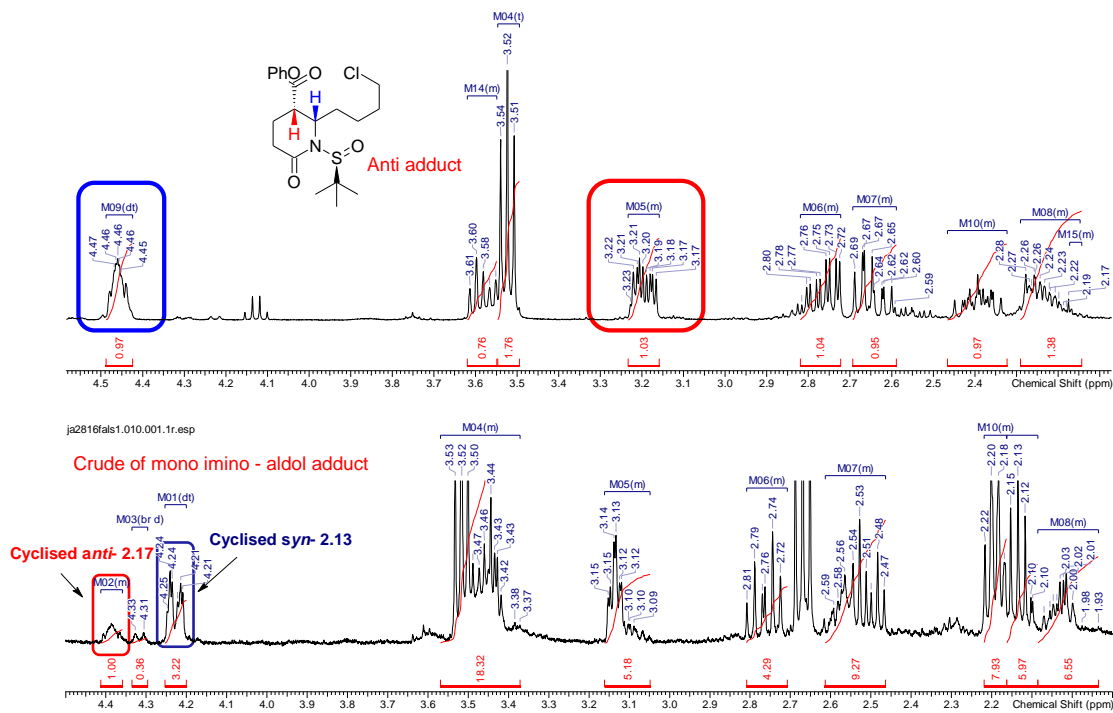


A.1.10 ^{13}C NMR (101 MHz) spectrum of (-)-sparteine ((-)-1.3) (CDCl_3)



Appendices

A.1.11 ¹H NMR spectrum of the crude mono imino-aldol reaction shows the mono *anti* and *syn* imino-aldol adducts 2.17 and 2.13 with impure *anti* imino-aldol adduct separated.



Appendix B X-Ray crystallography Data

B.1.1 Tricyclic imide product 2.40

Crystal Data and Experimental

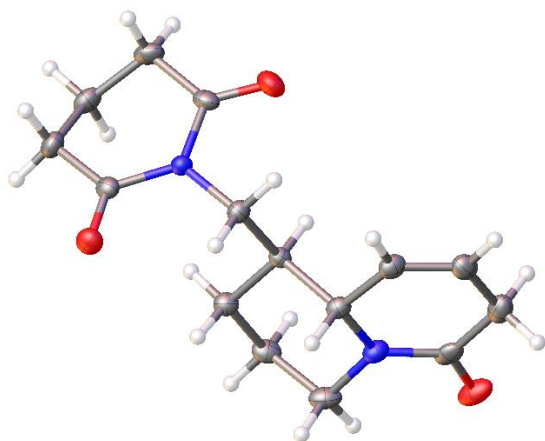
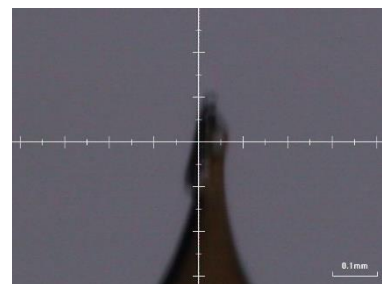


Figure 1: Thermal ellipsoids drawn at the 50% probability level.

Experimental. Single clear colourless fragment-shaped crystals of (**2016sot0040_R1_100K**) were recrystallised from DCM by slow evaporation. A suitable crystal (0.21×0.05×0.02) mm³ was selected and mounted on a MITIGEN holder with silicon oil on a Rigaku AFC12 FRE-VHF diffractometer. The crystal was kept at $T = 100(2)$ K during data collection. Using **Olex2** (Dolomanov et al., 2009), the structure was solved with the **ShelXT** (Sheldrick, 2015) structure solution program, using the Direct Methods solution method. The model was refined with version 2014/7 of **ShelXL** (Sheldrick, 2015) using Least Squares minimisation.

Crystal Data. C₁₅H₂₀N₂O₃, $M_r = 276.33$, monoclinic, P2₁ (No. 4), $a = 10.5786(7)$ Å, $b = 5.3217(3)$ Å, $c = 12.9067(9)$ Å, $\beta = 107.716(7)^\circ$, $\alpha = \gamma = 90^\circ$, $V = 692.14(8)$ Å³, $T = 100(2)$ K, $Z = 2$, $Z' = 1$, $\mu(\text{MoK}\alpha) = 0.093$, 7081 reflections measured, 3515 unique ($R_{\text{int}} = 0.0296$) which were used in all calculations. The final wR_2 was 0.0919 (all data) and R_1 was 0.0447 ($I > 2(I)$).

Compound	2016sot0040_R_100 K
Formula	C ₁₅ H ₂₀ N ₂ O ₃
$D_{\text{calc.}} / \text{g cm}^{-3}$	1.326
μ / mm^{-1}	0.093
Formula Weight	276.33
Colour	clear colourless
Shape	fragment
Size/mm ³	0.21×0.05×0.02
T/K	100(2)
Crystal System	monoclinic
Flack Parameter	0.0(8)
Hooft Parameter	-0.2(8)
Space Group	P2 ₁
$a/\text{Å}$	10.5786(7)
$b/\text{Å}$	5.3217(3)
$c/\text{Å}$	12.9067(9)
$\alpha/^\circ$	90
$\beta/^\circ$	107.716(7)
$\gamma/^\circ$	90
$V/\text{Å}^3$	692.14(8)
Z	2
Z'	1
Wavelength/Å	0.71073
Radiation type	MoK α
$\theta_{\text{min}}/^\circ$	2.978
$\theta_{\text{max}}/^\circ$	28.699
Measured Refl.	7081
Independent Refl.	3515
Reflections Used	2735
R_{int}	0.0296
Parameters	181
Restraints	1
Largest Peak	0.232
Deepest Hole	-0.215
Goof	1.022
wR_2 (all data)	0.0919
wR_2	0.0853
R_1 (all data)	0.0665
R_1	0.0447

Structure Quality Indicators

Reflections:	d min	0.74	I/ σ	15.5	R _{int}	2.96%	complete at 2 θ =61°	98%
Refinement:	Shift	0.000	Max Peak	0.2	Min Peak	-0.2	Goof	1.022
								-0.0(8)

A clear colourless fragment-shaped crystal with dimensions 0.21×0.05×0.02 was mounted on a MITIGEN holder with silicon oil. Data were collected using a Rigaku AFC12 FRE-VHF diffractometer equipped with an Oxford Cryosystems low-temperature apparatus operating at $T = 100(2)$ K.

Data were measured using profile data from ω -scans of 1.0° per frame for 10.0 s using MoK α radiation (Rotating Anode, 45.0 kV, 55.0 mA). The total number of runs and images was based on the strategy calculation from the program **CrystalClear** (Rigaku). The actually achieved resolution was $\Theta = 28.699$.

Cell parameters were retrieved using the **CrysAlisPro** (Rigaku, V1.171.38.41, 2015) software and refined using **CrysAlisPro** (Rigaku, V1.171.38.41, 2015) on 4012 reflections, 57 of the observed reflections.

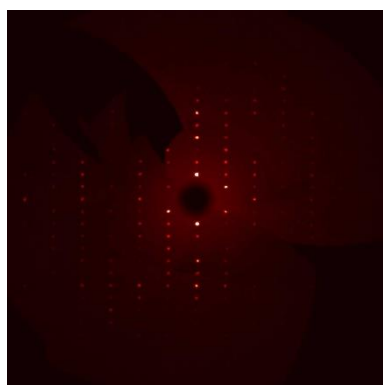
Data reduction was performed using the **CrysAlisPro** (Rigaku, V1.171.38.41, 2015) software, which corrects for Lorentz polarisation. The final completeness is 99.80 out to 28.699 in Θ . The absorption coefficient μ of this material is 0.093 at this wavelength ($\lambda = 0.71073$) and the minimum and maximum transmissions are 0.88651 and 1.00000.

The structure was solved in the space group P2₁ (# 4) by Direct Methods using the **ShelXT** (Sheldrick, 2015) structure solution program and refined by Least Squares using version 2014/7 of **ShelXL** (Sheldrick, 2015). All non-hydrogen atoms were refined anisotropically. Hydrogen atom positions were calculated geometrically and refined using the riding model.

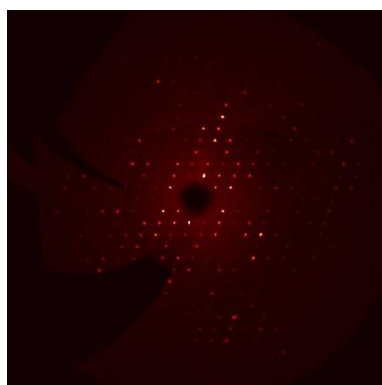
There is a single molecule in the asymmetric unit, which is represented by the reported sum formula. In other words: Z is 2 and Z' is 1.

The Flack parameter was refined to 0.0(8). Determination of absolute structure using Bayesian statistics on Bijvoet differences using the Olex2 results in -0.2(8). Note: The Flack parameter is used to determine chirality of the crystal studied, the value should be near 0, a value of 1 means that the stereochemistry is wrong and the model should be inverted. A value of 0.5 means that the crystal consists of a racemic mixture of the two enantiomers.

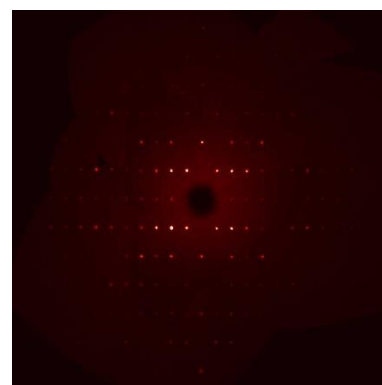
Generated precession images



0kl

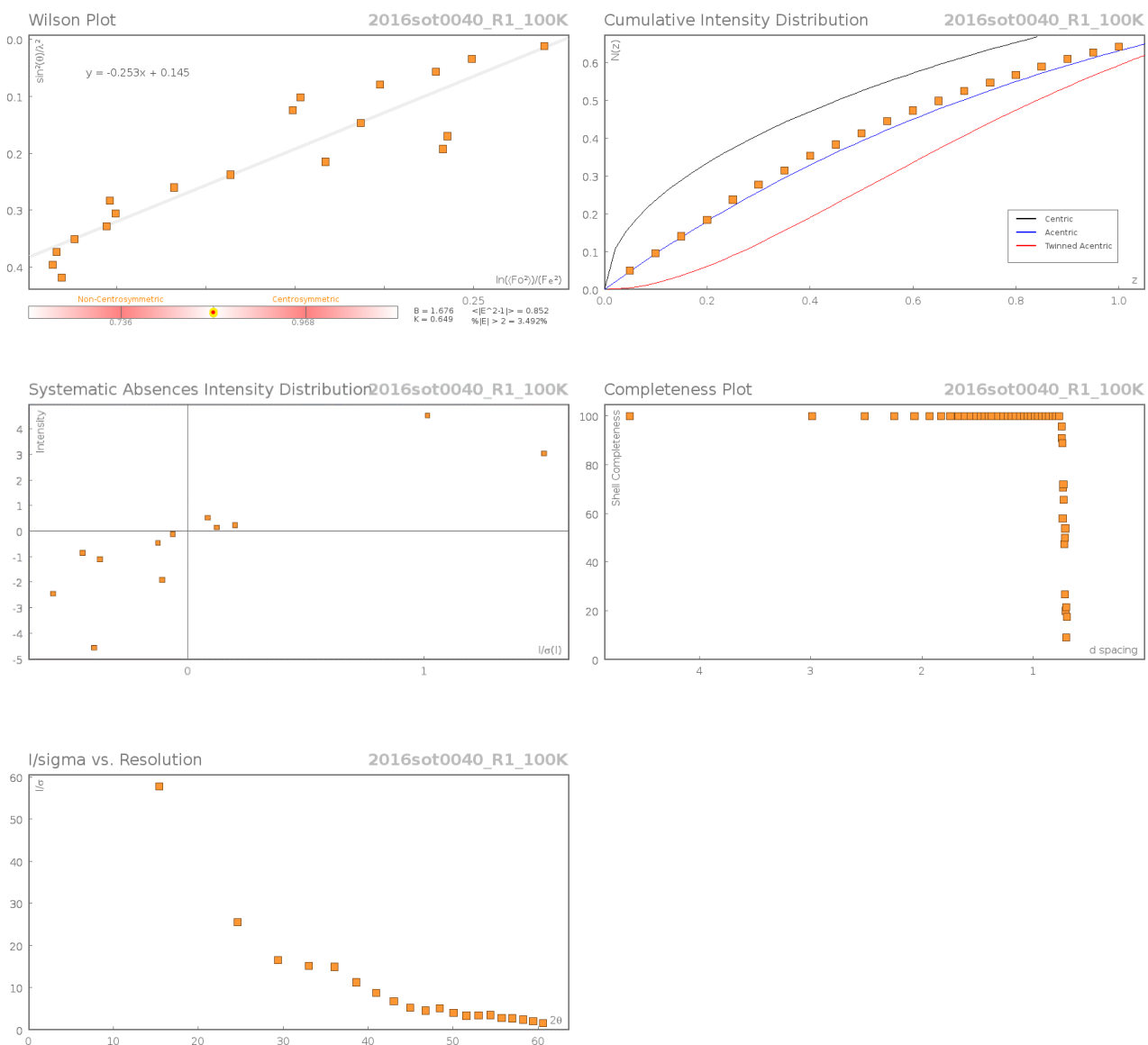


h0l

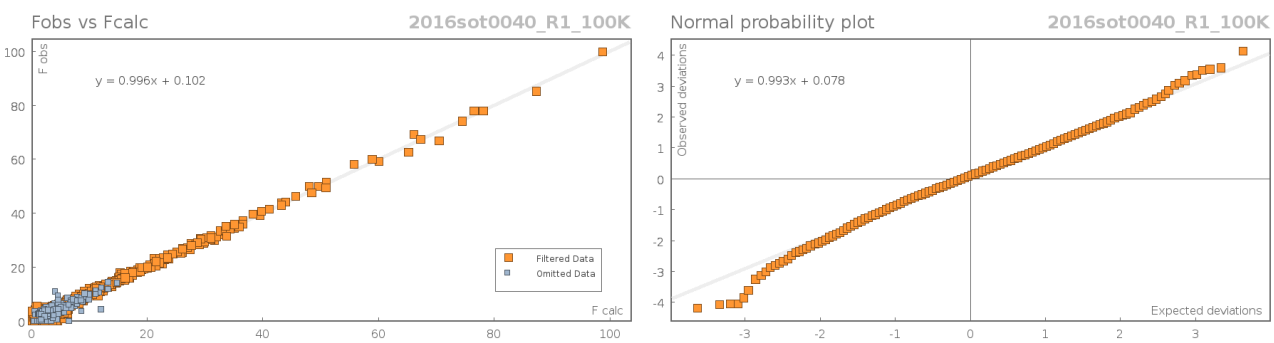


hk0

Data Plots: Diffraction Data



Data Plots: Refinement and Data



Appendices

Reflection Statistics

Total reflections (after filtering)	7093	Unique reflections	3515
Completeness	0.983	Mean I/σ	15.52
hkl_{\max} collected	(14, 7, 18)	hkl_{\min} collected	(-14, -7, -17)
hkl_{\max} used	(13, 7, 17)	hkl_{\min} used	(-14, -7, 0)
Lim d_{\max} collected	7.0	Lim d_{\min} collected	0.74
d_{\max} used	6.84	d_{\min} used	0.74
Friedel pairs	2209	Friedel pairs merged	0
Inconsistent equivalents	1	R_{int}	0.0296
R_{sigma}	0.0568	Intensity transformed	0
Omitted reflections	0	Omitted by user (OMIT hkl)	0
Multiplicity	(4402, 1117, 218, 21, 2)	Maximum multiplicity	8
Removed systematic absences	12	Filtered off (Shel/OMIT)	291

Table 1: Fractional Atomic Coordinates ($\times 10^4$) and Equivalent Isotropic Displacement Parameters ($\text{\AA}^2 \times 10^3$) for **2016sot0040_R1_100K**. U_{eq} is defined as 1/3 of the trace of the orthogonalised U_{ij} .

Atom	x	y	z	U_{eq}
O1	5371.7(15)	10048(3)	8544.4(14)	27.4(4)
O2	3883.7(15)	3549(3)	6200.3(14)	32.9(5)
O3	10403.9(15)	-92(3)	7465.4(16)	33.5(5)
N1	4683.3(17)	6702(4)	7409.6(15)	17.4(4)
N2	9066.7(17)	3223(4)	7515.6(16)	21.7(4)
C1	4595(2)	8305(4)	8248.3(18)	19.5(5)
C2	3535(2)	7752(4)	8779(2)	26.1(6)
C3	3030(2)	5068(5)	8615(2)	26.1(5)
C4	2619(2)	4481(4)	7403(2)	26.5(6)
C5	3749(2)	4808(4)	6942.5(19)	22.0(5)
C6	5816(2)	6948(4)	6973.5(19)	19.3(5)
C7	6866(2)	4903(4)	7449.3(17)	16.1(4)
C8	7331(2)	4988(4)	8699.4(18)	20.8(5)

Atom	x	y	z	U_{eq}
C9	8401(2)	3022(5)	9179.0(19)	23.8(5)
C10	9547(2)	3317(5)	8711(2)	26.7(6)
C11	8077(2)	5186(4)	7022.8(18)	18.8(5)
C12	7704(2)	5203(5)	5804.9(19)	23.1(5)
C13	8172(2)	3586(5)	5232(2)	25.3(5)
C14	9124(2)	1542(5)	5750(2)	28.9(6)
C15	9574(2)	1497(4)	6976(2)	23.9(5)

Table 2: Anisotropic Displacement Parameters ($\times 10^4$) **2016sot0040_R1_100K**. The anisotropic displacement factor exponent takes the form: $-2\pi^2[h^2a^{*2} \times U_{11} + \dots + 2hka^* \times b^* \times U_{12}]$

Atom	U_{11}	U_{22}	U_{33}	U_{23}	U_{13}	U_{12}
O1	26.0(8)	22.4(8)	34.4(10)	-6.0(8)	9.9(7)	-4.3(8)
O2	30.4(9)	36.2(10)	28.1(10)	-13.3(9)	2.7(8)	-3.1(8)
O3	20.1(8)	21.4(9)	57.2(12)	4.1(10)	9.1(8)	2.8(7)
N1	14.6(9)	18.4(9)	19.2(10)	-2.0(8)	5.4(7)	-1.6(8)
N2	17.3(9)	23.4(10)	23.7(11)	3.6(9)	5.4(8)	2.5(8)
C1	17.9(10)	17.5(11)	21.7(12)	-0.4(10)	3.8(9)	2.1(9)
C2	21.9(12)	28.7(13)	31.0(15)	-3.5(11)	13.0(11)	2(1)
C3	18.9(10)	29.4(12)	32.5(14)	5.0(12)	11.9(10)	1.0(11)
C4	17.7(11)	24.4(13)	35.5(15)	-1.5(11)	5.3(11)	-5.7(9)
C5	18.4(10)	21.9(11)	21.0(12)	-1.9(11)	-1.0(9)	-1.4(10)
C6	18.8(11)	19.9(11)	20.5(12)	1.6(10)	7.8(10)	0.3(9)
C7	17.9(10)	15.8(10)	14.4(10)	1.3(9)	4.4(8)	-1.9(9)
C8	20.8(10)	20.6(11)	20.5(12)	1.9(11)	5.6(9)	-0.7(10)
C9	24.6(11)	24.8(12)	19.1(12)	4.7(11)	2.2(10)	-2.5(10)
C10	19.4(11)	28.1(13)	28.1(13)	6.4(12)	0.7(10)	-2.5(11)
C11	16.9(10)	17.3(10)	22.0(12)	2.7(10)	5.7(9)	-0.5(10)
C12	20.3(11)	25.7(12)	24.4(13)	4.3(11)	8.6(10)	-1.1(10)
C13	24.5(11)	28.7(13)	24.4(13)	-1.5(11)	10.2(10)	-5.4(11)
C14	27.9(13)	23.5(12)	39.6(16)	-6.4(13)	16.5(12)	-3.7(11)
C15	15.3(11)	17.4(11)	40.0(15)	-0.2(12)	9.9(10)	-5.2(9)

Appendices

Table 3: Bond Lengths in Å for **2016sot0040_R1_100K**.

Atom	Atom	Length/Å	Atom	Atom	Length/Å
O1	C1	1.221(3)	C3	C4	1.523(3)
O2	C5	1.212(3)	C4	C5	1.498(3)
O3	C15	1.244(3)	C6	C7	1.543(3)
N1	C1	1.403(3)	C7	C8	1.538(3)
N1	C5	1.412(3)	C7	C11	1.547(3)
N1	C6	1.477(3)	C8	C9	1.527(3)
N2	C10	1.471(3)	C9	C10	1.518(3)
N2	C11	1.479(3)	C11	C12	1.500(3)
N2	C15	1.358(3)	C12	C13	1.325(4)
C1	C2	1.510(3)	C13	C14	1.495(3)
C2	C3	1.517(4)	C14	C15	1.508(3)

Table 4: Bond Angles in ° for **2016sot0040_R1_100K**.

Atom	Atom	Atom	Angle/°	Atom	Atom	Atom	Angle/°
C1	N1	C5	124.14(19)	O2	C5	C4	123.3(2)
C1	N1	C6	119.47(17)	N1	C5	C4	116.9(2)
C5	N1	C6	116.39(18)	N1	C6	C7	110.80(18)
C10	N2	C11	113.61(19)	C6	C7	C11	111.30(18)
C15	N2	C10	119.8(2)	C8	C7	C6	111.00(19)
C15	N2	C11	126.57(19)	C8	C7	C11	109.60(15)
O1	C1	N1	120.5(2)	C9	C8	C7	111.47(19)
O1	C1	C2	121.9(2)	C10	C9	C8	110.56(19)
N1	C1	C2	117.64(18)	N2	C10	C9	110.54(17)
C1	C2	C3	113.5(2)	N2	C11	C7	109.43(17)
C2	C3	C4	108.3(2)	N2	C11	C12	112.40(19)
C5	C4	C3	111.78(18)	C12	C11	C7	113.04(16)
O2	C5	N1	119.8(2)	C13	C12	C11	123.9(2)

Atom	Atom	Atom	Angle/°	Atom	Atom	Atom	Angle/°
C12	C13	C14	122.6(2)	O3	C15	C14	119.5(2)
C13	C14	C15	115.8(2)	N2	C15	C14	118.7(2)
O3	C15	N2	121.8(2)				

Table 5: Torsion Angles in ° for **2016sot0040_R1_100K**.

Atom	Atom	Atom	Atom	Angle/°
O1	C1	C2	C3	-158.3(2)
N1	C1	C2	C3	20.3(3)
N1	C6	C7	C8	-56.1(2)
N1	C6	C7	C11	- 178.44(17)
N2	C11	C12	C13	2.3(3)
C1	N1	C5	O2	178.1(2)
C1	N1	C5	C4	-1.6(3)
C1	N1	C6	C7	101.0(2)
C1	C2	C3	C4	-52.3(2)
C2	C3	C4	C5	58.5(2)
C3	C4	C5	O2	147.7(2)
C3	C4	C5	N1	-32.7(3)
C5	N1	C1	O1	-173.2(2)
C5	N1	C1	C2	8.1(3)
C5	N1	C6	C7	-78.6(2)
C6	N1	C1	O1	7.2(3)
C6	N1	C1	C2	- 171.45(19)
C6	N1	C5	O2	-2.3(3)
C6	N1	C5	C4	178.02(19)
C6	C7	C8	C9	- 178.31(18)
C6	C7	C11	N2	178.88(17)
C6	C7	C11	C12	-55.0(3)

Appendices

Atom	Atom	Atom	Atom	Angle/°
C7	C8	C9	C10	54.7(2)
C7	C11	C12	C13	-122.2(2)
C8	C7	C11	N2	55.7(2)
C8	C7	C11	C12	- 178.19(19)
C8	C9	C10	N2	-55.1(3)
C10	N2	C11	C7	-59.1(2)
C10	N2	C11	C12	174.45(19)
C10	N2	C15	O3	2.9(3)
C10	N2	C15	C14	-176.4(2)
C11	N2	C10	C9	58.9(3)
C11	N2	C15	O3	- 179.78(19)
C11	N2	C15	C14	1.0(3)
C11	C7	C8	C9	-55.0(2)
C11	C12	C13	C14	0.5(4)
C12	C13	C14	C15	-2.6(3)
C13	C14	C15	O3	-177.3(2)
C13	C14	C15	N2	1.9(3)
C15	N2	C10	C9	-123.4(2)
C15	N2	C11	C7	123.4(2)
C15	N2	C11	C12	-3.0(3)

Table 6: Hydrogen Fractional Atomic Coordinates ($\times 10^4$) and Equivalent Isotropic Displacement Parameters ($\text{\AA}^2 \times 10^3$) for **2016sot0040_R1_100K**. U_{eq} is defined as 1/3 of the trace of the orthogonalised U_{ij} .

Atom	x	y	z	U_{eq}
H2A	2779	8910	8478	31
H2B	3897	8089	9568	31
H3A	2261	4871	8894	31
H3B	3736	3896	9017	31
H4A	2293	2729	7284	32
H4B	1882	5607	7015	32
H6A	6224	8629	7158	23
H6B	5497	6796	6171	23
H7	6452	3224	7216	19
H8A	7687	6680	8944	25
H8B	6564	4684	8970	25
H9A	8730	3214	9979	29
H9B	8016	1319	9013	29
H10A	9998	4942	8949	32
H10B	10200	1955	8988	32
H11	8496	6846	7284	23
H12	7096	6447	5422	28
H13	7891	3731	4462	30
H14A	9918	1704	5501	35
H14B	8704	-93	5484	35

Citations

CrysAlisPro Software System, Rigaku Oxford Diffraction, (2015).

CrystalClear, Rigaku, (2009).

O.V. Dolomanov and L.J. Bourhis and R.J. Gildea and J.A.K. Howard and H. Puschmann, Olex2: A complete structure solution, refinement and analysis program, *J. Appl. Cryst.*, (2009), **42**, 339-341. Sheldrick, G.M., Crystal structure refinement with ShelXL, *Acta Cryst.*, (2015), **C27**, 3-8. Sheldrick, G.M., ShelXT-Integrated space-group and crystal-structure determination, *Acta Cryst.*, (2015), **A71**, 3- 8.

B.1.2 Anti-mono imino-aldol product 2.27

Crystal Data and Experimental

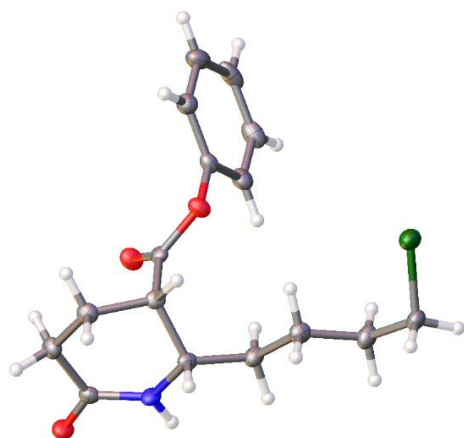
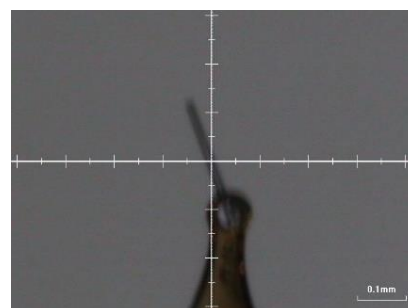


Figure 2: Thermal ellipsoids drawn at the 50% probability level.



Experimental. Single clear colourless needle-shaped crystals of (**2016sot0090_R1_100K**) were recrystallised from a mixture of hexane and ethyl acetate by slow evaporation. A suitable crystal (0.28×0.02×0.02) mm³ was selected and mounted on a MITIGEN holder with silicon oil on a Rigaku AFC12 FRE-VHF diffractometer. The crystal was kept at $T = 100(2)$ K during data collection. Using **Olex2** (Dolomanov et al., 2009), the structure was solved with the **ShelXT** (Sheldrick, 2015) structure solution program, using the Intrinsic Phasing solution method. The model was refined with version 2016/6 of **ShelXL** (Sheldrick, 2015) using Least Squares minimisation.

Crystal Data. C₁₆H₂₀ClNO₃, $M_r = 309.78$, monoclinic, P2₁/c (No. 14), $a = 18.7179(15)$ Å, $b = 5.3770(3)$ Å, $c = 16.4030(12)$ Å, $\beta = 109.501(8)^\circ$, $\alpha = \gamma = 90^\circ$, $V = 1556.2(2)$ Å³, $T = 100(2)$ K, $Z = 4$, $Z' = 1$, $\mu(\text{Mo K}\alpha) = 0.255$, 14451 reflections measured, 4003 unique ($R_{int} = 0.0794$) which were used in all calculations. The final wR_2 was 0.1678 (all data) and R_1 was 0.0724 ($I > 2(I)$). **Crystal Data.** C₁₆H₂₀ClNO₃, $M_r = 309.78$, monoclinic, P2₁/c (No. 14), $a = 18.7179(15)$ Å, $b = 5.3770(3)$ Å, $c = 16.4030(12)$ Å, $\beta = 109.501(8)^\circ$, $\alpha = \gamma = 90^\circ$, $V = 1556.2(2)$ Å³, $T = 100(2)$ K, $Z = 4$, $Z' = 1$, $\mu(\text{Mo K}\alpha) = 0.255$,

Compound	2016sot0090_R_100 K
Formula	C ₁₆ H ₂₀ ClNO ₃
$D_{calc.}/\text{g cm}^{-3}$	1.322
μ/mm^{-1}	0.255
Formula Weight	309.78
Colour	clear colourless
Shape	needle
Size/mm ³	0.28×0.02×0.02
T/K	100(2)
Crystal System	monoclinic
Space Group	P2 ₁ /c
$a/\text{Å}$	18.7179(15)
$b/\text{Å}$	5.3770(3)
$c/\text{Å}$	16.4030(12)
$\alpha/^\circ$	90
$\beta/^\circ$	109.501(8)
$\gamma/^\circ$	90
$V/\text{Å}^3$	1556.2(2)
Z	4
Z'	1
Wavelength/Å	0.71075
Radiation type	Mo K α
$\Theta_{min}/^\circ$	3.211
$\Theta_{max}/^\circ$	28.696
Measured Refl.	14451
Independent Refl.	4003
Reflections Used	2599
R_{int}	0.0794
Parameters	190
Restraints	0
Largest Peak	0.451
Deepest Hole	-0.300
GooF	1.026
wR_2 (all data)	0.1678
wR_2	0.1487
R_1 (all data)	0.1204
R_1	0.0724

Structure Quality Indicators

Reflections:	d min (Mo)	0.74	I/ σ	9.2	R _{int}	7.94%	complete at 2 θ =61°	100%
Refinement:	Shift	0.000	Max Peak	0.5	Min Peak	-0.3	Goof	1.026

A clear colourless needle-shaped crystal with dimensions 0.28×0.02×0.02 was mounted on a MITIGEN holder with silicon oil. Data were collected using a Rigaku AFC12 FRE-VHF diffractometer equipped with an Oxford Cryosystems low-temperature apparatus operating at $T = 100(2)$ K.

Data were measured using profile data from ω -scans of 1.0° per frame for 15.0 s using Mo K_{α} radiation (Rotating Anode, 45.0 kV, 55.0 mA). The total number of runs and images was based on the strategy calculation from the program **CrystalClear** (Rigaku). The actually achieved resolution was $\theta = 28.696$.

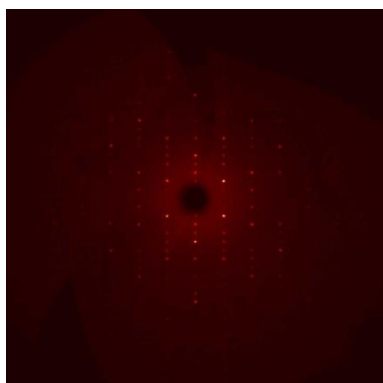
Cell parameters were retrieved using the **CrysAlisPro** (Rigaku, V1.171.39.9g, 2015) software and refined using **CrysAlisPro** (Rigaku, V1.171.39.9g, 2015) on 4225 reflections, 29 of the observed reflections.

Data reduction was performed using the **CrysAlisPro** (Rigaku, V1.171.39.9g, 2015) software, which corrects for Lorentz polarisation. The final completeness is 92.61 out to 28.696 in θ . The absorption coefficient μ of this material is 0.255 at this wavelength ($\lambda = 0.71075$) and the minimum and maximum transmissions are 0.51747 and 1.00000.

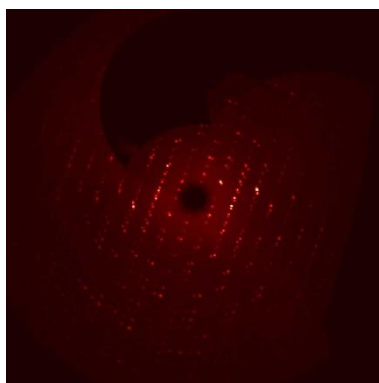
The structure was solved in the space group $P2_1/c$ (# 14) by Intrinsic Phasing using the **ShelXT** (Sheldrick, 2015) structure solution program and refined by Least Squares using version 2016/6 of **ShelXL** (Sheldrick, 2015). All non-hydrogen atoms were refined anisotropically. Hydrogen atom positions were calculated geometrically and refined using the riding model.

There is a single molecule in the asymmetric unit, which is represented by the reported sum formula. In other words: Z is 4 and Z' is 1.

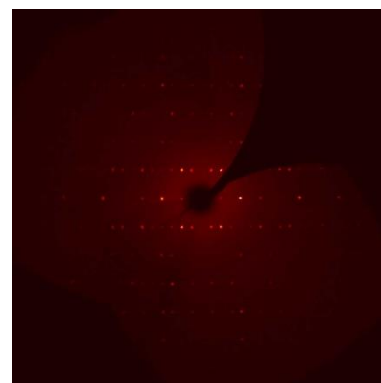
Generated precession images



0kl



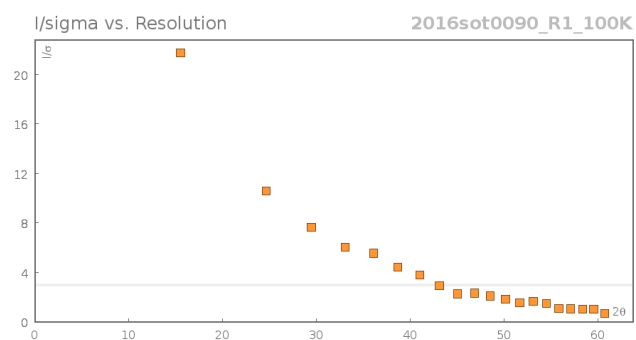
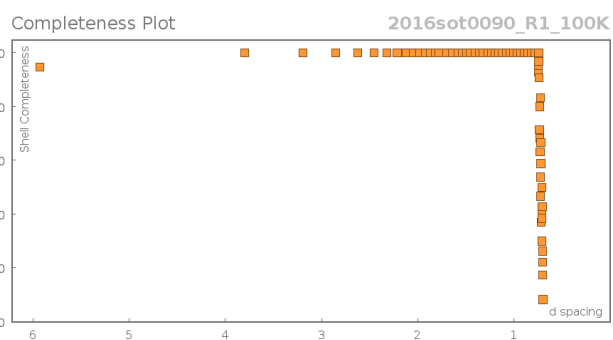
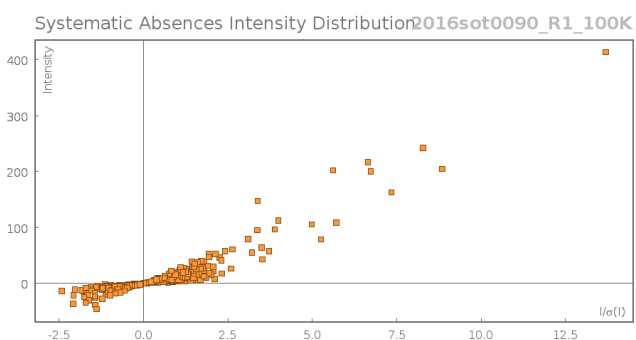
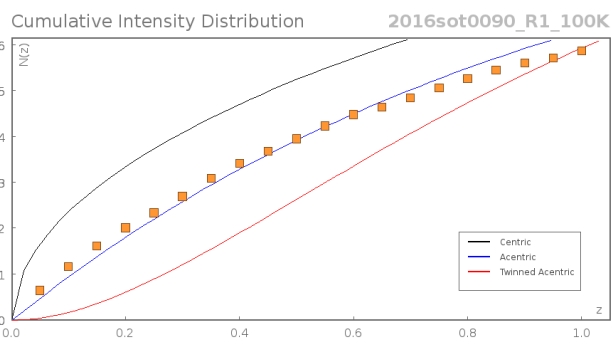
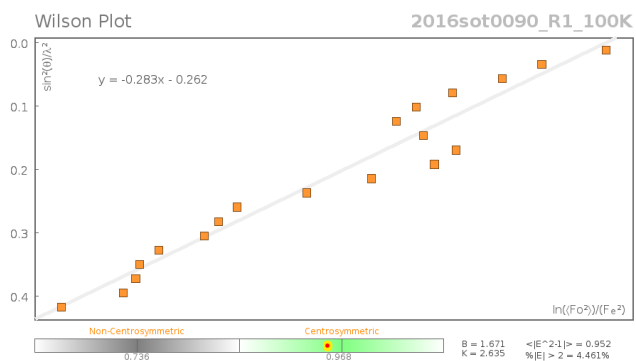
h0l



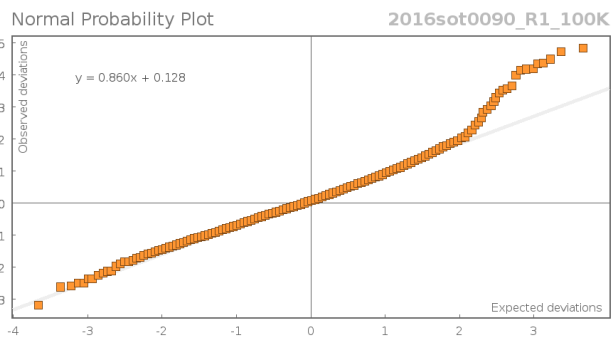
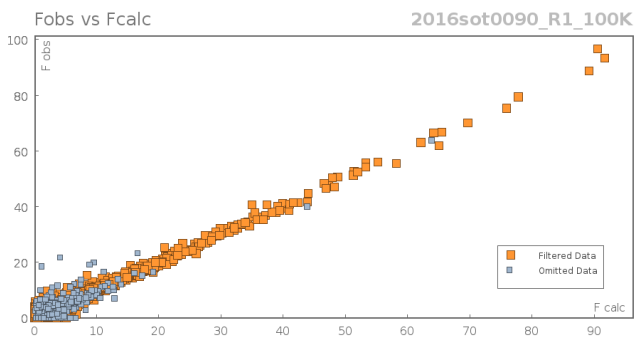
hk0

Appendices

Data Plots: Diffraction Data



Data Plots: Refinement and Data



Reflection Statistics

Total reflections (after filtering)	15302	Unique reflections	4003
Completeness	0.996	Mean I/σ	9.16
hkl_{\max} collected	(26, 7, 20)	hkl_{\min} collected	(-26, -7, -23)
hkl_{\max} used	(23, 7, 22)	hkl_{\min} used	(-25, 0, 0)
Lim d_{\max} collected	7.0	Lim d_{\min} collected	0.74
d_{\max} used	6.75	d_{\min} used	0.74
Friedel pairs	4719	Friedel pairs merged	1
Inconsistent equivalents	1	R_{int}	0.0794
R_{sigma}	0.0896	Intensity transformed	0
Omitted reflections	0	Omitted by user (OMIT hkl)	31
Multiplicity	(9198, 2607, 450, 41)	Maximum multiplicity	13
Removed systematic absences	820	Filtered off (Shel/OMIT)	624

Table 7: Fractional Atomic Coordinates ($\times 10^4$) and Equivalent Isotropic Displacement Parameters ($\text{\AA}^2 \times 10^3$) for **2016sot0090_R1_100K**. U_{eq} is defined as $1/3$ of the trace of the orthogonalised U_{ij} .

Atom	x	y	z	U_{eq}
Cl01	8701.2(5)	1534.5(16)	4957.3(5)	30.5(2)
O002	7883.5(11)	6276(4)	7136.5(13)	19.8(5)
O003	6992.1(11)	9043(4)	7168.5(14)	22.3(5)
O004	4780.6(11)	9682(4)	6003.5(13)	23.3(5)
N005	5605.7(13)	7426(4)	5580.7(15)	18.3(5)
C006	7155.0(15)	6986(5)	6995.3(17)	15.5(6)
C007	6156.9(16)	5430(5)	5651.8(18)	17.2(6)
C008	8457.8(16)	8076(5)	7478.2(19)	17.6(6)
C009	5268.7(16)	8010(5)	6155.0(19)	17.9(6)
C00A	6608.6(16)	4911(5)	6603.8(18)	16.3(6)
C00B	6622.2(17)	6085(5)	5076.9(19)	20.0(6)
C00C	8946.6(17)	7754(6)	8305(2)	22.8(7)
C00D	5513.0(17)	6704(6)	7012.9(19)	21.3(6)

Appendices

Atom	x	y	z	U_{eq}
C00E	6045.8(17)	4498(5)	7092(2)	19.9(6)
C00F	8529.9(17)	10022(6)	6969(2)	23.2(7)
C00G	7901.1(17)	2447(6)	4042.9(19)	23.2(7)
C00H	7475.1(19)	4579(6)	4276(2)	24.2(7)
C00I	7104.4(17)	3950(5)	4945(2)	21.9(7)
C00J	9111.2(18)	11718(6)	7300(2)	27.6(7)
C00K	9602.3(17)	11454(6)	8132(2)	29.5(8)
C00L	9526.6(18)	9463(6)	8638(2)	29.4(8)

Table 8: Anisotropic Displacement Parameters ($\times 10^4$) **2016sot0090_R1_100K**. The anisotropic displacement factor exponent takes the form: $-2\pi^2[h^2a^{*2} \times U_{11} + \dots + 2hka^* \times b^* \times U_{12}]$

Atom	U_{11}	U_{22}	U_{33}	U_{23}	U_{13}	U_{12}
Cl01	26.4(4)	42.4(5)	21.4(4)	-2.1(4)	6.3(3)	7.9(4)
O002	17.3(10)	14(1)	27.2(11)	-0.6(9)	6.0(9)	0.0(8)
O003	22.3(11)	14.1(10)	30.3(12)	-3.7(9)	8.4(9)	1.5(8)
O004	22.7(11)	23.8(11)	22.1(11)	2.4(9)	5.7(9)	9.2(9)
N005	21.0(13)	16.2(12)	15.5(12)	4.1(10)	3.2(10)	7.1(10)
C006	16.8(14)	16.2(14)	13.3(13)	4.4(11)	4.7(11)	1.4(11)
C007	17.7(14)	14.2(13)	17.5(14)	-3.1(12)	2.9(11)	3.7(11)
C008	16.1(14)	13.8(13)	24.4(15)	-1.7(12)	8.7(12)	-0.3(10)
C009	15.3(14)	16.0(14)	20.2(14)	-0.2(12)	3.0(11)	-0.9(11)
C00A	19.8(15)	8.5(12)	19.3(14)	0.9(11)	4.8(12)	2.3(11)
C00B	24.9(16)	17.9(14)	17.1(14)	1.7(12)	6.8(12)	4.5(12)
C00C	22.4(16)	21.7(15)	24.1(16)	1.7(13)	7.7(13)	2.8(12)
C00D	21.8(15)	20.2(15)	24.0(15)	3.7(13)	10.5(12)	-0.1(12)
C00E	21.5(15)	13.7(13)	24.4(15)	1.4(12)	7.5(12)	-0.5(11)
C00F	19.9(16)	21.4(16)	28.9(17)	3.1(14)	9.2(13)	5.2(12)
C00G	24.6(17)	29.1(16)	15.9(14)	-1.9(13)	6.8(13)	1.6(13)
C00H	32.4(18)	21.0(15)	21.0(15)	-0.1(13)	11.5(13)	5.1(13)
C00I	24.8(16)	17.6(14)	22.6(15)	-1.8(12)	6.9(13)	2.9(12)
C00J	27.0(17)	16.0(15)	45(2)	4.7(15)	18.7(15)	1.4(13)

Atom	U_{11}	U_{22}	U_{33}	U_{23}	U_{13}	U_{12}
C00K	19.2(16)	19.4(15)	54(2)	-11.9(16)	17.5(15)	-5.4(12)
C00L	20.9(17)	33.5(18)	30.0(17)	-8.1(15)	3.6(14)	3.2(13)

Table 9: Bond Lengths in Å for 2016sot0090_R1_100K.

Atom	Atom	Length/Å	Atom	Atom	Length/Å
Cl01	C00G	1.798(3)	C008	C00F	1.373(4)
O002	C006	1.359(3)	C009	C00D	1.501(4)
O002	C008	1.416(3)	C00A	C00E	1.537(4)
O003	C006	1.206(3)	C00B	C00I	1.519(4)
O004	C009	1.246(3)	C00C	C00L	1.388(4)
N005	C007	1.466(3)	C00D	C00E	1.527(4)
N005	C009	1.334(4)	C00F	C00J	1.384(4)
C006	C00A	1.505(4)	C00G	C00H	1.516(4)
C007	C00A	1.533(4)	C00H	C00I	1.520(4)
C007	C00B	1.523(4)	C00J	C00K	1.374(5)
C008	C00C	1.371(4)	C00K	C00L	1.391(5)

Table 10: Bond Angles in ° for 2016sot0090_R1_100K.

Atom	Atom	Atom	Angle/°	Atom	Atom	Atom	Angle/°
C006	O002	C008	117.5(2)	C00C	C008	C00F	122.0(3)
C009	N005	C007	127.0(2)	C00F	C008	O002	119.7(3)
O002	C006	C00A	111.4(2)	O004	C009	N005	121.1(3)
O003	C006	O002	122.4(3)	O004	C009	C00D	119.9(3)
O003	C006	C00A	126.2(3)	N005	C009	C00D	118.9(2)
N005	C007	C00A	110.4(2)	C006	C00A	C007	111.4(2)
N005	C007	C00B	108.3(2)	C006	C00A	C00E	111.8(2)
C00B	C007	C00A	116.0(2)	C007	C00A	C00E	108.4(2)
C00C	C008	O002	118.2(3)	C00I	C00B	C007	113.7(2)

Appendices

Atom	Atom	Atom	Angle/°
C008	C00C	C00L	118.8(3)
C009	C00D	C00E	115.4(3)
C00D	C00E	C00A	112.7(2)
C008	C00F	C00J	119.2(3)
C00H	C00G	Cl01	111.0(2)
C00G	C00H	C00I	114.8(3)
C00B	C00I	C00H	111.8(2)
C00K	C00J	C00F	120.0(3)
C00J	C00K	C00L	120.3(3)
C00C	C00L	C00K	119.8(3)

Table 11: Hydrogen Fractional Atomic Coordinates ($\times 10^4$) and Equivalent Isotropic Displacement Parameters ($\text{\AA}^2 \times 10^3$) for **2016sot0090_R1_100K**. U_{eq} is defined as 1/3 of the trace of the orthogonalised U_{ij} .

Atom	x	y	z	U_{eq}
H005	5483.87	8336.55	5108.3	22
H007	5863.8	3888.6	5409.59	21
H00A	6905.2	3345.67	6636.41	20
H00B	6274.05	6627.07	4505.54	24
H00C	6957.6	7504.38	5337.32	24
H00D	8889.33	6385.04	8644.32	27
H00E	5054.74	6110.58	7127.06	26
H00F	5767.46	7927.25	7468.47	26
H00G	5741.2	2991.88	6861	24
H00H	6332.24	4201.79	7710.65	24
H00I	8185.23	10201.42	6396.54	28
H00J	8078.13	2961.23	3562.99	28
H00K	7555.9	1010.52	3843.31	28
H00L	7077.79	5157.45	3742.78	29
H00M	7832.02	5975.01	4497.18	29
H00N	6782.62	2455.65	4755.75	26
H00O	7502.35	3556.88	5502.39	26
H00P	9170.46	13064.02	6953	33
H00Q	9995.32	12636.85	8361.77	35
H00R	9871.01	9273.34	9210.03	35

Citations

CrysAlisPro Software System, Rigaku Oxford Diffraction, (2015).

CrystalClear, Rigaku, (2009).

O.V. Dolomanov and L.J. Bourhis and R.J. Gildea and J.A.K. Howard and H. Puschmann, Olex2: A complete structure solution, refinement and analysis program, *J. Appl. Cryst.*, (2009), **42**, 339-341.

Sheldrick, G.M., Crystal structure refinement with ShelXL, *Acta Cryst.*, (2015), **C27**, 3-8.

Sheldrick, G.M., ShelXT-Integrated space-group and crystal-structure determination, *Acta Cryst.*, (2015), **A71**, 3-8.

B.1.3 *Syn,syn*-double imino-aldol product 2.2

Crystal Data and Experimental

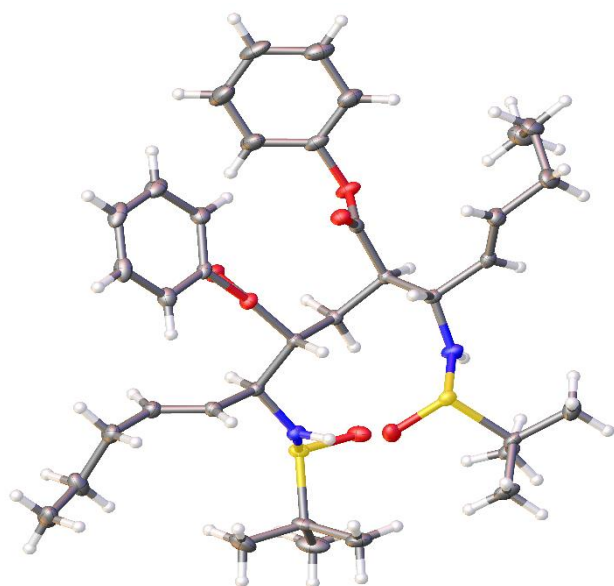
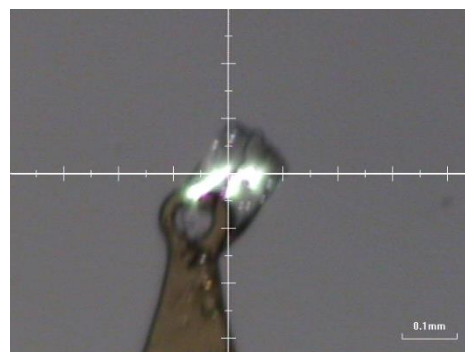


Figure 3: Thermal ellipsoids drawn at the 50% probability level.

Experimental. Single clear colourless Fragment-shaped crystals of (**2015sot0012**) were recrystallised from hexane by slow evaporation. A suitable crystal (0.20×0.14×0.02) was selected and mounted on a MITIGEN holder in perfluoroether oil on a Rigaku AFC12 FRE-HF diffractometer. The crystal was kept at $T = 100(2)$ K during data collection. Using **Olex2** (Dolomanov et al., 2009), the structure was solved with the ShelXT (Sheldrick, 2015) structure solution program, using the Direct Methods solution method. The model was refined with version of **ShelXL** (Sheldrick, 2008) using Least Squares minimisation.

Crystal Data. $C_{37}H_{54}N_2O_6S_2$, $M_r = 686.94$, tetragonal, $P4_32_12$ (No. 96), $a = 12.99897 \text{ \AA}$, $b = 12.99897 \text{ \AA}$, $c = 45.5533 \text{ \AA}$, $\alpha = \beta = \gamma = 90^\circ$, $V = 7697.3(2) \text{ \AA}^3$, $T = 100(2) \text{ K}$, $Z = 8$, $Z' = 1$, $\mu(\text{MoK}\alpha) = 0.183$, 79518 reflections measured, 12692 unique ($R_{int} = 0.0611$) which were used in all calculations. The final wR_2 was 0.0964 (all data) and R_1 was 0.0504 ($I > 2(I)$).



Compound	2015sot0012
Formula	$C_{37}H_{54}N_2O_6S_2$
$D_{calc.} / \text{g cm}^{-3}$	1.186
μ / mm^{-1}	0.183
Formula Weight	686.94
Colour	clear colourless
Shape	Fragment
Max Size/mm	0.20
Mid Size/mm	0.14
Min Size/mm	0.02
T / K	100(2)
Crystal System	tetragonal
Flack Parameter	0.00(2)
Hooft Parameter	0.004(17)
Space Group	$P4_32_12$
$a / \text{\AA}$	12.99897(14)
$b / \text{\AA}$	12.99897(14)
$c / \text{\AA}$	45.5533(8)
$\alpha / ^\circ$	90
$\beta / ^\circ$	90
$\gamma / ^\circ$	90
$V / \text{\AA}^3$	7697.3(2)
Z	8
Z'	1
$\mathcal{O}_{min} / ^\circ$	1.629
$\mathcal{O}_{max} / ^\circ$	32.085
Measured Refl.	79518
Independent Refl.	12692
Reflections Used	11093
R_{int}	0.0611
Parameters	440
Restraints	0
Largest Peak	0.337
Deepest Hole	-0.331
GooF	1.076
wR_2 (all data)	0.0964
wR_2	0.0928
R_1 (all data)	0.0622
R_1	0.0504

Structure Quality Indicators

Reflections:	d min	0.67	I/σ	20.3	Rint	6.11%	complete at $2\theta = 64^\circ$	94%
Refinement:	Shift/esd	0.002	Max Peak	0.3	Min Peak	-0.3	Goof	1.076

A clear colourless Fragment-shaped crystal with dimensions 0.20×0.14×0.02 was mounted on a MITIGEN holder in perfluoroether oil. Data were collected using a Rigaku AFC12 FRE-HF diffractometer equipped with an Oxford Cryosystems low-temperature apparatus operating at $T = 100(2)$ K.

Data were measured using profile data from ω -scans of 1.0° per frame for 15.0 s using MoK $_{\alpha}$ radiation (Rotating Anode, 45.0 kV, 55.0 mA). The total number of runs and images was based on the strategy calculation from the program **CrystalClear** (Rigaku). The actually achieved resolution was $\Theta = 32.085$.

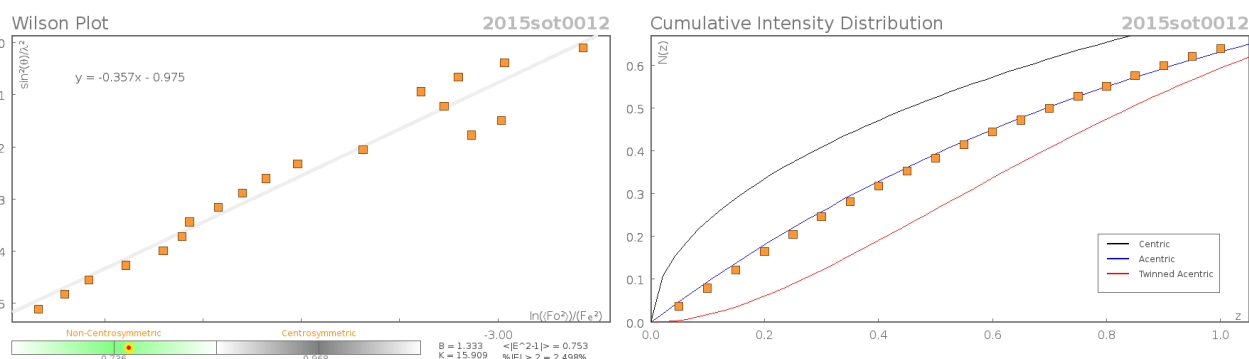
Cell parameters were retrieved using the **CrysAlisPro** (Agilent, V1.171.37.31, 2014) software and refined using **CrysAlisPro** (Agilent, V1.171.37.31, 2014) on 23670 reflections, 30 of the observed reflections.

Data reduction was performed using the **CrysAlisPro** (Agilent, V1.171.37.31, 2014) software which corrects for Lorentz polarisation. The final completeness is 100.00 out to 32.085 in Θ . The absorption coefficient (μ) of this material is 0.183 and the minimum and maximum transmissions are 0.89375 and 1.00000.

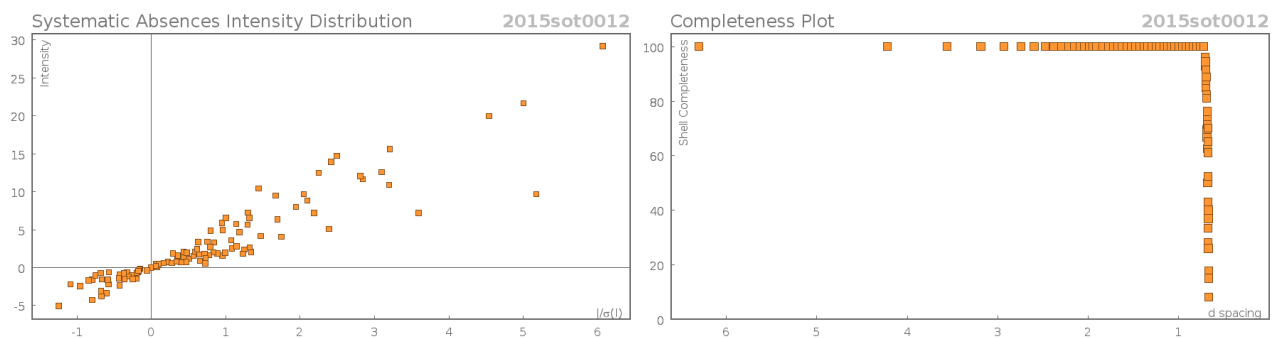
The structure was solved in the space group $P4_32_12$ (# 96) by Direct Methods using the ShelXT (Sheldrick, 2015) structure solution program and refined by Least Squares using version of **ShelXL** (Sheldrick, 2008). All non-hydrogen atoms were refined anisotropically. Hydrogen atom positions were calculated geometrically and refined using the riding model, with the exception of the N-H which were freely refined.

The Flack parameter was refined to 0.00(2), confirming the absolute stereochemistry. Determination of absolute structure using Bayesian statistics on Bijvoet differences using the Olex2 results in 0.004(17). Note: The Flack parameter is used to determine chirality of the crystal studied, the value should be near 0, a value of 1 means that the stereochemistry is wrong and the model should be inverted. A value of 0.5 means that the crystal consists of a racemic mixture of the two enantiomers.

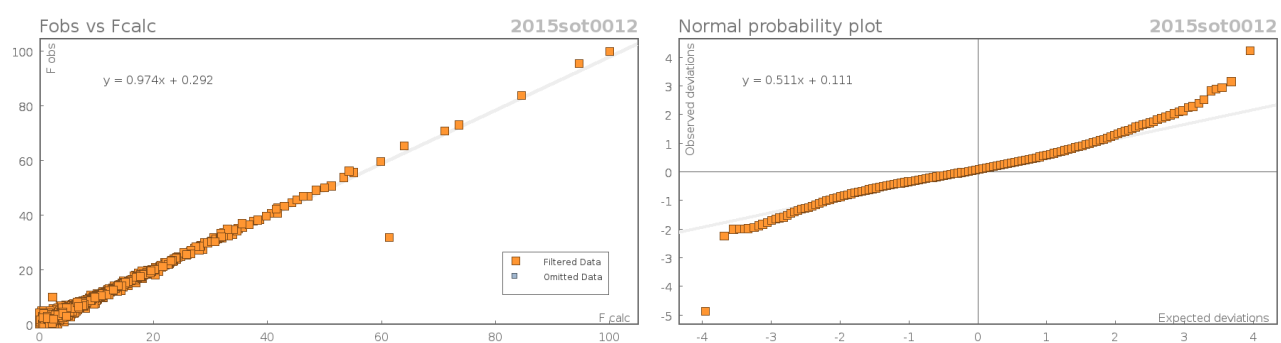
Data Plots: Diffraction Data



Appendices



Data Plots: Refinement and Data



Reflection Statistics

Total reflections	79647	Unique reflections	12692
Completeness	0.941	Mean I/σ	20.33
Max hkl collected	(19, 19, 67)	Min hkl collected	(-19, -19, -68)
Max hkl used	(13, 19, 68)	Min hkl used	(-12, 0, 0)
Lim d max	100.0	Lim d min	0.36
d max used	12.5	d min used	0.67
Friedel pairs	24835	Friedel pairs merged	0
Inconsistent equivalents	45	R_{int}	0.0611
R_{σ}	0.0471	Intensity transformed	0
Omitted reflections	0	Omitted by user	0
Multiplicity	(49546, 13012, 1343, 12)	ReflectionAPotMax	21
Removed Systematic Absences	129	Filtered Off	0

Table 12: Fractional Atomic Coordinates ($\times 10^4$) and Equivalent Isotropic Displacement Parameters ($\text{\AA}^2 \times 10^3$) for **2015sot0012**. U_{eq} is defined as 1/3 of the trace of the orthogonalised U_{ij} .

Atom	x	y	z	U_{eq}
S1	1867.3(4)	671.9(4)	4126.5(2)	15.16(10)
S2	3449.7(4)	30.1(4)	5122.5(2)	16.31(10)
O2	3884.9(12)	4027.4(12)	4161.1(3)	18.1(3)
O1	3416.5(13)	4836.6(12)	4577.6(4)	21.4(4)
O6	2402.0(13)	489.9(12)	5164.5(4)	22.1(4)
O3	5377.9(12)	2209.1(12)	4133.1(3)	16.0(3)
O4	5593.5(13)	2976.6(13)	4576.0(3)	19.2(3)
O5	2656.0(12)	-14.2(13)	4264.8(3)	20.8(3)
N1	1669.2(15)	1717.1(15)	4318.4(4)	17.3(4)
N2	3822.7(15)	146.7(15)	4780.6(4)	15.9(4)
C1	5100(2)	5601(2)	4586.7(6)	30.3(6)
C2	5745(2)	6415(2)	4517.0(7)	38.6(7)
C3	5371(2)	7251(2)	4364.6(6)	34.0(6)
C4	4349(2)	7291(2)	4281.0(6)	35.0(6)
C5	3697(2)	6477(2)	4349.5(6)	30.6(6)
C6	4084.8(19)	5650.9(19)	4500.8(5)	22.3(5)
C7	3403.3(17)	4034.6(16)	4385.8(4)	14.6(4)
C8	2739.9(16)	3161.5(16)	4498.4(4)	13.2(4)
C9	3404.4(17)	2397.8(17)	4676.8(4)	14.6(4)
C10	4202.8(16)	1771.0(16)	4509.0(4)	13.0(4)
C11	5123.9(17)	2409.1(16)	4417.9(4)	14.5(4)
C12	6278.9(16)	2652.6(18)	4019.8(4)	16.3(4)
C13	6988.6(18)	1981(2)	3903.4(5)	21.4(5)
C14	7883.6(19)	2366(2)	3778.1(5)	26.5(6)
C15	8048.5(19)	3416(2)	3774.2(5)	29.2(6)
C16	7323(2)	4081(2)	3890.1(5)	28.3(6)

Appendices

Atom	x	y	z	U_{eq}
C17	6419.5(19)	3703.4(19)	4013.2(5)	21.8(5)
C18	2144.5(17)	2694.2(17)	4235.4(4)	14.6(4)
C19	1331.3(17)	3451.3(17)	4137.7(5)	17.6(4)
C20	1430.0(19)	4153.4(19)	3928.7(5)	22.7(5)
C21	637(2)	4954(2)	3855.7(6)	29.3(6)
C22	876(2)	6013(2)	3986.7(6)	32.7(6)
C23	750(2)	6040(2)	4319.3(6)	35.7(6)
C24	630.1(18)	23.2(18)	4195.4(5)	18.5(4)
C25	-177.3(18)	602(2)	4017.7(5)	26.1(5)
C26	781(2)	-1069.5(18)	4077.5(5)	25.5(5)
C27	393.3(19)	11.4(19)	4524.3(5)	21.4(5)
C28	4632.7(16)	883.0(16)	4703.3(5)	14.7(4)
C29	5485.3(17)	311.8(17)	4548.6(5)	16.3(4)
C30	6448.5(18)	249.4(18)	4637.8(5)	20.1(4)
C31	7253.5(19)	-390.1(19)	4488.7(6)	24.1(5)
C32	7581(2)	-1313(2)	4675.1(6)	29.8(6)
C33	8211(2)	-2107(2)	4508.1(7)	31.9(6)
C34	3252(2)	-1378.1(17)	5142.0(5)	21.4(5)
C35	2507(2)	-1741.7(19)	4908.2(6)	28.9(6)
C36	2807(3)	-1561(2)	5448.1(6)	35.0(7)
C37	4309(2)	-1871(2)	5111.9(6)	32.9(6)

Table 13: Anisotropic Displacement Parameters ($\times 10^4$) **2015sot0012**. The anisotropic displacement factor exponent takes the form: $-2\pi^2[h^2a^{*2} \times U_{11} + \dots + 2hka^* \times b^* \times U_{12}]$

Atom	U_{11}	U_{22}	U_{33}	U_{23}	U_{13}	U_{12}
S1	16.8(2)	15.6(2)	13.1(2)	-2.51(19)	0.92(19)	-2.6(2)
S2	22.0(3)	14.9(2)	12.09(19)	0.86(19)	2.8(2)	0.0(2)
O2	18.8(8)	19.0(8)	16.6(7)	0.3(6)	3.6(6)	-2.8(6)

Atom	U_{11}	U_{22}	U_{33}	U_{23}	U_{13}	U_{12}
O1	25.6(9)	17.8(8)	20.9(8)	-6.3(6)	8.5(7)	-8.6(7)
O6	26.8(9)	17.9(8)	21.6(8)	0.6(6)	8.4(7)	1.6(7)
O3	15.0(7)	19.9(8)	13.1(6)	0.0(6)	3.7(6)	-2.7(6)
O4	19.1(8)	21.4(8)	17.2(7)	-1.7(6)	-0.5(6)	-4.5(7)
O5	19.5(8)	21.3(8)	21.8(7)	-5.5(7)	-3.5(6)	1.6(7)
N1	21.7(10)	14.6(9)	15.7(8)	-1.9(7)	7.3(7)	-4.4(7)
N2	18.3(9)	17.6(9)	11.8(7)	0.6(7)	0.4(7)	-2.8(7)
C1	27.0(13)	19.7(12)	44.2(15)	-3.9(11)	5.4(12)	-4.3(11)
C2	27.0(14)	29.7(15)	59.0(19)	-9.1(14)	8.4(14)	-9.2(12)
C3	37.7(15)	26.8(13)	37.6(14)	-7.9(12)	17.0(12)	-17.6(12)
C4	47.6(17)	25.7(13)	31.6(13)	2.4(11)	0.6(13)	-12.6(13)
C5	34.0(14)	27.4(13)	30.5(13)	-0.4(11)	-3.4(11)	-10.8(11)
C6	26.3(12)	18.3(11)	22.3(11)	-6.9(9)	8.0(9)	-8.3(10)
C7	13.3(9)	15.3(9)	15.1(9)	0.2(8)	-1.3(8)	1.4(8)
C8	12.8(9)	14.1(9)	12.8(8)	-0.6(8)	1.8(7)	-0.2(8)
C9	14.5(9)	15.9(10)	13.3(9)	0.7(8)	2.4(8)	0.2(8)
C10	13.5(9)	13.8(9)	11.5(8)	-0.1(7)	0.8(7)	-1.5(8)
C11	14.7(10)	15.1(10)	13.7(8)	1.0(8)	0.8(8)	1.6(8)
C12	12.4(10)	24.4(11)	12.0(8)	3.5(8)	0.7(7)	-2.9(8)
C13	19.1(11)	28.6(13)	16.6(10)	1.6(9)	2.5(9)	1.8(9)
C14	16.8(11)	44.9(16)	17.7(10)	2.2(11)	2.8(9)	2.5(11)
C15	18.5(11)	51.0(17)	17.9(10)	9.5(11)	1.7(9)	-10.0(12)
C16	27.8(13)	31.4(14)	25.7(12)	10.1(11)	-0.5(10)	-9.6(11)
C17	20.4(11)	23.4(12)	21.5(10)	5.6(9)	2.0(9)	-0.5(9)
C18	15.9(10)	15.1(10)	12.7(9)	-0.6(8)	2.1(8)	-2.6(8)
C19	14.9(10)	20.4(10)	17.4(9)	-1.5(9)	-0.9(8)	-2.8(9)
C20	21.4(12)	25.9(12)	20.7(10)	3.0(9)	-1.9(9)	-1.1(10)
C21	27.5(13)	30.8(13)	29.7(12)	9.3(11)	-9.4(11)	-0.9(12)

Atom	U_{11}	U_{22}	U_{33}	U_{23}	U_{13}	U_{12}
C22	33.9(15)	24.5(13)	39.7(15)	12.4(12)	-8.8(12)	1.0(11)
C23	39.4(16)	27.9(14)	39.9(15)	2.0(12)	2.3(13)	5.4(13)
C24	18.4(10)	18.5(10)	18.6(9)	-2.2(9)	1.3(8)	-7.7(9)
C25	19.7(12)	33.2(14)	25.4(11)	-0.3(11)	-4.5(9)	-3.5(10)
C26	33.5(14)	19.8(11)	23.2(11)	-5.3(9)	2.5(10)	-10.4(10)
C27	22.4(11)	22.0(11)	19.7(10)	-1.2(9)	3.4(9)	-7.6(10)
C28	14.6(9)	15.2(10)	14.4(9)	0.8(8)	0.1(8)	-2.0(8)
C29	17.4(10)	16.4(10)	14.9(9)	0.8(8)	1.7(8)	0.6(8)
C30	18.6(11)	19.3(11)	22.4(10)	-0.8(9)	0.5(9)	-0.3(9)
C31	16.4(11)	25.3(12)	30.7(12)	-0.5(10)	2.4(9)	-0.4(10)
C32	28.8(14)	32.8(14)	27.9(12)	-4.3(11)	-7.6(11)	9.8(11)
C33	22.5(13)	27.5(14)	45.7(16)	-8.7(12)	-3.0(12)	3.1(11)
C34	31.3(13)	13(1)	19.7(10)	5.2(8)	5.4(10)	3.1(9)
C35	37.2(15)	16.1(11)	33.4(13)	3(1)	1.1(11)	-6.2(11)
C36	55.1(19)	23.3(13)	26.7(12)	9.4(11)	14.4(13)	2.3(13)
C37	38.7(15)	22.9(12)	37.0(14)	2.9(11)	0.4(13)	11.4(12)

Table 14: Bond Lengths in Å for **2015sot0012**.

Atom	Atom	Length/Å	Atom	Atom	Length/Å
S1	O5	1.4978(17)	O3	C11	1.363(2)
S1	N1	1.6358(19)	O3	C12	1.404(3)
S1	C24	1.843(2)	O4	C11	1.198(3)
S2	O6	1.4994(18)	N1	C18	1.462(3)
S2	N2	1.6384(18)	N2	C28	1.466(3)
S2	C34	1.851(2)	C1	C2	1.388(4)
O2	C7	1.200(3)	C1	C6	1.377(4)
O1	C6	1.413(3)	C2	C3	1.378(4)
O1	C7	1.360(3)	C3	C4	1.382(4)

Atom	Atom	Length/Å	Atom	Atom	Length/Å
C4	C5	1.392(4)	C19	C20	1.325(3)
C5	C6	1.371(4)	C20	C21	1.502(4)
C7	C8	1.515(3)	C21	C22	1.532(4)
C8	C9	1.547(3)	C22	C23	1.525(4)
C8	C18	1.550(3)	C24	C25	1.524(3)
C9	C10	1.525(3)	C24	C26	1.531(3)
C10	C11	1.515(3)	C24	C27	1.530(3)
C10	C28	1.558(3)	C28	C29	1.509(3)
C12	C13	1.376(3)	C29	C30	1.319(3)
C12	C17	1.378(3)	C30	C31	1.499(3)
C13	C14	1.389(3)	C31	C32	1.530(4)
C14	C15	1.382(4)	C32	C33	1.522(4)
C15	C16	1.384(4)	C34	C35	1.515(4)
C16	C17	1.392(3)	C34	C36	1.529(3)
C18	C19	1.511(3)	C34	C37	1.523(4)

Table 15: Bond Angles in ° for **2015sot0012**.

Atom	Atom	Atom	Angle/°	Atom	Atom	Atom	Angle/°
O5	S1	N1	112.19(10)	C18	N1	S1	121.13(14)
O5	S1	C24	104.68(10)	C28	N2	S2	120.09(15)
N1	S1	C24	98.73(10)	C6	C1	C2	118.5(3)
O6	S2	N2	110.68(10)	C3	C2	C1	120.2(3)
O6	S2	C34	105.20(11)	C2	C3	C4	120.5(3)
N2	S2	C34	100.26(10)	C3	C4	C5	119.6(3)
C7	O1	C6	114.99(17)	C6	C5	C4	119.0(3)
C11	O3	C12	118.27(17)	C1	C6	O1	118.9(2)

Appendices

Atom	Atom	Atom	Angle/°	Atom	Atom	Atom	Angle/°
C5	C6	O1	119.0(2)	C19	C18	C8	108.77(17)
C5	C6	C1	122.1(2)	C20	C19	C18	126.3(2)
O2	C7	O1	123.2(2)	C19	C20	C21	124.7(2)
O2	C7	C8	125.4(2)	C20	C21	C22	113.4(2)
O1	C7	C8	111.34(17)	C23	C22	C21	112.7(2)
C7	C8	C9	109.92(17)	C25	C24	S1	106.54(16)
C7	C8	C18	108.44(16)	C25	C24	C26	111.1(2)
C9	C8	C18	115.69(18)	C25	C24	C27	112.7(2)
C10	C9	C8	117.36(17)	C26	C24	S1	104.65(16)
C9	C10	C28	110.80(16)	C27	C24	S1	110.29(15)
C11	C10	C9	112.51(17)	C27	C24	C26	111.1(2)
C11	C10	C28	106.13(17)	N2	C28	C10	111.26(17)
O3	C11	C10	110.35(17)	N2	C28	C29	108.57(18)
O4	C11	O3	124.5(2)	C29	C28	C10	111.26(17)
O4	C11	C10	125.12(19)	C30	C29	C28	125.7(2)
C13	C12	O3	116.1(2)	C29	C30	C31	123.9(2)
C13	C12	C17	122.1(2)	C30	C31	C32	112.2(2)
C17	C12	O3	121.7(2)	C33	C32	C31	113.8(2)
C12	C13	C14	119.5(2)	C35	C34	S2	111.32(16)
C15	C14	C13	119.4(2)	C35	C34	C36	110.5(2)
C14	C15	C16	120.4(2)	C35	C34	C37	112.5(2)
C15	C16	C17	120.5(3)	C36	C34	S2	104.47(17)
C12	C17	C16	118.1(2)	C37	C34	S2	106.67(18)
N1	C18	C8	110.59(17)	C37	C34	C36	111.0(2)
N1	C18	C19	110.26(18)				

Table 16: Hydrogen Fractional Atomic Coordinates ($\times 10^4$) and Equivalent Isotropic Displacement Parameters ($\text{\AA}^2 \times 10^3$) for **2015sot0012**. U_{eq} is defined as 1/3 of the trace of the orthogonalised U_{ij} .

Atom	x	y	z	U_{eq}
H1A	5347	5033	4689	36
H2A	6432	6397	4573	46
H3	5809	7792	4318	41
H4	4099	7859	4179	42
H5	3009	6492	4294	37
H8	2232	3458	4633	16
H9A	3760	2783	4828	17
H9B	2945	1921	4775	17
H10	3881	1477	4333	16
H13	6870	1276	3909	26
H14	8367	1921	3697	32
H15	8651	3678	3693	35
H16	7441	4787	3886	34
H17	5925	4147	4089	26
H18	2625	2575	4073	17
H19	700	3421	4234	21
H20	2034	4150	3819	27
H21A	-27	4725	3928	35
H21B	588	5017	3644	35
H22A	1577	6200	3937	39
H22B	422	6519	3899	39
H23A	53	5869	4369	54
H23B	907	6717	4390	54
H23C	1208	5550	4407	54
H25A	-223	1298	4087	39
H25B	-833	271	4040	39

Appendices

Atom	x	y	z	U_{eq}
H25C	15	602	3814	39
H26A	991	-1038	3876	38
H26B	146	-1443	4092	38
H26C	1302	-1413	4190	38
H27A	999	-187	4631	32
H27B	-149	-472	4563	32
H27C	182	686	4586	32
H28	4909	1180	4885	18
H29	5317	-26	4375	20
H30	6640	624	4803	24
H31A	7851	35	4449	29
H31B	6987	-634	4302	29
H32A	7982	-1067	4840	36
H32B	6969	-1644	4753	36
H33B	7822	-2354	4343	48
H33C	8372	-2672	4636	48
H33A	8837	-1797	4440	48
H35A	1863	-1389	4931	43
H35B	2400	-2469	4928	43
H35C	2787	-1597	4717	43
H36A	3262	-1276	5593	53
H36B	2732	-2286	5481	53
H36C	2146	-1234	5463	53
H37A	4579	-1735	4920	49
H37B	4252	-2601	5140	49
H37C	4765	-1589	5257	49
H1	1340(20)	1700(20)	4469(6)	24(7)
H2	3370(30)	0(30)	4651(7)	41(9)

Table 17: Hydrogen Bond information for **2015sot0012**.

D	H	A	d(D-H)/Å	d(H-A)/Å	d(D-A)/Å	D-H-A/deg
N2	H2	O5	0.85(3)	1.99(3)	2.804(2)	159(3)

Citations

CrysAlisPro Software System, Agilent Technologies UK Ltd, Yarnton, Oxford, UK (2014).

CrystalClear, Rigaku, (2009).

O.V. Dolomanov and L.J. Bourhis and R.J. Gildea and J.A.K. Howard and H. Puschmann, Olex2: A complete structure solution, refinement and analysis program, *J. Appl. Cryst.*, (2009), **42**, 339-341.

Sheldrick, G.M., A short history of ShelX, *Acta Cryst.*, (2008), **A64**, 339-341.

B.1.4 (+)-10,17-dioxo- β -isosparteine ((+)-1.4)

Crystal Data and Experimental

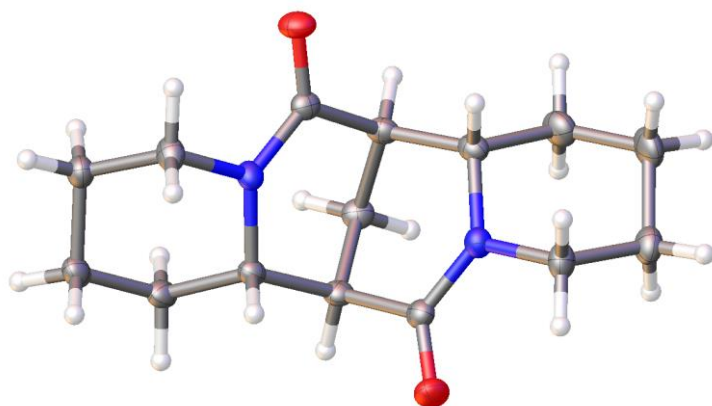
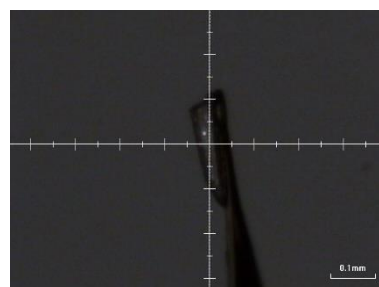


Figure 4: Thermal ellipsoids drawn at the 50% probability level.

Experimental. Single clear colourless prism-shaped crystals of (**2015sot0075-K-100K**) were recrystallised from DMSO by slow evaporation. A suitable crystal (0.23×0.07×0.04) was selected and mounted on a MITIGEN holder in perfluoroether oil on a Rigaku AFC12 FRE-HF diffractometer. The crystal was kept at $T = 100(2)$ K during data collection. Using **Olex2** (Dolomanov et al., 2009), the structure was solved with the **ShelXT** (Sheldrick, 2015) structure solution program, using the Direct Methods solution method. The model was refined with **ShelXL** (Sheldrick, 2008) using Least Squares minimisation.

Crystal Data. $C_{15}H_{22}N_2O_2$, $M_r = 262.34$, orthorhombic, $P2_12_12_1$ (No. 19), $a = 6.08925(15)$ Å, $b = 10.1967(2)$ Å, $c = 21.7891(7)$ Å, $\alpha = \beta = \gamma = 90^\circ$, $V = 1352.89(6)$ Å³, $T = 100(2)$ K, $Z = 4$, $Z' = 1$, $\mu(\text{MoK}\alpha) = 0.086$, 13342 reflections measured, 3496 unique ($R_{int} = 0.0305$) which were used in all calculations. The final wR_2 was 0.0855 (all data) and R_1 was 0.0377 ($I > 2(I)$).



Compound	2015sot0075-K-100K
Formula	$C_{15}H_{22}N_2O_2$
$D_{calc.}/\text{g cm}^{-3}$	1.288
μ/mm^{-1}	0.086
Formula Weight	262.34
Colour	clear colourless
Shape	prism
Max Size/mm	0.23
Mid Size/mm	0.07
Min Size/mm	0.04
T/K	100(2)
Crystal System	orthorhombic
Friedrich Mo, Cu	5, 28
Flack Parameter	0.2(6)
Hooft Parameter	0.8(4)
Space Group	$P2_12_12_1$
$a/\text{Å}$	6.08925(15)
$b/\text{Å}$	10.1967(2)
$c/\text{Å}$	21.7891(7)
$\alpha/^\circ$	90
$\beta/^\circ$	90
$\gamma/^\circ$	90
$V/\text{Å}^3$	1352.89(6)
Z	4
Z'	1
$\theta_{min}/^\circ$	3.444
$\theta_{max}/^\circ$	28.697
Measured Refl.	13342
Independent Refl.	3496
Reflections Used	3173
R_{int}	0.0305
Parameters	172
Restraints	0
Largest Peak	0.212
Deepest Hole	-0.168
GooF	1.023
wR_2 (all data)	0.0855
wR_2	0.0825
R_1 (all data)	0.0436
R_1	0.0377

Structure Quality Indicators

Reflections:	d min	0.74	I/σ	25.5	R _{int}	3.05%	complete at $2\theta=61^\circ$	100%
Refinement:	Shift	0.000	Max Peak	0.2	Min Peak	-0.2	Goof	1.023

A clear colourless prism-shaped crystal with dimensions 0.23×0.07×0.04 was mounted on a MITIGEN holder in perfluoroether oil. Data were collected using a Rigaku AFC12 FRE-HF diffractometer equipped with an Oxford Cryosystems low-temperature apparatus operating at $T = 100(2)$ K.

Data were measured using profile data from scans of 10.0° per frame for 1.0 s using MoK $_{\alpha}$ radiation (Rotating Anode, 45.0 kV, 55.0 mA). The total number of runs and images was based on the strategy calculation from the program **CrystalClear** (Rigaku). The actually achieved resolution was $\theta = 28.697$.

Cell parameters were retrieved using the CrysAlisPro (Agilent) software and refined using CrysAlisPro (Agilent) on 8106 reflections, 61 of the observed reflections.

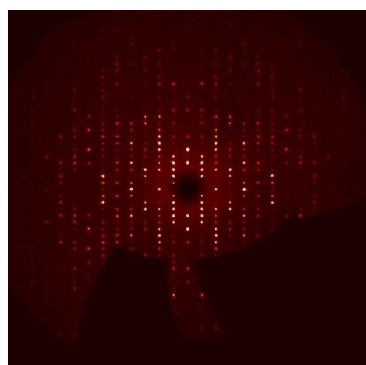
Data reduction was performed using the CrysAlisPro (Agilent) software that corrects for Lorentz polarisation. The final completeness is 99.80 out to 28.697 in θ . The absorption coefficient (μ) of this material is 0.086 and the minimum and maximum transmissions are 0.80173 and 1.00000.

The structure was solved in the space group P2₁2₁2₁ (# 19) by Direct Methods using the **ShelXT** (Sheldrick, 2015) structure solution program and refined by Least Squares using **ShelXL** (Sheldrick, 2008). All non-hydrogen atoms were refined anisotropically. Hydrogen atom positions were calculated geometrically and refined using the riding model.

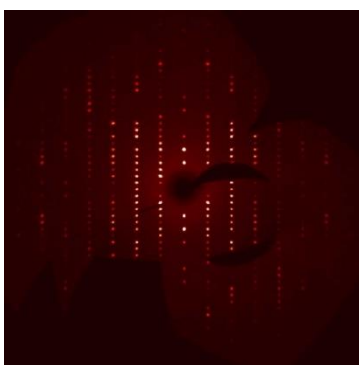
There is a single molecule in the asymmetric unit, which is represented by the reported sum formula. In other words: Z is 4 and Z' is 1.

The Flack parameter was refined to 0.2(6). Determination of absolute structure using Bayesian statistics on Bijvoet differences using the Olex2 results in 0.8(4). Note: The Flack parameter is used to determine chirality of the crystal studied, the value should be near 0, a value of 1 means that the stereochemistry is wrong and the model should be inverted. A value of 0.5 means that the crystal consists of a racemic mixture of the two enantiomers.

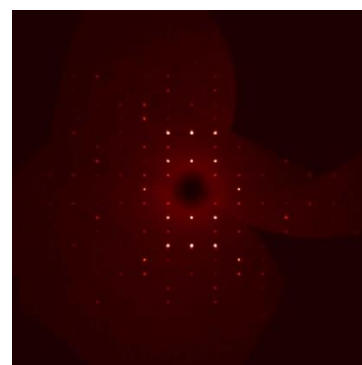
Generated precession images



0kl



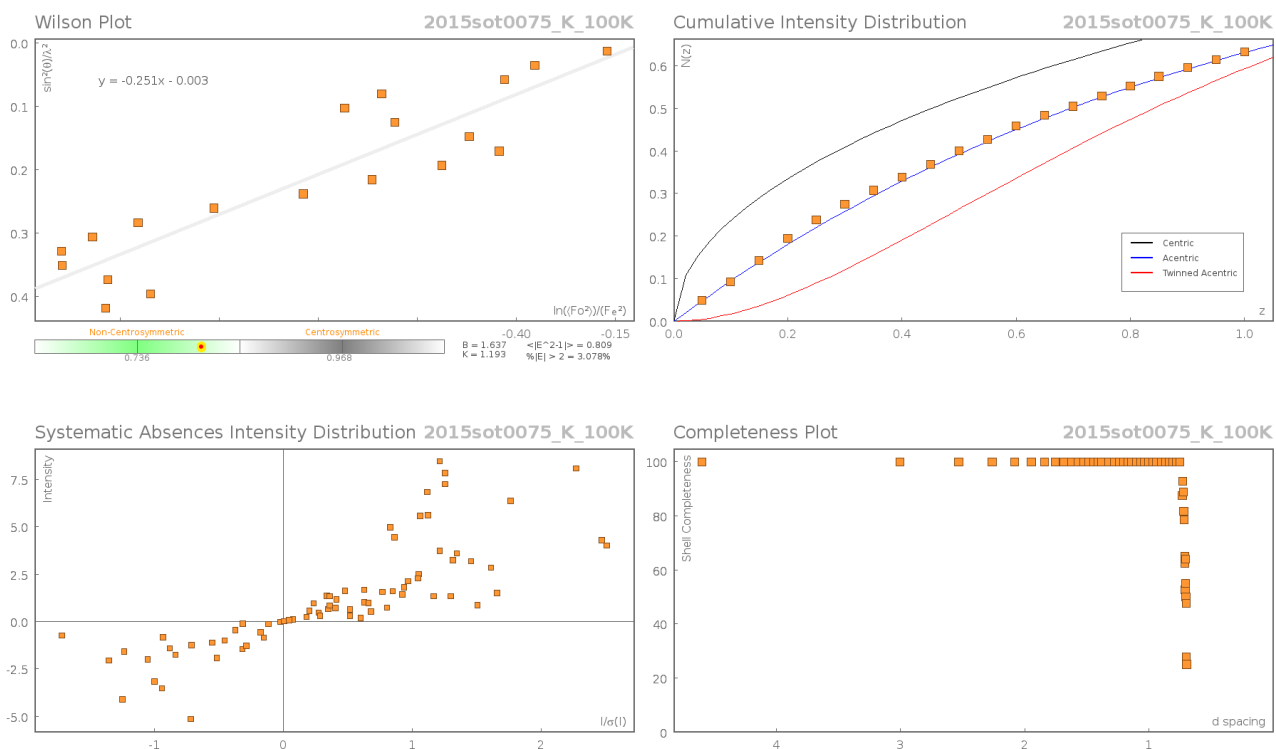
h0l



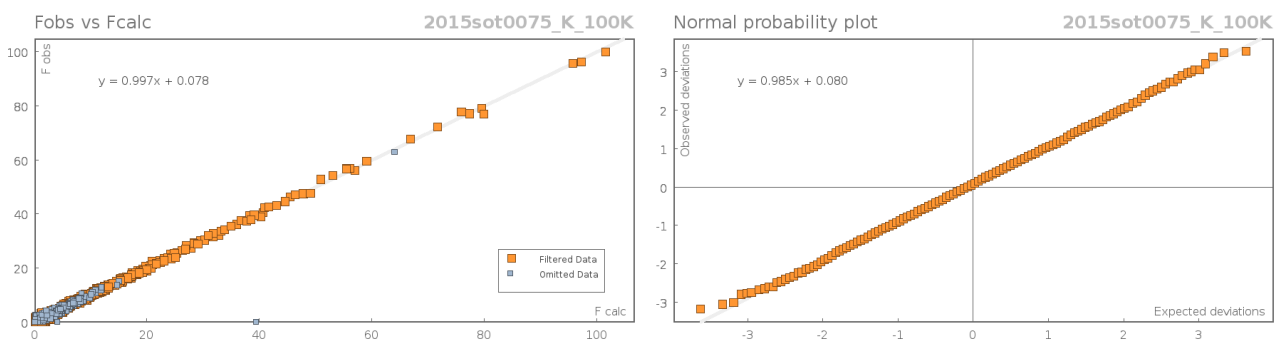
hk0

Appendices

Data Plots: Diffraction Data



Data Plots: Refinement and Data



Reflection Statistics

Total reflections (after filtering)	13413	Unique reflections	3496
Completeness	0.999	Mean I/σ	25.5
$hkl_{sub} > \max </sub>$ collected	(8, 13, 31)	$hkl_{sub} > \min </sub>$ collected	(-8, -14, -27)
hkl_{max} used	(8, 13, 29)	hkl_{min} used	(-8, 0, 0)
Lim d_{max} collected	7.0	Lim d_{min} collected	0.74

d_{\max} used	6.09	d_{\min} used	0.74
Friedel pairs	2486	Friedel pairs merged	0
Inconsistent equivalents	1	R_{int}	0.0305
R_{sigma}	0.0299	Intensity transformed	0
Omitted reflections	0	Omitted by user (OMIT hkl)	0
Multiplicity	(5041, 3799, 437, 24)	Maximum multiplicity	13
Removed systematic absences	71	Filtered off (Shel/OMIT)	633

Table 18: Fractional Atomic Coordinates ($\times 10^4$) and Equivalent Isotropic Displacement Parameters ($\text{\AA}^2 \times 10^3$) for **2015sot0075_K_100K**. U_{eq} is defined as 1/3 of the trace of the orthogonalised U_{ij} .

Atom	x	y	z	U_{eq}
O1	9480(2)	5742.5(13)	4771.9(6)	26.0(3)
O2	5798(2)	6708.8(14)	2442.2(6)	30.2(3)
N1	7169(2)	4881.4(14)	4061.1(7)	18.5(3)
N2	7998(3)	7603.1(14)	3170.1(7)	19.4(3)
C1	7887(3)	3537.6(17)	4193.9(9)	23.0(4)
C2	5997(3)	2754.3(18)	4464.8(9)	23.2(4)
C3	4038(3)	2759.4(18)	4031.2(9)	22.9(4)
C4	3373(3)	4168.6(19)	3880.0(9)	22.1(4)
C5	5317(3)	4953.3(17)	3627.2(8)	17.9(3)
C6	4690(3)	6378.1(17)	3479.8(8)	18.8(3)
C7	6205(3)	6918.9(17)	2985.7(8)	19.4(4)
C8	9423(3)	8211.5(17)	2706.0(9)	23.5(4)
C9	9290(3)	9701.7(18)	2752.9(9)	27.4(4)
C10	9863(4)	10149.6(19)	3400.5(10)	32.6(5)
C11	8410(4)	9465.1(18)	3874.6(10)	29.4(4)
C12	8520(3)	7972.8(17)	3807.4(8)	20.4(4)
C13	7071(3)	7251.1(17)	4273.1(8)	19.5(4)
C14	7994(3)	5889.0(17)	4393.8(8)	18.4(3)
C15	4706(3)	7208.6(18)	4056.2(8)	20.9(4)

Appendices

Table 19: Anisotropic Displacement Parameters ($\times 10^4$) **2015sot0075_K_100K**. The anisotropic displacement factor exponent takes the form: $-2\pi^2[h^2a^{*2} \times U_{11} + \dots + 2hka^* \times b^* \times U_{12}]$

Atom	U_{11}	U_{22}	U_{33}	U_{23}	U_{13}	U_{12}
O1	24.7(7)	29.2(7)	24.1(7)	-1.1(5)	-8.6(6)	2.6(6)
O2	36.8(8)	35.6(8)	18.2(7)	1.5(6)	-3.6(6)	-9.1(7)
N1	15.1(7)	16.9(7)	23.5(7)	1.3(6)	-1.3(6)	-0.2(6)
N2	20.1(7)	17.0(7)	21.0(7)	0.3(6)	1.1(6)	-0.2(6)
C1	19.6(8)	17.4(8)	32.1(10)	2.7(8)	-0.7(8)	1.5(7)
C2	26.6(9)	18.7(8)	24.2(9)	1.9(7)	-0.9(8)	-3.2(8)
C3	22.9(9)	23.9(8)	22.1(9)	-0.2(7)	0.7(7)	-6.9(7)
C4	18.3(8)	26.9(9)	21.0(9)	1.5(7)	-1.8(7)	-4.7(7)
C5	17.1(8)	19.5(8)	17.0(8)	-1.2(7)	-0.8(7)	-2.1(7)
C6	15.2(8)	20.9(8)	20.3(8)	-0.4(7)	-3.5(7)	1.5(7)
C7	21.4(9)	16.4(8)	20.5(8)	1.3(7)	-2.1(7)	2.0(7)
C8	23.4(9)	19.2(8)	28.1(10)	3.4(7)	4.8(8)	-1.0(8)
C9	28.1(10)	19.4(9)	34.9(11)	6.4(8)	-0.3(9)	-0.1(8)
C10	38.7(12)	16.2(9)	42.7(12)	-0.8(8)	-2.8(10)	-4.2(8)
C11	36.0(11)	18.9(9)	33.3(11)	-5.0(8)	-3.9(9)	-0.5(8)
C12	19.5(9)	18.1(8)	23.4(9)	-1.8(7)	-3.9(7)	1.6(7)
C13	19.4(8)	20.5(8)	18.5(8)	-4.8(7)	-2.2(7)	2.2(7)
C14	15.8(7)	21.9(8)	17.6(8)	0.1(7)	1.7(6)	0.5(7)
C15	18.1(8)	22.5(8)	22.0(9)	-1.5(7)	1.0(7)	3.6(7)

Table 20: Bond Lengths in Å for **2015sot0075_K_100K**.

Atom	Atom	Length/Å	Atom	Atom	Length/Å
O1	C14	1.233(2)	N2	C8	1.470(2)
O2	C7	1.229(2)	N2	C12	1.474(2)
N1	C1	1.467(2)	C1	C2	1.520(3)
N1	C5	1.474(2)	C2	C3	1.522(3)
N1	C14	1.354(2)	C3	C4	1.529(3)
N2	C7	1.356(2)	C4	C5	1.531(2)

Atom	Atom	Length/Å	Atom	Atom	Length/Å
C5	C6	1.536(2)	C10	C11	1.529(3)
C6	C7	1.521(2)	C11	C12	1.530(3)
C6	C15	1.515(2)	C12	C13	1.532(3)
C8	C9	1.525(2)	C13	C14	1.521(2)
C9	C10	1.524(3)	C13	C15	1.517(2)

Table 21: Bond Angles in ° for 2015sot0075_K_100K.

Atom	Atom	Atom	Angle/°	Atom	Atom	Atom	Angle/°
C1	N1	C5	113.64(14)	O2	C7	C6	119.77(16)
C14	N1	C1	119.52(15)	N2	C7	C6	117.70(15)
C14	N1	C5	126.14(14)	N2	C8	C9	110.06(16)
C7	N2	C8	119.24(15)	C10	C9	C8	110.41(16)
C7	N2	C12	125.75(15)	C9	C10	C11	110.89(17)
C8	N2	C12	114.40(15)	C10	C11	C12	111.36(17)
N1	C1	C2	109.99(15)	N2	C12	C11	109.58(15)
C1	C2	C3	110.52(15)	N2	C12	C13	112.15(14)
C2	C3	C4	110.16(15)	C11	C12	C13	112.90(16)
C3	C4	C5	111.34(14)	C14	C13	C12	109.91(14)
N1	C5	C4	109.55(14)	C15	C13	C12	110.73(15)
N1	C5	C6	111.79(14)	C15	C13	C14	112.24(15)
C4	C5	C6	112.18(14)	O1	C14	N1	122.55(16)
C7	C6	C5	109.90(14)	O1	C14	C13	119.82(16)
C15	C6	C5	110.73(14)	N1	C14	C13	117.60(15)
C15	C6	C7	112.36(14)	C6	C15	C13	106.27(14)
O2	C7	N2	122.52(17)				

Appendices

Table 22: Hydrogen Fractional Atomic Coordinates ($\times 10^4$) and Equivalent Isotropic Displacement Parameters ($\text{\AA}^2 \times 10^3$) for **2015sot0075_K_100K**. U_{eq} is defined as $1/3$ of the trace of the orthogonalised U_{ij} .

Atom	x	y	z	U_{eq}
H1A	9127	3557	4488	28
H1B	8400	3113	3811	28
H2A	5563	3140	4864	28
H2B	6476	1840	4538	28
H3A	2789	2297	4225	28
H3B	4423	2290	3648	28
H4A	2812	4601	4255	26
H4B	2175	4159	3573	26
H5	5793	4528	3236	21
H6	3161	6378	3313	23
H8A	8958	7929	2291	28
H8B	10959	7924	2770	28
H9A	10322	10104	2456	33
H9B	7787	9995	2648	33
H10A	9662	11111	3432	39
H10B	11423	9949	3487	39
H11A	6872	9759	3822	35
H11B	8893	9716	4292	35
H12	10073	7704	3887	24
H13	7116	7752	4667	23
H15A	3753	6813	4375	25
H15B	4167	8104	3966	25

Citations

CrystalClear, Rigaku, (2009).

O.V. Dolomanov and L.J. Bourhis and R.J. Gildea and J.A.K. Howard and H. Puschmann, Olex2: A complete structure solution, refinement and analysis program, *J. Appl. Cryst.*, (2009), **42**, 339-341.

Sheldrick, G.M., A short history of ShelX, *Acta Cryst.*, (2008), **A64**, 339-341.

B.1.5 (–)-10,17-dioxo- α -isosparteine ((–)-1.43)

Crystal Data and Experimental

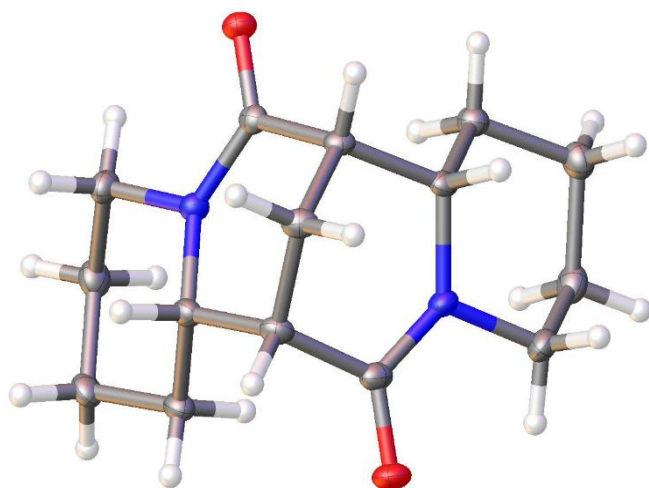
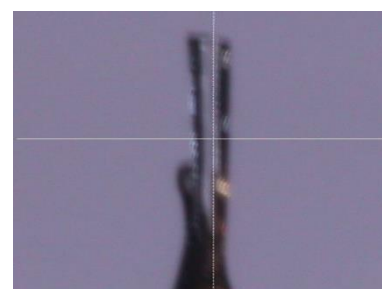


Figure 5: Thermal ellipsoids drawn at the 50% probability level.

Experimental. Single clear colourless rod-shaped crystals of (2017sot0020_R1_100K) were recrystallised from hexane by slow evaporation. A suitable crystal (0.54×0.08×0.05) mm³ was selected and mounted on a MITIGEN holder silicon oil on a Rigaku AFC12 FRE-VHF diffractometer. The crystal was kept at $T = 100(2)$ K during data collection. Using **Olex2** (Dolomanov et al., 2009), the structure was solved with the **ShelXT** (Sheldrick, 2015) structure solution program, using the Intrinsic Phasing solution method. The model was refined with version 2014/7 of **ShelXL** (Sheldrick, 2015) using Least Squares minimisation.

Crystal Data. C₁₅H₂₂N₂O₂, $M_r = 262.34$, orthorhombic, P2₁2₁2₁ (No. 19), $a = 6.2737(3)$ Å, $b = 11.5350(5)$ Å, $c = 18.4575(9)$ Å, $\alpha = \beta = \gamma = 90^\circ$, $V = 1335.72(11)$ Å³, $T = 100(2)$ K, $Z = 4$, $Z' = 1$, $\mu(\text{MoK}\alpha) = 0.087$, 12682 reflections measured, 3454 unique ($R_{\text{int}} = 0.0206$) which were used in all calculations. The final wR_2 was 0.0824 (all data) and R_1 was 0.0318 ($I > 2(I)$).



Compound	2017sot0020_R_100 K
Formula	C ₁₅ H ₂₂ N ₂ O ₂
$D_{\text{calc.}} / \text{g cm}^{-3}$	1.305
μ / mm^{-1}	0.087
Formula Weight	262.34
Colour	clear colourless
Shape	rod
Size/mm ³	0.54×0.08×0.05
T/K	100(2)
Crystal System	orthorhombic
Flack Parameter	0.0(3)
Hooft Parameter	-0.0(2)
Space Group	P2 ₁ 2 ₁ 2 ₁
$a/\text{Å}$	6.2737(3)
$b/\text{Å}$	11.5350(5)
$c/\text{Å}$	18.4575(9)
$\alpha/^\circ$	90
$\beta/^\circ$	90
$\gamma/^\circ$	90
$V/\text{Å}^3$	1335.72(11)
Z	4
Z'	1
Wavelength/Å	0.71073
Radiation type	MoK α
$\theta_{\text{min}}/^\circ$	3.430
$\theta_{\text{max}}/^\circ$	28.696
Measured Refl.	12682
Independent Refl.	3454
Reflections Used	3320
R_{int}	0.0206
Parameters	172
Restraints	0
Largest Peak	0.281
Deepest Hole	-0.180
GooF	1.064
wR_2 (all data)	0.0824
wR_2	0.0811
R_1 (all data)	0.0336
R_1	0.0318

Structure Quality Indicators

Reflections:	d min (Mo)	0.74	I/ σ	44.1	R _{int}	2.06%	complete at 2 θ =61°	100%
Refinement:	Shift	0.000	Max Peak	0.3	Min Peak	-0.2	Goof	1.064
								-0.0(3)

A clear colourless rod-shaped crystal with dimensions 0.54×0.08×0.05 was mounted on a MITIGEN holder silicon oil. Data were collected using a Rigaku AFC12 FRE-VHF diffractometer equipped with an Oxford Cryosystems low-temperature apparatus operating at $T = 100(2)$ K.

Data were measured using profile data from ω -scans of 1.0° per frame for 8.0 s using MoK α radiation (Rotating Anode, 45.0 kV, 55.0 mA). The total number of runs and images was based on the strategy calculation from the program **CrystalClear** (Rigaku). The actually achieved resolution was $\varnothing = 28.696$.

Cell parameters were retrieved using the **CrysAlisPro** (Rigaku, V1.171.39.9g, 2015) software and refined using **CrysAlisPro** (Rigaku, V1.171.39.9g, 2015) on 7528 reflections, 59 of the observed reflections.

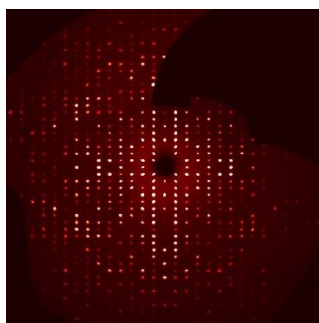
Data reduction was performed using the **CrysAlisPro** (Rigaku, V1.171.39.9g, 2015) software which corrects for Lorentz polarisation. The final completeness is 99.80 out to 28.696 in \varnothing . The absorption coefficient μ of this material is 0.087 at this wavelength ($\lambda = 0.71073$) and the minimum and maximum transmissions are 0.90833 and 1.00000.

The structure was solved in the space group P2₁2₁2₁ (# 19) by Intrinsic Phasing using the **ShelXT** (Sheldrick, 2015) structure solution program and refined by Least Squares using version 2014/7 of **ShelXL** (Sheldrick, 2015). All non-hydrogen atoms were refined anisotropically. Hydrogen atom positions were calculated geometrically and refined using the riding model.

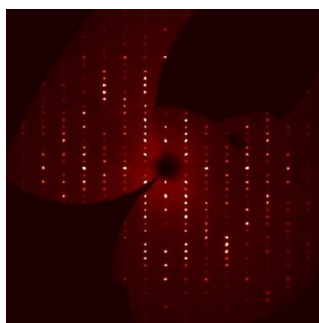
There is a single molecule in the asymmetric unit, which is represented by the reported sum formula. In other words: Z is 4 and Z' is 1.

The Flack parameter was refined to 0.0(3). Determination of absolute structure using Bayesian statistics on Bijvoet differences using the Olex2 results in -0.0(2). Note: The Flack parameter is used to determine chirality of the crystal studied, the value should be near 0, a value of 1 means that the stereochemistry is wrong and the model should be inverted. A value of 0.5 means that the crystal consists of a racemic mixture of the two enantiomers.

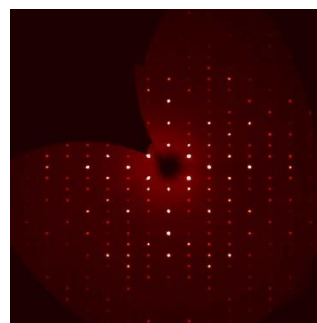
Generated Precession Images



0kl

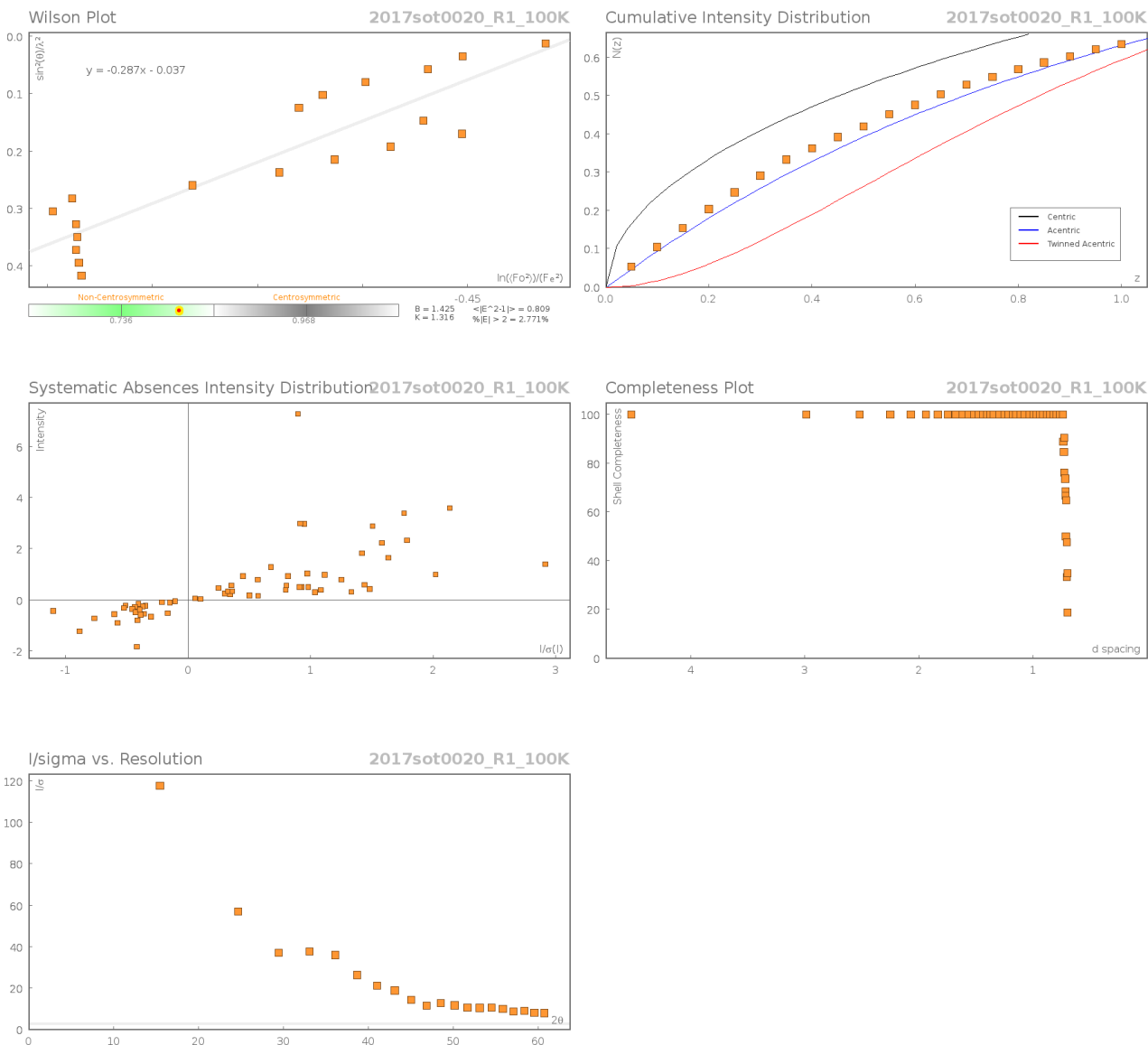


h0l

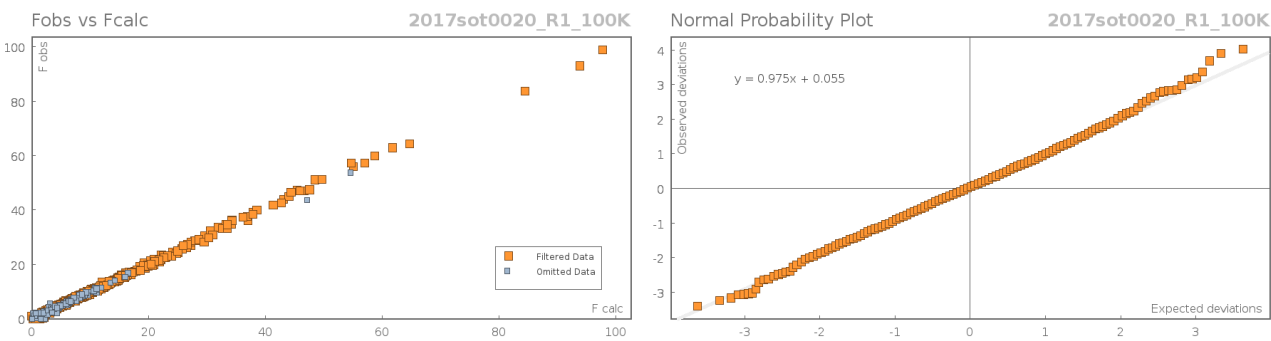


hk0

Data Plots: Diffraction Data



Data Plots: Refinement and Data



Appendices

Reflection Statistics

Total reflections (after filtering)	12747	Unique reflections	3454
Completeness	0.999	Mean I/σ	44.06
hkl_{\max} collected	(8, 15, 26)	hkl_{\min} collected	(-8, -16, -25)
hkl_{\max} used	(8, 15, 24)	hkl_{\min} used	(-8, 0, 0)
Lim d_{\max} collected	7.0	Lim d_{\min} collected	0.74
d_{\max} used	6.27	d_{\min} used	0.74
Friedel pairs	3098	Friedel pairs merged	0
Inconsistent equivalents	12	R_{int}	0.0206
R_{sigma}	0.0169	Intensity transformed	0
Omitted reflections	0	Omitted by user (OMIT hkl)	0
Multiplicity	(6621, 2570, 382, 83, 7)	Maximum multiplicity	13
Removed systematic absences	65	Filtered off (Shel/OMIT)	527

Table 23: Fractional Atomic Coordinates ($\times 10^4$) and Equivalent Isotropic Displacement Parameters ($\text{\AA}^2 \times 10^3$) for **2017sot0020_R1_100K**. U_{eq} is defined as 1/3 of the trace of the orthogonalised U_{ij} .

Atom	x	y	z	U_{eq}
O1	5257.4(16)	7595.3(9)	5697.8(6)	18.8(2)
O2	-575(2)	4407.2(10)	7232.0(6)	25.2(3)
N1	3371.1(19)	5916.8(10)	5610.7(6)	14.8(2)
N2	1938(2)	5801.7(10)	7387.7(6)	16.4(2)
C1	4707(2)	5517.6(13)	5008.8(8)	18.5(3)
C2	5197(3)	4227.1(13)	5079.2(8)	21.1(3)
C3	3147(3)	3525.4(13)	5140.2(8)	20.6(3)
C4	1766(2)	3991.7(12)	5755.8(8)	18.1(3)
C5	1320(2)	5291.3(12)	5668.6(8)	15.7(3)
C6	-149(2)	5765.0(12)	6265.0(8)	16.6(3)
C7	-74(2)	7087.6(12)	6270.0(8)	17.0(3)
C8	2202(2)	7415.4(12)	6469.5(7)	14.5(3)

Atom	x	y	z	U_{eq}
C9	3743(2)	6993.5(12)	5890.3(7)	14.2(3)
C10	367(2)	5272.0(12)	7006.5(8)	17.2(3)
C11	2393(3)	5379.3(14)	8122.4(8)	21.2(3)
C12	4768(3)	5415.4(14)	8283.9(8)	22.4(3)
C13	5643(3)	6634.3(13)	8169.3(8)	21.7(3)
C14	5135(2)	7029.5(12)	7397.8(8)	17.3(3)
C15	2747(2)	6985.5(12)	7237.5(7)	14.2(3)

Table 24: Anisotropic Displacement Parameters ($\times 10^4$) **2017sot0020_R1_100K**. The anisotropic displacement factor exponent takes the form: $-2\pi^2[h^2a^{*2} \times U_{11} + \dots + 2hka^* \times b^* \times U_{12}]$

Atom	U_{11}	U_{22}	U_{33}	U_{23}	U_{13}	U_{12}
O1	18.1(5)	18.1(5)	20.1(5)	1.2(4)	2.2(4)	-4.9(4)
O2	30.2(6)	19.2(5)	26.1(6)	2.5(4)	3.9(5)	-10.7(5)
N1	15.0(5)	14.1(5)	15.4(5)	0.1(5)	1.2(4)	-0.7(4)
N2	20.8(6)	13.3(5)	15.2(5)	2.2(4)	2.5(5)	-2.5(5)
C1	22.9(7)	17.4(6)	15.3(6)	-0.7(5)	3.6(6)	0.6(6)
C2	25.2(7)	18.9(7)	19.1(6)	-3.2(5)	1.1(6)	2.6(6)
C3	28.4(7)	14.7(6)	18.7(7)	-3.1(5)	-2.3(6)	-0.9(6)
C4	22.8(7)	13.4(6)	18.2(6)	-0.1(5)	-1.7(6)	-2.9(6)
C5	16.6(6)	14.8(6)	15.7(6)	0.4(5)	-2.8(5)	-2.7(5)
C6	13.2(6)	14.6(6)	21.8(6)	0.4(5)	-0.7(5)	-2.3(5)
C7	12.7(6)	14.5(6)	23.7(7)	2.3(5)	0.0(5)	0.9(5)
C8	15.1(6)	10.3(6)	18.0(6)	1.0(5)	1.0(5)	-0.2(5)
C9	14.6(6)	14.1(6)	13.9(6)	2.3(5)	-2.4(5)	0.6(5)
C10	18.7(6)	13.4(6)	19.5(6)	-0.5(5)	4.9(5)	-1.4(5)
C11	29.9(8)	19.2(7)	14.6(6)	2.6(6)	2.3(6)	-3.1(6)
C12	30.4(8)	20.3(7)	16.3(6)	1.8(5)	-1.3(6)	3.6(6)
C13	23.8(7)	22.2(7)	19.1(6)	-0.8(6)	-4.0(6)	-0.4(6)
C14	17.8(6)	15.8(6)	18.4(6)	0.5(5)	-0.9(5)	-1.8(5)
C15	16.6(6)	10.5(6)	15.6(6)	-1.2(5)	2.1(5)	-1.1(5)

Table 25: Bond Lengths in Å for **2017sot0020_R1_100K**.

Atom	Atom	Length/Å	Atom	Atom	Length/Å
O1	C9	1.2293(17)	C4	C5	1.5335(19)
O2	C10	1.2319(18)	C5	C6	1.536(2)
N1	C1	1.4661(18)	C6	C7	1.5263(18)
N1	C5	1.4794(18)	C6	C10	1.517(2)
N1	C9	1.3649(18)	C7	C8	1.5222(19)
N2	C10	1.356(2)	C8	C9	1.5214(19)
N2	C11	1.4690(18)	C8	C15	1.5401(19)
N2	C15	1.4829(17)	C11	C12	1.520(2)
C1	C2	1.525(2)	C12	C13	1.524(2)
C2	C3	1.524(2)	C13	C14	1.529(2)
C3	C4	1.527(2)	C14	C15	1.528(2)

Appendices

Table 26: Bond Angles in ° for **2017sot0020_R1_100K**.

Atom	Atom	Atom	Angle/°
C1	N1	C5	113.52(11)
C9	N1	C1	118.34(12)
C9	N1	C5	124.41(12)
C10	N2	C11	118.07(12)
C10	N2	C15	124.51(12)
C11	N2	C15	114.30(12)
N1	C1	C2	110.92(12)
C3	C2	C1	110.77(13)
C2	C3	C4	110.29(12)
C3	C4	C5	111.71(12)
N1	C5	C4	108.99(12)
N1	C5	C6	113.58(11)
C4	C5	C6	112.46(12)
C7	C6	C5	109.95(12)
C10	C6	C5	112.64(12)
C10	C6	C7	111.27(12)
C8	C7	C6	106.18(11)
C7	C8	C15	110.55(11)
C9	C8	C7	110.27(11)
C9	C8	C15	113.75(11)
O1	C9	N1	122.45(13)
O1	C9	C8	120.91(12)
N1	C9	C8	116.63(12)
O2	C10	N2	122.56(14)
O2	C10	C6	120.38(13)
N2	C10	C6	117.02(12)
N2	C11	C12	111.25(13)
C11	C12	C13	110.55(13)
C12	C13	C14	109.22(12)
C15	C14	C13	112.02(12)
N2	C15	C8	113.11(11)
N2	C15	C14	109.26(11)
C14	C15	C8	112.66(11)

Table 27: Hydrogen Fractional Atomic Coordinates ($\times 10^4$) and Equivalent Isotropic Displacement Parameters ($\text{\AA}^2 \times 10^3$) for **2017sot0020_R1_100K**. U_{eq} is defined as 1/3 of the trace of the orthogonalised U_{ij} .

Atom	x	y	z	U_{eq}
H1A	6031	5953	5004	22
H1B	3978	5659	4554	22
H2A	5997	3971	4659	25
H2B	6068	4097	5506	25
H3A	3489	2718	5231	25
H3B	2365	3570	4688	25
H4A	2484	3859	6214	22
H4B	425	3573	5765	22
H5	573	5392	5206	19
H6	-1610	5534	6145	20
H7A	-440	7393	5796	20
H7B	-1069	7396	6623	20
H8	2279	8264	6477	17
H11A	1882	4589	8170	25
H11B	1639	5855	8472	25
H12A	5509	4877	7968	27
H12B	5015	5178	8781	27
H13A	7173	6637	8245	26
H13B	5002	7163	8515	26
H14A	5643	7816	7331	21
H14B	5882	6536	7057	21
H15	2045	7511	7580	17

Citations

CrysAlisPro Software System, Rigaku Oxford Diffraction, (2015).

CrystalClear, Rigaku, (2009).

O.V. Dolomanov and L.J. Bourhis and R.J. Gildea and J.A.K. Howard and H. Puschmann, Olex2: A complete structure solution, refinement and analysis program, *J. Appl. Cryst.*, (2009), **42**, 339-341.

Sheldrick, G.M., Crystal structure refinement with ShelXL, *Acta Cryst.*, (2015), **C27**, 3-8.

Sheldrick, G.M., ShelXT-Integrated space-group and crystal-structure determination, *Acta Cryst.*, (2015), **A71**, 3-8.

B.1.6 *Syn* uncyclised imino-aldol product ((-)-2.17)

Crystal Data and Experimental

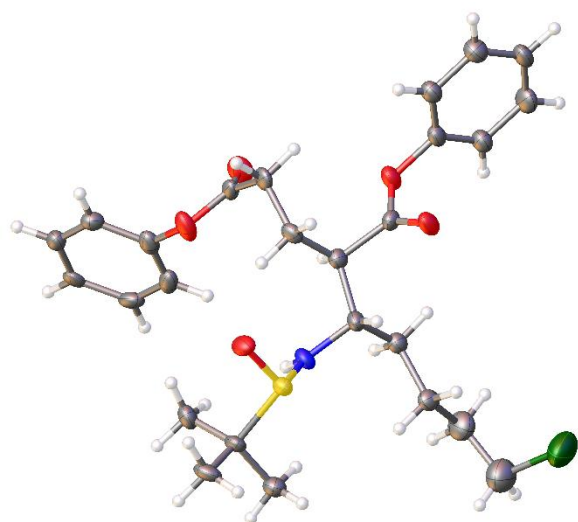


Figure 6: Thermal ellipsoids drawn at the 50% probability level. Disorder omitted for clarity.

Experimental. Single clear colourless needle-shaped crystals of (**2016sot0091_R1_100K**) were recrystallised from THF by slow evaporation. A suitable crystal (0.14×0.02×0.02) mm³ was selected and mounted on a glass fibre silicon oil on a Rigaku AFC12 FRE-VHF diffractometer. The crystal was kept at $T = 100(2)$ K during data collection. Using **Olex2** (Dolomanov et al., 2009), the structure was solved with the **ShelXT** (Sheldrick, 2015) structure solution program, using the Intrinsic Phasing solution method. The model was refined with version 2016/6 of **ShelXL** (Sheldrick, 2015) using Least Squares minimisation.

Crystal Data. C₂₆H₃₄ClNO₅S, $M_r = 508.05$, hexagonal, P6₅ (No. 170), $a = 29.3480(19)$ Å, $b = 29.3480(19)$ Å, $c = 5.4131(4)$ Å, $\alpha = 90^\circ$, $\beta = 90^\circ$, $\gamma = 120^\circ$, $V = 4037.7(6)$ Å³, $T = 100(2)$ K, $Z = 6$, $Z' = 1$, $\mu(\text{Mo K}\alpha) = 0.254$, 27278 reflections measured, 6945 unique ($R_{int} = 0.1557$) which were used in all calculations. The final wR_2 was 0.2642 (all data) and R_1 was 0.1018 ($I > 2(I)$).



Compound	2016sot0091_R_100 K
Formula	C ₂₆ H ₃₄ ClNO ₅ S
$D_{calc.} / \text{g cm}^{-3}$	1.254
μ / mm^{-1}	0.254
Formula Weight	508.05
Colour	clear colourless
Shape	needle
Size/mm ³	0.14×0.02×0.02
T/K	100(2)
Crystal System	hexagonal
Flack Parameter	0.02(9)
Hooft Parameter	0.06(8)
Space Group	P6 ₅
$a/\text{Å}$	29.3480(19)
$b/\text{Å}$	29.3480(19)
$c/\text{Å}$	5.4131(4)
$\alpha/^\circ$	90
$\beta/^\circ$	90
$\gamma/^\circ$	120
$V/\text{Å}^3$	4037.7(6)
Z	6
Z'	1
Wavelength/Å	0.71075
Radiation type	Mo K α
$\Theta_{min}/^\circ$	3.674
$\Theta_{max}/^\circ$	28.697
Measured Refl.	27278
Independent Refl.	6945
Reflections Used	3222
R_{int}	0.1557
Parameters	325
Restraints	367
Largest Peak	0.694
Deepest Hole	-0.910
GooF	1.005
wR_2 (all data)	0.2642
wR_2	0.2070
R_1 (all data)	0.2199
R_1	0.1018

Structure Quality Indicators

Reflections:	d min (Mo)	0.74	I/σ	5.5	Rint	15.57%	complete at $2\theta=62^\circ$	100%	
Refinement:	Shift	-0.001	Max Peak	0.7	Min Peak	-0.9	Goof	1.005	0.02(9)

A clear colourless needle-shaped crystal with dimensions 0.14×0.02×0.02 was mounted on a glass fibre silicon oil. Data were collected using a Rigaku AFC12 FRE-VHF diffractometer equipped with an Oxford Cryosystems low-temperature apparatus operating at $T = 100(2)$ K.

Data were measured using profile data from ω -scans of 1.0° per frame for 25.0 s using Mo K_α radiation (Rotating Anode, 45.0 kV, 55.0 mA). The total number of runs and images was based on the strategy calculation from the program **CrysAlisPro** (Rigaku, V1.171.39.9g, 2015). The actually achieved resolution was $\theta = 28.697$.

Cell parameters were retrieved using the **CrysAlisPro** (Rigaku, V1.171.39.9g, 2015) software and refined using **CrysAlisPro** (Rigaku, V1.171.39.9g, 2015) on 4937 reflections, 18 of the observed reflections.

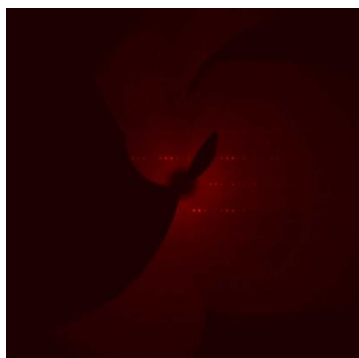
Data reduction was performed using the **CrysAlisPro** (Rigaku, V1.171.39.9g, 2015) software, which corrects for Lorentz polarisation. The final completeness is 93.29 out to 28.697 in θ . The absorption coefficient μ of this material is 0.254 at this wavelength ($\lambda = 0.71075$) and the minimum and maximum transmissions are 0.31574 and 1.00000.

The structure was solved in the space group $P6_5$ (# 170) by Intrinsic Phasing using the **ShelXT** (Sheldrick, 2015) structure solution program and refined by Least Squares using version 2016/6 of **ShelXL** (Sheldrick, 2015). All non-hydrogen atoms were refined anisotropically. Hydrogen atom positions were calculated geometrically and refined using the riding model.

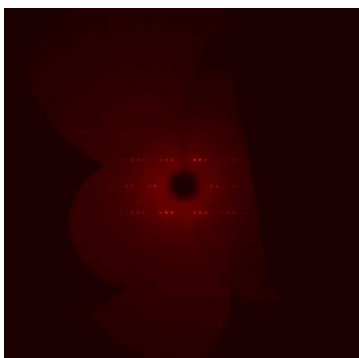
There is a single molecule in the asymmetric unit, which is represented by the reported sum formula. In other words: Z is 6 and Z' is 1.

The Flack parameter was refined to 0.02(9). Determination of absolute structure using Bayesian statistics on Bijvoet differences using the Olex2 results in 0.06(8). Note: The Flack parameter is used to determine chirality of the crystal studied, the value should be near 0, a value of 1 means that the stereochemistry is wrong and the model should be inverted. A value of 0.5 means that the crystal consists of a racemic mixture of the two enantiomers.

Generated precession images



0kl



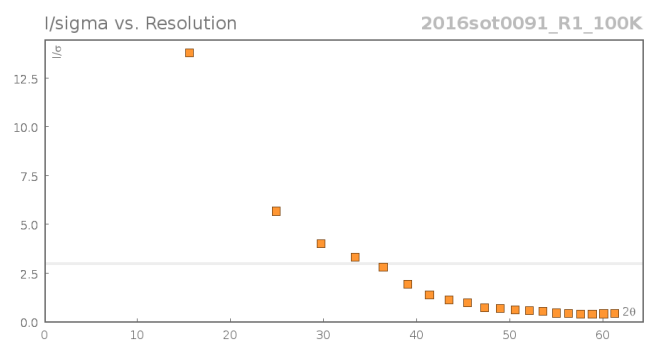
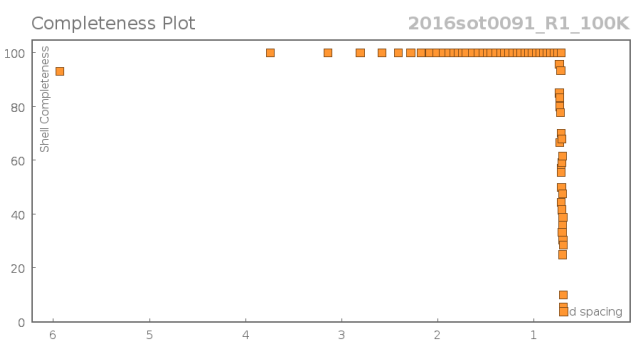
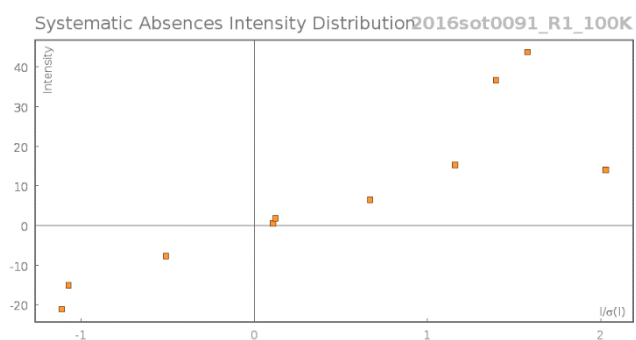
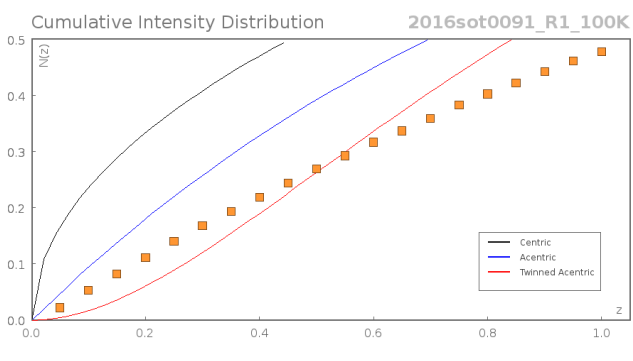
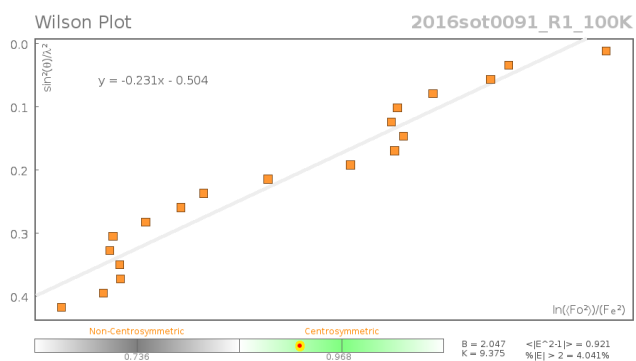
h0l



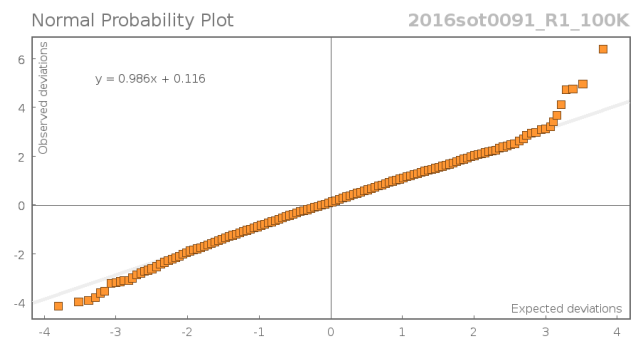
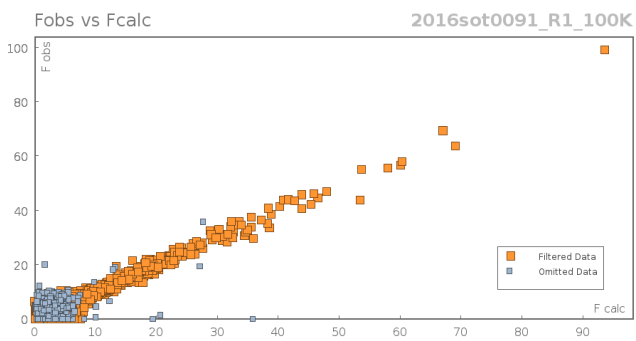
hk0

Appendices

Data Plots: Diffraction Data



Data Plots: Refinement and Data



Reflection Statistics

Total reflections (after filtering)	27321	Unique reflections	6945
Completeness	0.999	Mean I/σ	5.5
hkl_{\max} collected	(36, 39, 7)	hkl_{\min} collected	(-40, -40, -7)
hkl_{\max} used	(0, 39, 7)	hkl_{\min} used	(-33, 0, -7)
Lim d_{\max} collected	7.0	Lim d_{\min} collected	0.74
d_{\max} used	6.35	d_{\min} used	0.74
Friedel pairs	5200	Friedel pairs merged	0
Inconsistent equivalents	1	R_{int}	0.1557
R_{sigma}	0.2089	Intensity transformed	0
Omitted reflections	0	Omitted by user (OMIT hkl)	33
Multiplicity	(17211, 4965, 503, 2)	Maximum multiplicity	12
Removed systematic absences	10	Filtered off (Shel/OMIT)	1337

Table 28: Fractional Atomic Coordinates ($\times 10^4$) and Equivalent Isotropic Displacement Parameters ($\text{\AA}^2 \times 10^3$) for **2016sot0091_R1_100K**. U_{eq} is defined as 1/3 of the trace of the orthogonalised U_{ij} .

Atom	x	y	z	U_{eq}
Cl1A	1442.7(18)	1863(2)	7184(14)	101.4(18)
S1	3454.6(9)	1663.8(8)	1605(4)	30.6(5)
O1	5243(3)	2936(2)	4650(12)	43.3(16)
O2	5344(3)	3609(2)	6965(13)	45.6(17)
O3	4261(2)	3845(2)	5750(11)	34.3(14)
O4	3608(2)	3455(2)	2956(12)	38.5(16)
O5	3900(2)	1891(2)	-198(11)	35.7(15)
N1	3587(3)	2018(3)	4141(14)	31.7(17)
C1	5944(3)	2809(3)	6123(17)	32.1(19)
C2	6124(3)	2599(3)	7849(17)	32(2)
C3	5837(3)	2347(3)	9909(17)	31.1(19)
C4	5342(4)	2298(3)	10242(18)	37(2)
C5	5152(3)	2501(3)	8524(19)	37(2)
C6	5450(3)	2754(3)	6491(17)	35(2)
C7	5208(3)	3368(3)	5119(18)	32.7(19)
C8	4972(3)	3482(3)	2885(17)	34(2)
C9	4413(3)	3054(3)	2377(16)	29.1(19)
C10	4030(3)	2980(3)	4418(16)	29.0(18)
C11	3929(3)	3434(3)	4268(16)	29.2(19)
C12	4228(3)	4313(3)	5568(16)	30.3(19)
C13	4470(3)	4640(3)	3638(17)	33(2)
C14	4443(4)	5100(4)	3509(19)	40(2)
C15	4168(3)	5202(3)	5258(17)	37(2)
C16	3937(4)	4864(4)	7201(19)	43(2)
C17	3969(3)	4410(3)	7356(18)	35(2)
C18	3503(3)	2467(3)	4260(16)	32(2)
C19	3445(3)	1085(3)	2969(17)	31.5(19)

Appendices

Atom	x	y	z	U_{eq}
C20	3355(4)	718(3)	816(17)	38(2)
C21	3977(3)	1246(4)	4172(18)	38(2)
C22	2980(3)	834(3)	4708(18)	37(2)
C23A	3184(4)	2421(7)	6620(20)	30(3)
C24A	2603(4)	1982(5)	6390(20)	32(3)
C25A	2320(5)	1888(6)	8870(30)	51(4)
C26A	1735(6)	1535(8)	8770(40)	73(4)
Cl1B	1245(4)	1477(5)	10030(30)	101.4(18)
C26B	1572(12)	1439(17)	7410(70)	73(4)
C25B	2166(12)	1791(15)	7610(60)	51(4)
C24B	2501(11)	1927(13)	5260(50)	32(3)
C23B	3055(9)	2353(17)	6050(60)	30(3)

Table 29: Anisotropic Displacement Parameters ($\times 10^4$) **2016sot0091_R1_100K**. The anisotropic displacement factor exponent takes the form: $-2\pi^2[h^2a^{*2} \times U_{11} + \dots + 2hka^* \times b^* \times U_{12}]$

Atom	U_{11}	U_{22}	U_{33}	U_{23}	U_{13}	U_{12}
Cl1A	49(3)	89(3)	173(5)	43(4)	19(3)	40(3)
S1	26.7(12)	19.3(11)	46.5(12)	2(1)	4.6(10)	12(1)
O1	49(4)	38(4)	58(4)	-17(3)	-14(4)	33(3)
O2	45(4)	36(4)	59(4)	-14(3)	-10(3)	22(3)
O3	34(3)	26(3)	50(4)	-4(3)	-7(3)	20(3)
O4	31(3)	26(3)	64(4)	-4(3)	-13(3)	18(3)
O5	33(3)	26(3)	45(4)	6(3)	17(3)	13(3)
N1	35(4)	22(4)	44(4)	5(3)	5(3)	19(3)
C1	27(4)	21(4)	44(5)	3(4)	1(4)	9(4)
C2	25(4)	22(4)	52(5)	-2(4)	2(4)	13(4)
C3	29(4)	10(4)	51(5)	-6(4)	-6(4)	7(4)
C4	32(5)	16(4)	54(5)	1(4)	8(4)	5(4)
C5	24(4)	27(5)	61(5)	-17(4)	-6(4)	14(4)
C6	31(5)	26(5)	52(5)	-14(4)	-10(4)	17(4)
C7	21(4)	21(4)	58(5)	-11(4)	1(4)	12(4)
C8	33(4)	25(4)	51(5)	-8(4)	6(4)	20(4)
C9	35(5)	19(4)	35(4)	-4(4)	1(4)	15(4)
C10	24(4)	24(4)	41(5)	3(4)	0(4)	14(3)
C11	19(4)	26(4)	45(5)	5(4)	2(4)	13(4)
C12	25(5)	23(4)	47(5)	-2(4)	-5(4)	15(4)
C13	31(5)	25(4)	46(5)	-3(4)	-2(4)	15(4)
C14	38(5)	32(5)	52(5)	5(4)	2(5)	19(4)
C15	34(5)	23(5)	60(6)	-8(4)	-4(4)	18(4)
C16	40(6)	33(5)	62(6)	-11(4)	6(5)	22(5)
C17	33(5)	26(5)	51(5)	-3(4)	1(4)	17(4)
C18	27(4)	24(4)	52(5)	8(4)	8(4)	17(4)
C19	29(4)	14(4)	50(5)	1(4)	6(4)	10(4)
C20	47(6)	16(4)	48(5)	5(4)	6(4)	13(4)
C21	37(5)	30(5)	57(6)	-1(4)	0(4)	23(4)
C22	32(5)	24(5)	56(5)	5(4)	5(4)	13(4)
C23A	27(5)	24(5)	41(6)	1(5)	0(5)	14(5)
C24A	27(5)	27(5)	42(6)	6(6)	-1(5)	14(4)
C25A	51(6)	51(7)	55(7)	3(6)	14(5)	29(5)
C26A	56(6)	70(8)	100(9)	14(7)	3(6)	35(6)

Atom	U_{11}	U_{22}	U_{33}	U_{23}	U_{13}	U_{12}
Cl1B	49(3)	89(3)	173(5)	43(4)	19(3)	40(3)
C26B	56(6)	70(8)	100(9)	14(7)	3(6)	35(6)
C25B	51(6)	51(7)	55(7)	3(6)	14(5)	29(5)
C24B	27(5)	27(5)	42(6)	6(6)	-1(5)	14(4)
C23B	27(5)	24(5)	41(6)	1(5)	0(5)	14(5)

Table 30: Bond Lengths in Å for 2016sot0091_R1_100K.

Atom	Atom	Length/Å	Atom	Atom	Length/Å
Cl1A	C26A	1.797(18)	C10	C11	1.505(11)
S1	O5	1.495(6)	C10	C18	1.529(11)
S1	N1	1.647(8)	C12	C13	1.355(12)
S1	C19	1.838(8)	C12	C17	1.344(12)
O1	C6	1.403(10)	C13	C14	1.393(12)
O1	C7	1.347(10)	C14	C15	1.371(12)
O2	C7	1.174(10)	C15	C16	1.370(13)
O3	C11	1.368(10)	C16	C17	1.386(12)
O3	C12	1.429(9)	C18	C23A	1.547(13)
O4	C11	1.206(9)	C18	C23B	1.531(16)
N1	C18	1.458(10)	C19	C20	1.518(12)
C1	C2	1.364(12)	C19	C21	1.532(12)
C1	C6	1.390(12)	C19	C22	1.513(12)
C2	C3	1.370(12)	C23A	C24A	1.545(14)
C3	C4	1.400(12)	C24A	C25A	1.532(15)
C4	C5	1.365(13)	C25A	C26A	1.498(16)
C5	C6	1.370(13)	Cl1B	C26B	1.75(2)
C7	C8	1.511(13)	C26B	C25B	1.52(2)
C8	C9	1.511(12)	C25B	C24B	1.53(2)
C9	C10	1.514(12)	C24B	C23B	1.53(2)

Table 31: Bond Angles in ° for 2016sot0091_R1_100K.

Atom	Atom	Atom	Angle/°	Atom	Atom	Atom	Angle/°
O5	S1	N1	112.6(3)	C9	C8	C7	112.8(7)
O5	S1	C19	106.3(4)	C8	C9	C10	113.9(7)
N1	S1	C19	97.9(4)	C9	C10	C18	114.4(7)
C7	O1	C6	118.4(7)	C11	C10	C9	107.2(7)
C11	O3	C12	116.5(6)	C11	C10	C18	108.7(7)
C18	N1	S1	120.9(6)	O3	C11	C10	112.3(7)
C2	C1	C6	117.8(8)	O4	C11	O3	122.0(8)
C1	C2	C3	121.9(8)	O4	C11	C10	125.6(8)
C2	C3	C4	119.2(9)	C13	C12	O3	118.0(7)
C5	C4	C3	119.8(9)	C17	C12	O3	118.0(8)
C4	C5	C6	119.6(8)	C17	C12	C13	123.9(8)
C1	C6	O1	118.5(8)	C12	C13	C14	117.4(9)
C5	C6	O1	119.7(8)	C15	C14	C13	120.2(9)
C5	C6	C1	121.7(8)	C16	C15	C14	120.2(8)
O1	C7	C8	108.5(7)	C15	C16	C17	119.9(9)
O2	C7	O1	124.5(9)	C12	C17	C16	118.4(9)
O2	C7	C8	127.0(8)	N1	C18	C10	110.4(7)

Appendices

Atom	Atom	Atom	Angle/°	Atom	Atom	Atom	Angle/°
N1	C18	C23A	109.0(9)	C22	C19	C21	114.7(8)
N1	C18	C23B	110(2)	C24A	C23A	C18	112.0(10)
C10	C18	C23A	108.0(8)	C25A	C24A	C23A	110.8(11)
C10	C18	C23B	120.9(15)	C26A	C25A	C24A	115.1(14)
C20	C19	S1	105.3(6)	C25A	C26A	Cl1A	109.6(13)
C20	C19	C21	109.5(7)	C25B	C26B	Cl1B	112(2)
C21	C19	S1	110.1(6)	C26B	C25B	C24B	119(3)
C22	C19	S1	107.1(6)	C25B	C24B	C23B	105(2)
C22	C19	C20	109.7(7)	C18	C23B	C24B	116(2)

Table 32: Hydrogen Fractional Atomic Coordinates ($\times 10^4$) and Equivalent Isotropic Displacement Parameters ($\text{\AA}^2 \times 10^3$) for **2016sot0091_R1_100K**. U_{eq} is defined as 1/3 of the trace of the orthogonalised U_{ij} .

Atom	x	y	z	U_{eq}
H1	3710.71	1934.95	5442.11	38
H1A	6149.24	2987.36	4715.07	39
H2	6458.73	2627.85	7615.94	39
H3	5972.59	2207.09	11095.9	37
H4	5137.88	2123.48	11660.12	45
H5	4815.27	2468.32	8737.81	44
H8A	4977.67	3818.75	3147.5	41
H8B	5191.98	3524.23	1421.06	41
H9A	4409.54	2717.5	2125.19	35
H9B	4292.8	3137.47	824.31	35
H10	4196.88	2993.75	6046.52	35
H13	4651.42	4558.83	2419.78	40
H14	4615.24	5343.53	2205.52	48
H15	4136.96	5508.63	5121.89	44
H16	3756.52	4941.29	8438.72	52
H17	3811.75	4171.61	8693.41	42
H18	3305.72	2471.6	2764.39	39
H18A	3361.05	2477.61	2595.77	39
H20A	3003.52	594.76	125.9	58
H20B	3382.17	416.32	1392.34	58
H20C	3620.64	906.9	-460.56	58
H21A	4261.45	1481.32	3059.13	57
H21B	4002.96	931.33	4495.7	57
H21C	4006.66	1428.48	5732.31	57
H22A	3019.44	1086.86	5989.01	56
H22B	2962.75	523.56	5481.54	56
H22C	2654.84	726.93	3779.43	56
H23A	3346.13	2345.94	8049.3	36
H23B	3199.95	2760.94	6921.33	36
H24A	2424.65	2083.36	5135.73	38
H24B	2586.46	1652.49	5834.49	38
H25A	2466.75	1734.42	10033.79	61
H25B	2396.4	2232.62	9553.04	61
H26A	1591.84	1443.15	10468.03	88
H26B	1649.18	1205.51	7894.31	88

Atom	x	y	z	U_{eq}
H26C	1487.3	1069.87	7169.57	88
H26D	1445.07	1543.27	5937.71	88
H25C	2295.89	1621.44	8776.46	61
H25D	2235.74	2126.17	8374.89	61
H24C	2361.81	2061.2	3964.2	38
H24D	2506.05	1613.23	4624.71	38
H23C	3050.45	2684.28	6321.94	36
H23D	3136.05	2248.54	7659.8	36

Table 33: Atomic Occupancies for all atoms that are not fully occupied in **2016sot0091_R1_100K**.

Atom	Occupancy	Atom	Occupancy	Atom	Occupancy	Atom	Occupancy
Cl1A	0.7	H24A	0.7	H26B	0.7	H25D	0.3
H18	0.7	H24B	0.7	Cl1B	0.3	C24B	0.3
H18A	0.3	C25A	0.7	C26B	0.3	H24C	0.3
C23A	0.7	H25A	0.7	H26C	0.3	H24D	0.3
H23A	0.7	H25B	0.7	H26D	0.3	C23B	0.3
H23B	0.7	C26A	0.7	C25B	0.3	H23C	0.3
C24A	0.7	H26A	0.7	H25C	0.3	H23D	0.3

Citations

CrysAlisPro Software System, Rigaku Oxford Diffraction, (2015).

O.V. Dolomanov and L.J. Bourhis and R.J. Gildea and J.A.K. Howard and H. Puschmann, Olex2: A complete structure solution, refinement and analysis program, *J. Appl. Cryst.*, (2009), **42**, 339-341.

Sheldrick, G.M., Crystal structure refinement with ShelXL, *Acta Cryst.*, (2015), **C27**, 3-8.

Sheldrick, G.M., ShelXT-Integrated space-group and crystal-structure determination, *Acta Cryst.*, (2015), **A71**, 3-8.

B.1.7 Syn cyclised imino-aldol product ((-)-2.13)

Crystal Data and Experimental

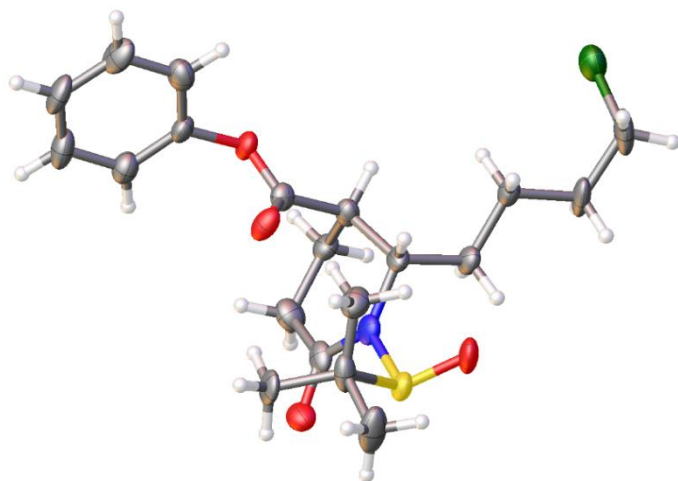
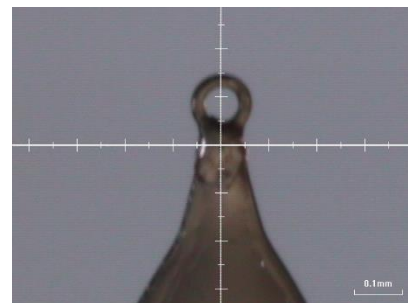


Figure 7: Thermal ellipsoids drawn at the 50% probability level.

Experimental. Single clear colourless plate-shaped crystals of (2015sot0035-R-100K) were recrystallised from chloroform by slow evaporation. A suitable crystal (0.13×0.09×0.02) was selected and mounted on a MITIGEN holder in perfluoroether oil on a Rigaku AFC12 FRE-VHF diffractometer. The crystal was kept at $T = 100(2)$ K during data collection. Using **Olex2** (Dolomanov et al., 2009), the structure was solved with the **ShelXT** (Sheldrick, 2015) structure solution program, using the Direct Methods solution method. The model was refined with version of **ShelXL** (Sheldrick, 2008) using Least Squares minimisation.

Crystal Data. $C_{20}H_{28}ClNO_4S$, $M_r = 413.94$, orthorhombic, $P2_12_12_1$ (No. 19), $a = 6.4385(7)$ Å, $b = 17.461(2)$ Å, $c = 19.3045(16)$ Å, $\alpha = \beta = \gamma = 90^\circ$, $V = 2170.3(4)$ Å³, $T = 100(2)$ K, $Z = 4$, $Z' = 1$, $\mu(\text{MoK}\alpha) = 0.296$, 11375 reflections measured, 5336 unique ($R_{int} = 0.1294$) which were used in all calculations. The final wR_2 was 0.3642 (all data) and R_1 was 0.1323 ($I > 2(I)$).



Compound	2015sot0035-R-100 K
Formula	$C_{20}H_{28}ClNO_4S$
$D_{calc.}/g\text{ cm}^{-3}$	1.267
μ/mm^{-1}	0.296
Formula Weight	413.94
Colour	clear colourless
Shape	plate
Max Size/mm	0.13
Mid Size/mm	0.09
Min Size/mm	0.02
T/K	100(2)
Crystal System	orthorhombic
Flack Parameter	0.2(2)
Hooft Parameter	0.14(11)
Space Group	$P2_12_12_1$
$a/\text{Å}$	6.4385(7)
$b/\text{Å}$	17.461(2)
$c/\text{Å}$	19.3045(16)
$\alpha/^\circ$	90
$\beta/^\circ$	90
$\gamma/^\circ$	90
$V/\text{Å}^3$	2170.3(4)
Z	4
Z'	1
$\theta_{min}/^\circ$	3.146
$\theta_{max}/^\circ$	28.699
Measured Refl.	11375
Independent Refl.	5336
Reflections Used	2937
R_{int}	0.1294
Parameters	247
Restraints	0
Largest Peak	1.366
Deepest Hole	-0.620
GooF	1.066
wR_2 (all data)	0.3642
wR_2	0.3192
R_1 (all data)	0.1958
R_1	0.1323

Structure Quality Indicators

Reflections:	d min	0.74	I/ σ	4.7	R _{int}	12.94%	complete at 2 θ =61°	95%
Refinement:	Shift	0.000	Max Peak	1.4	Min Peak	-0.6	Goof	1.066

A clear colourless plate-shaped crystal with dimensions 0.13×0.09×0.02 was mounted on a MITIGEN holder in perfluoroether oil. Data were collected using a Rigaku AFC12 FRE-VHF diffractometer equipped with an Oxford Cryosystems low-temperature apparatus operating at $T = 100(2)$ K.

Data were measured using profile data from ω -scans of 1.0° per frame for 20.0 s using MoK α radiation (Rotating Anode, 45.0 kV, 55.0 mA). The total number of runs and images was based on the strategy calculation from the program **CrystalClear** (Rigaku). The actually achieved resolution was $\Theta = 28.699$.

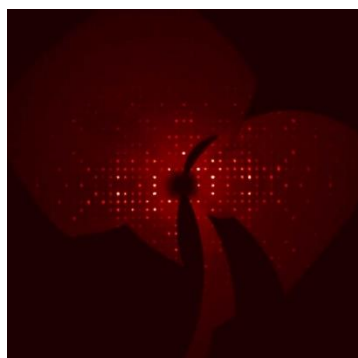
Cell parameters were retrieved using the **CrysAlisPro** (Agilent, V1.171.37.35, 2014) software and refined using **CrysAlisPro** (Agilent, V1.171.37.35, 2014) on 3143 reflections, 28 of the observed reflections.

Data reduction was performed using the **CrysAlisPro** (Agilent, V1.171.37.35, 2014) software which corrects for Lorentz polarisation. The final completeness is 99.50 out to 28.699 in Θ . The absorption coefficient (μ) of this material is 0.296 and the minimum and maximum transmissions are 0.43954 and 1.00000.

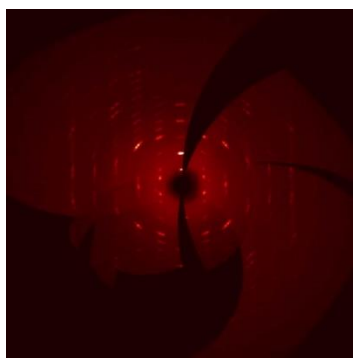
The structure was solved in the space group P2₁2₁2₁ (# 19) by Direct Methods using the **ShelXT** (Sheldrick, 2015) structure solution program and refined by Least Squares using version of **ShelXL** (Sheldrick, 2008). All non-hydrogen atoms were refined anisotropically. Hydrogen atom positions were calculated geometrically and refined using the riding model. The crystals were poorly formed plates that gave ill-defined reflections when viewed in the h0l plane.

The Flack parameter was refined to 0.2(2). Determination of absolute structure using Bayesian statistics on Bijvoet differences using the Olex2 results in 0.14(11). Note: The Flack parameter is used to determine chirality of the crystal studied, the value should be near 0, a value of 1 means that the stereochemistry is

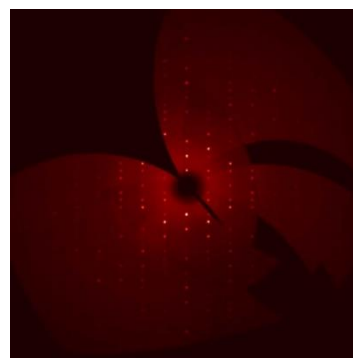
Generated precession images



hk0



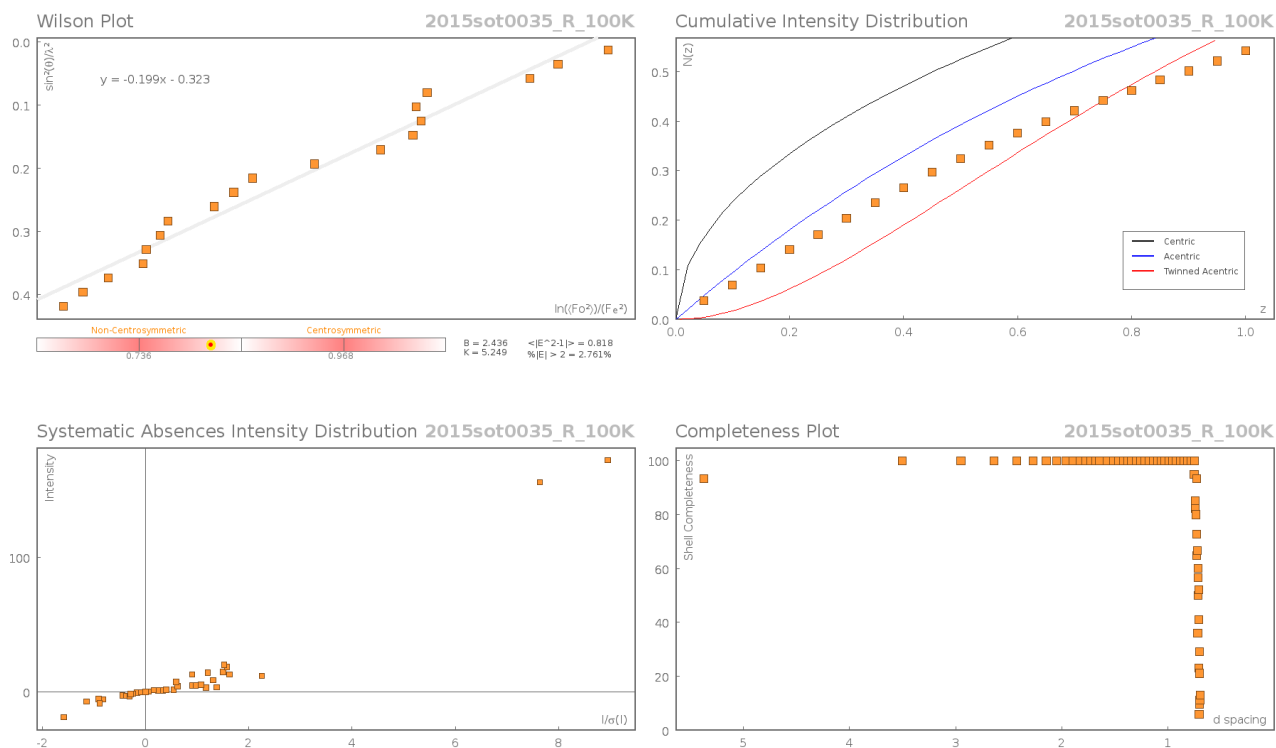
h0l



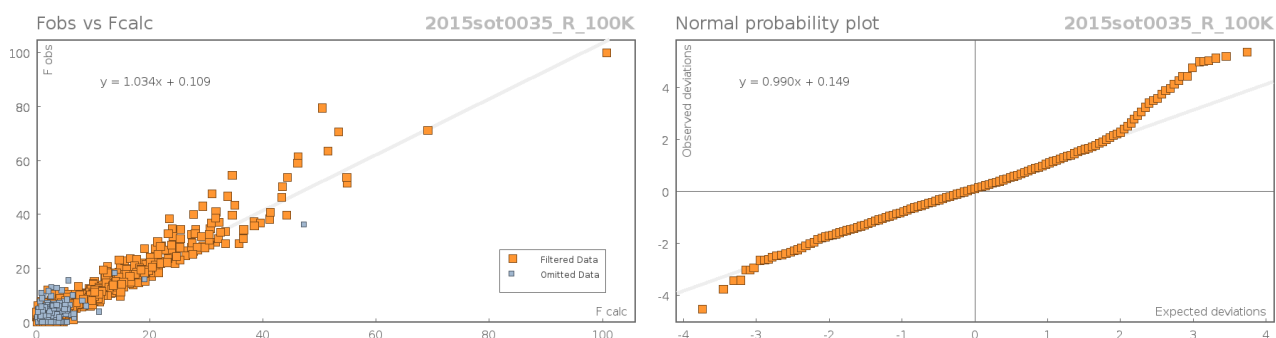
hk0

wrong and the model should be inverted. A value of 0.5 means that the crystal consists of a racemic mixture of the two enantiomers.

Data Plots: Diffraction Data



Data Plots: Refinement and Data



Reflection Statistics

Total reflections (after filtering)	11453	Unique reflections	5336
Completeness	0.954	Mean I/σ	4.69
hkls _{max} collected	(8, 24, 27)	hkls _{min} collected	(-9, -24, -25)
hkl _{max} used	(8, 23, 25)	hkl _{min} used	(-8, 0, 0)
Lim d _{max} collected	7.0	Lim d _{min} collected	0.74
d _{max} used	6.47	d _{min} used	0.74
Friedel pairs	3140	Friedel pairs merged	0
Inconsistent equivalents	91	R _{int}	0.1294
R _{sigma}	0.1639	Intensity transformed	0
Omitted reflections	0	Omitted by user (OMIT hkl)	28
Multiplicity	(10809, 544, 4)	Maximum multiplicity	8
Removed systematic absences	50	Filtered off (Shel/OMIT)	456

Table 34: Fractional Atomic Coordinates ($\times 10^4$) and Equivalent Isotropic Displacement Parameters ($\text{\AA}^2 \times 10^3$) for **2015sot0035_R_100K**. U_{eq} is defined as 1/3 of the trace of the orthogonalised U_{ij} .

Atom	x	y	z	U_{eq}
Cl1	-771(5)	3355(2)	508.7(15)	52.2(9)
S1	8243(4)	5732.2(16)	2436.6(12)	33.8(7)
O1	3445(12)	3364(4)	3897(3)	31.4(16)
O2	4822(12)	4548(4)	3894(4)	36.4(18)
O3	10622(11)	4596(5)	3011(4)	38.5(18)
O4	6709(14)	6038(5)	1933(3)	45(2)
N1	7411(14)	4800(5)	2613(4)	31.7(19)
C1	1311(19)	3655(6)	4876(6)	39(3)
C2	980(20)	3692(7)	5592(5)	47(3)
C3	2630(20)	3500(7)	6039(5)	46(3)
C4	4510(20)	3266(7)	5775(6)	46(3)
C5	4825(18)	3238(6)	5057(6)	37(3)

Atom	x	y	z	U_{eq}
C6	3192(17)	3428(6)	4631(5)	30(2)
C7	4355(16)	3986(6)	3596(5)	27(2)
C8	4677(17)	3818(6)	2818(5)	29(2)
C9	6367(16)	3207(6)	2738(5)	31(2)
C10	8409(18)	3505(7)	3026(6)	39(3)
C11	8893(17)	4332(6)	2879(5)	32(2)
C12	5270(14)	4552(6)	2418(5)	30(2)
C13	5084(17)	4417(6)	1626(5)	33(2)
C14	2834(16)	4350(6)	1374(5)	33(2)
C15	2690(20)	4281(7)	582(5)	48(3)
C16	480(20)	4249(8)	304(6)	57(4)
C17	7640(20)	6272(6)	3257(5)	39(3)
C18	5341(18)	6341(7)	3366(6)	41(3)
C19	8779(19)	5889(7)	3870(5)	39(3)
C20	8630(30)	7055(7)	3084(6)	61(4)

Table 35: Anisotropic Displacement Parameters ($\times 10^4$) **2015sot0035_R_100K**. The anisotropic displacement factor exponent takes the form: $-2\pi^2[h^2a^{*2} \times U_{11} + \dots + 2hka^* \times b^* \times U_{12}]$

Atom	U_{11}	U_{22}	U_{33}	U_{23}	U_{13}	U_{12}
Cl1	58(2)	63(2)	35.5(14)	3.7(14)	-12.8(14)	-8.6(16)
S1	39.8(14)	43.7(15)	18(1)	4.9(11)	-0.6(11)	-6.1(11)
O1	39(4)	38(4)	17(3)	1(3)	2(3)	-7(3)
O2	54(5)	30(4)	25(3)	-4(3)	11(3)	-6(3)
O3	31(4)	53(5)	32(4)	-4(3)	4(3)	3(4)
O4	62(6)	54(5)	20(3)	11(3)	-9(4)	-12(4)
N1	41(5)	39(5)	15(3)	-6(3)	0(4)	-3(4)
C1	46(7)	40(6)	31(5)	-3(5)	-9(5)	-6(5)
C2	66(8)	51(7)	25(5)	-12(5)	12(6)	-14(6)
C3	78(9)	40(7)	19(4)	3(5)	9(6)	-8(6)
C4	74(9)	41(7)	23(5)	5(5)	-1(6)	-2(6)
C5	46(7)	38(6)	28(5)	2(5)	2(5)	-2(5)

Appendices

Atom	U_{11}	U_{22}	U_{33}	U_{23}	U_{13}	U_{12}
C6	35(5)	34(5)	22(4)	7(4)	3(4)	-5(5)
C7	32(5)	23(5)	26(4)	1(4)	-1(4)	3(4)
C8	36(6)	28(5)	24(4)	0(4)	-5(4)	-6(4)
C9	33(5)	37(6)	23(4)	0(4)	7(4)	0(4)
C10	37(6)	41(7)	40(6)	-4(5)	-7(5)	9(5)
C11	39(6)	41(6)	16(4)	-7(4)	1(4)	11(5)
C12	25(5)	47(6)	18(4)	1(4)	3(4)	3(4)
C13	39(6)	42(6)	17(4)	-2(4)	1(4)	-7(5)
C14	37(6)	41(6)	21(4)	4(4)	1(4)	-6(5)
C15	80(9)	45(7)	17(4)	9(5)	-13(5)	-22(6)
C16	94(11)	51(7)	26(5)	6(6)	-27(6)	-7(8)
C17	64(8)	28(6)	24(4)	3(4)	-13(5)	1(5)
C18	38(7)	47(7)	37(6)	5(5)	7(5)	9(5)
C19	57(8)	50(7)	11(4)	-3(4)	-3(4)	-6(5)
C20	108(13)	39(7)	36(6)	9(5)	-13(8)	-20(8)

Table 36: Bond Lengths in Å for 2015sot0035_R_100K.

Atom	Atom	Length/Å	Atom	Atom	Length/Å
C11	C16	1.800(14)	C2	C3	1.408(18)
S1	O4	1.485(8)	C3	C4	1.374(18)
S1	N1	1.746(9)	C4	C5	1.401(15)
S1	C17	1.883(11)	C5	C6	1.375(15)
O1	C6	1.432(10)	C7	C8	1.545(13)
O1	C7	1.364(12)	C8	C9	1.531(14)
O2	C7	1.176(11)	C8	C12	1.544(14)
O3	C11	1.232(13)	C9	C10	1.519(15)
N1	C11	1.358(13)	C10	C11	1.504(16)
N1	C12	1.493(13)	C12	C13	1.552(12)
C1	C2	1.399(14)	C13	C14	1.533(14)
C1	C6	1.360(16)	C14	C15	1.538(12)

Atom	Atom	Length/Å
C15	C16	1.521(18)
C17	C18	1.500(17)

Atom	Atom	Length/Å
C17	C19	1.546(14)
C17	C20	1.544(16)

Table 37: Bond Angles in ° for 2015sot0035_R_100K.

Atom	Atom	Atom	Angle/°
O4	S1	N1	105.0(5)
O4	S1	C17	103.5(5)
N1	S1	C17	103.9(4)
C7	O1	C6	114.1(7)
C11	N1	S1	114.8(8)
C11	N1	C12	124.7(9)
C12	N1	S1	120.3(7)
C6	C1	C2	119.3(11)
C1	C2	C3	118.8(12)
C4	C3	C2	120.4(10)
C3	C4	C5	120.3(12)
C6	C5	C4	118.1(11)
C1	C6	O1	117.9(9)
C1	C6	C5	123.0(10)
C5	C6	O1	119.1(9)
O1	C7	C8	108.7(8)
O2	C7	O1	124.5(9)
O2	C7	C8	126.8(9)
C9	C8	C7	109.0(8)
C9	C8	C12	110.6(8)
C12	C8	C7	111.2(8)
C10	C9	C8	109.8(8)
C11	C10	C9	116.1(9)
O3	C11	N1	119.2(10)

Atom	Atom	Atom	Angle/°
O3	C11	C10	120.5(9)
N1	C11	C10	120.2(9)
N1	C12	C8	110.1(8)
N1	C12	C13	111.3(8)
C8	C12	C13	110.3(8)
C14	C13	C12	113.4(8)
C13	C14	C15	112.3(9)
C16	C15	C14	114.3(11)
C15	C16	C11	111.8(9)
C18	C17	S1	111.2(8)
C18	C17	C19	113.3(10)
C18	C17	C20	111.5(11)
C19	C17	S1	109.2(8)
C20	C17	S1	100.2(8)
C20	C17	C19	110.7(10)

Appendices

Table 38: Hydrogen Fractional Atomic Coordinates ($\times 10^4$) and Equivalent Isotropic Displacement Parameters ($\text{\AA}^2 \times 10^3$) for **2015sot0035_R_100K**. U_{eq} is defined as $1/3$ of the trace of the orthogonalised U_{ij} .

Crystals are poorly formed plates with many defects. Diffraction is a little messy and tails off at ca. 1angs. Collected as orthorhombic

Atom	x	y	z	U_{eq}
H20A	10118	6988	3001	92
H20B	8420	7407	3473	92
H20C	7972	7267	2668	92

Atom	x	y	z	U_{eq}
H1	228	3788	4564	47
H2	-324	3843	5773	57
H3	2444	3532	6526	55
H4	5600	3123	6080	55
H5	6131	3092	4870	45
H8	3350	3613	2623	35
H9A	5954	2737	2990	37
H9B	6536	3076	2243	37
H10A	8403	3431	3534	47
H10B	9548	3188	2835	47
H12	4278	4967	2552	36
H13A	5764	4847	1380	39
H13B	5838	3942	1504	39
H14A	2046	4807	1527	39
H14B	2184	3894	1589	39
H15A	3407	4724	370	57
H15B	3430	3812	435	57
H16A	506	4317	-206	68
H16B	-335	4676	504	68
H18A	4670	6477	2927	61
H18B	5062	6741	3710	61
H18C	4789	5851	3531	61
H19A	8211	5375	3946	59
H19B	8584	6197	4289	59
H19C	10264	5851	3765	59

Citations

CrysAlisPro Software System, Agilent Technologies UK Ltd, Yarnton, Oxford, UK (2014).

CrystalClear, Rigaku, (2009).

O.V. Dolomanov and L.J. Bourhis and R.J. Gildea and J.A.K. Howard and H. Puschmann, Olex2: A complete structure solution, refinement and analysis program, *J. Appl. Cryst.*, (2009), **42**, 339-341.

Sheldrick, G.M., A short history of ShelX, *Acta Cryst.*, (2008), **A64**, 339-341.

Sheldrick, G.M., ShelXT, *Acta Cryst.*, (2014), **A71**, 3-8.

List of References

1. Ohmiya, S.; Saito, K.; Murakoshi, I., Chapter 1 Lupine Alkaloids. In *The Alkaloids: Chemistry and Pharmacology*, Academic Press: **1995**; Vol. 47, pp 1-114.
2. Leonard, N. J., Chapter 19 Lupin Alkaloids. In *Alkaloids: Chemistry and Physiology*, Academic Press: **1953**; Vol. 3, pp 119-199.
3. Stenhouse, J. J. *Annalen*, **1851**, 78, 1–30.
4. Moureu, C.; Valeur, A. *Bull. Soc. Chim.* **1903**, 29, 1135.
5. Moureu, C.; Valeur, A. *Ann. Chem. Phys.* **1912**, 27, 245.
6. Clemo, G. R.; Leitch, G. C. *J. Chem. Soc.* **1928**, 1811.
7. Clemo, G. R.; Raper, R.; Tenniswood, C. R. S. *J. Chem. Soc.* **1931**, 429.
8. Clemo, G. R.; Raper, R. *J. Chem. Soc.* **1933**, 644.
9. Ing, H.R. *J. Chem. Soc.* **1932**, 2778.
10. Ing, H.R. *J. Chem. Soc.* **1933**, 504.
11. Clemo, G.R.; Leitch, G.C. *J. Chem. Soc.* **1928**, 1811.
12. Clemo, G.R.; Morgan, W. McG.; Raper, R. *J. Chem. Soc.* **1936**, 1025.
13. Okuda, S.; Kataoka, H.; Kyosuke, T. *Chem. Pharm. Bull.* **1965**, 13, 491.
14. Marion, L.; Turcotte, F.; Ouellet, J. *Can. J. Chem.* **1951**, 29, 22.
15. Winterfeld, K.; Rauch, C. *Arch. Pharm.* **1934**, 272, 273.
16. Carmack, M.; Douglas, B.; Martin, E. W.; Suss, H. *J. Am. Chem. Soc.* **1955**, 77, 4435.
17. Seeger, R.; Neumann, H.G. *Inst. Pharmakol. Toxikol.* **1992**, 132, 1577.
18. Yovo, K.; Huguet, F.; Pothier, J.; Durand, M.; Breteau, M.; Narcisse, G. *Planta Med.* **1984**, 50, 420.
19. Bobkiewicz-Kozłowska, T.; Dworacka, M.; Kuczyński, S.; Abramczyk, M.; Kolanoś, R.; Wysocka, W.; Garcia Lopez, P. M.; Winiarska, H. *Eur. J. Pharmacol.* **2007**, 565, 240.
20. Paolisso, G.; Sgambato, S.; Passariello, N.; Pizza, G.; Torella, R.; Tesauro, P.; Varricchio, M.; D'Onofrio, F. *Eur. J. Clin. Pharmacol.* **1988**, 34, 227.
21. Sgambato, S.; Paolisso, G.; Passariello, N.; Varricchio, M.; D'Onofrio, F. *Eur. J. Clin. Pharmacol.* **1987**, 32, 477.
22. Paolisso, G.; Sgambato, S.; Passariello, N.; Pizza, G.; Varricchio, M.; Torella, R.; D'Onofrio, F. *Horm. Metab. Res.* **1987**, 19, 389.
23. Schmeller, T.; Wink, M. In *Alkaloids: Biochemistry, Ecology, and Medicinal Applications*; Robers, M.F.; Wink, M., Eds.; Plenum Press: New York, **1998**, p 435.
24. Chuzel, O.; Riant, O. *Top. Organomet. Chem.* **2005**, 15, 59.
25. Hoppe, D.; Hintze, F.; Tebben, P. *Angew. Chem.* **1990**, 102, 1457.

26. Hoppe, D.; Hense, T. *Angew. Chem. Int. Ed. Engl.* **1997**, *36*, 2282.
27. Beak, P.; Basu, A.; Gallagher, D. J.; Park, Y. S.; Thayumanavan, S. *Acc. Chem. Res.* **1996**, *29*, 552.
28. Caddick, S.; Jenkins, K. *Chem. Soc. Rev.* **1996**, *25*, 447.
29. Seebach, D. *Angew. Chem. Int. Ed. Engl.* **1997**, *29*, 1320
30. Nozaki, H.; Aratani, T.; Noyori, R. *Tetrahedron Lett.* **1968**, *9*, 2087.
31. Nozaki, H.; Aratani, T.; Toraya, T. *Tetrahedron Lett.* **1968**, *9*, 4097.
32. Aratani, T.; Gonda, T.; Nozaki, H. *Tetrahedron Lett.* **1969**, *10*, 2265.
33. Aratani, T.; Gonda, T.; Nozaki, H. *Tetrahedron* **1970**, *26*, 5453.
34. Nozaki, H.; Aratani, T.; Toraya, T.; Noyori, R. *Tetrahedron* **1971**, *27*, 905.
35. Haasnoot, C. A. G. *J. Am. Chem. Soc.* **1993**, *115*, 1460
36. De Crisci, A. G.; Annibale, V. T.; Hamer, G. K.; Lough, A. J.; Fekl, U. *Dalton Trans.*, **2010**, *39*, 2888.
37. Galasso, V.; Asaro, F.; Berti, F.; Kovac, B.; Habus, I.; Sacchetti, A. *Chem. Phys.* **2003**, *294*, 155.
38. Jasiewicz, B.; Boczon', W.; Warzajtis, B.; Rychlewska, U.; Rafałowicz, T. *J. Mol. Struct.* **2005**, *753*, 45.
39. Beak, P.; Du, H. *J. Am. Chem. Soc.* **1993**, *115*, 2516.
40. Gallagher, D. J.; Du, H.; Long, S. A.; Beak, P. *J. Am. Chem. Soc.* **1996**, *118*, 11391.
41. Lutz, G. P.; Du, H.; Gallagher, D. J.; Beak, P. *J. Org. Chem.* **1996**, *61*, 4542.
42. Beak, P.; Kerrick, S. T.; Wu, S.; Chu, J. *J. Am. Chem. Soc.* **1994**, *116*, 3231.
43. O'Brien, P. *Chem. Commun.* **2008**, 655.
44. O'Brien, P.; Wiberg, K. B.; Bailey, W. F.; Hermet, J.-P. R.; McGrath, M. J. *J. Am. Chem. Soc.* **2004**, *126*, 15480.
45. Würthwein, E.-U.; Hoppe, D. *J. Org. Chem.* **2008**, *73*, 9055.
46. Carbone, G.; O'Brien, P.; Hilmersson, G. *J. Am. Chem. Soc.* **2010**, *132*, 15445.
47. Fassler, J.; McCubbin, J. A.; Roglans, A.; Kimachi, T.; Hollett, J. W.; Kunz, R. W.; Tinkl, M.; Zhang, Y.; Wang, R.; Campbell, M.; Snieckus, V. *J. Org. Chem.* **2015**, *80*, 3368.
48. Trend, R. M.; Stoltz, B. M. *J. Am. Chem. Soc.* **2008**, *130*, 15957.
49. Chopade (s), M. U.; Chopade A. U.; Nikalje, M. D. *Adv. Org. Chem. Lett.* **2016**, *3*, 4.
50. Osa, T.; Kashigawa, Y.; Yanagisawa, Y.; Bobbit, J. M. *J. Chem. Soc. Chem. Commun.* **1994**, 2535.
51. Clemo, G.R.; Raper, R.; Short, W.S. *J. Chem. Soc.* **1949**, 663.
52. Sorm, F.; Keil, B. *Coll. Czech. Chem. Commun.* **1948**, *13*, 544.
53. Sorm, F.; Keil, B. *Coll. Czech. Chem. Commun.* **1947**, *12*, 655.
54. Greenhalgh, R.; Marion, L. *Can. J. Chem.* **1956**, *34*, 456.
55. Blakemore, P. R.; Norcross, N. R.; Warriner, S. L.; Astles, P. C. *Heterocycles.* **2006**, *70*, 609.

List of References

56. Leonard, N. J.; Beyler, R. E. *J. Am. Chem. Soc.* **1948**, *70*, 2298.
57. Leonard, N. J.; Beyler, R. E. *J. Am. Chem. Soc.* **1950**, *72*, 1316.
58. Leonard, N. J.; Beyler, R. E. *J. Am. Chem. Soc.* **1949**, *71*, 757.
59. Leonard, N.J.; Hruda, L.R.; Long, F.W. *J. Am. Chem. Soc.* **1947**, *69*, 690.
60. Anet, E.; Hughes, G.K.; Ritchie, E. *Nature* **1950**, *165*, 35.
61. Anet, E. F. L. J.; Hughes, G. K.; Ritchie, E. *Aust. J. Sci. Res. A* **1950**, *3*, 635.
62. Schöpf, C.; Benz, G.; Braun, F.; Hinkel, H.; Rokohl, R. *Angew. Chem.* **1953**, *65*, 161.
63. Schöpf, C. *Angew. Chem.* **1957**, *69*, 69.
64. Moore, B.; Marion, L. *Can. J. Chem.* **1953**, *31*, 187.
65. Marion, L.; Leonard, N. J.; Moore, B. P. *Can. J. Chem.* **1953**, *31*, 181.
66. Tsuda, K.; Satoh, Y. *Pharma. Bull. (Tokyo)* **1954**, *2*, 190.
67. Galinovskiy, F.; Kainz, G. *Monatsh. Chem.* **1947**, *77*, 137.
68. Van Tamelen, E. E.; Foltz, R. L. *J. Am. Chem. Soc.* **1960**, *82*, 2400.
69. Van Tamelen, E. E.; Foltz, R. L. *J. Am. Chem. Soc.* **1969**, *91*, 7372.
70. Bohlmann, F.; Müller, H.-J.; Schumann, D. *Chem. Ber.* **1973**, *106*, 3026.
71. Oinuma, H.; Dan, S.; Kakisawa, H. *J. Chem. Soc., Chem. Commun.* **1983**, *12*, 654.
72. Oinuma, H.; Dan, S.; Kakisawa, H. *J. Chem. Soc., Perkin Trans. 1* **1990**, 2593.
73. Takatsu, N.; Noguchi, M.; Ohmiya, S.; Otomasu, H. *Chem. Pharm. Bull.* **1987**, *35*, 4990.
74. Takatsu, N.; Ohmiya, S.; Otomasu, H. *Chem. Pharm. Bull.* **1987**, *35*, 891.
75. Tufariello, J. J.; Mullen, G. B.; Tegeler, J. J.; Trybulski, E. J.; Wong, S. C.; Ali, S. A. *J. Am. Chem. Soc.* **1979**, *101*, 2435.
76. Wanner, M. J.; Koomen, G.-Jan. *J. Org. Chem.* **1996**, *61*, 5581.
77. Schöpf, C.; Braun, F.; Koop, H.; Werner, G.; Bressler, H.; Neisius, K.; Schmadel, E. *Liebigs Ann. Chem.* **1962**, *658*, 156.
78. Schöpf, C.; Braun, F.; Komzak, A. *Chem. Ber.* **1956**, *89*, 1821.
79. Smith, B. T.; Wendt, J. A.; Aubé, J. *Org. Lett.* **2002**, *4*, 2577.
80. Hayashi, T. *Acta Chem. Scand.* **1996**, *50*, 259.
81. Weissfloch, A.; Azerad, R. *Bioorg. Med. Chem.* **1994**, *2*, 493.
82. Milligan, G. L.; Mossman, C. J.; Aube, J. *J. Am. Chem. Soc.* **1995**, *117*, 10449.
83. Bourguet, E.; Baneres, J.-L.; Girard, J.-P.; Parello, J.; Vidal, J.-P.; Lusinchi, X.; Declercq, J.-P. *Org. Lett.* **2001**, *3*, 3067.
84. Hermet, J.P. R.; McGrath, M. J.; O'Brien, P.; Porter, D. W.; Gilday, J. *Chem. Commun.* **2004**, *16*, 1830.
85. Hoffmann, R. W.; Sander, T.; Hense, A. *Liebigs Ann. Chem.* **1993**, 771.
86. Sworin, M.; Lin, K. C. *J. Am. Chem. Soc.* **1989**, *111*, 1815.

87. Buttler, T.; Fleming, I.; Gonsior, S.; Kim, B.-H.; Sung, A. Y.; Woo, H.-G. *Org. Biomol. Chem.* **2005**, *3*, 1557.
88. Buttler, T.; Fleming, I. *Chem. Commun.* **2004**, 2404.
89. Norcross, N. R.; Melbardis, J. P.; Solera, M. F.; Sephton, M. A.; Kilner, C.; Zakharov, L. N.; Astles, P. C.; Warriner, S. L.; Blakemore, P. R. *J. Org. Chem.* **2008**, *73*, 7939.
90. Blakemore, P. R.; Kilner, C.; Norcross, N. R.; Astles, P. C. *Org. Lett.* **2005**, *7*, 4721.
91. Firth, J. D.; Canipa, S. J.; Ferris, L. O'Brien. P. *Angew. Chem. Int. Ed.* **2018**, *57*, 223.
92. Firth, J. D.; O'Brien, P.; Ferris, L. *Org. Biomol. Chem.* **2014**, *12*, 9357.
93. Hermet, J.-P. R.; Porter, D. W.; Dearden, M. J.; Harrison, J. R.; Koplin, T.; O'Brien, P.; Parmene, J.; Tyurin, V.; Whitwood, A. C.; Gilday, J.; Smith, N. M. *Org. Biomol. Chem.* **2003**, *1*, 3977.
94. Pousset, C.; Callens, R.; Haddad, M.; Larchevêque, M. *Tetrahedron: Asymmetry*, **2004**, *15*, 3407.
95. Scharnagel, D.; Goller, J.; Deibl, N.; Milius, W.; Breuning, M., *Angew. Chem., Int. Ed.* **2018**, *57*, 2432.
96. Nagai, N. *Yakugaku Zasshi.* **1889**, *9*, 54.
97. Xiao, P.; Li, J.; Kubo, H.; Saito, K.; Murakoshi, I.; Ohmiya, S. *Chem. Pharm. Bull.* **1996**, *44*, 1951.
98. Ding, P.-L.; Liao, Z.-X.; Huang, H.; Zhou, P.; Chen, D.-F. *Bioorg. Med. Chem. Lett.* **2006**, *16*, 1231.
99. Liu, X.-J.; Cao, M.-A.; Li, W.-H.; Shen, C.-S.; Yan, S.-Q.; Yuan, C.-S. *Fitoterapia* **2010**, *81*, 524.
100. Xiao, P.; Kubo, H.; Ohsawa, M.; Higashiyama, K.; Nagase, H.; Yan, Y.-N.; Li, J.-S.; Kamei, J.; Ohmiya, S. *Planta Med.* **1999**, *65*, 230.
101. Higashiyama, K.; Takeuchi, Y.; Yamauchi, T.; Imai, S.; Kamei, J.; Yajima, Y.; Narita, M.; Suzuki, T. *Biol. Pharm. Bull.* **2005**, *28*, 845.
102. Huang, J.; Xu, H., Matrine: Bioactivities and structural modifications. *Curr. Top. Med. Chem.* **2016**, *16*, (28), 3365.
103. Bohlmann, F., Winterfeldt, E., Friese, U. *Chem. Ber.* **1963**, *96*, 2251.
104. Mandell, L.; Singh, K. P.; Gresham, J. T.; Freeman, W. J. *J. Am. Chem. Soc.* **1963**, *85*, 2682.
105. Mandell, L.; Singh, K. P.; Gresham, J. T.; Freeman, W. J. *J. Am. Chem. Soc.* **1965**, *87*, 5234.
106. Okuda, S.; Yoshimoto, M.; Tsuda, K. *Chem. Pharm. Bull.* **1966**, *14*, 275.
107. Chen, J.; Browne, L. J.; Gonnella, N. C. *J. Chem. Soc., Chem. Commun.* **1986**, 905.
108. Kobayashi, G.; Furukawa, S.; Matsuda, Y.; Natsuki, R.; Matsunaga, S. *Chem. Pharm. Bull.* **1970**, *18*, 124.
109. Watkin, S. V.; Camp, N. P.; Brown, R. C. D. *Org. Lett.* **2013**, *15*, 4596
110. Ochiai, E.; Okuda, S.; Minato, H. *Yakugaku Zasshi.* **1952**, *72*, 781.

List of References

111. Okuda, S.; Kamata, H.; Tsuda, K.; Murakoshi, I. *Chem. & Ind. (London)*, **1962**, 1326.
112. Kobayashi, G.; Furukawa, S.; Matsuda, Y.; Natsuki, R.; Matsunaga, S. *Chem. Pharm. Bull.* **1970**, *18*, 124
113. Kobayashi, G.; Furukawa, S.; Matsuda, Y.; Matsunaga, S. *Yakugaku Zasshi*, **1969**, *89*, 203 ;
Chem. Abstr. **1969**, *70*, 106328.
114. Wenkert, E.; Jeffcoat, A. R. *J. Org. Chem.* **1970**, *35*, 515.
115. Hua, D. H.; Miao, S. W.; Bravo, A. A.; Takemoto, D. J. *Synthesis* **1991**, 970.
116. Tonelli, M.; Vazzana, I.; Tasso, B.; Boido, V.; Sparatore, F.; Fermeglia, M.; Paneni, M. S.;
Posocco, P.; Pricl, S.; La Colla, P.; Ibba, C.; Secci, B.; Collu, G.; Loddo, R. *Bioorg. Med. Chem.*
2009, *17*, 4425.
117. Tonellia, M.; Pagliettib, G.; Boidoa, V.; Sparatore, F.; Marongiuc, F.; Marongiuc, E.; La
Collac, P.; Loddoc, R. *Chem. Biodiv.* **2008**, *5*, 2386.
118. Casagrande, M.; Basilico, N.; Parapini, S.; Romeo, S.; Taramelli, D.; Sparatore, A. *Bioorg.*
Med. Chem. **2008**, *16*, 6813.
119. Vazzana, I.; Budriesi, R.; Terranova, E.; Ioan, P.; Ugenti, M. P.; Tasso, B.; Chiarini, A.;
Sparatore, F. *J. Med. Chem.* **2007**, *50*, 334.
120. Sparatore, A.; Basilico, N.; Parapini, S.; Romeo, S.; Novelli, F.; Sparatorec, F.; Taramelli,
D. *Bioorg. Med. Chem.* **2005**, *13*, 5338.
121. Ercoli, M.; Mina, L.; Boido, C. C.; Boido, V.; Sparatore, F.; Armani, U.; Piana, A. *IL Farmaco*
2004, *59*, 101.
122. Pohmakotr, M.; Numechai, P.; Prateeptongkum, S.; Tuchinda, P.; Reutrakul, V. *Org.*
Biomol. Chem. **2003**, *1*, 3495.
123. Pohmakotr, M.; Seubsai, A.; Numeechai, P.; Tuchinda, P. *Synthesis* **2008**, 1733.
124. Remuson, R. Gelas.-Mialhe., Y *Mini-Rev. Org. Chem.* **2008**, *5*, 193.
125. Amorde, S. M.; Jewett, I. T.; Martin, S. F. *Tetrahedron* **2009**, *65*, 3222.
126. Wasserman, H. H.; Vu, C. B.; Cook, J. D. *Tetrahedron* **1992**, *48*, 2101.
127. Hiemstra, H.; Sno, M. H. A. M.; Vijn, R. J.; Speckamp, W. N. *J. Org. Chem.* **1985**, *50*, 4014
128. Schreiber, S. L.; Claus, R. E.; Reagan, J. *Tetrahedron Lett.* **1982**, *23*, 3867.
129. Su, D.; Wang, X.; Shao, C.; Xu, J.; Zhu, R.; Hu, Y. *J. Org. Chem.* **2011**, *76*, 188.
130. Cheng, G.; Wang, X.; Su, D.; Liu, H.; Liu, F.; Hu, Y. *J. Org. Chem.* **2010**, *75*, 1911.
131. Kitahara, K.; Toma, T.; Shimokawa, J.; Fukuyama, T. *Org. Lett.* **2008**, *10*, 2259.
132. Ahari, M. h.; Perez, A.; Menant, C.; Vasse, J.-L.; Szymoniak, J. *Org. Lett.* **2008**, *10*, 2473.
133. Hajri, M.; Blondelle, C.; Martinez, A.; Vasse, J.-L.; Szymoniak, J. *Tetrahedron Lett.* **2013**, *54*,
1029.
134. Cutter, A. C.; Miller, I. R.; Keily, J. F.; Bellingham, R. K.; Light, M. E.; Brown, R. C. D. *Org.*
Lett. **2011**, *13*, 3988.

135. Watkin, S. V. *PhD Thesis*. University of Southampton, **2013**.
136. Kise, N.; Inoue, Y.; Sakurai, T. *Tetrahedron Lett.* **2013** *54*, 3281.
137. Brambilla, M.; Davies, S. G.; Fletcher, A. M.; Roberts, P. M.; Thomson, J. E. *Tetrahedron*, **2016**, *72*, 7417.
138. Davies, S. G.; Fletcher, A. M.; Roberts, P. M.; Thomson, J. E. *Synlett*, **2017**, *28*, 2697.
139. Ionut, A. P. *PhD Thesis*. University of Southampton, **2015**.
140. Nagao, Y.; Dai, W.; Ochiai, M.; Tsukagoshi, S.; Fujita, E. *J. Org. Chem.* **1990**, *55*, 1148.
141. Kinghorn, A. D. *J. Agric. Food Chem.* **1982**, *30*, 796.
142. Nagao, Y.; Dai, W. M.; Ochiai, M.; Tsukagoshi, S.; Fujita, E. *J. Am. Chem. Soc.* **1988**, *110*, 289.
143. Koley, D.; Krishna, Y.; Srinivas, K.; Khan, A. A.; Kant, R. *Angew. Chem. Int. Ed.* **2014**, *53*, 13196.
144. Evans, D. A.; Nelson, J. V.; Taber, T. R. Stereoselective Aldol Condensations. In *Topics in Stereochemistry*; Allinger, N. L., Eliel, E. L., Wilen, S. H., Eds.; John Wiley & Sons, Inc.: Hoboken, NJ, **1982**; Vol. *13*.
145. Tang, T. P.; Ellman, J. A. *J. Org. Chem.* **2002**, *67*, 7819.
146. Humphries, P. S.; Do, Q-Q. T.; Wilhite, D. M. *Beilstein J Org Chem.* **2006**, *2*, 1.
147. Tsunoda, T.; Yamamiya, Y.; Ito, S. *Tetrahedron Lett.* **1993**, *34*, 1639.
148. Gaetjens, E.; Morawetz, H. *J. Am. Chem. Soc.* **1960**, *82*, 5328.
149. Simion, A. M.; Hashimoto, I.; Mitoma, Y.; Egashira, N.; Simion, C. *Synth commun.* **2012**, *42*, 921.
150. Raghavan, S.; Krishnaiah, V.; Sridhar, B. *J. Org. Chem.* **2010**, *75*, 498.
151. Chen W.; Ren J.; Wang M.; Dang L.; Shen X.; Yang X.; Zhang H. *Chem. Commun.* **2014**, *50*, 6259.
152. Cropper, E. L.; White, A. J. P.; Ford, A.; Hii, K. K. *J. Org. Chem.* **2006**, *71* (4), 1732.
153. Miller, I. R. *PhD Thesis*. University of Southampton, **2008**.
154. Gray, D.; Gallagher, T., *Angew. Chem. Int. Ed.* **2006**, *45*, 2419.
155. Lui, G.; Cogan, D. A.; Owens, T. D.; Tang, T. P.; Ellman, J. A. *J. Org. Chem.* **1999**, *64*, 1278
156. Bogdal, D. *Molecules* **1999**, *4*, 333.
157. Huang, Z.; Zhang, M.; Wang, Y.; Qin, Y. *Synlett* **2005**, *2005*, 1334.
158. Han, P.; Si, C. M.; Mao, Z. Y.; Li, H. T.; Wei, B. G. *Tetrahedron* **2016**, *72*, 862.

List of References